1993

MEASUREMENT AND ANALYSIS OF SEA WAVES NEAR A REFLECTIVE STRUCTURE

BIRD, PAUL ANDREW DELVES

MEASUREMENT AND ANALYSIS OF SEA WAVES NEAR A REFLECTIVE STRUCTURE

by

PAUL ANDREW DELVES BIRD

A thesis submitted to the University of Plymouth
in partial fulfilment for the degree of

DOCTOR OF PHILOSOPHY

School of Civil and Structural Engineering
Faculty of Technology

June 1993

The author and student divers with the wave recorder, Plymouth Sound.

'Remember, when discoursing about water, to induce first experience, then reason'

- Leonardo da Vinci, quoted by Le Mehaute.

AUTHOR'S DECLARATION

This work is the result of my own investigation. All other sources have been acknowledged. At no time during the registration for the degree of Doctor of Philosophy was I registered for any other award.

I attended the International Conference on Measuring Techniques of Hydraulic Phenomena in London, 1986, and the couse Design Criteria in Maritime Engineering at Plymouth Polytechnic in 1986.

I have made presentions on this work as part of the programmes of research seminars of the School of Civil and Structural Engineering and of the Institute of Marine Studies at the University of Plymouth, to the Single Layer Armouring Research Club, to members of the Science and Engineering Research Council, and to the Southern Branch of the Institute of Water and Environmental Management at Littlehampton, West Sussex.

In 1991 I presented the paper 'Field measurements of the wave climate' at the Symposium on Developments in Coastal Engineering at the University of Bristol. Other papers are in preparation.

Signed.....P.E. Bird.....

Date.....30 June 1993.....

NOTICE

This thesis contains material that is commercially confidential. It has been registered as such with the University's Academic Registry, and is supplied to the reader in confidence. The thesis is not to be passed on to any third party, nor copied, without the author's permission until 1 July 1995.

From that date the thesis will be made available for consultation in the library of the University of Plymouth, and may be photocopied or lent to other libraries for study purposes subject to the normal conditions of acknowledgement. Copyright will remain with the author and no quotation from the thesis nor information derived from it may be published without the author's prior written consent.

MEASUREMENT AND ANALYSIS OF SEA WAVES NEAR A REFLECTIVE STRUCTURE

by

Paul Andrew Delves Bird

ABSTRACT

Methods and equipment for the measurement of ocean waves were reviewed and their suitability assessed for the aim of this project: field measurement of sea waves near a reflective coastal structure such as a breakwater. None was found to be suitable. The functional and performance objectives are set out for a new system. The evolution of the final design, based on an array of pressure sensors, is described. The whole system is intended to be deployed on the sea-bed. It is fully self contained and independent of shore based services. Located away from the surf zone it is well placed to survive storm conditions and unauthorised interference.

Theoretical methods for the re-construction of surface elevation records from measured sub-surface pressures, and the experimental findings of other workers, are presented. Available methods of estimating the wave directional spectrum from a spatial array of surface elevation records are reviewed, and the most appropriate one implemented.

The system has given extensive service at a number of coastal defence sites. The results of subsequent analysis of selected data sets are presented in detail. They show the pronounced nodal structure in amplitude expected in the presence of wave reflection, clearly demonstrating that a single point measurement is likely to give misleading estimates of incident wave height. For near-calm to moderate, shore-normal incident wave conditions the results were found to agree with theoretical predictions both of wave height as a function of distance offshore, and of the structure's frequency-dependent reflection coefficient. For rougher conditions, in which both theoretical and physical models are less applicable, the results agreed with visual observations.

ACKNOWLEDGEMENTS

I would like to record my thanks to all who have helped in this project. In particular:

To Prof G.N. Bullock, director of studies, for conceiving the idea of the wave recording system, commissioning it and securing funds for its development, and so providing me with the most interesting design project of my career to date; to my supervisors Prof D.J. Mapps and Dr T. Donnelly for their regular encouragement and advice; to Mr J. Driver for sharing his wide experience of wave recording at the outset of the work; to Mr K. Stott for fabricating the electronic assemblies, and Mr J. Hutchinson for manufacturing the housings, and other academic and technical staff members throughout the faculty for their specialist advice and contributions; to Mr J. Barker and Mr F. Rendell for planning the deployment procedure and, with Mr F. Knott, for the high standard of organisation and seamanship in carring it through; to the divers - Messrs F. Rendell, S. Edmunds, D. Mellor, A. Tapp, W. Millar, and many students; to Mr D.E.G. Honeywell for invaluable conversations over many years on mechanical engineering practice and engineering design in general, and Mr B.G. Hagan for advice on pressure housing design; to Prof D.A. Huntley for helpful discussions on the daunting subject of directional wave analysis, Dr M.A. Davidson for his contributions to the analysis, and Dr E. Ifaechor for general advice on digital signal processing; to Mr N.W.H. Allsop of Hydraulics Research Ltd for his support and assistance; to the Queen's Harbourmaster and the Property Services Agency for permission to deploy the system near Plymouth Breakwater, and Arun District Council for the same at Elmer; and to the National Advisory Body and the Science and Engineering Research Council for providing funds for the project.

I am grateful also to my colleagues for their patience while I have had to put other tasks aside in order to complete this thesis, and most of all to my family: Eileen for keeping everything running at home during this period, and Anna and Katie - for helping to stick the pictures in.

TABLE OF CONTENTS

LIST OF FIGURES

LIST OF TABLES

LIST OF PLATES

LIST OF SYMBOLS

a	amplitude
A	amplitude
c	wave celerity (speed)
c	co-spectrum
c_g	group velocity
C_r	reflection coefficient
d	mean depth
D	sensor separation
E	energy
f	frequency
g	gravitational acceleration
G	directional spreading function
G	gain
H	wave height
$\mathbf{i}$	unit vector
$\mathbf{I}$	identity matrix
Ir	Iribarren number
j	$\sqrt{-1}$
$\mathbf{k}$	unit vector
$\mathbf{k}$	wave number vector
k	magnitude of wave number vector
k	index for discrete sequence
k	integer
l	sensor separation
L	wave length
m	sensor identifier
m	integer
n	sensor identifier
n	integer
n	index for discrete sequence
N	integer
N	pressure attenuation calibration factor

p	pressure
P	pressure - standing value
P	power
q	noise signal
Q	cross-spectral density function
Q	cross-spectral density matrix
r	position vector
R	autocorrelation matrix
s	parameter for directional spreading function
S	variance spectrum
t	time
T	wave period
T	propagation delay
Ur	Ursell number
v	speed
V	particle velocity
w	window function
W	Fourier transform of window function
x	distance or displacement
x	general input variable
X	relative distance in x direxion
y	distance or displacement
y	general output variable
Y	relative distance in y direction
z	distance or displacement
z	offset signal
z	amplitude spectrum (omni-directional)
Z	amplitude directional spectrum

α	complex weighting factor for estimate of directional spectrum
β	bed slope angle (to horizontal)
ε	phase angle
ϕ	phase angle
η	surface elevation
Φ	velocity potential
ρ	density
κ	scaling factor for directional spectrum
θ	wave direction
ω	radian frequency
Ω	generalised frequency variable for a discrete sequence

Subscripts

a	atmospheric
a	from Airy theory
i	incident
o	deep water
p	peak-to-peak value
pk	peak value
r	reflected
r	image position
s	standing part
v	varying part
x	component in x direction
y	component in y direction

Superscripts

T	matrix transpose
*	complex conjugate
^	estimate

CHAPTER 1
INTRODUCTION

CHAPTER 1
INTRODUCTION

1.1 SCOPE OF THE WORK

The aim of the project was to develop a new instrumentation system to measure, at full scale, the complex wave conditions near a reflecting structure. The system was to be capable of operating unattended for long periods, and to be robust enough to survive storms conditions. Specifications of the form which the instrument was to take, and its performance, were to be set after a review of previous work, the equipment available on the market, and in the light of the current state of electronics technology. Sophisticated analysis methods were to be developed and implemented in a series of software routines. These would derive from the measured quantities the required information on wave conditions: the directional wave spectrum. The wave recording system would be capable of acquiring long-term wave statistics at a coastal site, and also (of more interest initially) capable of providing information on the performance of coastal structures - particularly their wave reflection properties.

The work was started in 1986. After design, development and initial trials a full-performance wave recording system was first deployed in 1988. A second system was made in 1992, and at the time of writing (1993) the two system have delivered a total of nearly one year's wave data from four different sites.

The work falls into two main parts: the instrumentation itself, and the analysis of the measured data. Chapter 1 sets out the information required of the new system, and contains a review of wave measurement techniques and instrumentation available for purchase. Chapter 2 gives an account of how the specification for the new instrument was arrived at, and describes the system itself. Chapter 3 completes the instrumentation part of the project with a description of operational considerations such as deployment

and recovery from site, together with the initial data-handling procedures which give the files of sub-sea pressure data.

The second part of the work consisted of the analysis procedures in which required information on the wave field was extracted from the measured data. Chapter 4 presents a brief review of the relevant aspects of wave theory before going into detail on how surface elevation (wave) data is constructed from sub-surface pressure fluctuations, and how the directional wave spectrum is calculated from wave records taken simultaneously from an array of transducers. Examples of the results are given in Chapter 5, together with discussion.

The account of the project concludes at that point. The implications of these results for the design of coastal structures is the subject of ongoing work at the University of Plymouth.

1.2 BACKGROUND TO THE WORK

Some 35% of the coastline of England and Wales is protected by man-made defences from erosion or flooding, an investment valued in 1984 at four billion pounds, and receiving maintenance work costing one hundred million pounds per year. Many of these works were constructed before 1960 so that maintenance costs are rising. The damage caused in the UK by the fierce storms and exceptionally high tides of January and February 1990, together with fears of a rise in mean sea level due to global warming, all point to the need for more investment in coastal protection work. It has been argued (Maritime Engineering Group 1985, Coastal Engineering Research 1985, CIM 1989) that coastal protection schemes could be considerably more cost effective if more were known about the basic processes by which sea waves and currents affect structures, and how they erode, transport and deposit the materials making up the shoreline.

These phenomena are studied in three ways: by constructing computer programs to predict behaviour from basic physical laws; by constructing scale models and making measurements in the laboratory; and by making measurements on the sea and real shorelines and structures. This latter is in general the most difficult because the available site is unlikely to be idealised to reveal one desired characteristic alone. Also, interesting events do not happen to order and must be waited for, and the equipment must be capable of surviving storm and other damage. However the data obtained from field work can be the most valuable of the three as it is not subject to the assumptions implicit in numerical model and laboratory model approaches. This field data is therefore often used to check or calibrate the performance of the other methods. The coastal engineering research community has assigned a high priority to the collection of comprehensive, quality field data, both for the better understanding of basic processes, and for the validation of models.

The present study addresses the problem of measuring sea waves near coastal structures. It includes the development of a new instrument, since no existing equipment could meet all the requirements. The two key features are that it should cope with rough seas (partly as those are the conditions for which computer and physical modelling is least useful) and that it can measure both incident and reflected waves. The new instrument, and the associated methods of analysis, will find two kinds of application in coastal engineering. Firstly, in the monitoring of structural performance it is necessary to relate measurements of, for example, impact loads, and internal stresses and strains, to the waves causing them - the incident waves. Any wave measuring device incapable of distinguishing between incoming and reflected waves will lead to an incorrect interpretation of the structural measurements. An example of such an application is in the design of breakwaters with single layer armouring blocks. There is an urgent need to obtain performance measurements for this sort of armouring to improve breakwater designs. New design methods and guidelines are required to avoid both the failure of inadequate structures (for example at Sines, Portugal in 1978), and the unnecessary costs of 'over-design'. Measurements

of internal stresses and strains in the armour units of such a breakwater are currently being made by collaborating organisations, and it is hoped to deploy the wave recorder as part of that project.

Secondly, reflection itself is important because it causes scour that can undermine the structure's foundations; it causes unpleasant and dangerous seas states in nearby waterways; and it is a major mechanism by which a structure prevents wave energy reaching the shoreline (what is not transmitted is either reflected or absorbed). And in another application, wave power devices must absorb, rather than reflect, energy. The present system will be capable of measuring the reflection performance of structures. Rock island breakwaters are a new type of coastal defence, and the wave recorder is to be deployed next to some of these. It is hoped to determine how the reflection coefficient depends on, for example, angle of slope.

1.3 A REVIEW OF WAVE MEASUREMENT

1.3.1 Purpose

Waves have been measured in the coastal zone over the past few decades for purposes as diverse as the interests of the organisations carrying out the work. The armed forces, academic and research institutions, civil engineering consultants and their local authority clients, oil companies, and national environmental monitoring agencies are all active in the field. They may be endeavouring to improve understanding of wave behaviour, to determine likely wave loading on structures, or, as in the present case, to improve the capabilities of wave measuring instruments themselves.

Wave recording with instruments began seriously in the Second World War to help ensure the safe landing of troops on foreign shores. From a more theoretical point of view, observing the behaviour of real waves is an important input to the development of more accurate analytical descriptions

of waves, including the effects of non-linearities. The interaction between waves and currents, sea bed features, and structures is at present imperfectly understood and in need of further refinement.

The engineer planning a new coastal structure needs to know as much as possible about the wave climate to which it will be exposed in order to avoid inadequate performance, or excessive cost. In particular, the expected return periods of waves of a given height should be known with some confidence, and these can only be obtained from data covering at least one year, and preferably longer. An estimated 55 million observations of wave height and wind speed have been collated by the UK Meteorological Office Marine Data Bank. That data is made available in printed form (BMT 1986, Draper 1991) and more comprehensively as a personal computer database (BMT 1990). The British Oceanographic Data Centre at the Proudman Oceanographic Laboratory, Bidston, also maintains a national bank of wave data, and can give sources of data for other areas.

Having estimated the design wave conditions, the engineer then needs guidelines and procedures to design the structure (eg CERC 1984). These incorporate the experience from past structures and the outcome of a large body of research into the interaction between waves and structures.

The subject of electrical power generation from sea waves has undergone several changes in political fortune in the last twenty years. Although a commercially viable device, competitive with mainland fossil fuel stations, has not yet been built, there may well be a brighter future for combined power-generating and coastal defence structures. Much wave data, with direction an important parameter, has been collected for the wave power programme (Crabb 1984).

The need for better instrumentation to measure waves more comprehensively and cheaply is recognised (Dean 1981). The characteristic least well provided for is direction of wave propagation. Work is proceeding to develop methods of measuring the directional spectra of

waves routinely and continuously, both remotely from satellites and aircraft, and locally at a particular site.

1.3.2 Methods

The many and various ways of detecting waves are either 'direct' methods, in that they measure the actual height of the water surface above a datum (eg sea bed or mean sea level), or 'indirect', measuring a quantity that is related to wave height, such as pressure below the surface. Perhaps the easiest way to classify the methods is by location of the sensor: above the water surface, on or piercing the surface, and below the surface. The diagram in Figure 1.1 provides a graphical summary. The measurement of wave direction is discussed separately. All the systems described, particularly the remote sensing systems, have benefited from advances in technology. The improvements in sensors, analog integrated circuits and batteries have enabled greater accuracy, longer periods of unattended operation, and greater functionality (Bird and Bullock 1991). For example, the problem of measuring wave direction implies greater complexity in both accelerometer buoys (pitch and roll as well as heave), and also in subsurface sensors (synchronised reading of several channels). But perhaps the most significant advances have been made in the way measured data is accessed by the user. The old methods of data storage - rolls of paper charts and pens requiring frequent replacement - have given way to magnetic tape, and to semiconductor memory. The digital format of the later methods is necessary for any subsequent analysis by computer.

1.3.2.1 Sensor above the surface

This includes radar, the radio altimeter, laser, ultrasonic rangefinder, and still and video photography. The equipment may be mounted locally on a structure such as a pier (or possibly on a nearby shoreline), or remotely on an aircraft or satellite. In favourable conditions with the sensor on a stable platform near the sea surface very good resolution and accuracy are obtainable. In rough conditions the spray and aerated water of breaking

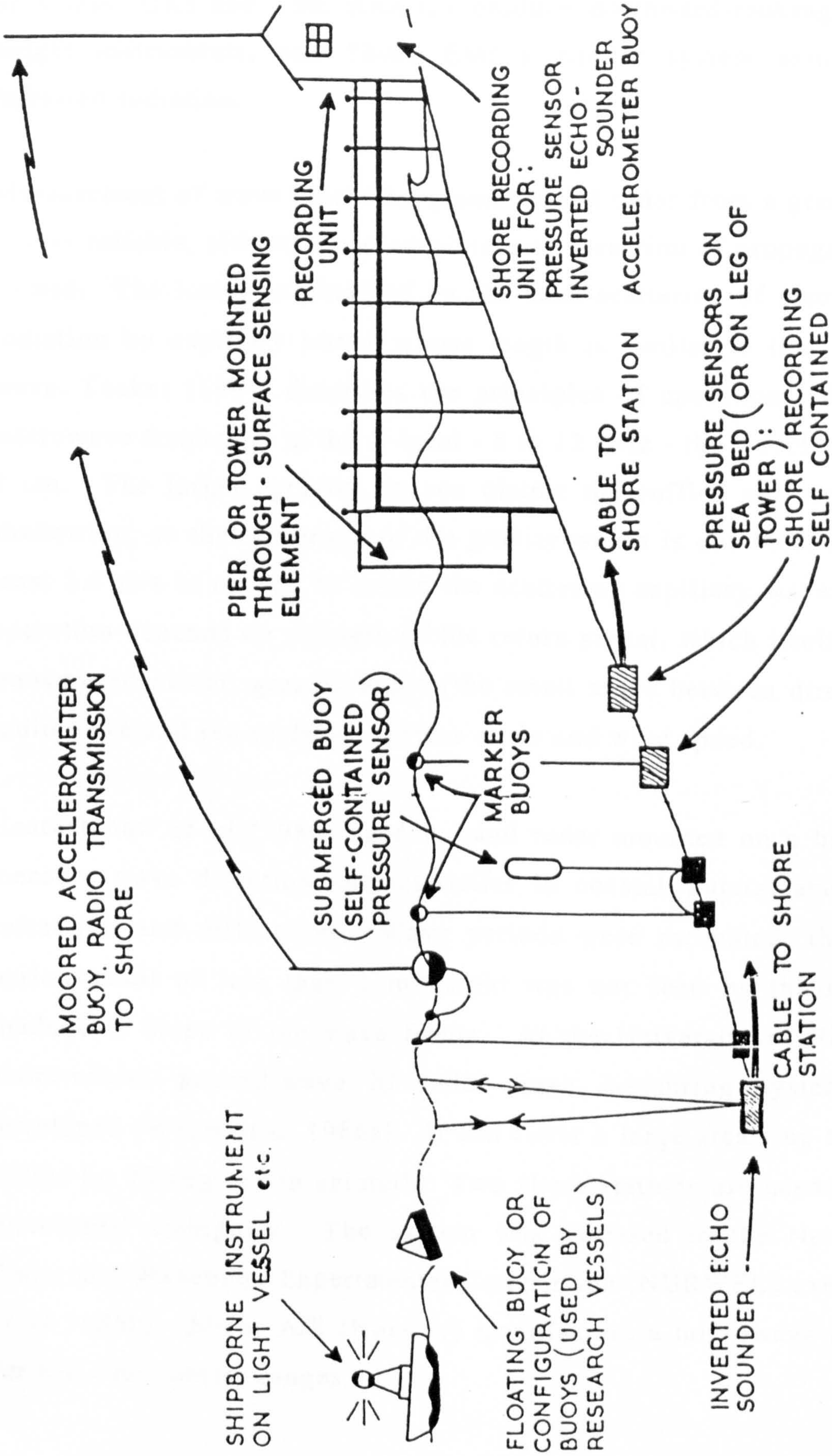

Figure 1.1: Methods used for recording sea waves (from Draper, 1966)

wave crests introduce uncertainty in fixing water surface level. Marex (Isle of Wight, UK) and TSK America produce downward-looking radar wave height instruments, and Thorn EMI a similar system using pulses of infra-red radiation.

Measurement of wave height by ground-based radar from a greater distance is less reliable, although a good picture of direction of propagation may be gained. The image is obtained by the back-scattering of electro-magnetic radiation by capillary waves whose length is similar to that of the radio wave. Tucker (1991) describes the principles of operation. For a typical microwave frequency in the X band - 8 to 12 GHz - the wavelength is about 3 cm. The larger, gravity, waves distort the ruffled surface, and cause shadowing, so that an image of the gravity waves is obtained. A wind of at least 2.5 m/s is needed to create the scattering capillary waves. Range of operation depends on strength of the return signal, which itself depends on transmitted power, grazing angle (the small angle between direction of the radio wave and sea surface), surface slope and wind speed.

Heathershaw *et al* (1980) used X band radar mounted on a breakwater to measure wave direction characteristics in coastal waters, and to observe refraction and diffraction. Wave periods were estimated, though longer period swell of less than 1 m height was not seen by the radar due to inadequate slope of the wave fronts. At the University of Birmingham a shore-based, ground-wave hf radar wave measuring system has been developed (Wyatt *et al* 1986a). It can cover a large area - up to 200 km in radius by 90 degrees in azimuth. Two shore stations are needed to remove directional ambiguity. The system was assessed in the Netherlands/UK Radar and Wavebuoy Experimental Comparison (NURWEC) exercise (Wyatt *et al* 1986b). Miros A/S (Norway) manufacture a microwave radar system for use over shorter ranges.

Remote sensing with radar has the potential to offer routine and reliable collection of data over a wide area (Carter *et al* 1988). The synthetic aperture radar (SAR) technique yields images of the high resolution

required for wave observation. An aircraft or satellite flies in a straight path, emitting pulses continuously at a precisely controlled frequency so that the transmitted power is coherent. The return signals are processed such that an antenna of aperture as long as the flight path is simulated, thereby giving the high resolution. Frequencies in the L band (1 to 2 GHz, with a wavelength of 15 to 30 cm) are normally used; small waves are again necessary for scattering. Clouds and rain do not attenuate signals at that frequency (Rayleigh scattering by water drops becomes serious at wavelengths of 3 cm or less) so that data can be collected during storms. Although it is possible to derive wave height from the data, techniques are still being refined (Jain 1977).

A system developed by NASA in the USA (Walsh *et al* 1981) consists of a computer controlled radar that produces in real time a topographical map of the surface beneath the aircraft carrying it. Later off-line processing gives the directional wave spectra. In another NASA program, a radar for use on either aircraft or satellite was developed (Jackson *et al* 1981). When satellite mounted, spectra are produced for locations at typically every 100 nautical miles along the satellite's track.

The Seasat satellite launched in 1978 was equipped with a synthetic aperture radar (SAR) which produced images of 100 km wide strips of the ocean's surface. It provided information on wave direction and length, as well as ocean currents (Mattie *et al* 1980).

However, more work is needed to bring the full potential of remote sensing - accurate wave measurements over large areas at reasonable cost. A comprehensive review of the remote sensing of waves is given by Huang (1982).

In some circumstances photographic methods of recording waves are a possibility. For a ground-based installation there must be a support structure for equipment, a graduated staff, adequate lighting and a clear line of sight. From an aircraft, wave visibility depends on surface slope, and on

the alignment of the wave fronts relative to the source of illumination. In principle surface heights can be obtained by analysis of stereo photographs, although in practice in requires much analysis (Stillwell 1969). The Stereo Wave Observation Project (SWOP) (Cote *et al* 1960) was a major trial of this method. With these limitations, and the high cost of operating aircraft, aerial photography is limited to examining the spatial behaviour of waves (such as refraction) at a particular location, and to checking other systems more suited to routine measurement.

1.3.2.2 Sensor at or piercing the surface.

A graduated staff fixed in the sea bed or on some supporting structure, and observed by eye or camera, must be the simplest and most direct way of measuring waves. But difficulties in defining the actual water surface in a storm, or even in seeing the scale at all, as well as in availability of manpower will render this method unsuitable in many cases.

There are electrical equivalents, widely used in the laboratory, which pick up the resistive or capacitive linkage between two vertical wires that pass through the surface. Signals from these can be logged with conventional equipment. In practice it is difficult to engineer a system strong enough to survive storms in exposed locations although a system for deployment on beaches has been developed by Chadwick (1989). Aeration and spray can complicate the interpretation, while splashing with water well above the true surface produces a spurious pulse that may be misleading.

Floating buoys, located by compliant moorings and fitted with accelerometers (such as the 'Waverider' buoy from Datawell bv, Netherlands, shown in Figure 1.2) have been used extensively for many years. An accelerometer on a stabilised platform within the buoy's waterproof housing gives an electrical output proportional to vertical acceleration. This is integrated twice to give vertical displacement, or heave. The buoy is fitted with circuitry for modulating a carrier at between 27 and 30 MHz, and sends the signal via a whip aerial to the shore station

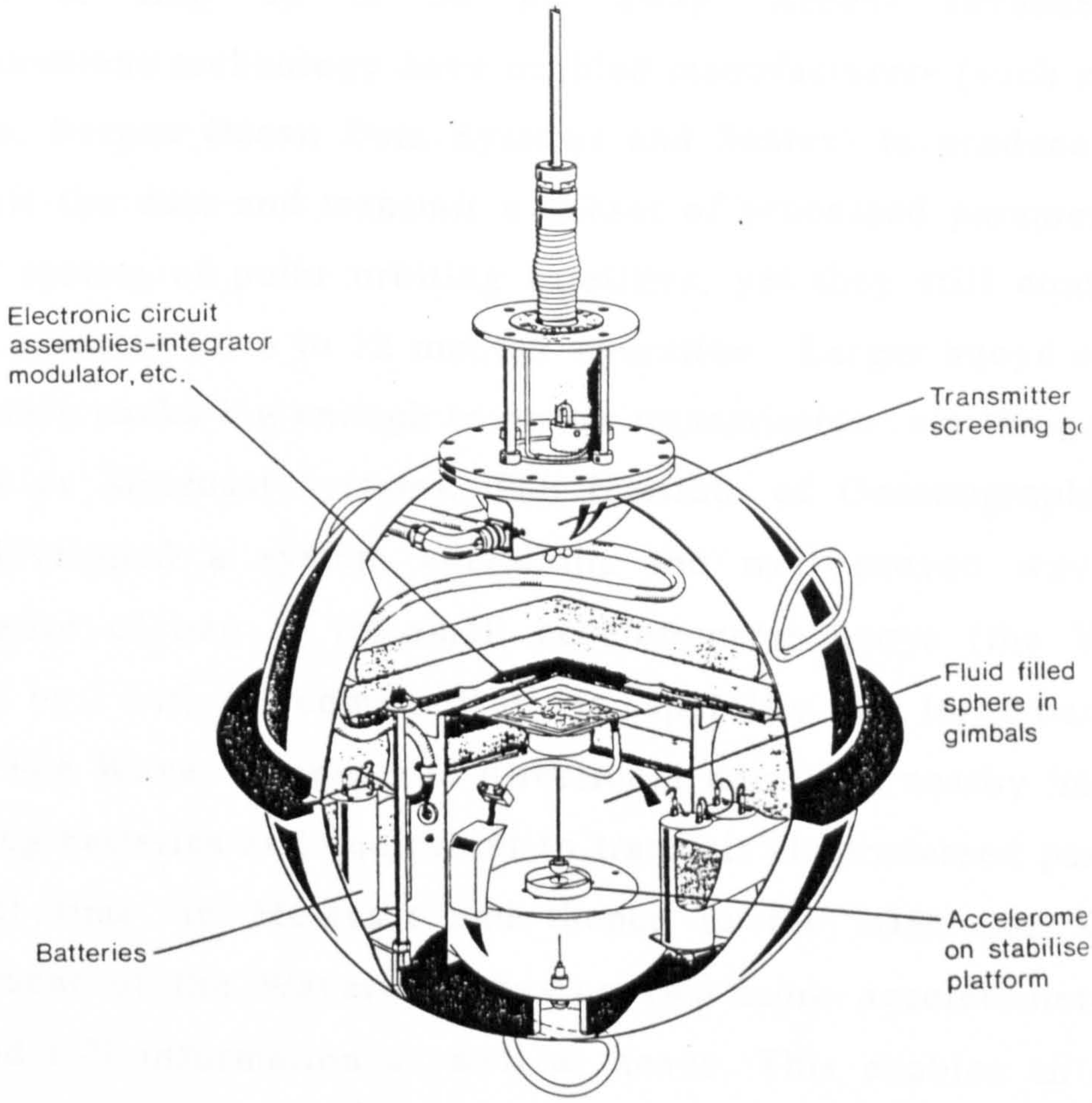

Figure 1.2: Cutaway view of Waverider buoy (from Driver, 1980)

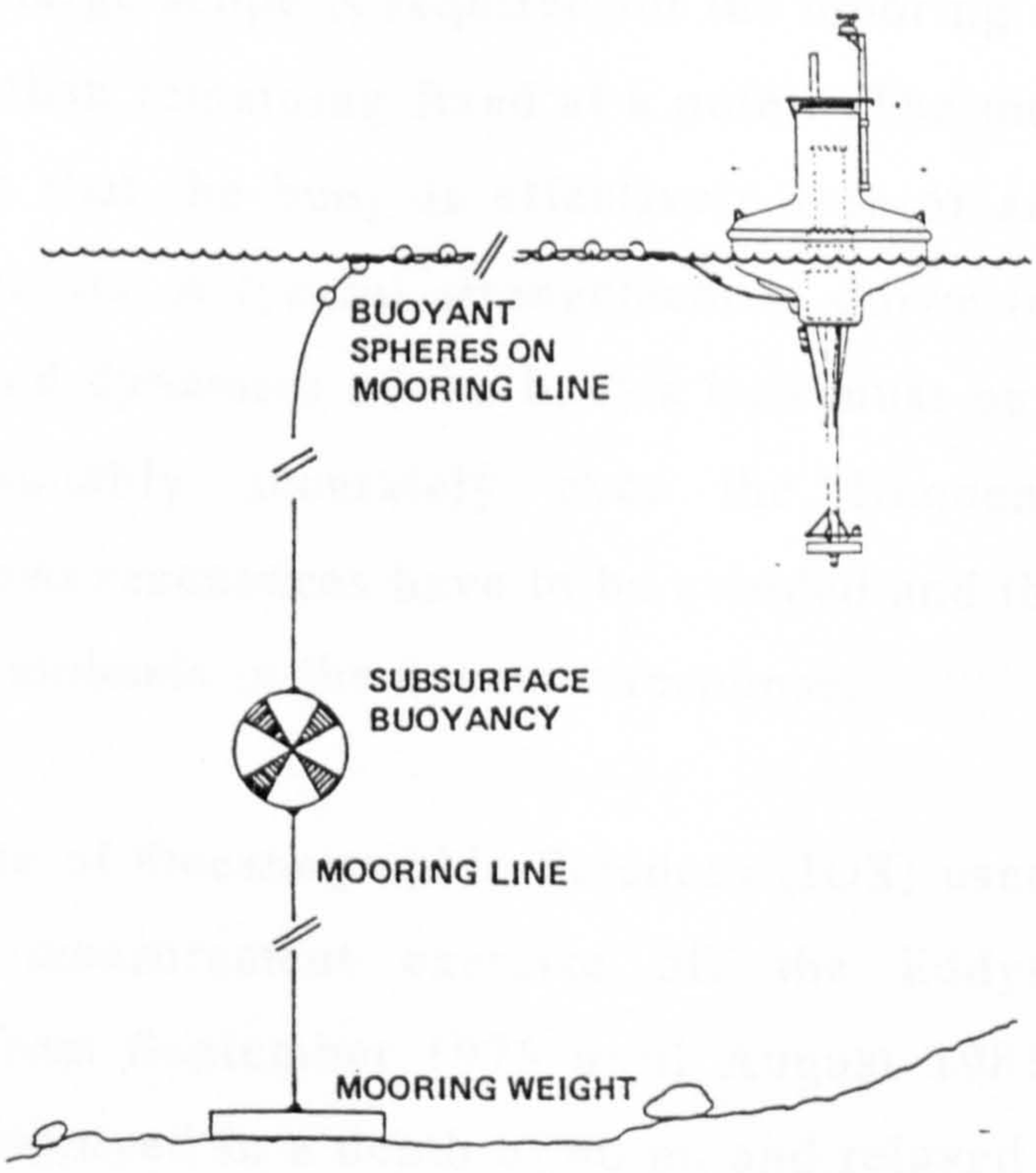

Figure 1.3: Mooring for Pitch-roll-heave buoy

platform or ship up to 50 km away. Recent advances in data communications technology have enabled manufacturers (such as Datawell, Nereides, Bergen Ocean Data Systems and Seatex) to produce buoys that record all the data and transmit a subset of processed parameters via the ARGOS system of polar orbiting satellites, yet they still contain enough battery capacity for 6 to 12 months' operation. Larger buoys can be fitted with battery packs big enough to power transmission via the geostationary Inmarsat or Meteosat systems. The Institute of Oceanographic Sciences (IOS) developed a system combining the well proven wave-following performance of one of its small accelerometer buoys (the Wavec from Datawell bv.) with the communications capability of a large buoy (Clayson 1989). The Wavec telemetered directional data to a nearby 'mother buoy' containing batteries and equipment to transmit all processed parameters, in near real time, to Meteosat and thence to the IOS. The Wavec is a development of the Waverider, having two more accelerometers to give pitch and roll information as well as heave. This enables an estimate of wave direction to be made.

In general, wave-measuring buoys can be vulnerable to vandalism and theft, and since a large scope is required for the mooring cable they range over an area rather than remaining fixed at a point. The mooring must be carefully designed so that the buoy is effectively free of any frictional, inertial or elastic restraints. A typical arrangement is shown in Figure 1-3. Similarly, the shape and dynamics of the buoy's hull must be such that it follows the waves reasonably accurately over the frequency range of interest. Under-damped resonances have to be avoided and the data corrected for any remaining emphasis in the dynamic response.

The Institute of Oceanographic Sciences (IOS) used a Waverider buoy in a long term measurement exercise off the Eddystone Rocks, south of Plymouth from September 1978 until August 1981 (Fortnum 1982). The buoy was deployed in a depth of 40 m, and relayed its data by radio link to a shore station at Wembury, east of Plymouth. There the demodulated signal was digitised and stored on magnetic cartridge for later analysis at

the IOS in Taunton. As a backup the analog signal was recorded directly on to magnetic tape. The data was received, processed and recorded for periods of 17 minutes every three hours, using a sampling frequency of 2 Hz. To indicate the difficulty of working in these conditions, nearly 30% of the records over the three years were missing or invalid, although some of those were captured by the tape backup. The buoys were calibrated on-shore before and after deployment by rotating them in a large frame and examining the received radio signal. Sensitivity of the Waverider, radio link and demodulation equipment was stable to within +/- 3% over the period of deployment.

The measurements taken during the Joint North Sea Wave Project (JONSWAP) in September 1973 (Hasselmann *et al* 1980) attempted, unlike the work at the Eddystone, to obtain wave direction information as well as surface height records. Two buoys were used: a heave, pitch and roll buoy from the IOS, and a 'meteorological buoy' from the University of Hamburg. The latter was a comprehensively instrumented conical shaped buoy, containing three accelerometers, a gyroscope, two inclinometers, a compass and two pressure transducers.

In January 1980 the Norwegian Continental Shelf Institute deployed a heave, pitch and roll buoy off the coast of Norway (Andensen *et al* 1983) to measure wave height and direction. It was developed by that organisation in conjunction with the Christian Michelsen Institute and manufactured by Bergen Ocean Data. The hull was a discus shape with a subsurface leg and ballast weight, and on top was a mast for supporting meteorological instrumentation and an Argos satellite transmitting aerial, Figure 1-3. Inside were the accelerometers, a sea temperature sensor, and a Sea Data digital tape recorder. As in the previously mentioned examples the mooring was designed for minimum effect on the motion of the buoy. Data was recorded over several years, with a 10 to 20 % loss rate. Winds of up to 35 m/s, and waves up to 19 m were experienced, resulting in the mooring breaking twice; here the Argos tracking system assisted swift recovery. Calibration was performed on shore with a vertically rotating carousel with

six degrees of freedom, and the heave component further checked at sea by comparison with a Waverider buoy.

The shipborne wave recorder (Tucker 1956, Haine 1980) consisting of accelerometers and pressure sensors fitted to the hull of a ship, has also been extensively used. The accelerometers measure vertical displacement or heave of the ship, while the pressure transducers measure depth of immersion. Combining data from the two yields the actual water surface record. Measurements are normally made when the ship is stationary, and the transducers are carefully sited to minimise the effects due to the ship's pitch and roll; wave direction is not measured. These systems are more accurate for longer period waves than for short. They have provided a cost effective way of obtaining large amounts of wave data.

The manual equivalent of the shipborne wave recorder - simple visual observation by mariners - has yielded an enormous quantity of wave data (Hogben and Lumb 1967); for many parts of the world this is the only source. A formal procedure for making these observations and interpreting the results was made in 1944 (Munk), and subsequently work has been done to assess their reliability (Jardine 1979).

1.3.2.3 Sensor below the surface

Instruments mounted below the sea surface usually have improved chances of survival as they are less visible, and so less at risk from vandalism and theft, and may be less vulnerable to storm damage. Measuring water pressure variations at the sea bed, or at some intermediate depth, was the principle used by some of the first wave recording instruments and remains in use today. The major disadvantage is the reduction, at depth, of the pressure fluctuation due to the waves. Thus a sensor near the surface would experience a fluctuation in pressure similar to the hydrostatic value that would arise from the equivalent water level changes. But at greater depth the pressure changes are only a small proportion of this. The effect is more marked with higher frequency waves, and is discussed more in Chapter 4.

Sub-surface pressure sensing is therefore used only if the transducer can be mounted at a depth of less than about 20 m.

The pressure sensor itself may operate on a number of principles. Normally the pressure causes (either directly or through an interposed fluid) a diaphragm to flex. The amount of movement is picked up by strain gauges, or by capacitive or inductive changes in linked circuits. Wave measurement by pressure sensing at the sea bed was chosen for this project, so a more detailed discussion of practical considerations appears later.

Carmel, Inman and Golik (1985) describe a measurement made from February 1979 to August 1981 off the coast of Israel near Haifa in which they used two pressure sensors in a 6m depth of water, connected by armoured cable to a shore based data recording system. Recordings were made twice daily for 25 minutes, sampling each channel at 4 Hz, on to hi-fi cassette tapes that were later sent to the Scripps Institute for Oceanography in California for analysis. The ambiguity inherent in inferring wave direction from just two sensors was resolved with additional information. Data for the first 10 months was intermittent and unreliable, but improved in the remaining period after modifications were made.

Motion of water due to waves can be measured with current meters. These instruments are of a number of types, based on the effect of moving water on a spinning impeller, or on voltages induced in electromagnetic coils, or on the travel time of acoustic impulses between fixed points, or on drag-inducing shapes bending strain-gauged bars. Some of these measure components of current along only one axis, others are omni-directional.

Sherman and Greenwood (1986) used two bi-directional electromagnetic current meters and a vertical, resistive, wave staff to measure wave heights and angles at Wendake Beach, Ontario, Canada. The measurement was of rather short duration, from 31 May to 1 June 1980, but good accuracy and resolution of wave direction were claimed.

Use of ultrasonic ranging (echo-sounding) from above the water has already been mentioned; echo sounders are also available that operate 'upside down'. They are located on the sea bed and point upwards to measure distance to the water surface. Temperature and salinity changes, an aerated surface, and noise interference can cause errors, and the devices tend to consume more electrical power than pressure sensors. Accuracy under favourable conditions, however, can be high.

1.3.2.4 Determining wave direction

The preceding sections have indicated that only some of the measuring techniques are capable of yielding the direction of propagation of waves, or wave components in a complex field, others giving only time histories of wave heights. In general if directional information is required then it is necessary either to use one of the imaging techniques such as radar or photography, or to measure a vector quantity such as water movement at a point (or several quantities in the case of the pitch-roll-heave buoy), or to measure scalar quantities simultaneously at a number of points.

Comparative studies have been done of several possible approaches. Over a period of six days in March 1977, Mattie, Hsiao and Evans (1981) performed an experiment to determine the applicability of four methods to obtain wave direction. Three were remote sensing techniques: photography from an aircraft at a height of about 18 km, a synthetic aperture radar also on an aircraft, and a standard X band marine radar situated on shore. The fourth method was an array of five pressure transducers fixed to a tower at a depth of 19 m. They report good agreement in the results for wavetrains with a single predominant direction, but poor agreement over multiple wavetrains of similar period travelling in different directions. They point out that results from the pressure transducer array are dependent largely on the type of analysis used, and they used an algorithm of low directional resolution. The pressure sensing method was the only one able to give wave heights.

A comprehensive study of five means of obtaining wave direction was carried out in 1980 as part of the US Atlantic Remote Sensing Land Ocean Experiment (ARSLOE) (Grosskopf *et al* 1984). The output from four subsurface gauges and a shore based radar were compared. Two gauges contained current meters aligned orthogonally and a pressure sensor. One consisted of three orthogonally aligned current meters only, and the final gauge was an array of four pressure transducers. In general the results were well correlated, except that height estimates from the three current meter system were significantly low; it was recommended that a non-current means of acquiring wave height should be included. The radar could distinguish well wavetrains of similar period travelling in different directions, but not wavetrains of different period going the same way. The opposite was true of the subsurface gauges, although again a relatively simple analysis procedure for evaluating wave direction was used; more complex 'data-adaptive' techniques were expected to resolve directions of wavetrains of similar period. The paper contains a thorough discussion of error sources inherent in the methods, many of which were relevant to the present work. It is of course necessary to avoid excessive errors from all sources if the final results are to be accurate, and these include not just in the performance of sensors and electronic instrumentation but also in the positioning of equipment, and the processing and analysis of the results. The pressure sensor array was open to fewer error sources than the other methods examined.

1.4 SPECIAL FEATURES OF THE MEASUREMENT

The information required was a complete description of the wave conditions close to a structure. The description was to include the height of the waves, periods and their directions of propagation. Linearity was assumed so that the wave pattern could be considered made up of sinusoidal wave components, each with its own period and direction. The wave field was thus described by its 'directional spectrum', the distribution of wave energy over frequency and direction. As the layout of the test site was known,

those components corresponding to waves travelling in towards the structure (the incident waves) could be identified and distinguished from the reflected waves. Comparison of the two gives the amount of reflection of wave energy.

The general arrangement of the instrumentation system needed was governed by operational considerations and features of the site. Firstly, severe storms were expected; the instrument would be expected to survive these and operate normally throughout. Previous experience of this type of work by members of the department indicated that it was difficult to design equipment strong enough to survive in the area of breaking waves, the 'surf zone'. Therefore if there were to be sub-surface sensors then it was desirable that any processing and recording equipment should also be mounted underwater. Alternatively, cables could be led to a sheltered area before leaving the water, but this could result in rather long cable runs.

Secondly, there is the danger that expensive equipment left out in the open could be stolen or tampered with. The first test site envisaged - Plymouth Breakwater - was in an area extensively used by divers, fishermen and yachtsmen, so the new system had to be hidden from view as far as possible.

Thirdly, long periods of operation were needed to collect data during a wide range of sea states without frequent attention by the operators. That implied either a large data storage capacity, or a means of transmitting data to an operator on shore a few kilometres away.

Radar imaging was not appropriate as accurate wave height data was required. Optical methods placed unacceptable limits on the periods data would be obtainable. No suitable pier or tower existed at the test site, nor could one be built, ruling out the local above-surface methods. And as the region of interest was very close to a structure, an instrumented buoy ranging widely on the scope of a compliant mooring would have been impractical. A buoy would also have been vulnerable to theft and vandalism. Sub-surface sensors were clearly indicated, and in view of the

reasoning above, a sub-surface processing and storage unit. Acoustic ranging devices were expected to consume rather too much electrical power. The choice of sensor therefore narrowed to pressure or current. The latter has a high consumption of electrical power. In addition pressure transducers are more robust than current meters, and less prone to errors that are difficult to calibrate out.

In view of these results and arguments an array of sub-surface pressure transducers, with suitable analysis, was the method chosen in this investigation to measure wave height and direction.

1.5 A PROPRIETARY WAVE RECORDER?

The department possessed and had used at a number of sites a self-contained sea-bed mounted wave recorder (the DNW-5 from NBA Controls Ltd.), which used a pressure transducer and stored data on cassette tape. Approaches to the manufacturer revealed that it would not be practical to modify the design to enable a number of these units to be deployed in an array for synchronised operation. In any case its accuracy, data storage capacity, battery life and inflexibility of operation (no communication was possible without recovery) were not really adequate. A thorough search for a suitable proprietary instrument commenced with the aid of the specialist technical press (eg Underwater Systems Design 1987), trade exhibitions (eg Oceanology '86, 1986), and experts in the field (Draper and Driver 1980, Driver 1985). A list of manufacturers approached appears in Appendix A. The search revealed nothing that would meet the requirements.

Looking further afield at the general instrumentation market, it was also discovered that there were no general purpose data loggers capable of operating in such an environment without attention for long periods. A decision was taken to design and build a new instrument, referred to here as the 'new wave recording system'. Development of the instrument from the general requirements set out above is described in the next Chapter.

REFERENCES

Audensen T. Barstow S. F. and Krogstad H. E. (1983)
Analysis of wave directivity from a heave, pitch, roll buoy operated offshore Norway
Internal report of the Continental Shelf Institute, Trondheim, Norway.

Bird P.A.D. and Bullock G.N. (1991)
Field measurements of the wave climate
in *Symp. on Developments in Coastal Engineering*, Eds D.H. Peregrine and J.H. Loveless, University of Bristol, UK, 15 Mar 1991.

British Maritime Technology Ltd. with Unwins Ltd. (1986)
Global Wave Statistics.

British Maritime Technology Ltd. (1990)
PC Global Wave Statistics

Carmel Z. Inman D.L. and Golik A. (1985)
Characteristics of storm waves off the Mediterranean Coast of Israel
Coastal Engineering 9, 1-19.

Carter D.J.T. Challenor P.G. and Srokosz M.A. (1988)
Satellite remote sensing and wave studies into the 1990's
Int. Jnl. of Remote Sensing, 9 (10-11).

Chadwick A.J. (1989)
Measurement and analysis of inshore wave climate
Proc. Inst. Civ. Engrs. Pt2 87 23-38.

Clayson C.H. (1989)
Directional wave measurements - southern North Sea
IOS Report No.266.

Coastal Engineering Research (1985)
Reports prepared by the working parties on beaches and sea walls; siltation, dredging and dispersion; and coastal harbours, breakwaters and offshore islands.
Thomas Telford, July 1985.

Coastal Impact Modelling Committee (1989)
Coastal impact modelling - the way forward, May 1989.

Coastal Engineering Research Center (1984)
Shore protection manual, vol II
Coastal Engineering Research Center, US Army Corps of Engineers Dept of the Army.

Cote L.J. Davis J.O. Marks W. M°Gough R.J. Mehr E. PiersonW.J. Ropek J.F. Stephenson G. and Vetter R.C. (1960)
The directional spectrum of a wind generated sea as determined from data obtained by the Stereo Wave Observation Project
Meteorol. Papers, N.Y.U. Coll. of Eng. **2** (6) 88pp.

Crabb J.A. (1984)
Assessment of wave power available at key UK sites
IOS Report No.186, IOS Deacon Laboratory, Wormley, Godalming, UK.

Dean R.G. (1981)
The NRC workshop on wave measurement technology: a summary
Proc Symp & Workshop on wave measurement technology, Apr 22-24, 1981, Washington DC, USA.

Draper L. (1966)
The problems of sea wave recording
in *Proc Conf on Electrical Engineering in Oceanography*
IERE, University of Southampton, UK, 12-15 Sept 1966, pp 3/1 to 3/4.

Draper L. and Driver J. (1980)
Wave recording instruments for civil engineering use
Appendix to Institute of Oceanographic Sciences Report No 103.

Draper L. (1991)
Wave climate atlas of the British Isles HMSO, UK.

Driver J.S. (1980)
A Guide to sea wave recording
IOS Report No 103, IOS Wormley, Godalming, UK.

Driver J.S. (1985)
Personal communication, Dec 1985.

Fortnum B.C.H. (1982)
Waves recorded off the Eddystone Lighthouse, Sept '78 - Aug '81
Institute of Oceanographic Sciences Report No. 132.

Grosskopf W. G. Aubrey D. G. Mattie M. G. and Mathiesen M. (1984)
Field intercomparison of nearshore directional wave sensors
IEEE Journal of Oceanic Engineering vol **OE-8** 254-271, Oct1984.

Haine R.A. (1980)
Second generation shipborne wave recorder
Transducer Technology **2** (2) 25-28.

Hasselmann D. E. Dunckel M. and Ewing J. A. (1980)
Directional wave spectra observed during JONSWAP, 1973
Journal of Physical Oceanography **10** 1264-1280.

Heathershaw A.D. Blackley M.W.L. and Hardcastle P.J. (1980)
Wave direction estimates in coastal waters using radar
Coastal Engineering **3** 249-267.

Hogben N. and Lumb F.E. (1967)
Ocean Wave Statistics
National Physical Laboratory, London, UK.

Huang, N.E. (1982)
A general survey of remote sensing techniques for wave measurement.
Proceedings of the U.S. National Research Council on Wave Measurement Technology 38-79.

Jackson F.C. Walton W.T. and Baker P.L. (1981)
Directional spectra from air- and space- borne radar
Proc ASCE Conf Directional Wave Spectra Applications
Sept 1981 299-314.

Jain A. (1977)
Determination of ocean wave heights from synthetic aperture radar imagery
Applied Physics **13** (4) 371-382, Aug 1977.

Jardine T.P. (1979)
The reliability of visually observed wave heights
Coastal Engineering, **3** 33-38.

Maritime Engineering Group, Institution of Civil Engineers (1985)
Research requirements in coastal engineering.
Thomas Telford, Feb 1985.

Mattie M.G. Lichy D.E. and Beal R.C. (1980)
Seasat detection of waves, currents and inlet discharges
Int Jnl of Remote Sensing **1** (4) 377-398.

Mattie M.G. Hsiao S. V. and Evans D. D. (1981)
Wave direction measured by four different systems
IEEE Journal of Oceanic Engineering, vol **OE-6** (3) 87-93, July 1981

Munk W.H. (1944)
Proposed uniform procedure for measuring waves and interpreting instrument records
Wave Project, Scripps Institute of Oceanography, La Jola. California.

Oceanology '86
Exhibition Catalogue
Brighton, March 1986.

Sherman D. J. and Greenwood B. (1986)
Determination of wave angle in shallow water
ASCE Journal of Waterway, Port, Coastal & Ocean Engineering, **112** (1) 129-139, Jan 1986.

Stilwell D.,Jnr. (1969)
Directional energy spectra of the sea from photographs
Journal of Geophysical Research **74** (8) 1974-1986, April 1969.

Tucker M.J. (1956)
A shipborne wave recorder
Transactions of the Institution of Naval Architects, London, **98** 236-250.

Tucker M.J. (1991)
Waves in ocean engineering
Ellis Horwood, London.

Underwater System Design, pp6-9, July 1987.
Product review: data logging
Also many advertisements in *Sea Technology*, and *Transducer Technology*.

Walsh E.J. Hancock D.W. and Hines E. (1981)
Surface contour radar remote sensing of waves
Proc ASCE Conf Directional Wave Spectra Applications
Sept 1981 pp 281-297.

Wyatt L.R. Venn J. Burrows G.D. and Moorhead M.D. (1986a)
Ocean surface wave and current measurement with hf ground-wave radar
Int Conf on Measuring Techniques of Hydraulic Phenomena in Offshore, Coastal and Inland Waters, London, UK.

Wyatt L.R. Venn J. Burrows G.D. Ponsford A.M. Moorhead M.D. and Heteren J.van (1986b)
HF measurements of ocean wave parameters during NURWEC
IEEE J. Ocean. Eng, vol **OE-11** (2) 219-234.

CHAPTER 2

THE NEW WAVE RECORDING SYSTEM

CHAPTER 2
THE NEW WAVE RECORDING SYSTEM

2.1 INTRODUCTION

The design and manufacture of the wave recording system are described in this chapter. The nature of the measurement was discussed in Section 1.4 where it was concluded that subsurface pressure transducers were to be used, with any processing and data storage units also mounted underwater. In Section 2.2 the process of refining the requirements and selecting equipment and methods is continued, leading to a statement of what the measuring system should do: the 'functional specification'. Further consideration of the task enables numerical limits to be put to the major parameters and these are expressed in the 'performance specification'. While fulfilling those specific objectives it was hoped to develop the new instrument in such a way that it would be easily adaptable to the measurement of other physical quantities, and so meet a need for a precision, high capacity data logger for automatic operation in hostile environments.

The two specifications form the starting point for the design of mechanical and electrical hardware, and the controlling software. The design passes through a number of stages as different ideas and solutions are considered (in Section 2.4). Before that, in 2.3, the designs of related, existing, equipment are examined.

The design that was finally settled on is described in detail along with the performances of individual parts of the system in Section 2.5. The reader may like to look ahead to Section 2.5.1 and Appendices B and C for a preview of the end point before following these next sections through. Included there are a descriptive data sheet of the wave recording system (renamed the 'Marine and Site Recorder' to emphasise its more general

potential applications), and a copy of a newspaper article giving a general overview of the recorder and its application.

All manufacturing operations were carried out at the University with the exception of welding and hard anodising the aluminium case, making the printed circuit boards and the battery pack, and assembling underwater connectors to armoured cable, all of which were done by specialist companies. The Department was well placed to undertake this project. The engineering skills and workshop equipment needed to design and make such an instrument were in place. Two suitable boats and crews were available, and among staff and students were divers, to deploy and recover the underwater equipment. The University is situated within a couple of miles of a suitable site for trials - Plymouth Breakwater - and was able to obtain permission to work there and cooperation from the Queen's Harbourmaster and the Property Services Agency. The sum of £17,000 for components and materials was provided by the Science and Engineering Research Council.

2.2 REQUIREMENTS OF THE WAVE RECORDING SYSTEM

The *overall* requirements of the wave recording system are developed in this section. Those of the major component units are developed in later sections - the 'top-down' method.

2.2.1 Functional Specification

To this point it had been decided (Section 1.4) that the system should be self-contained and situated on the sea bed, measuring water pressure at several locations. Still to be considered were the means of deploying, operating and recovering the system at typical sites.

As has been mentioned the environment would not be favourable for precision measuring equipment. Firstly, violent storms were to be expected. Previously at Plymouth these had pushed the 25 and 50 tonne concrete

armouring blocks right over the Breakwater. In 1990 a particularly bad storm moved two of the largest, 100 tonne, blocks over to the shoreward side. Secondly, no mains power could be provided. Thirdly, access to the data would not be easy due to the remoteness of potential sites.

To permit different analysis techniques to be tried, and to minimise any uncertainty that would arise in the case of unforeseen events such as the loss of a transducer, the instrument was to preserve the 'raw' data - samples of water pressure - rather than more compact, statistical, representations of it. Analysis of the measured data was to be performed on a personal computer or workstation: hardware (and associated software) far more powerful than any microprocessor likely to be fitted into the underwater unit. The wave recording system's output was therefore required on a computer disc.

Since the primary purpose was to measure waves reflected from nearby structures, the typical site for deployment would not be in deep water, enabling sea bed mounted pressure transducers to pick up wave activity. Records from each transducer in the array would have to be synchronised, providing a series of 'snapshots' of sea surface height at a number of locations. The wavelengths expected indicated that the array would be spread out over tens or hundreds of metres.

In order to permit measurements of wave-induced loading on structures and other quantities, made by separate instruments, to be related to the wave measurements a real-time clock was required. Date and time of the records could then be stored along with the data.

Based on these arguments, the following functional specification was drawn up. The wave recording system will:-

- be sea bed mounted with integral power supply and data store
- measure water pressures at several locations simultaneously
- record times and dates of measurements

- present the measured data on a computer disc
- have sufficient data- and battery-capacity to record pressure data over a fairly long period
- enable the user to set up measurement parameters, and to check for correct operation from time to time, without full recovery of the equipment
- be robust enough to survive storms, and be located to avoid unauthorised interference.

2.2.2 Performance Specification

The next stage in specifying the equipment was to add quantitative limits to the features described qualitatively in the previous section. Careful consideration was given to setting the limits to avoid, on the one hand, unnecessarily difficult design targets, and on the other hand underestimating necessary requirements. The result is the 'performance specification'.

2.2.2.1 Accuracy

In deciding the accuracy with which waves were to be measured it must be remembered that they are detected as small variations in pressure superimposed upon a much larger standing value. Additionally, as has already been noted, the fluctuating, wave-related, component of pressure is attenuated at depth. Expressing error limits as a percentage of full range of the transducer would be unhelpful, since any reasonable value (for example 0.5%) would be comparable to the signal corresponding to a fairly large wave. The following error limits were set as an achievable target that would not noticeably degrade the information in the signal.

Max. error in measuring steady component: +/- 1% of reading (steady part)

Max. error in measuring varying component:

+/- 1% of reading (varying part)

or 5mm (whichever is greater)

The limits are expressed as percentages of reading rather than of full scale, and split into the steady (mean water level) and varying (wave) components. That is more meaningful in this application than an overall limit of, for example, 1% full scale, although the quoted limits are in absolute terms considerably tighter.

Related to the question of accuracy is that of resolution: the smallest change in measurand that can be reliably detected. Here a figure of +/- 1% of the varying component (or 5mm) was chosen as being compatible with the accuracy specification.

2.2.2.2 Sampling Rate

To make best use of a given data storage capacity the rate at which the analog pressure signals are sampled and converted into digital form must be set as low as possible. Nyquist's 'sampling theorem' states that no information will be lost provided that the sampling frequency is at least twice the highest frequency component in the input signal. That is a theoretical limit, however, and is not attainable in practice. Also, it assumes that the maximum frequency of the signal is known. The highest frequency waves of interest for the present site are of about three seconds period (0.33 Hz). For this maximum frequency a fairly conservative choice of 2 Hz sampling frequency was made - three times the Nyquist limit. At other sites shorter period waves might be expected so the sampling period was to be easily adjustable.

2.2.2.3 Duration of operation

The difficulty of deploying and recovering underwater equipment, even with skilled personnel and all the right facilities, was not to be underestimated

and so a long period of operation on one set of batteries was required. That had implications for circuit design (current consumption), battery sizing, instrument control (automatic powering down when not in use), mechanical design (corrosion and sealing), and data storage.

It is not necessary to measure waves continuously as it is assumed that over the period of an hour or so their statistical properties ought not to change much. It has become customary for instruments to measure for some minutes and then switch off for several hours. That feature was to be included in the new unit, together with 'threshold detection', in which a particular sea state would initiate measurement. The threshold values need not be fixed at this stage; the requirement is that they can easily be set and changed.

2.2.2.4 Number of transducers

At least three point-measurements of surface elevation are needed to get an unambiguous estimate of wave direction, although the resolution of direction from that number is poor. More measurement locations lead to the possibility of higher directional resolution of a complex sea. (The resolution obtainable from various sensor patterns is discussed in Chapter 4). Moreover, the resilience of the system is improved with more transducers as loss of one or two channels (not unlikely given the environment) will leave enough for some useful information. Unfortunately a large part of the overall cost is in the transducers and their housings, connectors and cable assemblies. Six transducers were specified.

2.2.2.5 Data capacity

A commonly used measurement cycle consists of 17 minutes measurement in every three hour period. That was used as a guide in planning the data storage requirements of the new instrument. So, at two readings per second from each of six transducers, every 17 minute cycle would generate about 12 thousand readings, that is 96 thousand per day. The capacity needed for

four months would therefore have to accommodate about 12 million readings, rather more than was practicable at the time (1987). Sufficient data storage for 4 million readings was specified, with the proviso that it would be re-writeable in situ so that the data could be collected after any period up to six weeks without loss and then reset for subsequent periods of six weeks until the batteries became exhausted.

2.2.2.6 Summary

The performance of the envisaged wave recording system was specified as follows:-

- Accuracy: steady component: +/- 1% rdg
  varying component: +/- 1% rdg, or 5mm
- Resolution: 1% of rdg of varying component, or 5mm
- Sample rate: 2 Hz
- Measuring cycle: automatic operation subject to input activity, of pre-set timing (typically 17 mins every 3 hours, but alterable).
- Transducers: 6 No., pressure. Sea bed mounted in an array. (Simultaneous readings required from each).
- Data storage capacity: 4 million readings. (May be reused after downloading data, without recovering instrument).
- Battery life: Four months.
  (and housing life)

2.3 PREVIOUS DESIGNS

Other organisations working in the oceanographic and coastal fields had also come to the conclusion that there was no data acquisition system available which would do the job described in the last section. They were similarly obliged to design and build their own, and accounts of these were reviewed before embarking on the new design.

Prothero (1980) described his 'ocean bottom seismometer' of the late 1970's which houses three geophones, a C90 cassette drive for data storage, and a serial interface for downloading data to a host computer. It was housed a cylindrical hard-anodised aluminium casing weighing 136 kg, and powered by rechargeable lead-acid batteries. The Intersil IM6100 microprocessor (a low-power complementary metal oxide semiconductor - CMOS - type) with 32 kilobytes (KB) of random access memory (RAM) performed rudimentary digital filtering on the signal before storage. Recovery was effected by sending an acoustic signal to the unit causing it to detonate explosive bolts and rise to the surface. The main problem reported was jamming of the cassette drive.

Rather less sophisticated was Mitchell's (1981) microprocessor-based underwater tension meter which measured and logged the output of an integral load cell. The RCA 1802, CMOS, 8 bit processor was equipped with 512 bytes of program memory and 2 KB battery-backed RAM for storing the data. Sixteen dry cells gave a continuous operating time of 60 hours. The voltage-to-frequency technique of digitising the load signal proved difficult to set up, and prone to drift, so it was later replaced by an 8 bit analog to digital converter (ADC).

A system based on a high-density cassette drive for measuring nearshore waves was described by Boyd and Lowe (1985). They managed to store about 6 MB onto a C90 data cassette, although no microcomputer is incorporated so that measurement scheduling was rather inflexible.

The submersible data logging system of Papij (1986) was most interesting in that it was not necessary to open the case at all during normal operation, despite there being no electrically conductive connections. The depth, temperature and water conductivity sensors were all included in the cylindrical housing, and data was transferred through its walls inductively. Having recovered the unit, it was placed into the coils of a special transceiver assembly, which was connected to a personal computer by serial link. The unit's internal batteries were recharged by electrical power also

transferred through the case inductively, using the same coils. A review of inductively coupled connections for underwater was presented by Allen (1987).

In 1987 Birch and Pascal described a meteorological instrumentation system for installation in buoys or on board ship. Like some of the above examples it incorporates RCA's 1802 processor, and uses the RCA Microbus to interface with a 12 bit analog-to-digital converter and a real time clock. The authors point out the importance of careful grounding and shielding of the more sensitive circuits, as well as DC isolation of the sensors.

The main features of interest in these designs are the general layouts, and the choice of the key components. All except one was microprocessor controlled for increased flexibility of operation, and for provision of limited data processing and control of the user interface. The processors selected were all CMOS types for low power consumption, the CDP1802 from RCA being one of the most popular in the late 1970's and early '80s. The appeal of Intersil's IM6100 was its similarity to the famous PDP-8 minicomputer. Tape cassette was the preferred medium of data storage.

2.4 GENERAL ARRANGEMENT

The specifications set down in Section 2.2 define fairly closely what was wanted from the system, but they do not define the form of the instrument that will do the job. Instead, they raise questions on how to implement the required functions (data storage, signal conditioning etc), how to separate the functions into different physical units, and how these units are to communicate. The next stage of the design is to generate a number of possible options for arranging the functions, and then to select the most promising on the basis of ease of use, performance available from the latest components and circuit techniques, cleanness of the interfaces between units, and cost.

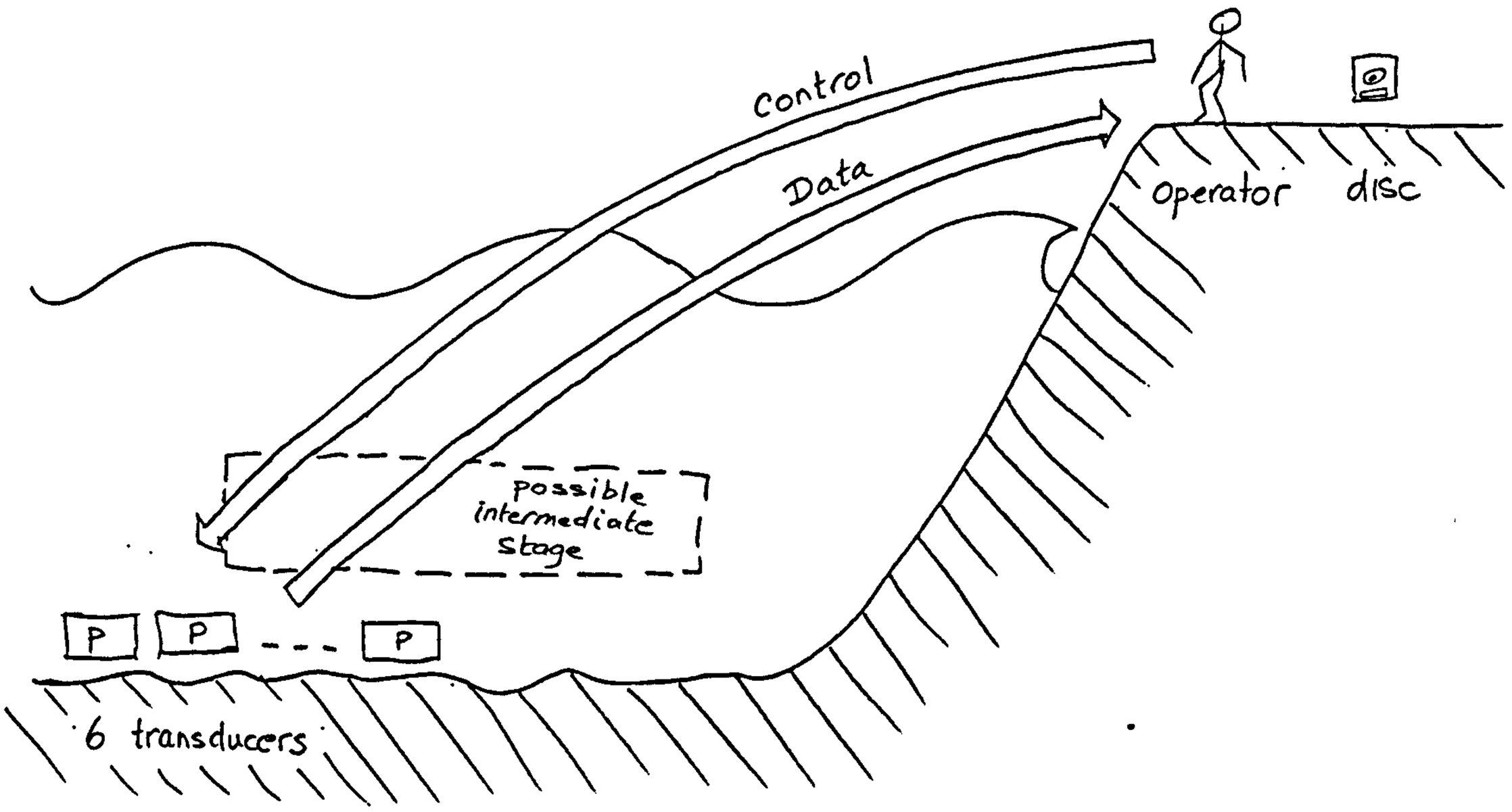

Figure 2.1 : Overview of the measurement

All that has been specified so far are the two ends of the system: inputs (pressures) and output (digital data on disc). These are represented in Figure 2.1 . Also the assumptions have been made that the pressure transducers will require a number of signal conditioning stages and conversion into digital form, and that there will be some data compression and storage, and internal scheduling of measurement operations with some degree of control by the user. The intermediate stage shown includes any functions housed separately from the individual sensor units. The specification does not call for such a unit so it is drawn with a dotted line, but the arguments below indicate that it would bring benefits.

It is often best to evaluate possible layouts by examining the implied interfaces between sections, and to start with the interface between instrument and user.

2.4.1 Communications link to the user

The possibilities envisaged were:-

a) A separate module for the data store that could be hauled aboard or lifted by a diver. Any control information would have to be inserted into the module before reconnection.

b) A cable link to a shore station. The link could be copper or optical fibre.

c) A cable link to a radio buoy transmitting to a shore station.

d) A cable link normally lying on the sea bed that could be hauled or lifted aboard a boat.

e) An ultrasonic link from boat to sub-sea unit(s).

f) A data collection unit carried by a diver, communicating with the sub-sea units either by waterproof connectors or an inductive connection through the case wall.

As the end point is a computer magnetic disc holding measured data, the system must include a disc drive. That could be in the instrument itself, or in a personal computer at the end of the communication link.

Option (a) lacks flexibility, particularly in the user's control of parameters. If the operation is to be carried out by boat, with no diver, then there will be a unit of considerable value which is rather vulnerable to theft. However, there are advantages: the arrangement is relatively simple, it would permit the use of the type of memory components that need to be erased out-of-circuit, and (if a battery pack were included) would extend the duration of operation between deployments, and relax the low current consumption requirement.

Option (b) would require a long cable (several kilometres) as it would have to be diverted to come to the surface at a sheltered location.

Options (e) and (f) are the only ones that avoid the need for some intermediate unit without incurring undue complication: (e) as it might be

possible to communicate with all sensors at once with a sort of broadcast, frequency division multiplex, ultrasonic link, and (f) by the diver 'harvesting' data from units one after the other. However routine use of the instrument was not to be dependent on diving support, ruling out (f). The ultrasonic link has the great advantage of not needing any underwater cable or connectors at all. However the data rates are high for the transmission medium of sea water and so require a narrow beamwidth and accurate positioning of the boat. The method is worthy of future investigation for communication from a boat to a single point, although any 'broadcast' technique would be considerably more difficult.

Clearly, the possibility of a connection for data and control from the wave recorder to the Polytechnic was attractive (option c). The value of the buoy and its transmitting equipment would have to be kept low in case it were stolen. Perhaps the nicest solution for the longer term would be to use the radio buoy and an ultrasonic link from buoy to instrument.

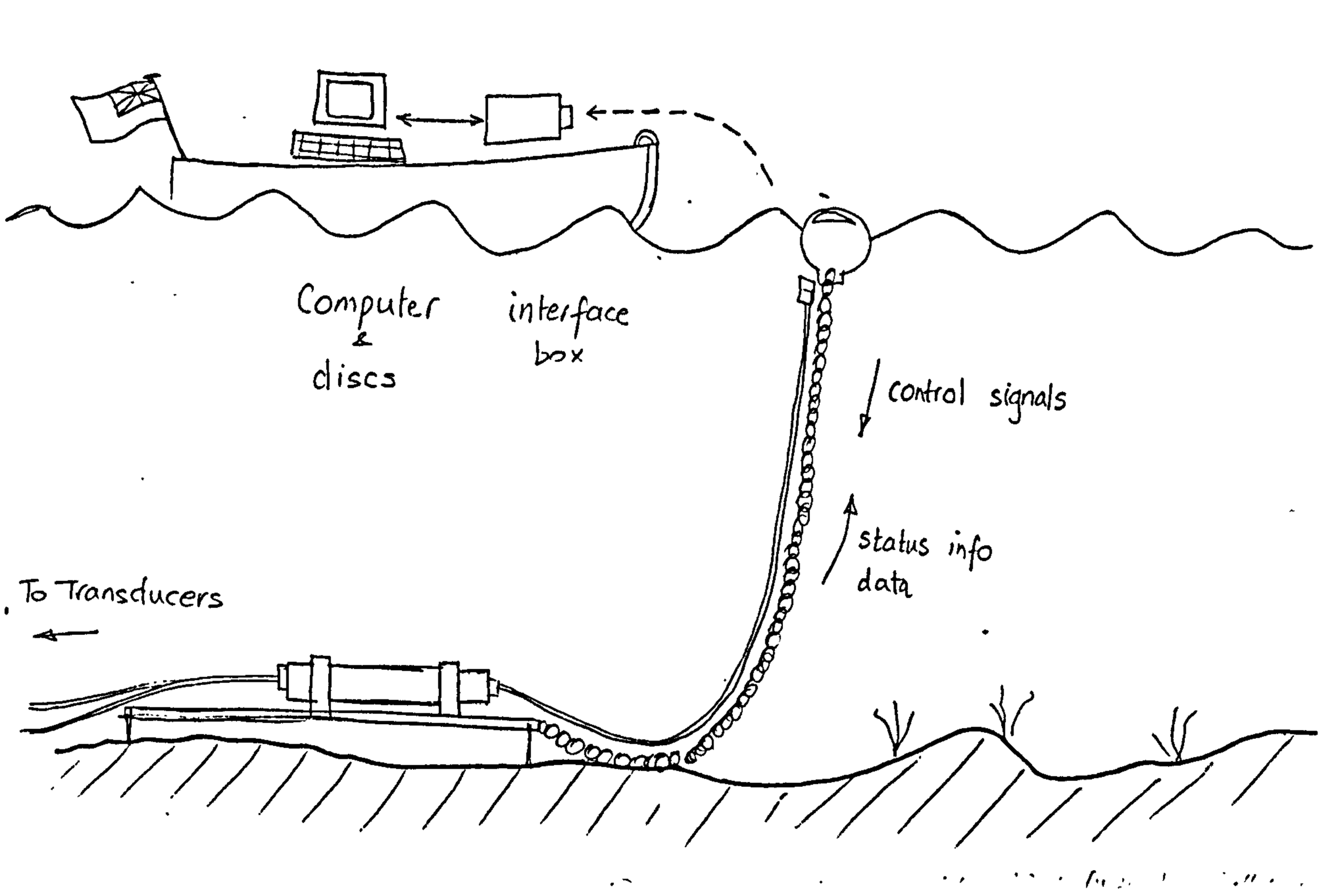

Figure 2.2 : Permanent data cable link

The simplest of the options - (d) - was eventually chosen in order to shorten development time. A cable permanently connected to a central signal conditioning and data storage unit lies on the sea bed, and is marked by a small buoy (Figure 2.2).

The operator visits the site by boat, hauls aboard the cable and connects it to the personal computer. Instrument status may be examined on the screen, control parameters set from the keyboard and uploaded to the wave recorder, and data downloaded onto the computer's disc. (Note that conventional data communication terminology works upside-down in this application!) The cable would be somewhat vulnerable to interference so precautions were taken to minimise any damage to the system in that event. It was necessary to ensure that a violent tug on the cable would cause connector breakage before threatening the case sealing. In addition, some protection was given against electrical damage by fitting all cable interface circuits with opto-isolators.

2.4.2 Arrangement of underwater sections

In the previous section the case was made for a single point for communications from the user. This implies a central unit to which all pressure signals are led. The question now is how much signal processing to include in the remote pressure sensing units, and how much in the central unit. The two extremes are:-

- maximum at centre, minimum remote. Only the pressure transducers themselves are at remote locations, all amplifiers, signal conditioning, ADC, control, data store and power supplies are placed in the central unit; and
- minimum at centre, maximum remote, in which all those functions are placed remotely except control of timing and the communications link.

Many other combinations between these extremes are possible and were carefully considered.

The criteria for judging the best arrangement of functional layout include cost of parts: in many cases a function located centrally will serve all six sensors. Possibly more important is the form of the resulting interface between remote and central units. Ideally these interfaces should be simple (underwater connectors are expensive and limited in configuration), free from errors due to interference and ground loops, and should allow the system to continue to operate at reduced performance in the case of loss of one or two remote units. Power supply arrangements need similar consideration: should there be batteries with each transducer, or a larger pack for all components in the central unit?

Pressure transducers for this sort of application produce only millivolt level signals, usually from a strain gauge bridge bonded to the back of a flexing diaphragm. Conducting those signals for tens or hundreds of metres would not result in the qualities mentioned. At a minimum, preamplification of the signal at the transducer would be needed.

At the other extreme, if all the functions were included with the transducers there would be considerable replication, raising the total cost. However, the sensors would communicate to the central unit with digital signals which are much less prone to electrical errors than signals in analog form.

In fact, the most significant feature of an arrangement is whether the interfaces are analog or digital. (A 'hybrid' method using voltage to frequency conversion and sending a square wave signal was also considered). In its favour the *digital* form is electrically more robust. It also opens the possibility of using optical fibre rather than copper (bringing the benefits of speed and electrical isolation) although that was discounted as optical fibres cannot carry power to the remote units. (Cables with mixtures of optical fibre and copper cores are available, but suitable connectors are much harder to obtain.)

On the other hand, it was felt that a high level *analog* signal (for example: 0 to 5 V, or 4 to 20 mA) would be acceptable. Also there were arguments for keeping as many as possible of the control functions central, for example, to achieve simultaneous timing of the pressure measurements. Also it was anticipated that the analog signal conditioning would turn out to be fairly complex in order to give the required accuracy. Features such as automatic range switching and calibration are more costly distributed than implemented centrally.

For these reasons it was decided to place only pre-amplifiers with the pressure transducers and to link the high level analog signals to a central unit which would contain all the other functions (Figure 2.3). This layout had the additional advantage of enabling later adaptation to measuring other physical quantities. Only the transducers and initial signal conditioning circuits would need to be changed. The instrument could then meet the need for a precision, high capacity data logger for automatic operation in hostile environments.

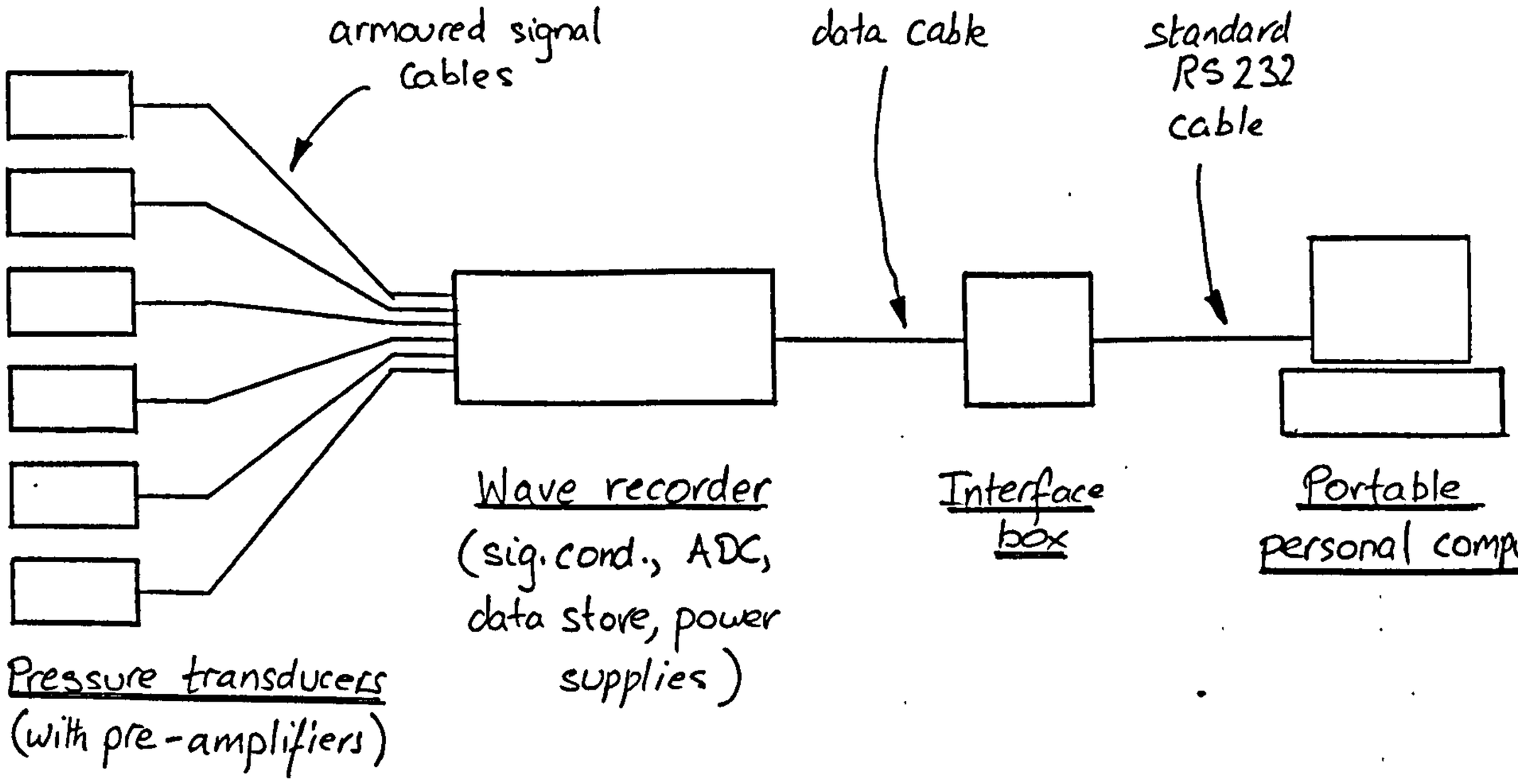

Figure 2.3 : General arrangement of the wave recording system

2.5 DESCRIPTION OF THE SYSTEM

2.5.1 Overview

Figure 2.3 shows the general arrangement of the new wave recording system. The central signal conditioning and data storage unit, the transducers, the interface unit and the 'laptop' personal computer are illustrated in Plate 1. The transducers and the recorder are in sealed enclosures which are held in position on the sea bed in specially fabricated supports. Armoured cables with underwater-mateable connectors link the transducers to the recorder. Data can be downloaded when convenient through the communications cable via the interface unit to the computer. Control parameters may also be sent from the computer to the recorder. The data transfer cable normally rests on the sea bed and can be located by means of a small marker buoy, while both the interface unit and the computer may easily be carried in a boat. Consequently no diving is necessary for information transfer.

The recorder has a large data storage capacity (four megabytes) in CMOS random access semiconductor memory. It will store typically six weeks' wave data from the full complement of six transducers. Thus visits by boat to collect the data may be up to six weeks apart; typically one would plan monthly visits and have two weeks in hand for unsuitable weather. After data collection the memory is re-used. The internal battery pack lasts for four months. Only after that period need the recorder be recovered, allowing a full winter season's use. Although the transducers could be left in place, normally they would be recovered at the same time for cleaning and calibration.

The instrument is microprocessor-controlled to give flexibility of measurement scheduling, control of signal conditioning stages, and control of the communication link. The system conforms to the specifications set out in Section 2.2.2 .

Plate 1 : Wave recording system

Inside the housing are fitted four printed circuit board (PCB) assemblies and the battery pack (Plates 2 and 3). The PCB's are double sided, through-hole plated, glass fibre boards, except for the power supply assembly which is shown in prototype stripboard implementation. The data store assembly has a solder resist coating, that being the normal standard envisaged for fully developed boards. That one also has a small 'piggy-back' circuit which would not fit in to the main area. As pictured, the data store has only one-sixteenth of the full memory complement fitted, and the signal conditioning PCB only three of the six channels The latest electronic components available were selected to reduce size, as well as to achieve low power consumption and good accuracy. Because of the fairly dense packing, attention had to be given to the control of electrical interference between sections. The board assemblies are connected to each other by ribbon cables with insulation displacement connectors, and to the wiring assemblies from batteries and transducers by heavier duty headers and sockets.

In general the procedure followed the sequence of defining the specifications; identifying potentially the most difficult sections; searching the relevant literature and data sheets; making preliminary sketches and then breadboards; testing, modifying and re-testing (using proprietary and specially made test equipment), trying out with other sections; and designing the printed circuit boards. A formal drawing control system kept track of the many changes involved in the test-modify-retest cycle.

Printed circuit boards were laid out with the aid of the computer aided design (CAD) package 'Redboard' from Racal Ltd, and the resulting output sent on floppy disk to a specialist company for laser photo-plotting and manufacture. Redboard's auto-route facility was unable to produce designs for the digital sections, tending to place the easiest 90% of the tracks and leaving the designer 'painted into a corner' with the remaining 10%. For the analog circuits no PCB CAD package at the time could, in the author's view, take account of the more varied requirements to produce a good design; that was still a job for the human designer. The layouts of all four boards were

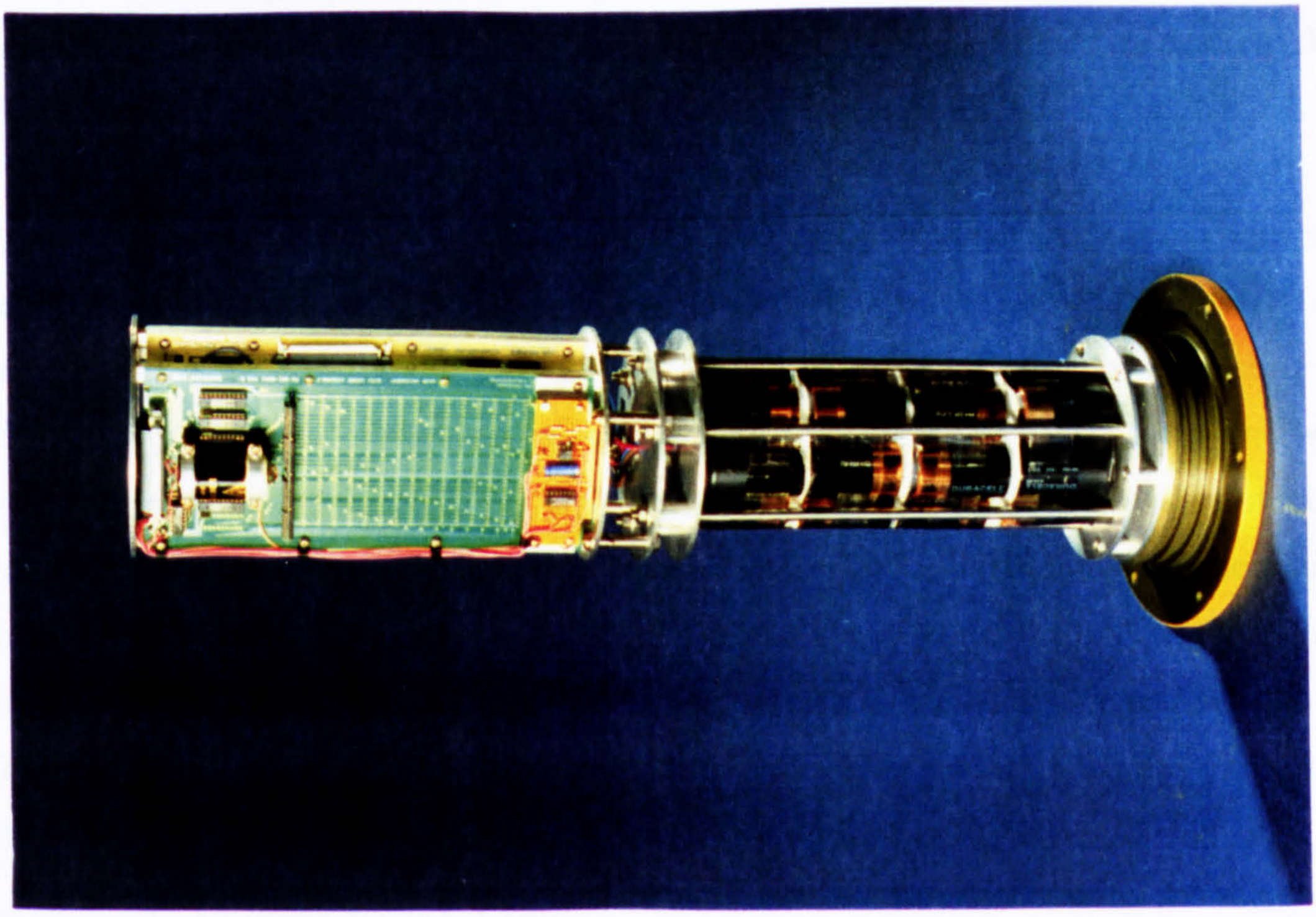

Plate 2 : Wave recorder chassis showing batteries,
printed circuit board assemblies and chassis.

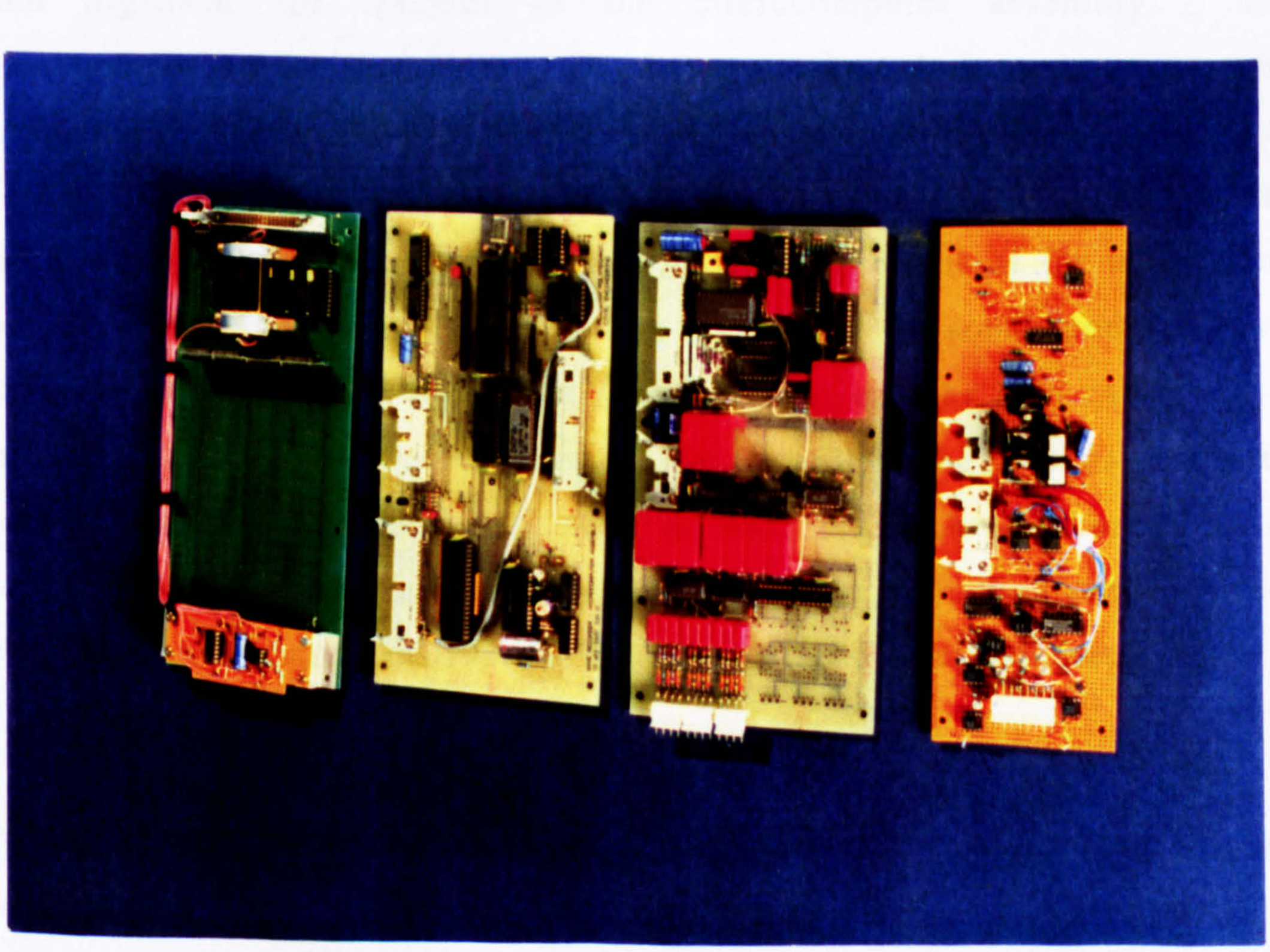

Plate 3 : The four main circuit board assemblies.
From the left: data store, microcomputer,
signal conditioning, and power supply.

designed in rough with coloured pencils on tracing film at twice full size before transfer to the computer which replaced the coloured tapes of the older technique.

The functional sections are shown in Figure 2.4 . These are power supply control, signal conditioning, microcomputer, and data store. Each section is implemented on its own PCB, shown in Plate 3. The fifth main section is the battery pack. Connections between sections are shown as broad arrows, with the number of conductors written in. Apportioning functions to circuit boards was carefully worked out to achieve logical interfaces and minimum interference, taking account of the different board sizes and associated headroom. An early scheme in which all sections were connected to a common 'instrument bus' turned out to be rather cumbersome and was abandoned.

The six transducers are connected to the signal conditioning board where their outputs are amplified, filtered, multiplexed into a single channel, and then digitised for transfer to the microcomputer assembly. The microcomputer puts the readings as they are taken during a measurement cycle into a memory buffer. At the end of the cycle it compresses them into a block of data, adds the time and date, and sends the block across to the data store. The microcomputer schedules all the actions of the instrument, and handles communication with the operator's personal computer via isolating amplifiers (on the power supply board) and the data cable. (It is only by this route that the recorder can be controlled, the personal computer is the system's control panel. Even an on-off switch is impractical on sub-sea equipment.) An early examination of the functions required soon ruled out any simpler instrument layout without a microcomputer, such as that of Boyd and Lowe (1985).

The power supply assembly provides regulated voltages to the other sections, and to the pressure transducers. Supplies for digital and analog parts are kept separate to minimise conducted interference. The control circuit in the power supply acts with the microcomputer and its real-time

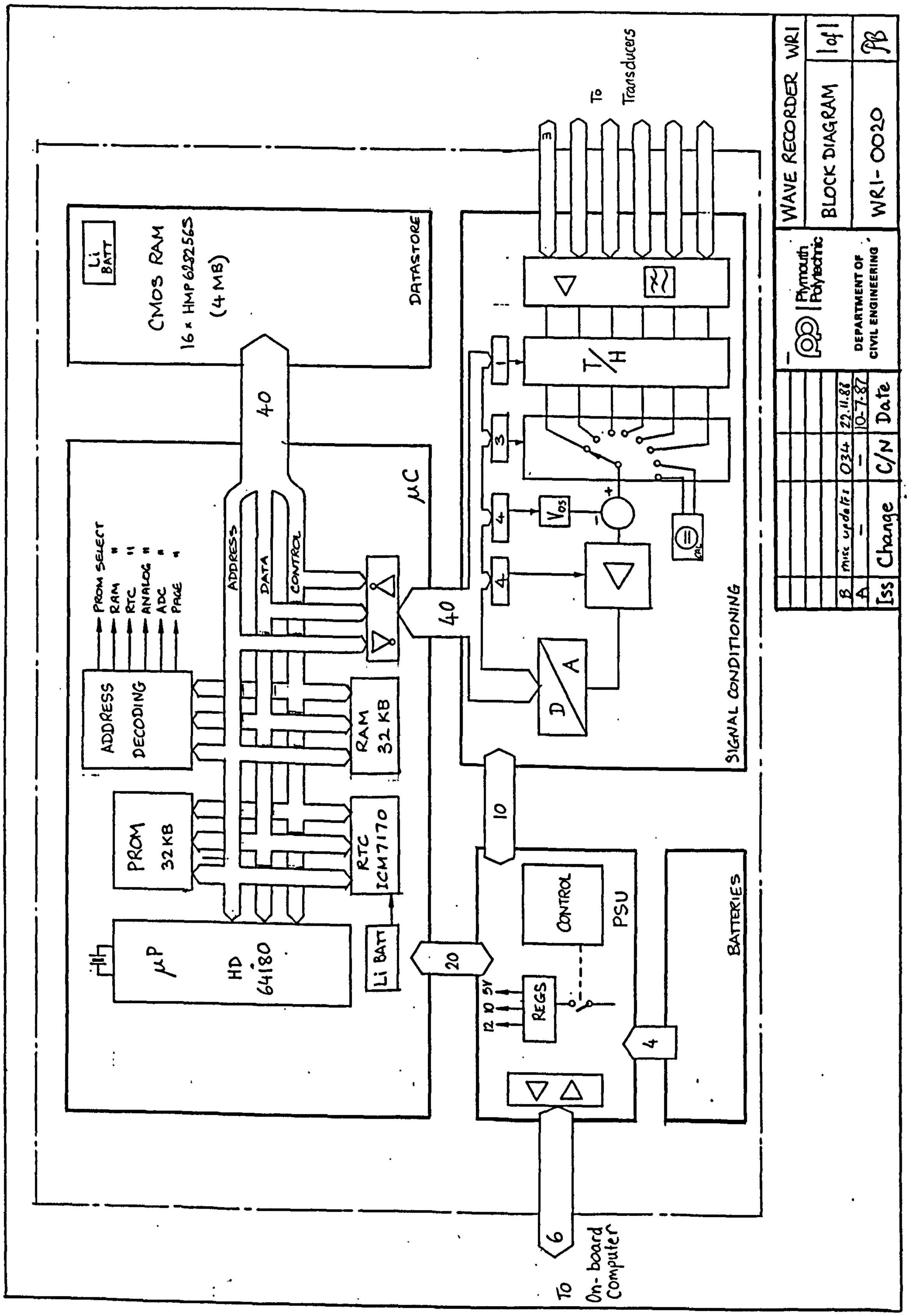

Figure 2.4 : Block diagram of wave recorder

clock (RTC) to shut down the instrument after a complete measurement cycle to save battery power, and to switch it back on again after a pre-set interval. Each circuit technique and component was scrutinised for its power demand. The battery power budget was severely limited by the required deployment period.

2.5.2 Pressure transducers

Pressure (after temperature) is one of the most commonly measured physical quantities in industry, so there is a large range of transducers on the market. This application, though demanding, did not require the design of a new transducer. However, a special housing to protect it from corrosion was needed.

Gauge rather than absolute pressure was required, as that is related to water height independently of atmospheric pressure. But to obtain gauge pressure, atmospheric pressure must be applied to the back of the sensing diaphragm. That could not be done as the pressure inside the sealed housing would not follow atmospheric, indeed it would be strongly related to temperature. 'Sealed gauge' sensors contain an inert gas at standard pressure, and incorporate electronic temperature compensation, but these also are unable to account for changes in atmospheric pressure. Absolute pressure reading sensors were therefore selected, envisaging that a correction would be made to each record from a barograph at the analysis stage. A range of 40 metres water-gauge (40mWG), approximately 4 bar, was specified to permit operation down to about 30 metres (allowing one bar for atmosphere). Fine resolution, with low hysteresis and dead-band errors, was essential to pick up millimetre changes in water head within such a large range.

The companies Druck, Schaevitz, RDP, ESI, Shape, Schlumberger and Transamerica all offered promising products. In the end (after a false start with a company now out of business) the PDCR 130 from Druck was chosen, costing about £330. This transducer (whose data sheet is reproduced

in Appendix D) is made of stainless steel which corrodes during long term immersion in sea water, so a housing was designed to incorporate an intermediate chamber filled with oil. The micro-machined silicon pressure sensor has strain gauges diffused into the surface: the 'integrated bridge' which is a speciality of the company. An amplifier within the body requires a DC supply of between 10 and 32 volts, and produces a signal of 0 to 5 volts proportional to pressure. An un-amplified millivolt-level strain gauge output on a long cable run would have been too susceptible to noise and interference but the 5V output was suitable for this application. (Later a cheaper, even higher specification, transducer became available from the same company with a 4-20 mA interface, and this was selected for the second system, built in 1992). Power consumption was quoted at 20 milliamps, but in practice most units took only 9 or 10mA. That was a crucial performance figure as the wave recorder's batteries had to supply six transducers. Non-linearity, hysteresis, and temperature related errors were all carefully examined to determine their effect on overall measurement accuracy (Section 2.5.3.7).

To calibrate the transducers a means of applying a known pressure had to be found. The adjustment screws provided for gain and offset of the internal amplifiers could then be trimmed, or alternatively the corrections applied at the data analysis stage. A 'dead-weight pressure tester' is conventionally used to generate accurately known pressures. Employing first principles, a piston of known mass and diameter presses down on oil in a matching cylinder. Surprisingly, although the principle is very simple, it was not easy to get it to work. Neither a laboratory demonstration rig nor a geotechnics pressure tester proved to be anything like accurate or repeatable enough, achieving typically +\- 3%. However, when finely engineered, as in the Budenberg company's deadweight tester, accuracy of better than 0.05% is obtained. The transducers were calibrated against one of these before each deployment. BS1780:1985 gives advice on the calibration of pressure gauges.

2.5.3 Signal Conditioning

2.5.3.1 Overview

This section of the instrument, shown at the bottom right of Figure 2.4, and in more detail in Figure 2.5, converts the useful information in the six analog signal inputs into a stream of binary numbers that can be read by the microprocessor. Initial conditioning is applied to each channel individually but most of the work is done by just one set of components, the six signals being connected one after the other under the control of the microprocessor.

Following the signal path on the diagram, the first function encountered is an active low pass filter which removes any 'high' frequency content (above about one hertz) that would, if present, be aliased down to the frequency range of interest. All channels are sampled (at typically 2 Hz) simultaneously by a track-and-hold circuit. Thus there is no appreciable delay between readings taken at the different seabed locations. During the 'hold' interval the multiplexer (rotary switch in the diagram) connects each channel in turn through for amplification and digitisation. The rectangular boxes shown in Figure 2.4 connected to the microprocessor bus are latches which hold binary data from the microprocessor (the number of bits is indicated in the box) thereby permitting it to control the associated analog function. The one-bit latch on the right sets track or hold mode, the next determines which channel is connected to the amplifiers, and the other two set the amplifiers' offset and gain.

Two extra positions of the multiplexer are shown on Figure 2.5. These are connected to accurately-set voltage levels to provide a calibration check on subsequent stages. This procedure is known as 'semi-automatic' calibration: the calibration source is applied automatically, but adjustment for any error is left until the data is interpreted.

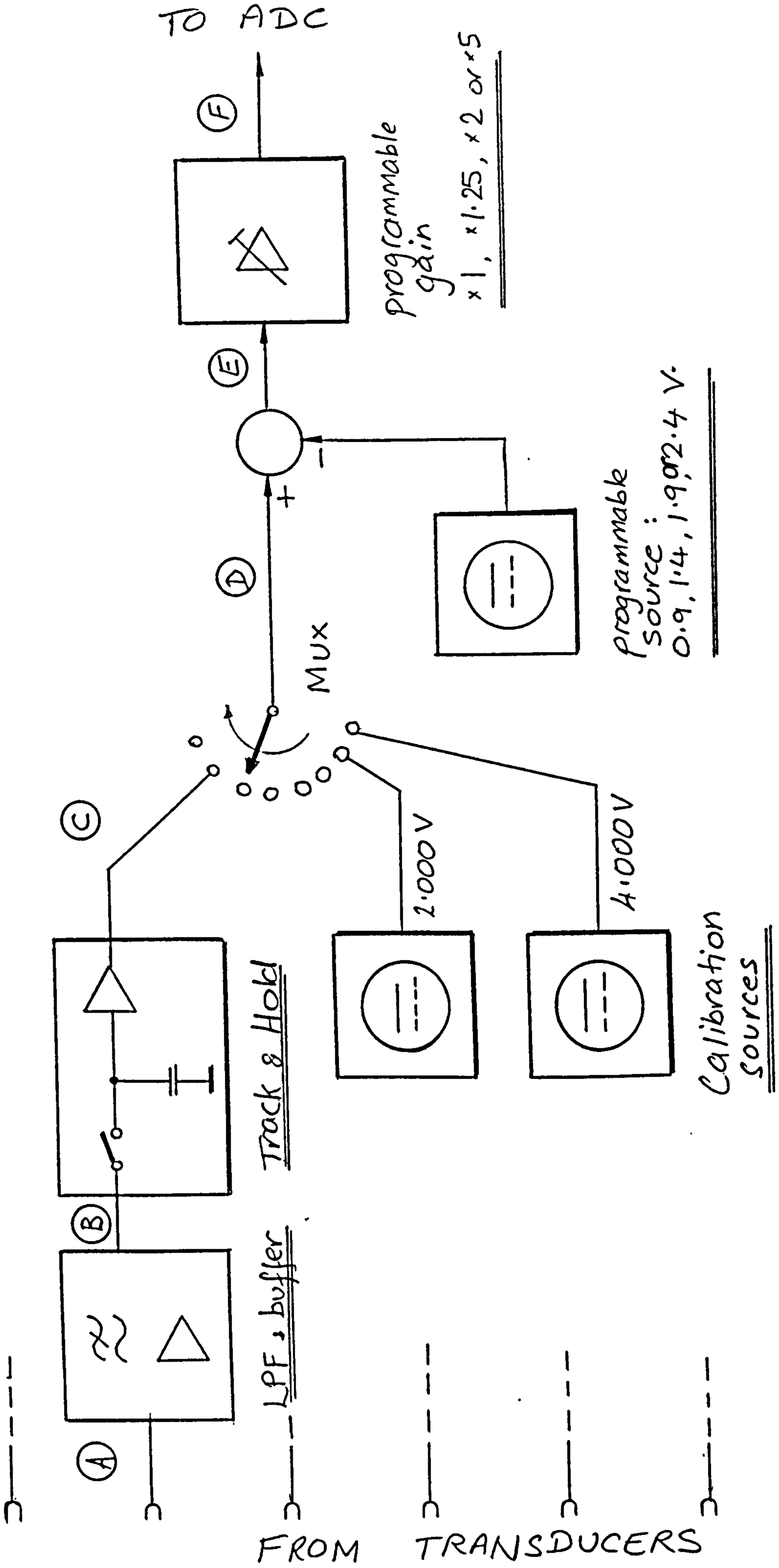

Figure 2.5 : Block diagram of the signal conditioning assembly

Power supplies are brought in from the microprocessor board: separate 5V lines for analog and digital sections, a 10V supply, and a 12-18V unregulated supply for onward connection to the transducers.

2.5.3.2 Input signal characteristics

Signal levels

The pressure transducers are supplied with amplifiers that produce an output in the range 0 to 5V corresponding to their full range of pressure: 0 to 4 bar (absolute). This voltage is 'single-ended', that is to say it is referred to the 0V power supply potential.

Waves cause an excursion of only a small proportion of that pressure range. Most of the signal represents atmospheric pressure and the head of pressure corresponding to still water level. Pressure changes at the sea bed due to the waves themselves are attenuated with depth (the effect is described in Chapter 4). As an example, a wave train of 5 seconds period and 0.5m height in a depth of 15m will cause 5 centimetres water gauge (cmWG), or 5mb, pressure variation. Peak to peak output will therefore be only 6.25mV on a standing level of 3.125V. The pressure attenuation of 10 in this example is the greatest envisaged in practice for this instrument.

Signal frequency band

Except for sheltered conditions the coastal engineer is concerned with wind waves whose periods are between approximately 3 and 30 seconds, together with long period oscillations due to harbour resonances, 'infra-gravity' waves and tides. Mean depth of water is also important so that the height of water on any neighbouring structure can be found and pressure attenuation with depth be predicted. The frequency band of signals of interest was therefore 0 to 0.33Hz. (The instrument was actually designed to be capable of much higher frequencies to permit measurement of other quantities at a later date).

Signal impedance

The pressure transducers' amplifiers ensured low output impedance which helped to reduce interference picked up on the cable. The input impedance of several kilohms of typical amplifier would not appreciably load such a signal.

Protection against abnormal inputs

Each channel has a network of resistors and diodes giving protection against input voltages up to +/-90 V. Fuses are fitted to all lines, selected to blow if the wave recorder is inadvertently switched on with the underwater connectors not mated. (In that condition currents flow through the sea water causing rapid damage to the electrodes and loss of battery charge.)

2.5.3.3 Input filters

When a continuous signal is sampled to obtain a representation in the form of a sequence of discrete values it is necessary to ensure that there are no signal components whose frequency is greater than half the sampling frequency. Any such components, whether from waves, turbulent flow or electrical noise, would appear in the data set at an altered frequency - the phenomenon of 'aliasing'. An analog low pass filter was provided for each channel to remove those components.

The filter had to pass signal components from 0 to 1Hz (since the sampling frequency was 2Hz) and stop any above 1Hz; this ideal characteristic is shown in Figure 2.6 . An acceptable, non-ideal but realisable, characteristic is also shown, and is defined by the corners - less than +/-0.02 dB attenuation up to 0.4 Hz, less than +/-0.1 dB up to 0.5 Hz, and greater than 40 dB at 1Hz and above. Phase response was also important since certain time domain analysis techniques were to be applied to the data. Phase lag increasing linearly with frequency was wanted as that is equivalent to a constant time delay for all frequencies, thus avoiding distortion of the time waveform. Again in practice some distortion is inevitable, so a target maximum difference between time delay at any two frequencies up to about

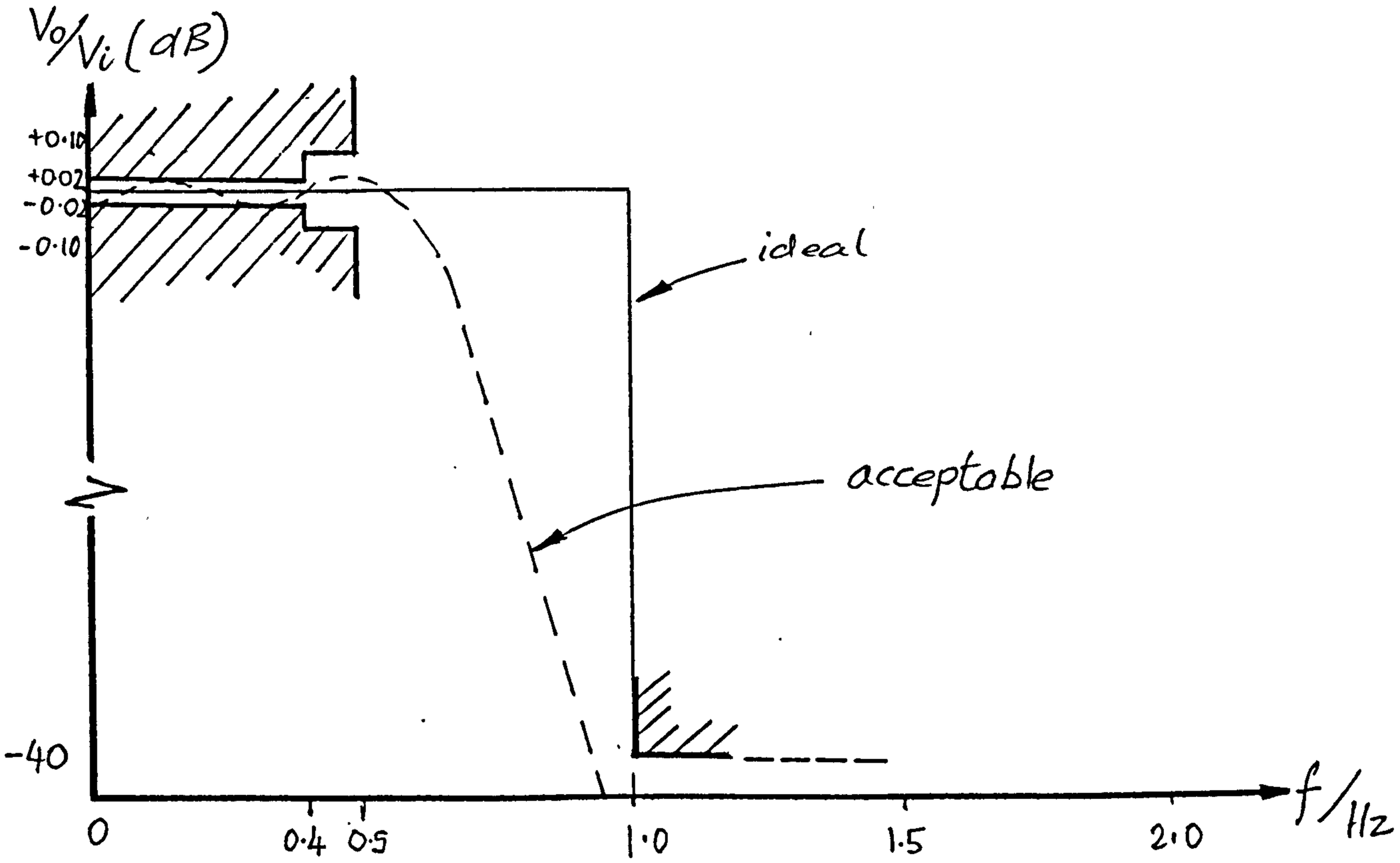

Figure 2.6 : Amplitude response specification for input filters

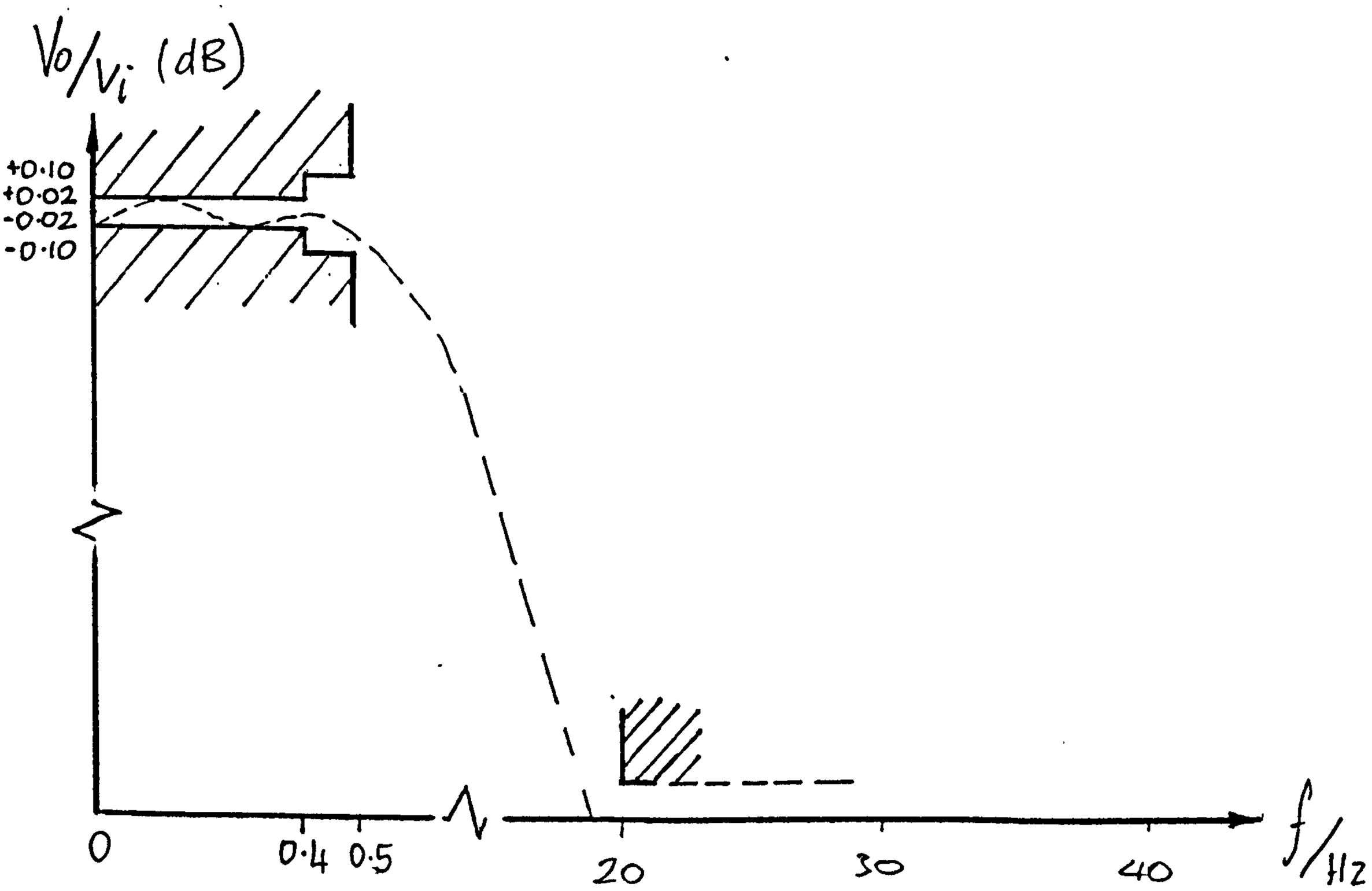

Figure 2.7 : Amplitude response of filter for use with digital decimation

the 20 dB point was set at 0.1s. That figure was considered sufficiently small compared to the time of travel between two locations in the array.

Unfortunately, it would have taken a 10th order Butterworth class or a 6th order Chebyshev class filter to achieve the amplitude response, and both would have distorted the waveform excessively. Also it had been hoped to use a second order filter, since six filters were needed in a small space. The solution was to increase the sampling rate to 40Hz, and thereby relax the specification on the analog filters. After digitisation, a digital decimation filter performed by the microprocessor would reduce the number of data points for storage back to two per second from each channel (Rabiner and Crochiere 1975, and Rabiner 1977). This new specification is shown in Figure 2.7. (At the time of writing the digital decimation filter remains to be implemented.)

This was achievable by a 2-pole Butterworth filter, implemented by a voltage-controlled, voltage source type active circuit that required little PCB area (one operational amplifier, two resistors and two capacitors) and having no undue sensitivity to component tolerances or op-amp performance. Before construction the circuit was simulated using Mentor Graphics' MSPICE software on an Apollo Domain workstation to verify the calculations. A benefit of computer aided design is the ease with which the effect of component tolerances can be evaluated. Contrary to expectations a 5% tolerance on capacitor value appeared to be permissible; these were far cheaper than the 1% capacitors initially thought necessary.

Board space was further economised by using a quad op-amp: the LT1014 from Linear Technology Corporation which offers reasonably good input offset voltage and bias currents at low power from a single supply.

When tested, the prototype circuit was only just inside the specification. However, on inspection the capacitors were found to be on the high limit; allowing for that the computer simulations were almost identical to physical

performance. Phase response was fairly linear at -45deg/Hz, giving an almost constant group delay of 0.125s.

2.5.3.4 Signal sampling and selection

Each of the six filtered and buffered input signals is next fed to a track and hold circuit, shown functionally in Figure 2.5 . The switches are normally closed so that the signals at C follow those at B. On receipt of a signal from the microprocessor the six switches open and points C hold their levels irrespective of changes at the inputs. Subsequent stages then digitise each channel in turn. Thus all channels are sampled at effectively the same instant. The two calibration sources are constant and so do not need track and hold circuits.

Component selection is critical. The capacitor is a polypropylene metal-foil type, chosen for low dielectric absorption. The switches are CMOS integrated circuits for small size and easy digital control with low current consumption. Low power relays were considered but even the latest ones need rather too much coil current. Latching types are more difficult to interface, and in any case would take up too much board area. Another alternative, JFET switches, require power supply potentials outside the signal range. Using CMOS and quad op-amps, all track and hold circuits are realised by four IC's and associated passive components. Additional resistors and schottky diodes prevent charge stored in the capacitors damaging the switch and amplifier inputs.

2.5.3.5 Amplifiers

The 'Input signal characteristics' section above illustrates with an example how the wave signal is dominated by a large standing value. Figure 2.5 shows the circuits that remove the standing value and amplify the remainder to the full range of the analog-to-digital converter (ADC). Four monolithic integrated circuits using switched capacitor and chopper stabilising techniques implement this function, along with precision (0.1%) resistors.

Extra components protect IC inputs and outputs from charge stored on the capacitors during power down. The four offset and gain settings together provide many combinations to suit prevailing wave conditions. The microprocessor controls the settings via the latches that can be seen in Figure 2.4 .

The effects of different settings in systems like this one are best shown on signal level diagrams which trace the signals right through the system, in this case from pressure to ADC input. Figures 2.8 (a) and (b) give examples at minimum and maximum gain. In (a) it can be seen that the full range ADC input is traversed by a pressure change of 0.9 to 4.9 bar. On maximum gain Figure 2.8 (b) indicates that a span of only 1 bar corresponds to full ADC range, for example 0.9 to 1.9 bar, or 1.4 to 2.4 bar etc, depending on the offset value. A 50% overlap in ranges enables the microprocessor to select a high gain range in which the signal is almost centrally placed.

2.5.3.6 Analog to digital conversion

Analog signal conditioning is complete at the output of the amplifier described above; the signal is then ready for conversion into digital form. The most important specification here is the resolution. Eight, ten and twelve bit converters were commonly available in monolithic integrated circuit form. The 12-bit successive-approximation type AD1205 from National Semiconductor was selected for high resolution with low power consumption and a microprocessor compatible interface (Electronic Design, 1984).

A test box was made to take the place of the microcomputer board during development. Switches enabled the user to set the digital control lines, and alpha-numeric displays showed the ADC output in hexadecimal form. A second specially made test box generated accurate dc levels to simulate transducer signals.

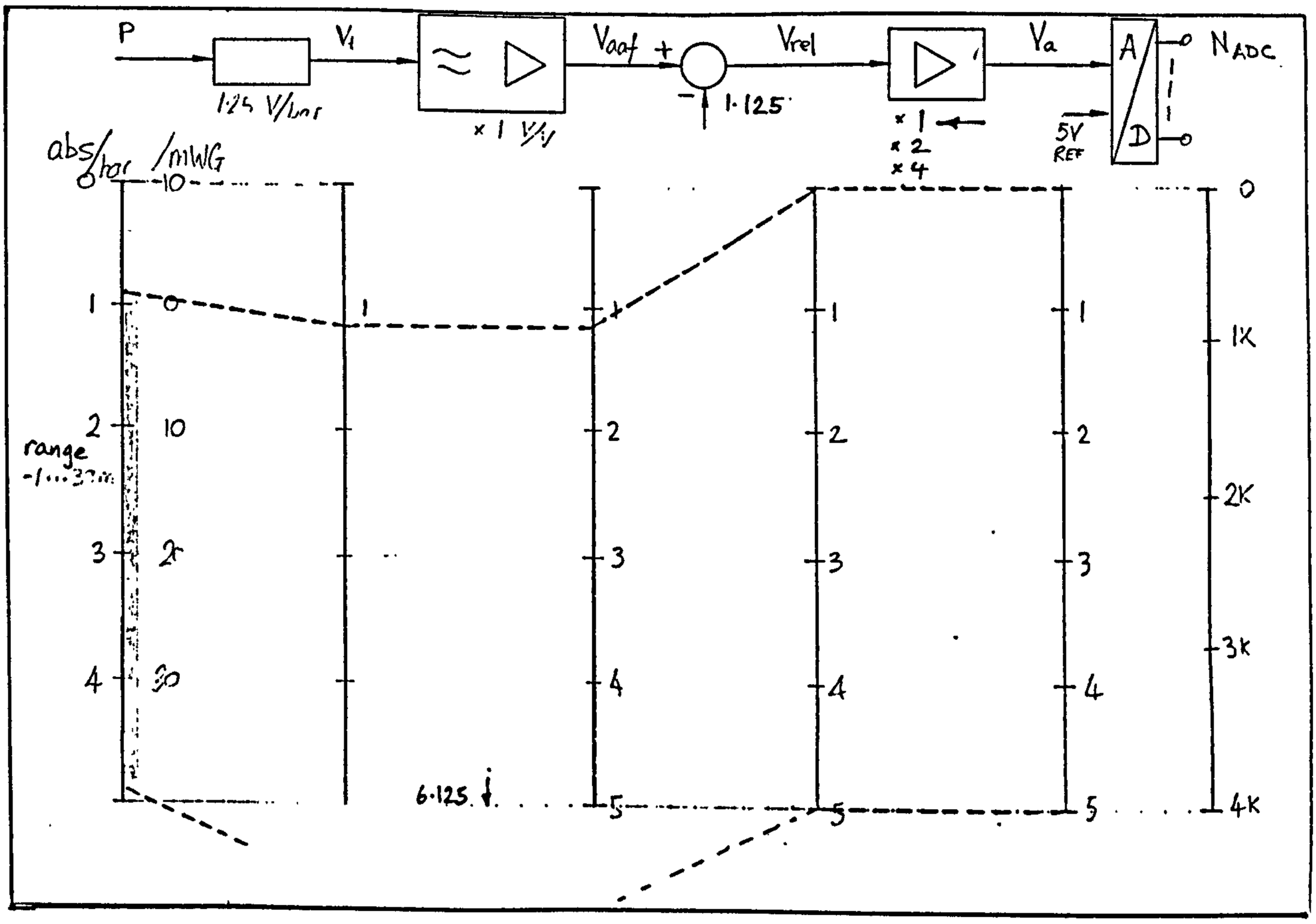

a) minimum gain

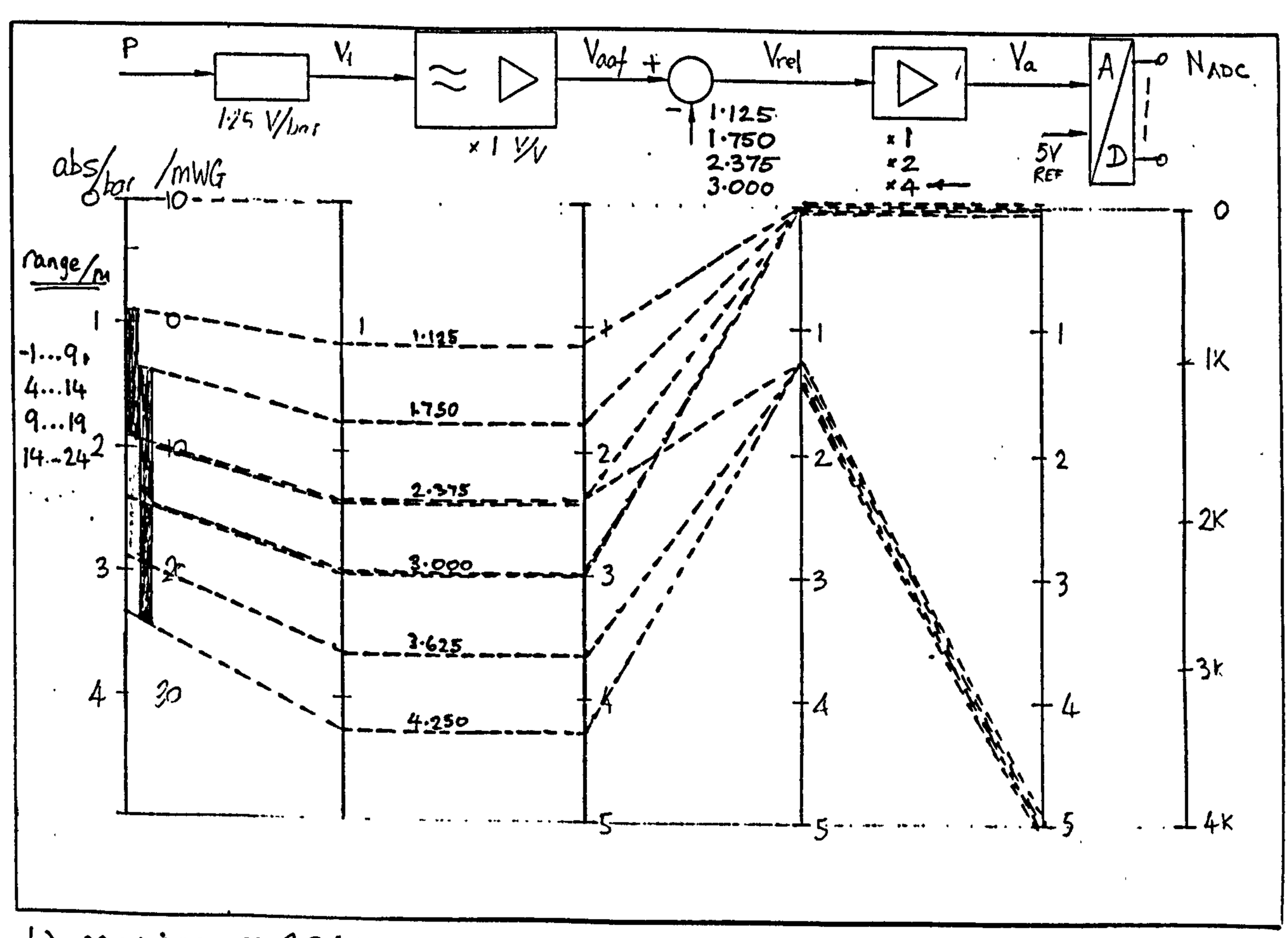

b) maximum gain

Figure 2.8 : Signal level diagrams

Resolution

A 12 bit ADC resolves its full input range into 2^{12}, or 4096, steps. The 5 volt range in this circuit is therefore divided into 1.2 mV intervals. The level diagrams show that that interval is equivalent to about 1 mb on a gain setting of unity, and 0.2 mb at a gain of 5. In terms of still water depth these figures correspond to 10 mm and 2 mm respectively. However, allowing for a worst case attenuation factor of 10 between hydrostatic and actual sea-bed pressure excursions makes the effective resolutions in wave height 100 mm and 20 mm. Referring to the overall instrument specification (Section 2.2.2) it can be seen that the 5 mm resolution of wave height will not be met at this extreme value of attenuation, although in most cases there will be plenty in hand. This shortcoming in performance was considered relatively minor. Greater amplifier gain would have improved resolution, but at the risk of full wave excursion going out of range, and an impaired signal (ie wave) to noise ratio.

2.5.3.7 Measurement errors

As stated in Sections 2.2.2.1 and 2.5.3.6 high accuracy was a prime requirement. Once the signal is turned into digital form it can be assumed that, barring malfunctions, no further errors will be introduced, provided that ADC resolution is adequate. It is therefore the analog sections, transducers to ADC in Figure 2.4, that require the most careful design for accuracy. An 'error budget' was deduced from the specifications and became, together with power consumption and circuit board space, one of the main determinants of the signal conditioning design.

After all the components had been selected and the circuits designed to conform to their own allowance in the budget, an error analysis was carried out to ensure that the whole system was within limits. Types of error in such a system are many and various, and exist in all parts of the analog section: imperfections in transducer sensitivity and offset, resistive voltage drop in the long marine cables, offsets and bias currents in the amplifiers, resistor tolerances and dynamic errors in the switching circuits, and in the

analog part of the ADC. Moreover, the magnitudes of many of these errors are functions of environmental parameters such as temperature and power supply voltage. The impact of each error source on the data obtained depends on whether it applies to the varying (wave induced) or standing (mean depth) part of the signal.

To calculate overall error, each part of the analog section was modelled as a functional block, multiplying its input by a factor and adding a fixed 'offset'. Thus the factor for a transducer is its sensitivity, and for an amplifier, its gain. The offset produced by a transducer should be zero, and that produced by the offset amplifier: exactly its design value. These functional blocks are cascaded together and the overall error calculated. This is most conveniently done by referring all errors to the input: pressure. The treatment of errors, and the statistical basis for combining them, are set out in Appendix E.

In the literature authors tend to differ somewhat on the classification of error types, and the terminology used to describe them. Sydenham (1982) takes as the broadest classification 'systematic' and 'random' errors. The former (alternatively called 'deterministic') are known and may be allowed for by calibration. Choosing the nearest available resistor value to the exact one required will give an error of that sort. Random errors change from reading to reading, and are due to fundamental imperfections such as noise, dead-band and hysteresis effects; these cannot be calibrated out. However, limits to these are normally known, either as an absolute maximum discrepancy, or as the standard deviation of a statistical distribution. Errors that depend on some environmental parameter (eg resistor temperature coefficient) are termed 'parametric errors', and may fall into either one of the two main categories.

The question of how to treat the common tolerances in component value is not obvious. At the design stage these are not known, so the resulting errors are 'random'. However, once the circuit is made from individual components it can be calibrated, and the now 'systematic' errors removed by

adjustment or later correction of the data. In the present case, calibration was used extensively at circuit and sub-system levels as well as on the overall instrument. It is not, though, possible to calibrate out all tolerance errors due to the many different signal paths: six channels share the same amplifiers, and the amplifiers themselves have sixteen different gain and offset combinations. Moreover, in-circuit adjustments can be fiddly to set and often drift over time. The circuits, therefore, were designed to be inherently accurate enough to meet the specification without adjustments.

Appendix F contains an example of an error calculation worked through for the case of 2 bar mean pressure (approximately atmospheric pressure plus 10m depth) with 0.01 bar peak-to-peak fluctuation (equivalent to an un-attenuated wave height of 10cm, or in the worst case to 1m wave height attenuated by a factor of 10). The result is an error in mean depth of +2.0/-0.5% of reading, and in wave height of 1.0 / -0.7 % of reading, all based on maximum error values. If individual errors were to take their typical as opposed to their maximum values the total errors would fall to about one-third to one-half of the maximum. Calibration further reduces the figures. The dominant error was the ADC span error (+/- 0.73%). This could in future be adjusted out, though no such provision was made on the present unit. Removing this source would leave +0.6/-0.3% error in wave height.

2.5.4 Data Storage

2.5.4.1 Data storage capacity

Initial calculations indicated that a suitable coding scheme would enable each reading (full size of 12 bits) to be represented by one byte in memory. At four megabytes (Section 2.2.2.5) the capacity envisaged was much larger than that fitted into commercially available instrumentation of the type. Moreover, due to the specification of battery life the data store had to consume little current during read and write operations, and very little or none when just retaining data. In fact the requirements of size and consumption work against each other: if more capacity is available then data can be collected over a longer period, so that one would want a large data store to consume less power than a small one. The store had to be re-usable without special out-of-circuit erasing procedures; it had to be compact enough to fit inside the pressure housing; and although likely to be one of the most expensive parts of the system, should not take the total cost over budget. Fortunately there was one feature not pressed to the limit: reading and writing speed, which could be quite low by current standards.

2.5.4.2 Choice of storage type

One of the fundamental aspects of the design was the choice of a storage medium for the wave data. The ideal data storage device can be imagined as having enormous capacity in a small physical size; and as being non-volatile, convenient to interface (easy reading and writing of data), fast, requiring no current, reliable over extremes of environment, and cheap.

The technologies available were (eg Duthie 1984):-

a) magnetic tape and disc

b) magnetic bubble memory

c) semiconductor memory.

Most instrumentation for underwater work that was available at the commencement of the project used cassette tape. A typical wave recorder, the DNW-5 from NBA Controls Ltd, used a cassette tape, which, with an industry standard format, stored about 400 kilobytes (one-tenth the capacity required here) and had a fairly high power consumption. Research was in hand to increase the capacity of standard digital cassette tape by a factor of ten (Donnelly *et al* 1987) but such systems were not at the time fully developed. Magnetic disc storage was another possibility, but the drives were too bulky and drew too much current.

Magnetic bubble memory (Jalbert *et al* 1983, Garcia and Pokoski 1981, and Jones 1986) was initially favoured. It was small for the required capacity, and research promised further improvements. It needed no power to retain data, and was finding applications in many areas such as portable electricity-billing machines, telephone exchanges, and communications satellites. However, on further investigation and after comparison with the fast developing field of semiconductor memory its disadvantages of relatively complex interfacing circuitry and high current consumption during read and write operations led to the selection of semiconductor memory.

There are many types of semiconductor memory, and the number increases as manufacturers seek the ideal memory device for the enormously valuable memory market (eg Sommers 1985). They include the non-volatile, cheap read-only memory (ROM), and the random-access memory (RAM) to which data can be written but is lost as soon as power is removed. There is a spectrum of types in between: new ROM technologies acquiring the functionality of RAM but without the disadvantage of volatility. A summary of features and performance of several memory types is given in Appendix G.

It was apparent at an early stage that the specification could be met with at least one of these storage media, so detailed design of the other sections could go ahead first. The decision on which type to use was deferred until

other sections had been designed, previous experience in the industry having indicated that significant improvements in performance and cost would be likely over the period.

Electrically programmable ROM (EPROM) is normally programmed in a special unit, but it would have been possible to design the recorder to program the memory with data in circuit. However programming is not quite the same as writing data - normally programming requires 'empty' memory locations whereas the writing of data does not. The question then is whether the memory can be erased in circuit. The electrically erasable and programmable ROM (EEPROM) does offer that feature, but at a high cost and only moderate density.

In the end battery-backed static random access memory, in the low power consuming complementary metal oxide semiconductor (CMOS) technology was chosen for its high density at reasonable cost. The dynamic RAM used in most mains powered computers has even more capacity (and is much cheaper) due to its configuration of one transistor per cell (ie per bit) compared to the static version's six. However the accompanying refresh circuits need far too much power. The memory was bought in in the form of single-in-line packages of 1/4 megabyte each, manufactured from industry standard integrated circuits.

The pace of development in this field is so fast that such judgements become dated fairly rapidly. In particular Flash EEPROMS may soon provide a better solution, or even the miniature hard disc drives now becoming available.

2.5.4.3 Implementation

The sixteen single-in-line modules (SIMMs) of RAM with decoding circuits, buffers and backup battery take up one of the four printed circuit boards (Plate 3). (Each SIMM is referred to in this account as a 'rampack'.)

Functionally it forms an extension of the microcomputer assembly and is connected to it by a ribbon cable (Figure 2.4).

Power supply

Power for the RAM is taken either from the wave recorder main battery (via the microcomputer) or, when that is disconnected during power-down mode, from an on-board lithium cell (Small 1986). A control circuit monitors these two supplies, together with two signal lines from the microprocessor: 'data store connect' and 'reset'. When communication to the RAM is not required the control circuit generates a signal causing buffers to isolate all the RAM lines. Time delays are included to assure stability of the microprocessor before allowing it to connect to the RAM. The memory ICs are in CMOS technology, as are all buffers and decoders, resulting in a low total current drain in standby mode.

Address decoding

The eighteen address lines of each rampack are connected together in a bus which is driven by the microprocessor via tri-state buffers. The microprocessor selects one of the sixteen rampacks by writing four data bits into a latched decoder. The decoder outputs are gated with a microprocessor control line : 'data store select'.

This and the safeguards mentioned above ensure that access to the data is only possible if the wave recorder supply is up and stable, and the microprocessor is not reset, and it has signalled 'data store connect' and 'data store select'.

Data bus

Like the address lines, the eight data lines of each rampack are connected together in a bus, interfacing with the microcomputer data bus via three-state transceivers. The rampacks' inputs together present a fairly substantial electrical load to the transceivers, which are in high speed CMOS technology. With the various line driving circuits all connected to the same bi-directional bus the condition of two circuits trying to drive the

same line simultaneously must not be permitted, otherwise data errors or damage could result.

Bus timing

Considerable care was taken to avoid such bus contention problems, and to satisfy the timing requirements of each component. Timing analysis can be quite intricate and generate reams of calculations covering all foreseeable conditions. The read, write, power-up and power-down processes are broken down into their basic sequences (eg: bus release by transceiver, output enable signal asserted, data bus driven by RAM). There are eleven such sequences in the data read process alone, and each of these sequences is the result of the actions of several preceding circuits. Each process was checked using the figures for propagation delay, set-up time, hold time and so on quoted for the devices at various temperatures and loadings. Where such analysis revealed any violations of specification then either the microprocessor was programmed to allow 'wait states', or the circuit design changed.

2.5.5 Microcomputer Assembly

It was clear from the specification that the wave recorder would need microcomputer control to achieve the required functions and give the user the ability to change settings. The tasks of such a control section include scheduling transducer readings, controlling the analog circuits and the real-time clock, reading and writing data to the data store assembly, managing communication to the user's personal computer, and carrying out simple data processing. Microcomputer hardware and software naturally work together to achieve these tasks, and designs of the two proceeded together. Overall program functions were specified first, then a suitable hardware 'platform' on which to run the software was sketched out. The detailed, low level, program modules could only be written after drawing the microcomputer circuits. The controlling program is described in Section 2.5.8 . The assembly occupies one printed-circuit board, and

incorporates a real-time clock (RTC) chip, backed up by its own lithium cell. Figure 2.4 shows how the microprocessor fits into the system.

2.5.5.1 Microprocessor selection

There are a number of approaches to the provision of microcomputer control for a data acquisition system. They can be characterised by the amount of design work that remains to be done to adapt the purchased components to the specific application. The spectrum ranges from the general purpose computer (eg the PC) which is readily adapted to many different tasks, through the proprietary single board computer (SBC), to the purpose designed PCB fitted with a microcontroller or microprocessor integrated circuit. The parts cost of the options tend to descend in the order listed, but as this was a low-volume product that consideration was not as important as development time. This increases from the general purpose computer to the specific microprocessor I.C. based design. The microprocessor and microcontroller routes involve considerable design work in selecting components, designing the logic and laying out the PCB, work that is largely done by the manufacturers of the single-board computer and general purpose computer. In addition, program development requires certain software 'tools' (assembler and/or compiler, simulator) which are often incorporated into the SBC.

Thus there were strong reasons for purchasing a SBC for this application, but unfortunately no proprietary product was available of the right size and shape to fit the housing, or with sufficiently low power consumption (*Electronic Engineering* 1985). So it was decided to design a dedicated assembly using a microprocessor integrated circuit. The HD64180 microprocessor (*Electronic Design* 1985, *EDN* 1987, Hitachi 1987) from Hitachi was selected: a development of the well known Z80, but with a serial port, timers and memory management facilities all integrated on chip. Extra instructions were included, such as multiplication, and the part was available in low-power CMOS versions, and was able to operate at reasonably high speed.

2.5.5.2 Address mapping

The 64180's 'address space' - the range of numbers that can appear in coded form on the address bus - in common with most microprocessors may be used for two purposes: for addressing memory, and for addressing input/output (I/O) devices. The microprocessor's 'memory enable' and 'I/O enable' outputs determine which type of device responds to the address. Two decoder integrated circuits on the PCB decode memory and I/O addresses. The connections to these decoders determine the allocation of addresses to devices; boundaries between device addresses are chosen to be round numbers to keep the connections simple.

The microprocessor's memory, which may be called 'system memory' to distinguish it from the data store assembly, consists of 32 kilobytes (KB) of electrically programmable read-only memory (EPROM) to hold the program, and 32 KB of random access memory (RAM) for data and working area. As always, low power consumption in standby mode is essential whilst retaining reasonable speed of operation; CMOS technology chips were used.

The 64180 (in the version chosen) has nineteen address lines, enabling it to address 512 K locations: the 'physical address space'. Machine instructions can only address 64 K locations: the 'logical address space'. Conversion between the two is done by the microprocessor's on-chip memory management unit (MMU).

Figure 2.9 shows a map of the memory address space. In normal operation pressure readings are written to the system RAM one by one as they are taken. Both the RAM and ROM are mapped by the MMU into the first 64 K of address space. At the end of a measuring period (say 17 minutes), before the wave recorder powers down, the MMU registers are changed and the resulting block of data is transferred to the next free section of one of the rampacks.

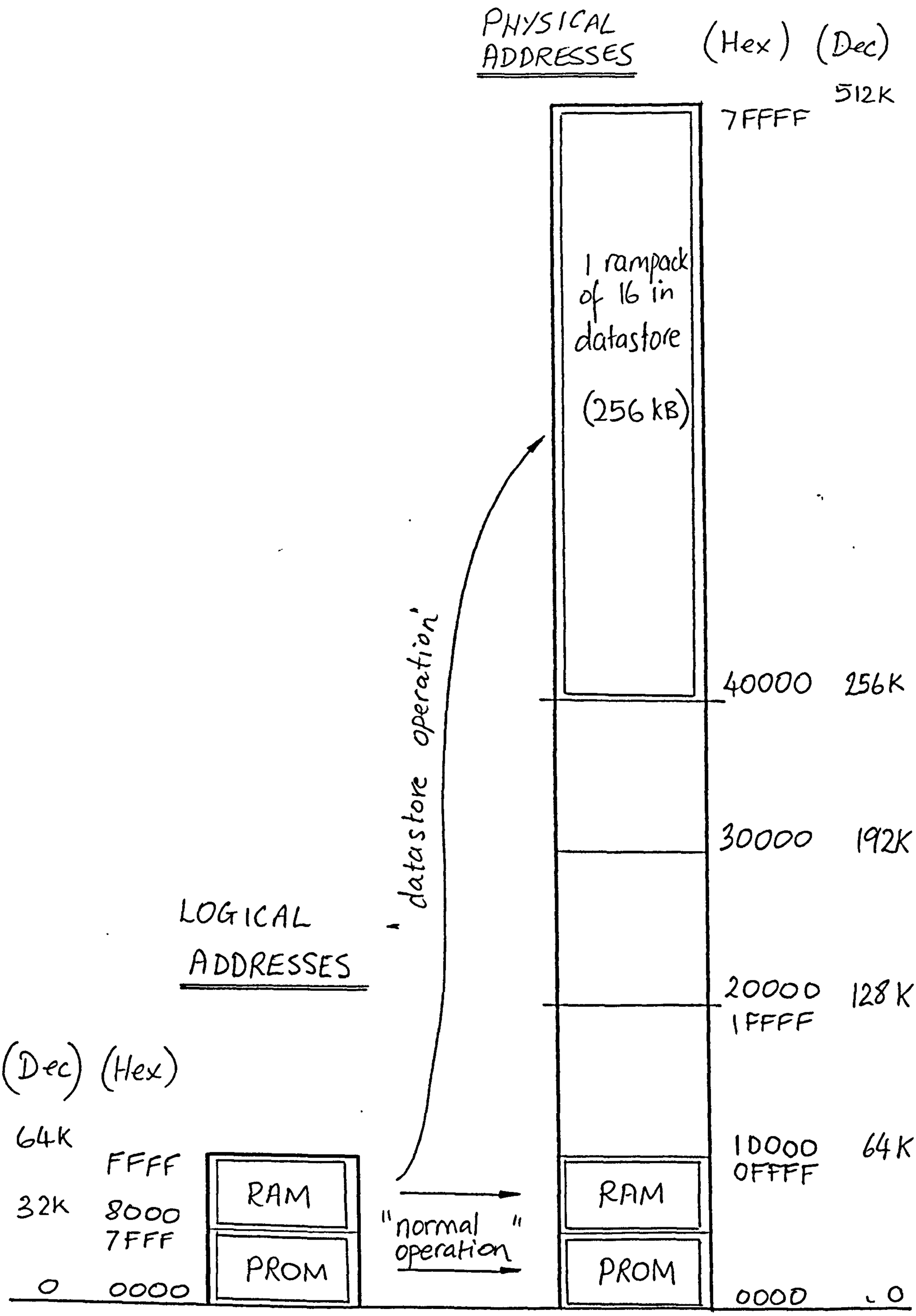

Figure 2.9 : Memory address map

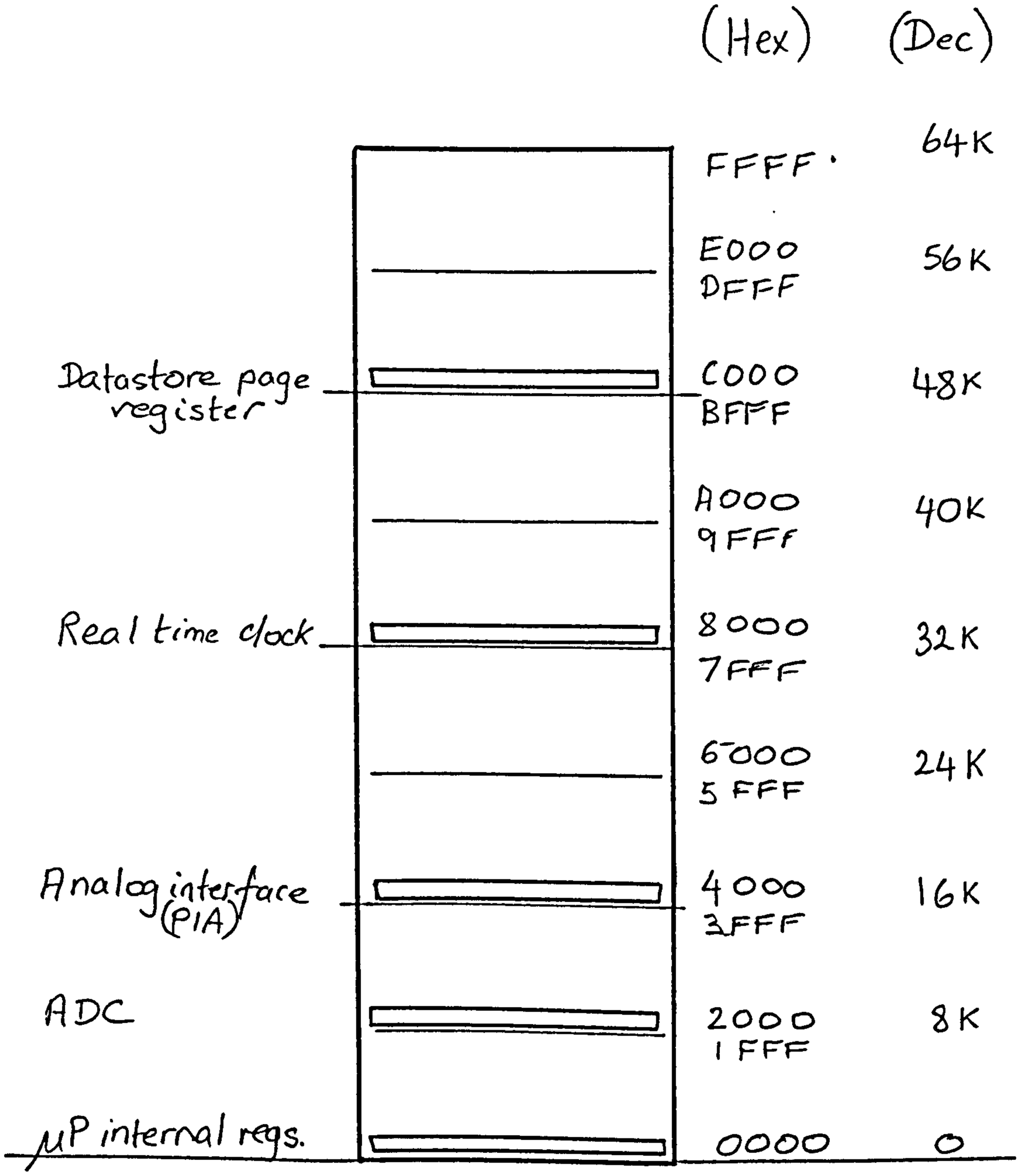

Figure 2.10 : I/O address map

Figure 2.10 shows a map of the input/output address space. The device addresses are distributed on an 8 K grid for simple decoding. Their functions are explained in more detail below. Figure 2.4 gives the overall arrangement.

2.5.5.3 Datastore interface

The 64180's ability to address 1/2 MB of memory rather than the 64 KB more usual for its type is an advantage, but is still not enough for the 4 MB in this application. Further memory management had to be implemented to select one of the sixteen 1/4 MB rampacks to appear in the top half of the

microprocessor's physical address space (Figure 2.9). This is done by providing a register on the data store board as an I/O device to which the microprocessor can write a byte specifying the active rampack. In addition, a number of control signals is required by the data store: read, write, chip select and page select. These are generated on the microcomputer board and connected across to isolating buffers on the data store assembly along with the address and data buses.

2.5.5.4 Analog interface

The microprocessor is required to control the track/hold circuit, multiplexer, programmable gain amplifier, and analog to digital converter (ADC) on the signal conditioning board, as well as to read the ADC's data. The latter has a microprocessor-compatible interface so the 64180 data bus is taken across to the signal conditioning board for direct connection. Control lines for the other circuits, though, are provided by a peripheral interface adaptor (PIA) - a proprietary IC which contains the latched, bi-directional registers needed to interface a microprocessor to typical peripheral circuits. Fourteen of the sixteen PIA outputs are used to control those circuits, one is used as a control line to connect data store to microprocessor buses, and the remaining output carries the 'power down' command signal to the power supply assembly. Level shifters convert between the 5 volt microprocessor supply to the 10 volt analog supply.

Since the data bus was to be connected to the signal conditioning board it would have been possible to put the PIA (or discrete latches) also on the signal conditioning assembly. The pros and cons of each arrangement were quite finely balanced; as in many other decisions of this sort the effect of each option is evaluated on board space, functional simplicity, connector requirements, signal interference, signal loading, current consumption and development time.

A clock signal is required by the ADC. This is derived from the microprocessor system clock and connected across to the signal

conditioning board. Three flip-flops and a selector switch give the choice of a number of divide ratios so the ADC clock can be kept within limits over a wide range of system clock speed. The system clock speed was 6 MHz in development, but could be raised to a 12 MHz maximum for the integrated circuits selected.

2.5.5.5 Real-time clock

The real-time clock (RTC) performs two functions. It provides the microprocessor with the current date and time so that measured data can be stored time and date stamped. It also acts as an alarm clock when the recorder is powered down, sending a 'wake up' signal to the power supply at the start time of the next measurement cycle. It is therefore equipped with its own lithium cell so that when the wave recorder is switched off the RTC remains active, though in a very low power standby mode.

The real-time clock is connected to the address and data buses, and is treated as a set of I/O registers by the microprocessor. It has a small 32 kHz watch crystal attached. This gives limited accuracy of time keeping, but errors may be calibrated out during the data decoding process.

The Intersil ICM7170 was selected from a number of RTC chips for microprocessor bus interfacing (Liebson 1986, Kahn and Alexander 1987, Peek 1986). Its advantages include the ability to switch over automatically from system power to backup power, and the provision of an 'alarm' signal. The details of this circuit required particularly careful consideration: track layout of the oscillator section was critical, the alarm signal requires level translation from negative voltages, and it was found that not all types of lithium cell had acceptable terminal voltages. (More information on the power supply switching arrangements is given in the 'Power supply control' section below.)

2.5.5.6 Signal timing and loading

Once the major chips had been selected and the intervening logic and signal connections designed, it was necessary to check that all the timing requirements were met. The procedure is similar to that described in Section 2.5.4.3 for the data store, but applied to the ROM, RAM, RTC, PIA, ADC and power supply control circuits.

2.5.6 Power Supply

The power supply section consists of a printed circuit board assembly and battery pack (Figure 2.4). Its function is to provide electrical power for the six remote transducers and the analog and digital circuitry within the wave recorder.

The user (via the data link), the microprocessor and the real-time clock are all able to initiate switching power on and off. In addition, battery condition detector circuits make the power supply switch off before low voltage levels can cause unreliable operation. A control section is therefore incorporated within the power supply to handle these commands in an ordered and reliable manner.

2.5.6.1 Batteries

A pack of twenty-eight D size alkaline-manganese cells provide the wave recorder's electrical power requirements for approximately four months. That number of cells can be neatly arranged into a cylinder of four banks of seven cells. It fills half the space inside the recorder (Plate 2). The cell terminals are wired to form series and parallel combinations with outputs of 20 amp-hour capacity at 10 to 18 volts, and 10 amp-hours at 6 to 9 volts.

Primary cells were chosen as they have much greater capacity than secondary (rechargeable) types. Also, recharging from a boat was not practical as it would take several hours. Volumetric energy densities and

discharge curves for several battery couples were considered, the former to achieve maximum capacity in the available space (weight was not important), and the latter to maximise use of that capacity. A steep discharge curve (the plot of terminal voltage against time as current is drawn) is undesirable because a linear regulator drops the difference between terminal voltage and regulated voltage across a power-dissipating element. Switched-mode regulators make use of this energy, but they are more complex and generate electrical noise and so need careful shielding.

The alkaline - manganese dioxide couple was selected for its good performance and low cost. The other contender was lithium thionyl chloride, and it would be possible to specify that type in the future. That type would provide three times the charge capacity, but at four times the price.

2.5.6.2 Regulators

Figure 2.11 shows the four supplies provided: 12V (nominal) for the transducers, 10V and 5V for the analog circuits, and a 5V line for the digital circuits (separated from the analog to avoid interference). Distribution is carefully organised to minimise interference arising from currents sharing non-zero impedance paths. The transducers have their own built-in regulators, and can accept a supply anywhere in the range 10 to 32 volts. Hence only a switch, consisting of a power MOSFET, appears between battery and transducer supply line. This component has a low 'on' resistance and does not draw the coil energising current a relay would require. The 10 volt supply to the analog circuits is derived from this switched line by a low-dropout integrated-circuit regulator. The 5 volt output, led separately to the analog and digital sections, is regulated by a MOSFET operating as a linear pass element which can supply more current than the IC alternative. This 'cascade' arrangement, in which a regulator depends on the one before, has the advantage that only one control line is needed. Operating that line initiates a 'domino effect', switching all supplies on and off together.

PROJECT	made	Plymouth Polytechnic	DEPARTMENT OF CIVIL ENGINEERING		
WAVE RECORDER WR-1	PB				
SECTION	**date**	**JOB NO.**	**SHEET NO.**	**rev.**	
SYSTEM POWER DISTRIBUTION	10.6.93	WR1-0026	1/1	B	

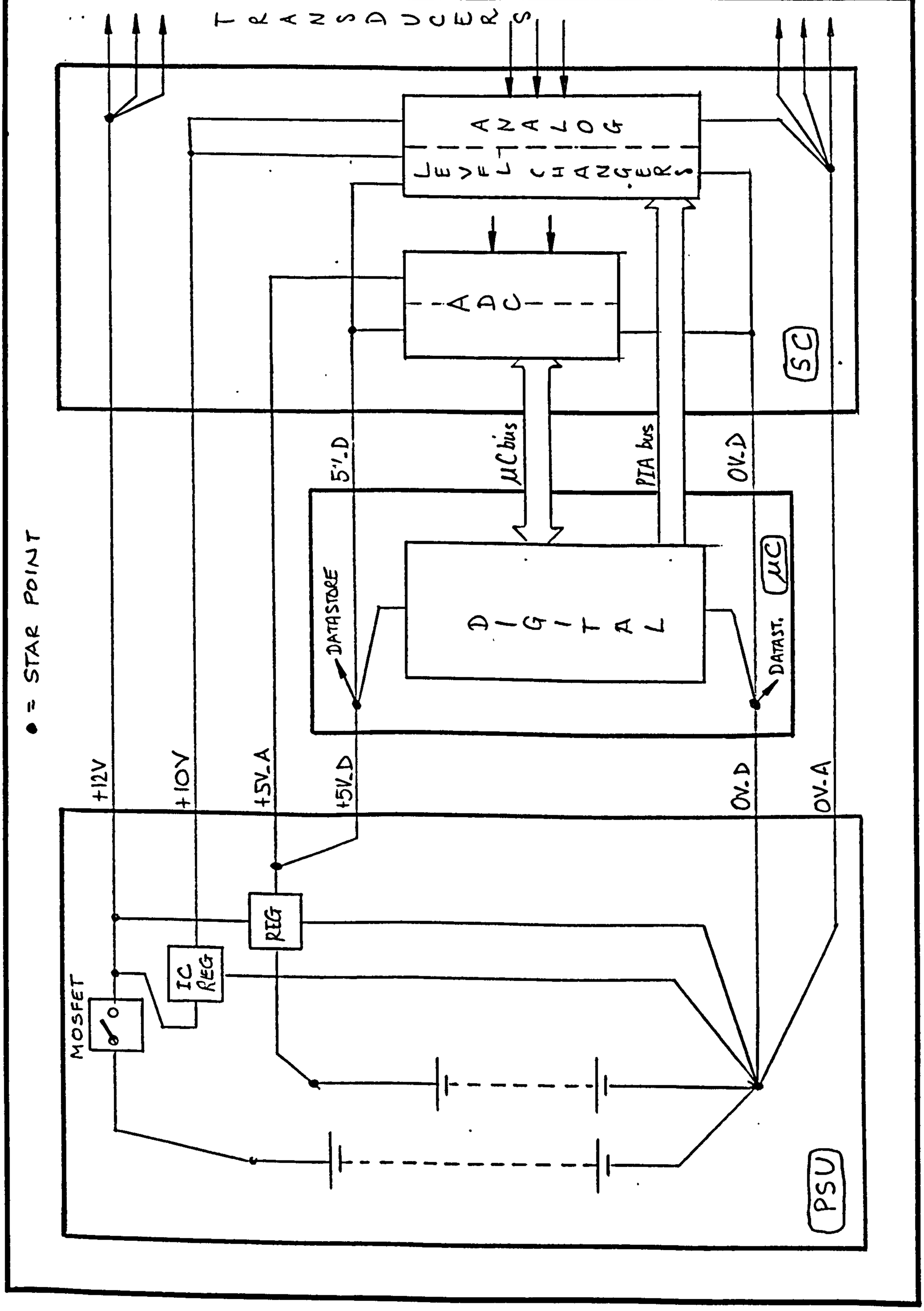

Figure 2.11 : System power distribution

To maximise battery life linear regulators should have a low dropout voltage (the minimum difference between input and output that permits correct operation), and should consume little current. Most proprietary regulators do not offer those characteristics, though the Linear Technology Corp. integrated circuit selected does, up to a limit of 125 mA. In the 5 volt regulator, advantage was taken of the availability of higher voltage lines. These are used to supply its control circuit and enable, with the MOSFET, the design of a very low dropout voltage.

Protection

Fuses are fitted to each of the battery supply lines. The 5 volt output has a 'crowbar' circuit to limit it to a maximum of 6 volts in case of regulator failure. Also each PCB assembly has diodes to guard against reverse polarity power supply line connection, and zener diodes as extra insurance against over-voltage. Circuits that use several power supply levels are at risk if those voltages do not rise, and fall, in the correct sequence, or if the circuit inputs remain present after the supply has fallen. Even with the centralised power supply arrangement described here there is a considerable number of potential failure modes that can arise from power supply sequencing; all of these have been guarded against with extra passive components. This potential for failure is an argument against an arrangement of distributed regulators.

All PCB assemblies have power supply filtering components fitted near their connectors, and ceramic capacitors at each group of integrated circuits to decouple the effects of rapidly changing currents.

2.5.6.3 Power supply control and supervision

This part of the circuit receives inputs from a number of other sections and generates the 'power on' signal that controls the main MOSFET switch in the regulator section. It also controls the microprocessor's RESET input. The arrangement is shown in Figure 2.12 . A battery-condition monitoring circuit is included for both battery supplies. These compare terminal

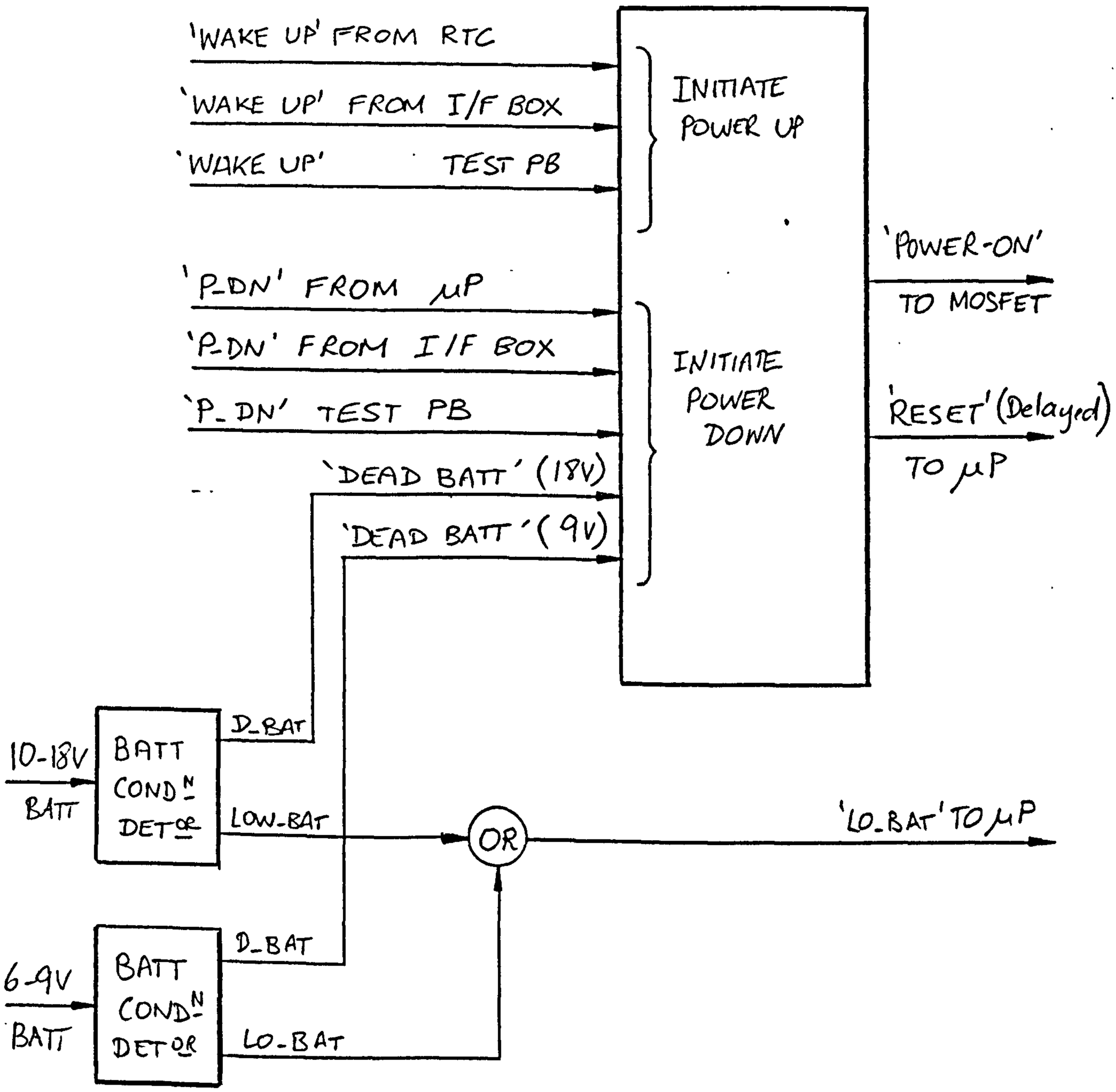

Figure 2.12 : Block diagram of power supply control section

voltages against two levels. The 'low battery' condition is indicated to the microprocessor which places a message, with time of occurrence, in the parameter page of the data store for the user to see during a subsequent communication session. The 'dead battery' condition, in which the terminal voltage is too low for reliable operation, causes immediate power down without reference to the microprocessor.

Figure 2.12 also shows the other inputs to the control section. 'Power down' may be initiated by the microprocessor at the end of a measurement period, or by an on-board push-button for use in development, or by the 'dead-battery' condition signal. In addition, a switch inside the interface box gives the user the ability to switch off the wave recorder. (Switching off and on again is the only way to reset the microprocessor from the surface.) Three inputs cause the control circuit to switch power on. These come from the real-time clock's alarm, from the interface box, and from the test push-button on the power supply board.

The control arrangements of instruments that can switch themselves on and off usually require careful thought if they are to perform correctly in all circumstances. In this case, firstly, the seven inputs originate in different parts of the wave recorder, many of which have different power supply levels, and which may or may not be switched on. Level translation is therefore needed between sections. The safest method, adopted here, is an 'open-collector' convention. Thus the sender circuit indicates an active state by connecting one of the receiver's lines to ground. At other times the line is allowed to float.

Secondly, logic levels that represent control signals must be chosen in the light of prevailing on/off states. For example, the microprocessor's 'power down' output signal should be active-high, otherwise the low signal level the microprocessor is bound to produce when switched off would prevent the wave recorder's power ever being switched on. Also the 'power-on' signal should be active-high, so that the signal cannot be made without

there being at least a few volts from the battery to ensure the battery condition monitors are working.

Thirdly, stable but illegal logic states must be forseen and designed out. An example of such a state is power off without the real-time clock alarm set, or set to a time before the time of switch off. The arrival of interrupts at awkward moments can bring this about and so are guarded against. Another illegal state may occur if, for example, the microprocessor enters a 'HALT' state or an endless loop, thus failing to reach the power down procedure. That one is particularly serious if the interrupts are disabled, resulting in incoming commands being ignored. A further example concerns the latches in the control section. Their output states must be defined in the case of contradictory inputs arriving simultaneously.

Fourthly, the system must deal with unstable and transitional states, including contact bounce in switches and differing rise times of the power supply rails on each board. Controlled delays are inserted where necessary. Also, the control section incorporates a latch so that the appropriate output change is maintained even if the input transition is brief. The software reinforces this latching action. For example, on receipt of a 'low battery' signal the program should not switch the recorder off only to let it go on again as soon as the low battery signal is de-asserted. This would cause 'hunting' as the battery terminal voltage dropped under load and recovered when disconnected. Rather, the program causes controlled termination of the measuring period including setting the RTC's alarm.

All the power supply control circuits operate continuously, even when the main circuits are off, and so are made from low-current devices.

2.5.7 Communication to User's PC

The arrangement chosen to allow the user to set recording parameters and to recover measured data was described in outline in Section 2.4.1 . It is shown in block diagram form in Figure 2.13 .

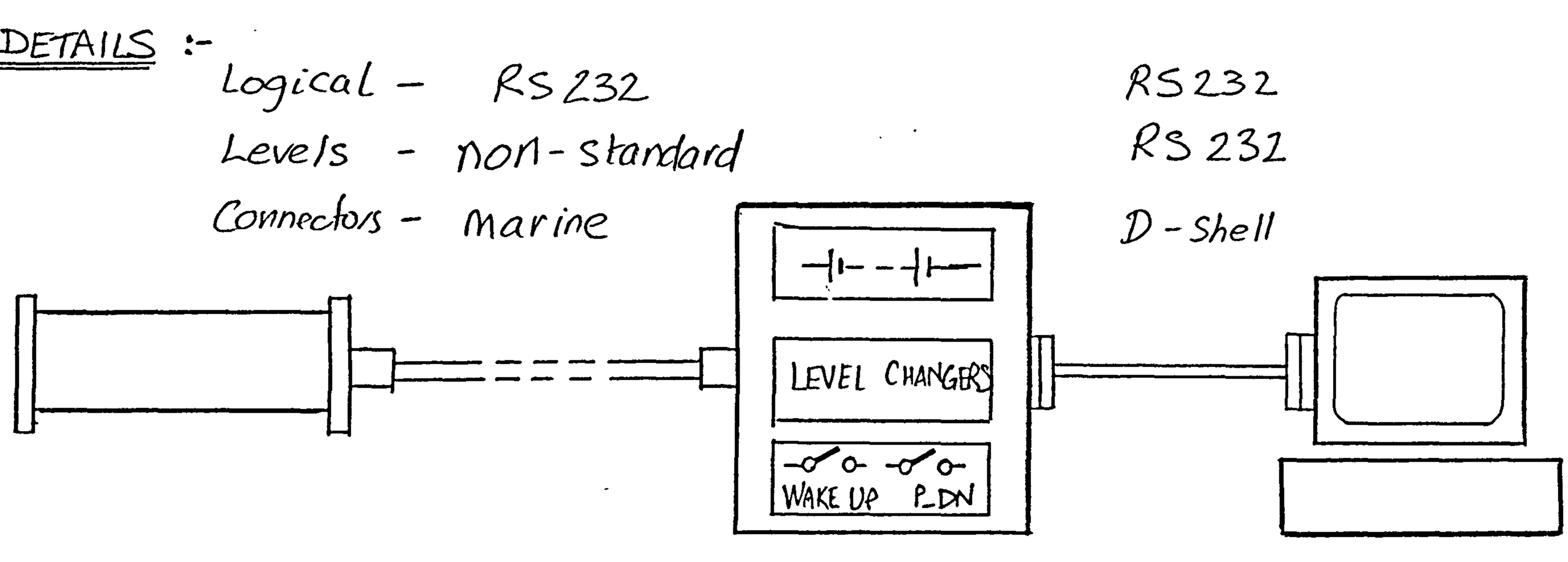

Figure 2.13 : Interface between wave recorder and user's PC

A parallel interface would have been preferred for increased data transfer rate, but to economise on connector costs the simpler serial scheme was chosen.

The HD64180 microprocessor is equipped with two serial ports, one of which incorporates hardware 'handshaking', or flow-control. In the wave recorder these lines drive opto-coupler circuits and amplifiers before going to the data cable and interface unit. The opto-couplers ensure DC isolation of the wave recorder from the equipment on the boat to avoid ground loop interference.

The amplifiers are designed to drive the 30 metre data cable at 19200 baud. A higher rate would have required more current. That is equivalent to about 2 kilobytes per second (KB/s). At that rate it would take half an hour to download all 4 MB of data. Initially, this rate was not achieved because the Amstrad PPC640 laptop PC in use with the system could not accept more than 9600 baud, and that only with long pauses to allow its buffers to clear. In later deployments data rates closer to the design value were anticipated with higher performance portable PCs. The download time would clearly be shorter if the user were to select which records to collect, and leave those which a knowledge of weather conditions over the period suggests will be uninteresting.

The RS232 signals 'transmit data', 'receive data', 'request-to-send' and 'clear-to-send', are all used, although they do not conform to that standard's voltage levels or polarities. Conversion to these is carried out in the interface unit so that the lines are electrically and mechanically compatible to the standard PC serial port.

The interface unit has its own batteries, and is housed in a robust, sealed (though not submersible) box. It has a switch to generate the 'wake-up' signal. The user operates this switch if he wants to communicate with the wave recorder when it is powered down between measurement cycles. The user's 'power-down' facility has already been mentioned.

The user's laptop personal computer (PC) plays a relatively simple part in the system. It acts as a terminal to the wave recorder's microcomputer and provides mass storage to collect the data. A proprietary communications package is run on the PC, giving the user control over its serial interface and disc drive. When the user presses a key its ASCII code is sent down to the wave recorder. When the wave recorder issues a character code to the PC it is displayed on the screen, and (if desired) stored on disc.

The operating system running in the wave recorder recognises certain characters, such as 'T', 'P', '0', '1', '2' etc and takes the appropriate action. Others result in the message 'unrecognised' being sent back for display on the PC screen. More detail on the command set is given in the next section.

2.5.8 Controlling program

The wave recorder's controlling program occupies about 2 KB of the microcomputer PROM. It has five main tasks:

i) Measurement control: scheduling the transducer readings, operating the track-and-hold and multiplexer circuits, setting the auto-range and auto-offset amplifiers, and controlling and reading the ADC.

ii) Measurement processing: compressing the readings to 1 byte each, implementing the decimation filter*, time and date stamping the records, comparing wave activity with a pre-set threshold*.

iii) Memory control: loading and restoring status parameters (such as address of the next free page in the data store and messages for the user) to the non-volatile data store, loading and reading measured records, memory bank switching.

iv) Power supply control: calculating and setting RTC alarm time, handling low-battery interrupt.

v) Handling the communication link: receiving and interpreting characters, sending status information and data to PC, accepting user-supplied measurement settings*.

(Functions marked with an asterisk had not been implemented at the time of writing)

The program was written with the aid of design structure diagrams (BS6224:1987) in a 'top-down', modular fashion. The modules were designed to be as independent as possible. This enabled easier testing, clearer logical flow, and improved reliability of the complete program; and it facilitated any subsequent modification or extension. The top level of the version called 'DEP3' is illustrated in Figure 2.14 by its design structure diagram. The upper half shows the preliminary sections of the listing that set values for the assembler. The run-time sections follow. There are three possible entry points to the code: microprocessor reset following power-up (initiated for example by the RTC alarm, or by the user via the interface unit), an interrupt signalling that a character has been received on the

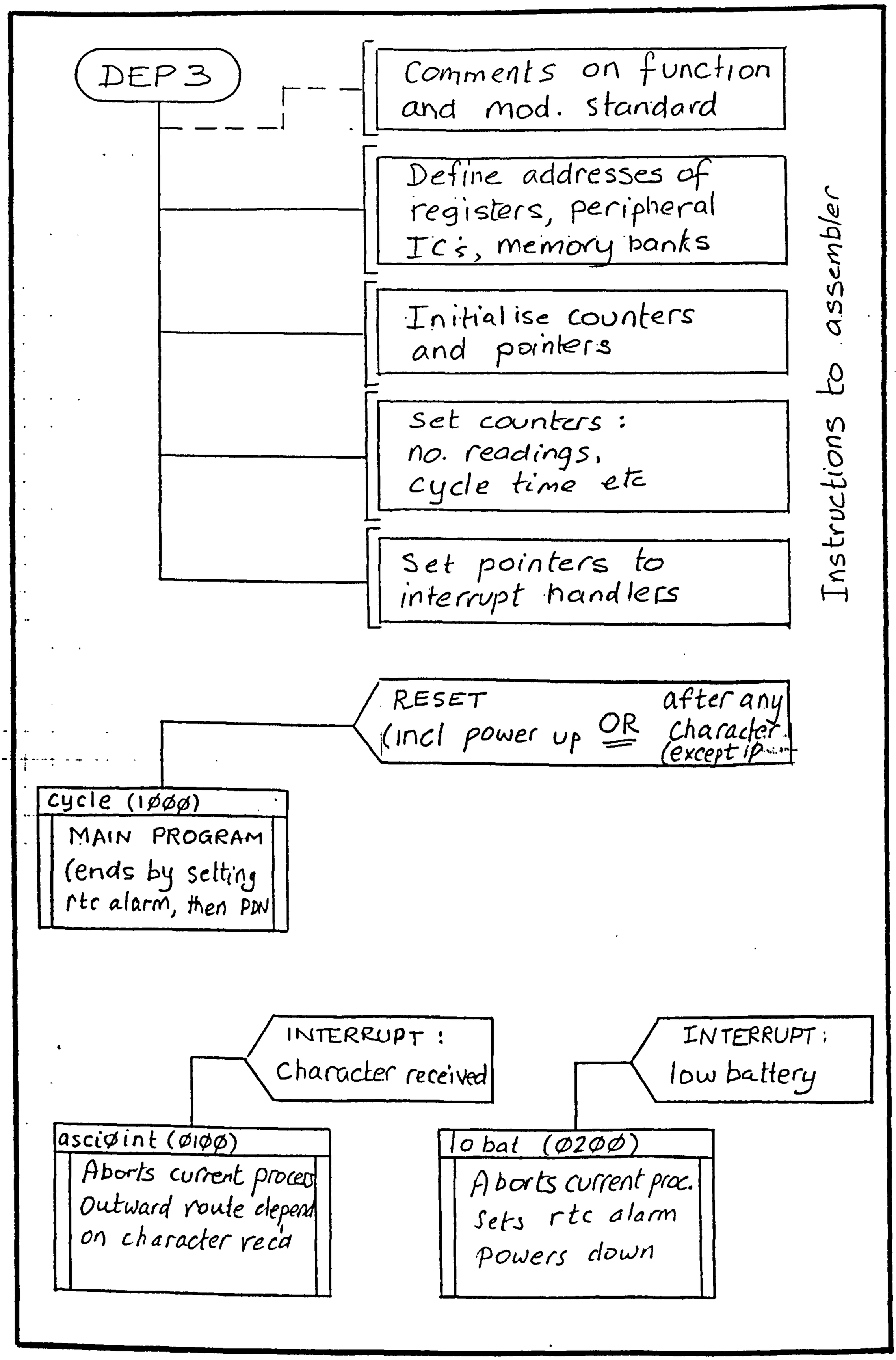

Figure 2.14 : Design structure diagram (level 1) for controlling program

communication link, and an interrupt from the power supply unit warning of a low-battery condition.

The module 'cycle' is part of the second level of the structure diagram, and is shown in Figure 2.15. The symbol for each of the modules is a box which contains the module's name, its start address in ROM, and the sheet number in the diagram where its own structure may be found. Brackets with dotted connecting lines supply further information. Flow passes from top to bottom, always taking a branch before continuing down the diagram. In a loop-type control structure the parallel bars indicate the point at which the loop test is made, with the test condition itself written at the head of the loop.

Data compression

To start with the simple method was used of masking off the four most significant bits of the twelve bit ADC output, leaving only one byte to be stored for each reading. Full length readings were stored at the beginning and end of each record. The full ADC range is thus effectively split into 16 segments. The 8 bits stored give the position within a segment, but identification of the segment is not defined. That was determined at the data decoding stage, based on the departure from the previous reading. It is expected that a more sophisticated compression scheme will be implemented at a later date.

Program development

The complete program contained about 40 modules, defined on a similar number of sheets. It was written in the microprocessor's assembly language (Hitachi 1987), on a 286-type personal computer, using a standard ASCII editor, and cross-assembled into 64180 object code. A relocating linker took all the modules' object files and linked them into absolute code for downloading to a PROM programmer. The loaded PROM was then transferred to the microcomputer board assembly. During development an EPROM emulator was used. This machine contained RAM that plugged into the EPROM socket on the microcomputer board, and was connected to the

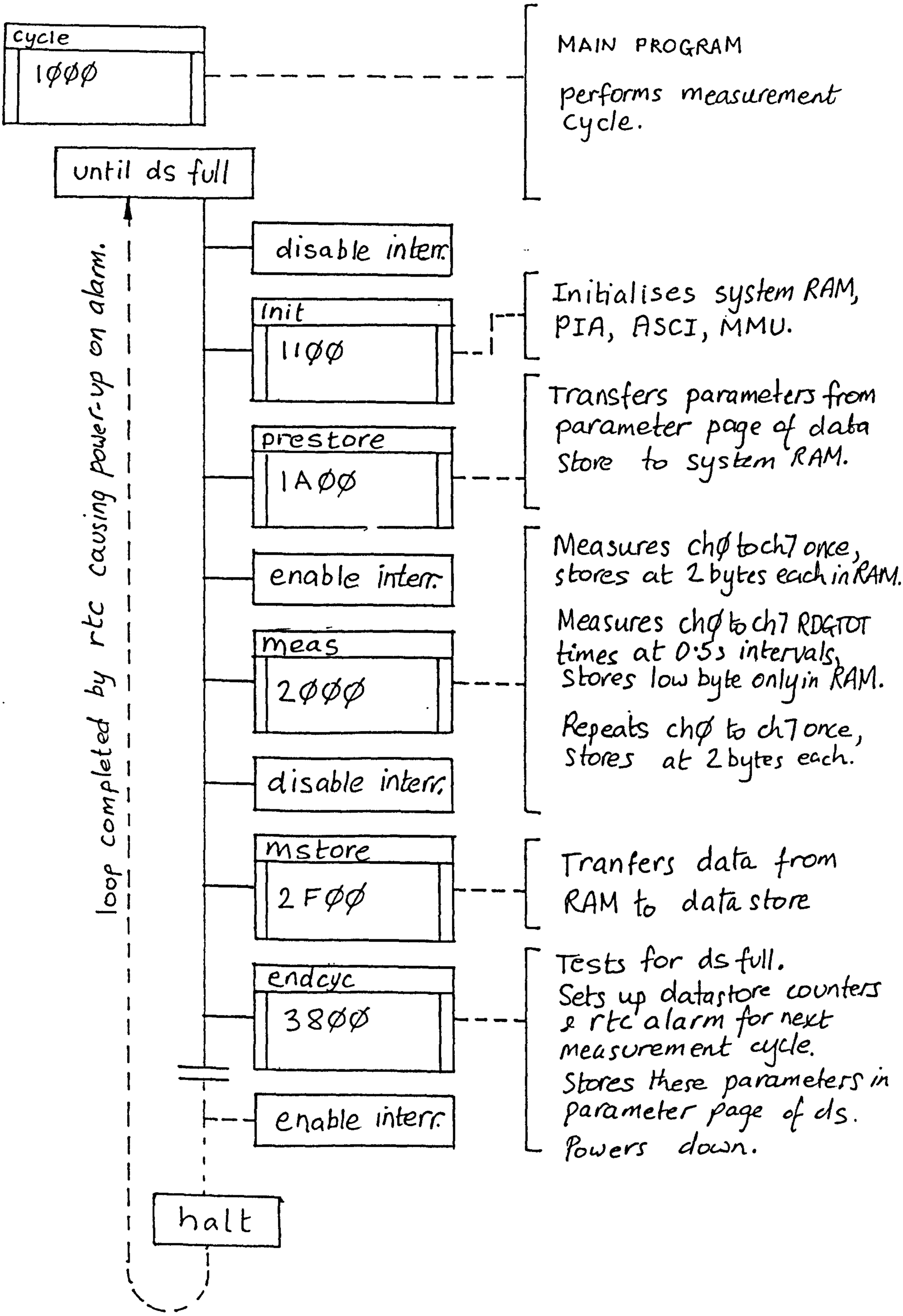

Figure 2.15 : Design structure diagram for the level 2 module 'cycle'.

```
669                     ;*************************************************
670                     ;                                                *
671                     ;         title   :  meas (subroutine)           *
672                     ;         defn    :  measures ch0 to ch7 & stores *
673                     ;                     in RAM once at start & end. *
674                     ;                     HI & LO bytes.             *
675                     ;                    measures ch2,3,4,5,6,7 at 1\2s*
676                     ;                    intervals RDGTOT times.LO byte*
677                     ;         notes   :  uses hl to point to RAM      *
678                     ;                     address for data.          *
679                     ;                    MMU must be reset before exec.*
680                     ;                                                *
681                     ;*************************************************
682
683                               org     2000h
684
685  2000               meas    :                       ;subroutine start
686  2000  F5                    push    af
687  2001  C5                    push    bc
688  2002  D5                    push    de
689  2003  E5                    push    hl
690
691  2004  21 A000              ld      hl,BUFFST   ;init buffer pointer
692  2007  22 800A              ld      (BUFFPTR),hl
693
694  200A  21 8020    ontimerd :ld      hl,ONT01S   ;read on time
695  200D  CD 2B00              call    rtcrd
696  2010  21 8020              ld      hl,ONT01S   ;transfer to buffer
697  2013  ED 5B 800A           ld      de,(BUFFPTR)
698  2017  01 0010              ld      bc,0010h
699  201A  ED B0                ldir
700  201C  ED 53 800A           ld      (BUFFPTR),de;update buffer pointer
701
702
703  2020  CD 2800              call    initsc      ; offset, gain ,track
704
705  2023  CD 2380              call    measlong    ;measures and stores all
706                                                 ;channels, 2 bytes each.
707
708  2026  CD 2400              call    measshrt    ;measures and stores
709                                                 ;in RAM, transducers
710                                                 ;RDGTOT times, 1 byte ea
711
712  2029  2A 800A            ld      hl,(BUFFPTR);align neatly in record
713  202C  23                  inc     hl
714  202D  23                  inc     hl
715  202E  23                  inc     hl
716  202F  23                  inc     hl
717  2030  22 800A              ld      (BUFFPTR),hl
718
719  2033  CD 2380              call    measlong    ;measures and stores all
720                                                 ;channels, 2 bytes each.
721
722  2036  CD 3880              call    offtime     ;reads rtc into scr
723                                                 ;and last line of buff
724
725  2039               measend :
726  2039  E1                    pop     hl
727  203A  D1                    pop     de
728  203B  C1                    pop     bc
729  203C  F1                    pop     af
730
731  203D  C9                    ret
732
```

Figure 2.16 : Listing of the level 3 module 'meas'

PC by a serial link, so new sections of code could be tried quickly without the lengthy process of erasing and programming a PROM. The emulator also provided some simple de-bugging facilities such as setting breakpoints and tracing program flow.

An in-circuit emulator would have been superior, but the greater cost was not considered justified. Similarly, it would have been quicker to write the program in the higher-level language 'C', but cross-compilers were much more expensive than cross-assemblers. A page of the 2000 line listing file, the assembled code from the 3rd level module 'meas', is reproduced in Figure 2.16.

2.5.9 Mechanical Design

The wave recording electronics and pressure transducers were fitted into watertight pressure housings capable of reliable long-term sealing to a depth of 100 metres in sea water. Section 2.5.9.1 to 2.5.9.5 refer mainly to the wave recorder housing. Transducer housings are described separately in Section 2.5.9.7.

Plates 1, 4 and 5 show the recorder housing. It is of tubular construction, with removable end caps sealed by 'O' rings and retained by nuts and bolts through the flanges. Connectors for the transducers are fitted to the end caps and also sealed using 'O' rings.

Polyacetal brackets provide a non-conducting (to avoid galvanic corrosion) means of securing the instrument to its frame, and points of attachment for the detachable rope carrying handle, as well as protection against damage to the casing when set down on a rough surface. The method of fixing the instrument to the brackets, and the brackets to the frame, is designed to deter theft. To ease the removal of end caps during disassembly threaded holes are provided that take nylon jacking bolts. These bear on the flanges to draw out the end caps against any partial vacuum.

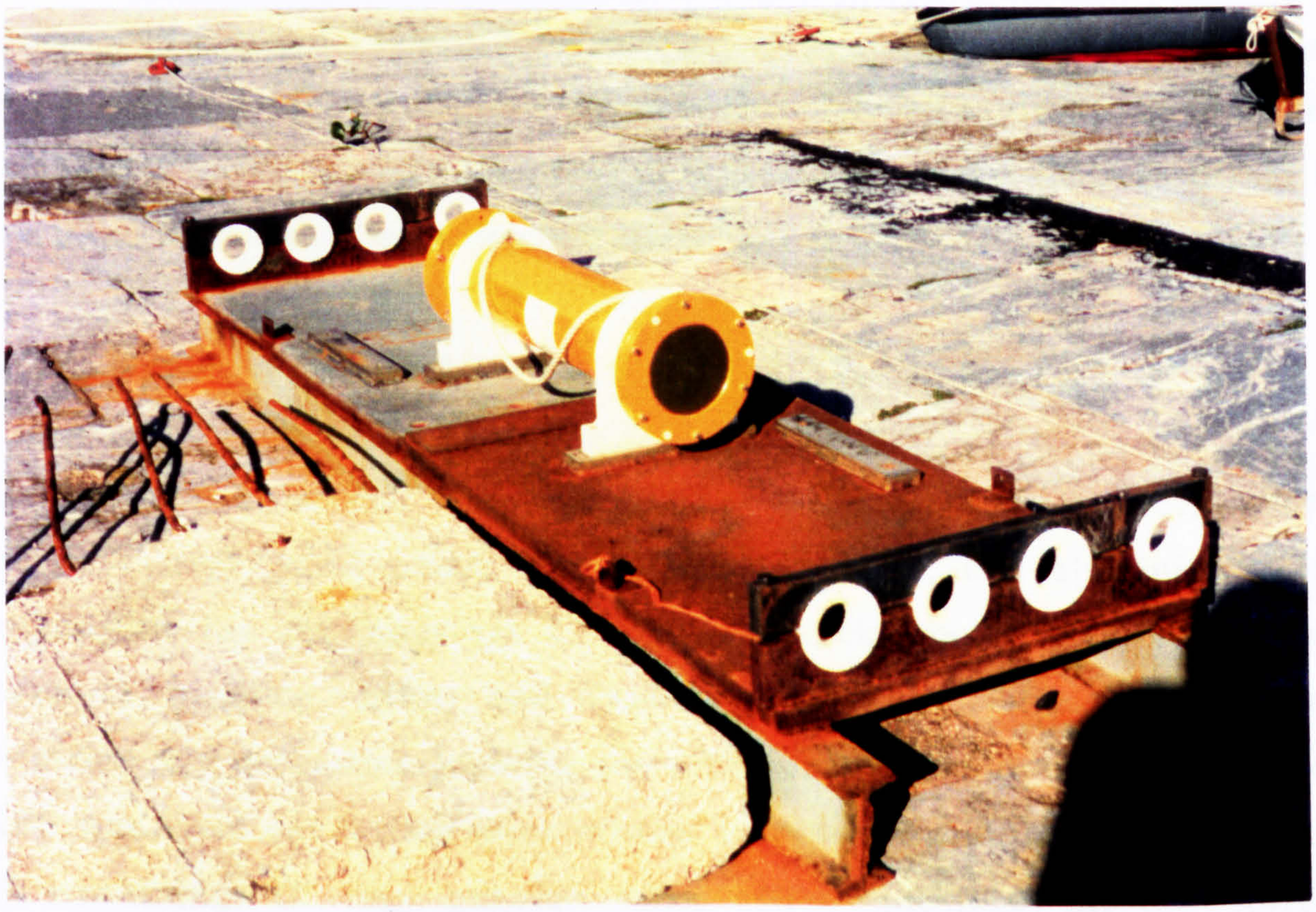

Plate 4 : Recorder housing fitted to its support frame.

Plate 5: Recorder housing components

The diameter of the housing (150 mm) is determined mainly by the arrangement of connectors, allowing enough clearance for a diver to turn the locking rings. Its length (675 mm) provides adequate space for batteries and printed circuit boards, making allowance for future development. The complete recorder weighs 18 kg in air, and displaces 14.8 litres so that in sea water it weighs a more convenient 3.3 kg.

2.5.9.1 Material Selection

Acrylonitrile butadiene styrene (ABS) and other plastics, mild steel, stainless steel, some nickel based alloys, bronzes, and aluminium were considered for the housings (Tuthill and Schillmoller (1965), Fulmer Research Institute, Elliot and Tupholme). The material was selected primarily for properties enabling the achievement of a good, reliable seal. ABS was ruled out for the more critical recorder housing due the difficulty of machining 'O' ring grooves (also called housings) to the correct dimensional tolerances and surface finish, although it had the advantages of corrosion resistance, easy fabrication and low cost. Mild steel corrodes too fast unless given a protective coating which would itself degrade tolerances and finish of the 'O' ring housings. Stainless steels have a tendency to suffer pitting and crevice corrosion in sea water, and corrode quickly if immersed for long periods in water with insufficient oxygen to maintain the protective oxide layer. Again, the danger was to the seal integrity so this material was not selected for the recorder. However, 'A4' grade stainless steel (BS6105, BS3643, BS3692 and BS4168) comprising approximately 18 per cent chromium and 12 per cent nickel (previously known as 'type 316', BS970) was used for the fasteners. Nickel based alloys, such as Monel metal, were too expensive.

Aluminium alloy was selected as it is easy to machine and weld and is light and cheap. Its disadvantage of high corrosion rate was overcome by the application of a hard anodic oxide coating. The particular alloy chosen was type 6082 (BS1471, BS1474) (previously designated H30 by the same standards before amendment), an alloy containing silicon, magnesium and

manganese which is well suited to machining, welding and hard-anodising operations, and which is readily available in bar and tube form. Tube for the housings was bought in in drawn rather than extruded condition since the softness of the latter would permit deformation under machining. Lengths of round bar for the end caps were supplied in extruded condition. Weld filler rod recommended for use with this alloy is type 4043A (previously designated N21), (BS3019).

2.5.9.2 Sealing

The joint between each end cap and the tube is sealed by three elastomeric toroidal sealing rings ('O' rings), one in axial compression (a 'face seal'), and two in radial compression ('piston seals'), Plate 5. The simpler gasket seals were not considered sufficiently reliable. The housings in which the 'O' rings sit are formed in the end caps to precise dimensional tolerances and surface finish. Design of these details and selection of the 'O' rings was made in accordance with BS4518, Dowty Seals Ltd(1990) and BS6442. A good design imparts the right amount of squeeze to the ring, while ensuring that stretch is not excessive, that it does not tend to 'spiral' on assembly, nor extrude under pressure. Tolerances on the 'O' ring housing dimensions, clearance between components, corner radii, lead-in chamfers and surface roughness were all carefully controlled. A medium hardness nitrile rubber was selected for its compatibility with sea water.

2.5.9.3 Machining and Fabrication

Drawn tube and plates were initially prepared on a centre lathe. A local engineering company attached the flanges to the tube by tungsten inert gas welding, following a weld procedure that incorporated the requirements of BS3091, BS499 and BS2901.

Machining the welded assembly was continued on the lathe. Supporting the workpiece was carefully considered: one end was held in the jaws of the chuck and the other supported on running centres bearing on a short length

of tube already turned to a precise outside diameter. This arrangement took advantage of the known roundness and concentricity of the (previously machined) flanges, while avoiding inaccuracy due to the out-of-round surface of drawn tube. The short machined sections of tube were used later to take the plastic support brackets.

However, even this procedure did not permit the tight tolerances of the bore to be obtained, and it turned out excessively oval. The problem was rectified by selecting fatter 'O' rings, re-calculating dimensions and tolerances, and further machining. It was concluded that the correct tool for machining the bore is a horizontal borer in which the workpiece remains stationary and the cutting tools rotate in a circle that does not depend for its accuracy on other surfaces of the workpiece.

The two polyacetal (Delrin) support brackets, and the faired discs for the transducers described below, were cut from 25 mm thick sheet material on a Bridgeport computer numerical controlled (CNC) universal milling machine.

Surfaces touching the 'O' ring seals were finished to the specified average roughness figure by lapping with diamond paste. Surface roughnesses were checked with a Rank Taylor Hobson Talysurf 5-120 gauge, and by comparison to electro-formed surface roughness standards. Dimensional tolerances were checked with a variety of standard bore-, micrometer- and vernier- gauges.

2.5.9.4 Surface Protection

Aluminium left unprotected would not have survived the required immersion time without severe corrosion. This would have led first to failure of the seals, and possibly even to complete penetration of the six millimetre wall-thickness case. The tube assembly and end caps were therefore sent out to receive a hard anodic oxide coating to BS 5599. This process, which is to be distinguished from the softer 'architectural'

anodising treatments, produces a 50μm layer of aluminium oxide of very high electrical resistance and resistance to corrosion. About 25μm extends down into the original dimension of the metal. (Allowance was made for the build up during design of the 'O' ring grooves.) Adhesion is excellent. The surface has a hardness comparable to that of a tool steel, and thus very good resistance to abrasion, but the underlying metal is relatively soft, and so care had to be taken during manufacture and later handling to avoid heavy impacts.

The colour of hard-anodised aluminium is a 'drab olive green' (Plate 5) - difficult to see in water that may be rather murky. A yellow chlorinated rubber topcoat was applied on to a two-part liquid plastic copolymer priming coat. The chlorinated rubber topcoat was selected for its claimed resistance to a wide range of chemicals (including the ones likely to be present in this application) as well as its durability and hard wearing qualities.

A range of adhesive labels was tested underwater, and a satisfactory one chosen to carry the Department's name and telephone number, together with the instrument's function and warnings to deter unauthorised interference.

2.5.9.5 Chassis

A framework of square and round bars, and discs, mainly in aluminium, was designed and fabricated to support the circuit boards and battery pack (Plate 2). Particular attention was paid to strength and stiffness, and to the accommodation of dimensional tolerances, and to minimise electrical interference between circuit boards.

The chassis is fixed to one of the end caps. Although not as rigid as if half of the weight were taken by each end cap, the arrangement does avoid the need for connectors to join the two halves midway along the tube, with the consequent tricky tolerancing and difficult access.

Cells were supplied by the manufacturer already made up into a battery pack, glued together, and connected electrically as called for in the purchase specification. The pack was held by a cage of bars and discs close to the supporting end cap (since the battery pack is the heaviest component), in an arrangement permitting adjustment for pack length.

The circuit board frame consisted of two discs separated by six square bars. The boards were arranged to provide a logical flow of signals (minimising cable lengths and interference) subject to the mechanical constraints of component heights and required board area. Thin tin-plated steel sheets were folded and fitted in between boards and their supporting bars to shield electrically the low level analogue signals from fast high level digital signals.

2.5.9.6 Sea-bed fixings

Plate 4 shows the recorder fastened to its mounting frame, specially fabricated on the quay side from heavy section plates and I-beams. Stainless steel blocks with pre-drilled and tapped fixing holes were welded onto the plate. Doughnut shaped Delrin bushes were incorporated into the ends to give a straight, chafe-free lead in for the cables. The frame weighed about half a tonne. The whole layout is designed to avoid as far as possible the danger of damage due to fouling by debris and marine equipment. If an anchor fluke should catch a cable, then the connector would break its locking ring and pull out rather than drag the instrument from the frame, or frame from the sea bed.

Each transducer is held in place on the sea bed by a concrete mounting block (Plate 6) incorporating a vertical mild steel post with a fixing plate on top. The blocks were fitted with eyes for attaching locating chains and cable ties. All the steelwork was protected against corrosion by zinc sacrificial anodes.

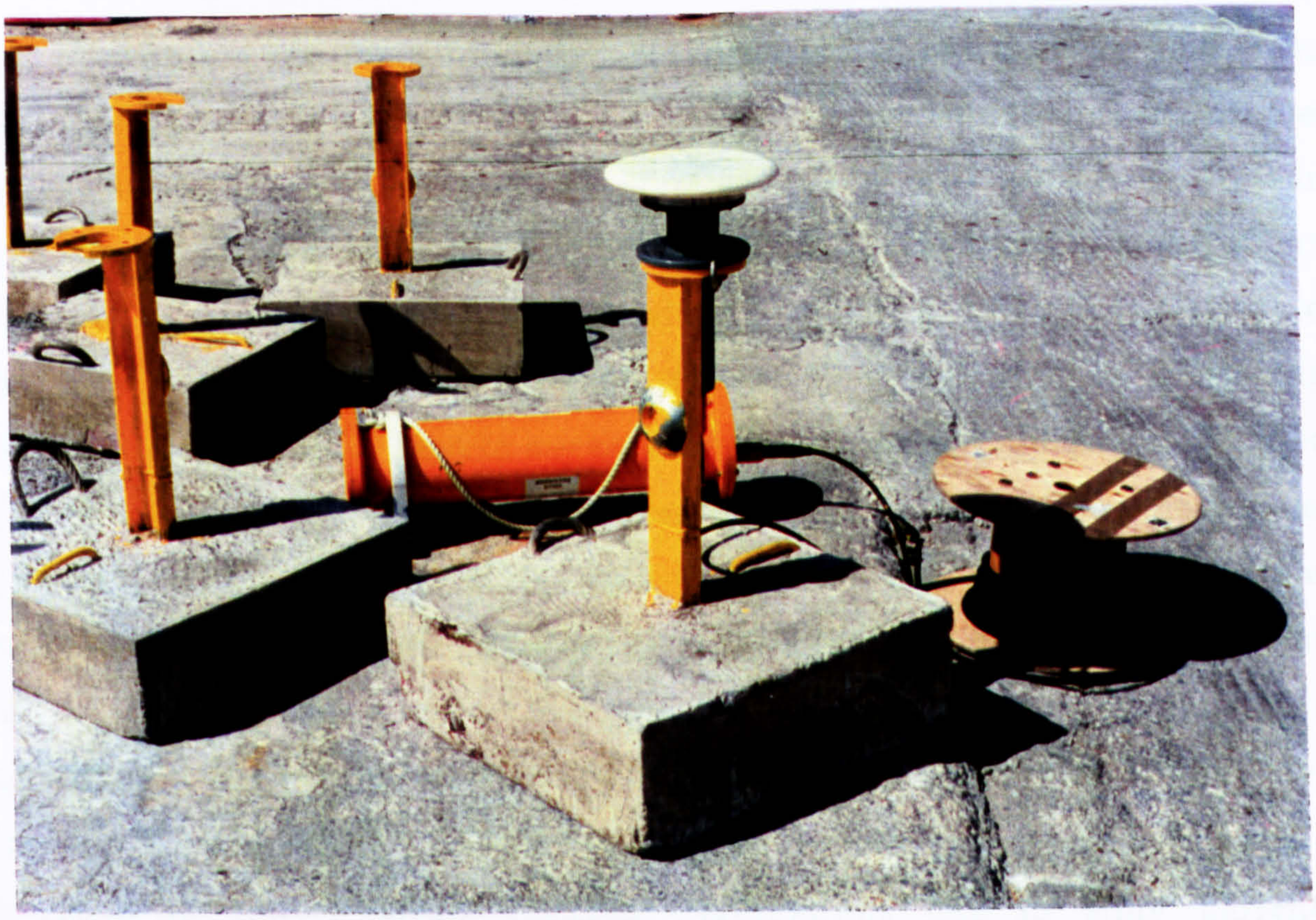

Plate 6 : Transducer mounting blocks

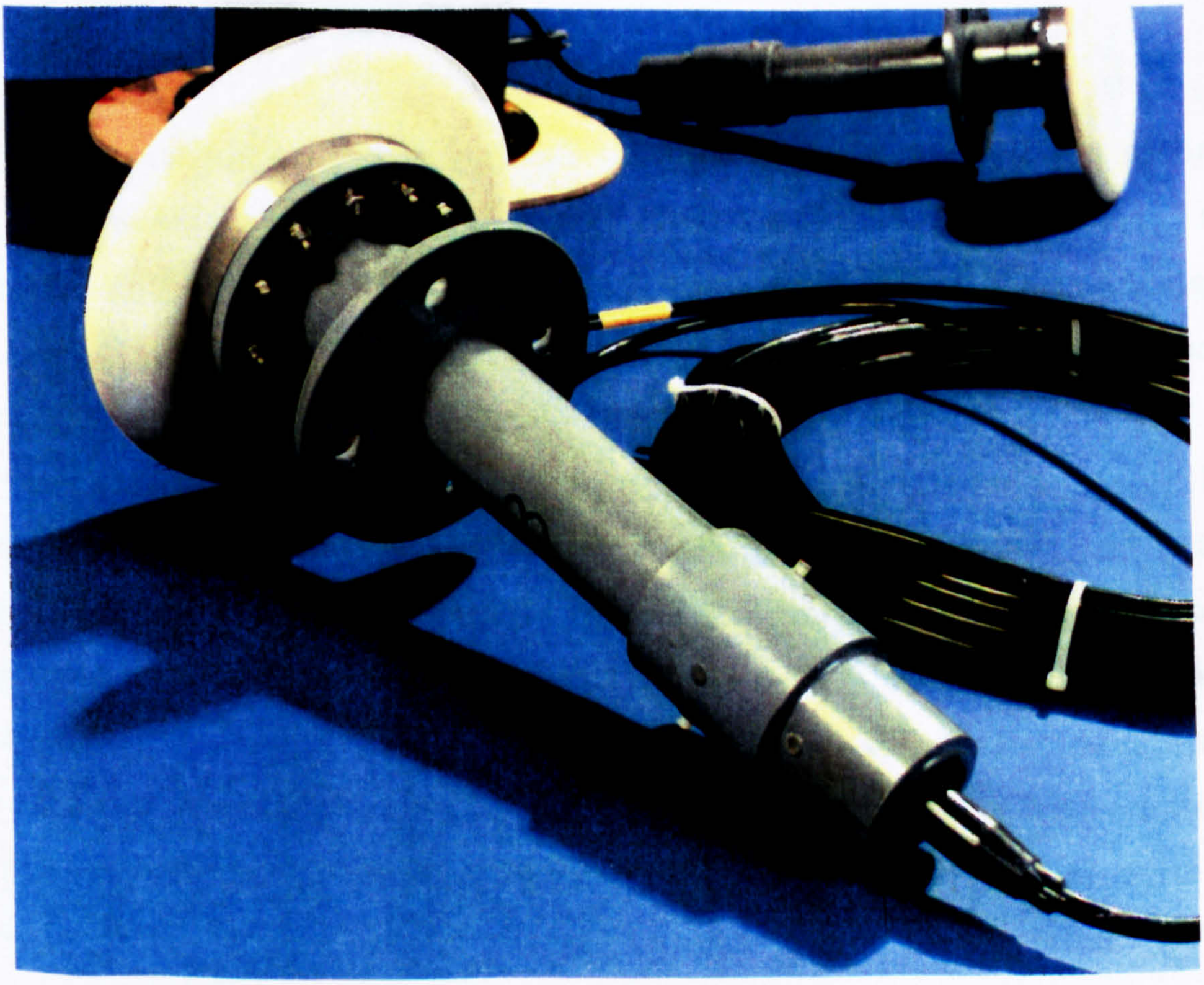

Plate 7 : Transducer housing

2.5.9.7 Transducer Housing

The transducers are made from stainless steel which can corrode badly after prolonged immersion in sea water. A special casing was therefore designed for the transducer (Plate 7). It transfers sea water pressure to the pressure port via an intermediate oil-filled chamber. The transducer is screwed into one side of a stainless steel circular plate. A drilling through the centre of the plate leads to a depression on the other side which is filled with degassed silicone oil. That is covered with a neoprene diaphragm, the other side of which is in contact with the sea water. The transducer housing and electrical connector are kept dry by a tubular housing in ABS that butts up to the stainless steel disc. Sealing arrangements and material selection are not as critical as they are in the recorder housing as the consequences of failure are much less serious. (No sealing failures, though, have yet occurred.) The white disc with well rounded edges in the photograph is designed to reduce small pressure fluctuations due to eddy currents; drillings allow water through to the neoprene diaphragm below.

2.5.9.8 Underwater connectors

The wave recording system consists of eight separate units: the recorder, six transducer assemblies and the portable computer interface unit. Considerable thought was given to the way electrical power and signals were to be transferred between units as it was known that interconnection deficiencies were a common cause of failure in this type of equipment. The problem was to transfer reliably a number of signals and power lines through the wall of a housing, all insulated from one another and without allowing water to penetrate. Various methods of inductive and capacitive coupling had been tried (Papij 1986, Allen 1987) which did not require holes in the housing, but these would have taken substantial development for this application, and may have degraded accuracy. Alternatively, optical fibres could have conveyed the information in digital form, but suitable connectors were not readily available, and the decision had been taken to keep the interfaces in analog form (Section 2.4.1). So conventional

electrically conductive paths were provided between sections: a conductor passes through a hole in the casing, but is separated from it by insulating material. The simplest way of achieving this is to drill the case and pass the insulated cable through, sealing the joint with an adhesive. The experience of other workers , however, had indicated that this sort of approach was unreliable, with failure of bonding likely after a short time. Furthermore, a 'water-block' is desirable at each entry point, so that if the cable were to be cut, water entering and travelling along inside ('wicking') would be prevented from getting into the case. Some sort of feed-through or 'penetrator' is therefore needed, and after giving some thought to making these directly in the housing it was concluded that the most reliable seal would be obtained by buying in components from specialist manufacturers who have experience of the relevant materials and processes and fitting them to the case with conventional 'O' rings.

Connectors, rather than feed-throughs, were used to ease deployment on site; substantial lengths of armoured cable can be unwieldy even without equipment attached to the ends. Furthermore, these connectors were to be coupled underwater, so waterproof ones for mating in the dry would not do: underwater-mateable (also called 'wet-pluggable') types were needed. Many of these are extremely expensive: one type to a military specification cost over £1000 per pair. A list of manufacturers contacted is given in Appendix H. The 'Subcon' range, imported into the UK by PDM Ltd, was finally selected as an economic and effective type, available in configurations suitable for both the transducer and data signals. Both halves are moulded in neoprene, with each individual socket-way having a set of four annular ridges that close onto the plug like 'O' rings, insulating it (together with a small amount of trapped water) from the sea water outside. The body of the bulkhead mounting half is sealed to the case with an 'O' ring, while the free half is soldered to the cable conductors and moulded by the supplier to the cable sheath. These cost in the region of £60 per pair, and have performed well.

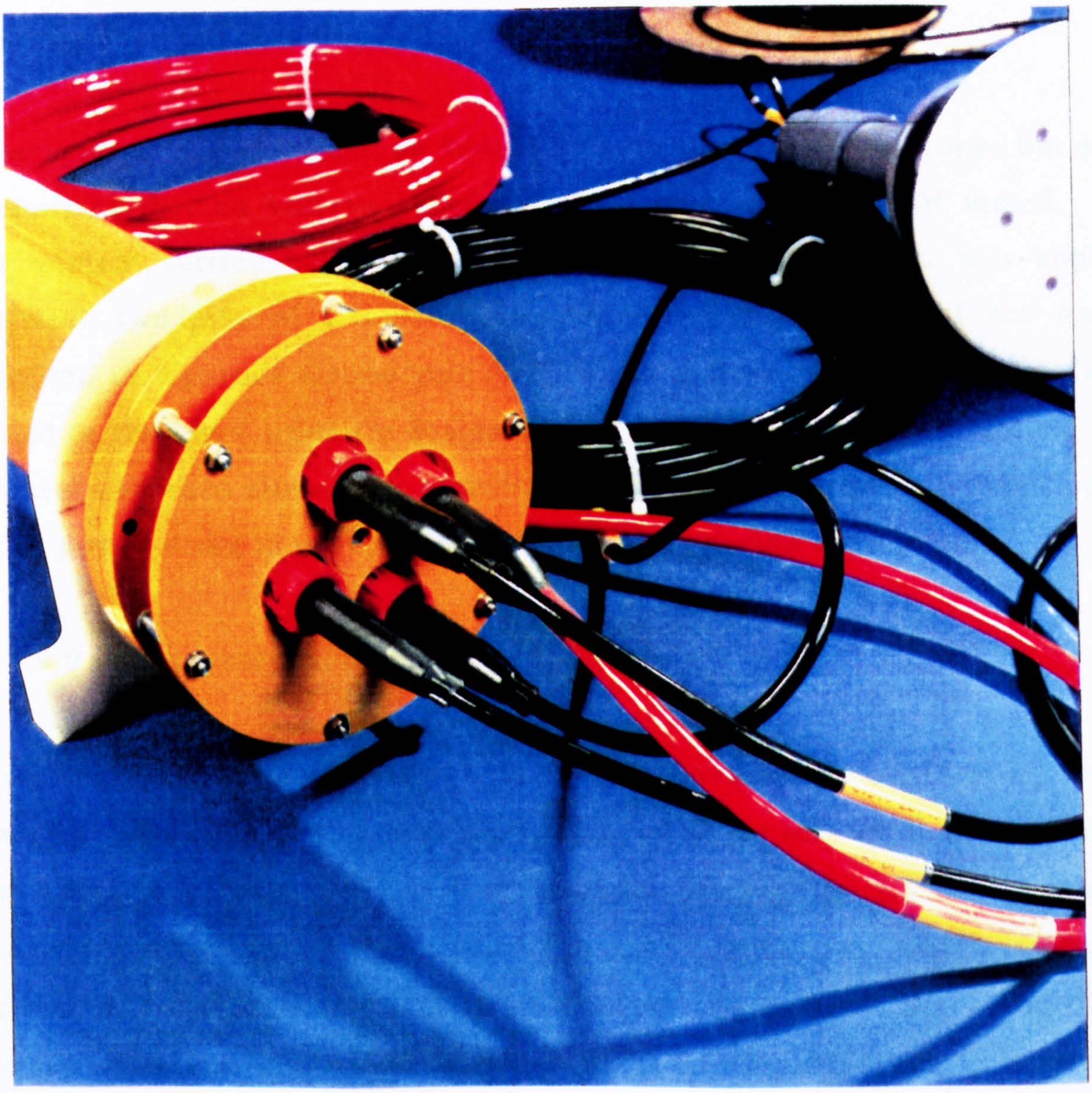

Plate 8 : Marine cable connection detail

Various alternative arrangements were examined to reduce the number of connectors needed. 'Daisy-chaining' the transducers was the most effective, but unacceptable due to the resulting dependency of the system on one connection. Bifurcated cables, allowing cables from two transducers to use a single connector to the recorder, and a 'manifold box' splitting one large cable from the recorder into six were other options, but none was considered superior to the simple one-per-transducer layout, and so that was retained.

Plastic locking rings keep the connectors properly mated, and extra plates (at the recorder) and sleeves (at the transducers) prevent sideways loads causing excessive bending (Plates 7 and 8).

The system may therefore be lowered to the sea-bed in sections, but it is important that no voltage be applied to the connectors until mated. An experiment carried out in the laboratory, in which 20V dc. was applied between two pins of a Subcon plug immersed in a beaker of sea water, resulted in vigorous electrolysis and a current flow of over 1 A. The fuses fitted to the input lines are designed to blow if this occurs in practice. The control software allows the user to disable the automatic 'wake-up' signal after power-down to prevent connector damage during deployment.

2.5.9.9 Underwater cable

Like the specialised connectors described above, cable conforming to the exacting electrical and mechanical specification for this application tends to be rather expensive. The error analysis of Section 2.5.3.7 implied a maximum resistance in the transducer signal connections, which imposed a minimum cross sectional area for the copper conductors. Screening of the signal wires was also required. Mechanically, the cable had to be strong, resistant to chafe, and waterproof.

For the first deployment a non-armoured cable was chosen to speed development; later a full-specification cable was manufactured to special order by De Regt Special Cable bv, Holland. Other companies approached are listed in Appendix I. Seven conductors of 0.75mm^2 cross sectional area are laid together, and covered by a winding of aluminium tape with a 'drain' wire to form a screen. This is covered by a pvc sheath, a helically-wound armouring layer of galvanised steel wire, and finally by a jacket of polyurethane. The grade of polyurethane is selected for nominally static use in temperate climates. This cable cost £10 per metre for the minimum order quantity of 300m, with a charge of £500 for shipping from the

manufacturer to the connector supplier. Complete moulded cable assemblies were then called off from the latter as required.

The data cable has eight conductors, arranged as four screened pairs. It is a standard cable, not armoured, as failure would probably not disrupt measurement.

REFERENCES

Allen J. (1987)
Inductively connected electrical control systems - their role in remotely installed subsea systems
Underwater Systems Design (Jan/Feb 1987) 8-14.

Birch K.G. and Pascal R.W. (1987)
A meteorological system for research applications
Proc 5th Int Conf on Electronics for OceanTechnology (24-26 Mar 1987)7-12.

Boyd W. and Lowe R. (1985)
A high density cassette data acquisition system : operation and applications
Proc Conf: Oceans'85 Ocean Engineering and the Environment (Nov '85) 606-9.

BS 499
Welding terms and symbols
British Standards Institution, UK.

BS 970:Part1:1983
Wrought steels for mechanical and allied engineering purposes

BS 1134:1972
Assessment of surface texture

BS 1471:1972
Wrought aluminium and aluminium alloys for general engineering purposes. Drawn tube.

BS 1474:1972
Wrought aluminium and aluminium alloys for general engineering purposes.Bars, extruded round tube and sections

BS1780:1985
Specification for bourdon tube pressure and vacuum gauges
Appendix E: Testing apparatus and methods, and
Appendix F: Corrections to dead-weight testers (pressure balances) and mercury columns.

BS 2901:Part4:1983
Filler rods and wires for gas shielded arc welding :Part 4 : Aluminium and magnesium alloys

BS 3019:Part1:1984
TIG welding of aluminium, magnesium and their alloys

BS 3643:Part1:1981
Iso metric screw threads : Part 1 : Principles and basic data

BS 3692:1967
Iso metric precision hexagon bolts,screws and nuts

BS 4168:Part1:1981
Hexagon socket screws and wrench keys : Part 1 : Hexagon socket head cap screws

BS 4518:1982
Metric dimensions for toroidal sealing rings ('O'rings) and their housings

BS 5222
Aluminium piping systems

BS 5599:1978
Hard anodic oxide coatings on aluminium for engineering purposes

BS 6105:1981
Corrosion-resistant stainless steel fasteners

BS 6224:1987
Design structure diagrams for use in program design and other logic applications

BS 6442:1984
Limits on surface imperfections on elastomeric toroidal sealing rings ('O'rings)

Donnelly T. Mapps D.J. and Wilson R. (1987)
High density data storage on audio compact cassette tape using a low-cost tape transport
Jnl of IERE **57** (5) 235-238 Sept/Oct 1987.

Dowty Seals Ltd (1990)
O-ring catalogue, Parts 1 & 2
Tewkesbury UK.

Duthie I. (1984)
ROMS to Bubbles - the selection of non-volatile memory
Electronics and power (Nov/Dec 1984) 865-869.

EDN Magazine (1987)
13th annual microprocessor/microcomputer chip directory
(27 Nov '87)

Electronic Design (1984) (Oct 31) 227-238
12-bit A-D converter slips smoothly into analog and digital realms

Electronic Design (1985) (14 Mar)
8-bit microcomputer chips - special edition report

Electronic Engineering (1985)
Product focus - bus oriented boards (July '85)

Elliot D. and Tupholme S. M.
An introduction to steel selection. Part 2 : Stainless steel
BSI Design Centre Guide / Oxford University Press

Fulmer Research Institute:
The Fulmer Materials Optimiser

Garcia E.P. and Pokoski J.L. (1981)
An application of magnetic bubble memory in ocean instrumentation
Proc Conf Oceans '81: The ocean...an international workplace
Boston MA USA, IEEE, 1 306-310, Sept 16-18 1981.

Hitachi Ltd. (1987)
HD64180 Hardware manual 3rd ed

Hitachi Ltd (1987)
HD64180 programming manual 3rd ed

Jalbert J.C. and Chappell S.G. (1983)
Bubble memory recorder for Eave-East vehicle
Proc Conf Ocean '83 160-162, 1983.

Jones P. (1986)
Bubble memory - present and future
New Electronics (9 Dec 1986) 31.

Kahn A and Alexander M. (1987)
Interface a real-time clock chip to an IBM PC or Apple II
EDN Magazine (12 Nov '87) 209-216.

Leibson S.H. (1986)
Clock/calendar chips add system features
EDN Magazine (12 June '86) 73-77.

Mitchell R.B. (1981)
A microprocessor-based underwater tension meter
Int Conf Electronics for Ocean Technology (1981) 329-336.

Papij A. (1986)
A submersible data logging system
Jnl Elec & Electr Engineering, Australia **6** (1) 40-45.

Peek G.D. (1986)
ICM7170 application summary (Issue 1) Oct '86, Intersil Corporation

Prothero W.A. (1980)
Earthquake signal processing and logging with a battery powered microcomputer
Bull. Seismol. Soc. Am. (USA) **70** (6) 2275-90.

Rabiner and Chrochiere (1975)
Optimum FIR digital filter implementation for decimation, interpolation and narrow band filtering
IEEE Trans on Acoustics, Speech and Signal Processing (Oct '75) 444.

Rabiner (1977)
A simplified computational algorithm for implementing FIR digital filters
IEEE Trans on Acoustics, Speech and Signal Processing (June '77) 259

Small C.H. (1986)
Backup batteries (special report)
EDN Magazine (30 Oct '86) 132-150.

Sommers R. (1985)
Special edition report - non-volatile memories
Electronic Design (6 June 1985) 77-96, .

Sydenham P. (Ed) (1982)
Handbook of measurement science Vol 1: Theoretical fundamentals
Sections 3.2.3 & 6.1.2

Tuthill A H and Schillmoller C M (1965)
A guide to the selection of marine materials
Ocean science & Oc. Eng. Conf, Washington DC.

CHAPTER 3

USING THE WAVE RECORDING SYSTEM

CHAPTER 3
USING THE WAVE RECORDING SYSTEM

3.1 INTRODUCTION

The wave recording system has now been described; this chapter discusses the problems considered in putting it to use in the difficult environment just seaward of a breakwater. These include how best to fix the equipment to the sea bed so that it stays in place undamaged, and how to survey the transducer positions accurately underwater. Also discussed are the procedures for collecting data, processing it into standard format files of pressure measurements, and archiving. The word 'processing' is used here to mean converting the raw, compressed data from the recorder's datastore into pressure records. The term 'analysis' is reserved for subsequent operations such as deriving surface elevation records from the measured sub-sea pressures, and estimating directional spectra. More detail on the topics covered in this chapter is contained in the Operator's Manual (Bird, 1992)

3.2 DEPLOYMENT AND RECOVERY

Mindful of the harshness of the environment into which the recorder was to be used careful thought was given to the arrangements for keeping the equipment in place. Movement, including tilting of the transducers, over time had to be minimised, and chafe and stress concentration in the cables avoided.

A rectangular steel platform of about 400 kg was provided for the recorder, and six smaller platforms of concrete and steel for the transducers. Lengths of chain running from one platform to the next in the array served to define the spacings, and to restrain the cables which were fixed to the chain at intervals with plastic ties. Tying cables at intervals to rock-bolted fixings

was considered, but apart from increasing the difficulty of deployment this would have created undesirable local flexing.

The steel recorder platform and concrete transducer mounting blocks were set out first, with the blocks previously having been linked together by the chain. Spread along the side of the deploying vessel, the platforms were cut free as the vessel moved along the line of the array (Plate 9). The line was straightened by an extra pull on the last block before it was released. The off-line platform in the array was dropped into its approximate position and manoeuvred by divers with the aid of air-bags. Good weather conditions were essential as the vessel was working close to the armouring blocks on the breakwater. Also, excessive rolling would have increased the risk of injury from heavy pieces of equipment.

Originally it had been planned to place two large cruciform-shaped anchors at the inner and outer extremities of the array so that the boat could be moored and its position controlled by hauling on lines. These were fabricated and placed, but unfortunately they were carried away before the date of deployment by, it is thought, people trying to steal the buoys, chain and shackles.

In the next stage the recorder, and transducers with cables attached, were taken down to their platforms and bolted on (Plate 10). The cables were then unrolled from the transducers to the recorder and tied at intervals to the chain. Finally the connectors were mated at the recorder, and the locking rings tightened.

The array pattern of transducers is selected to suit the analysis method subsequently to be used and the range of wave periods expected: the next chapter describes that procedure. Figure 3.1 shows a typical arrangement. It is not in general practical to place each component into position with great accuracy, so that after deployment a survey was made to establish actual positioning. Results from the survey are used in later analysis. Two methods of fixing transducer locations were carried out (Rendell 1989):

Plate 9 : 'Deepwater' with transducer mounting blocks alongside

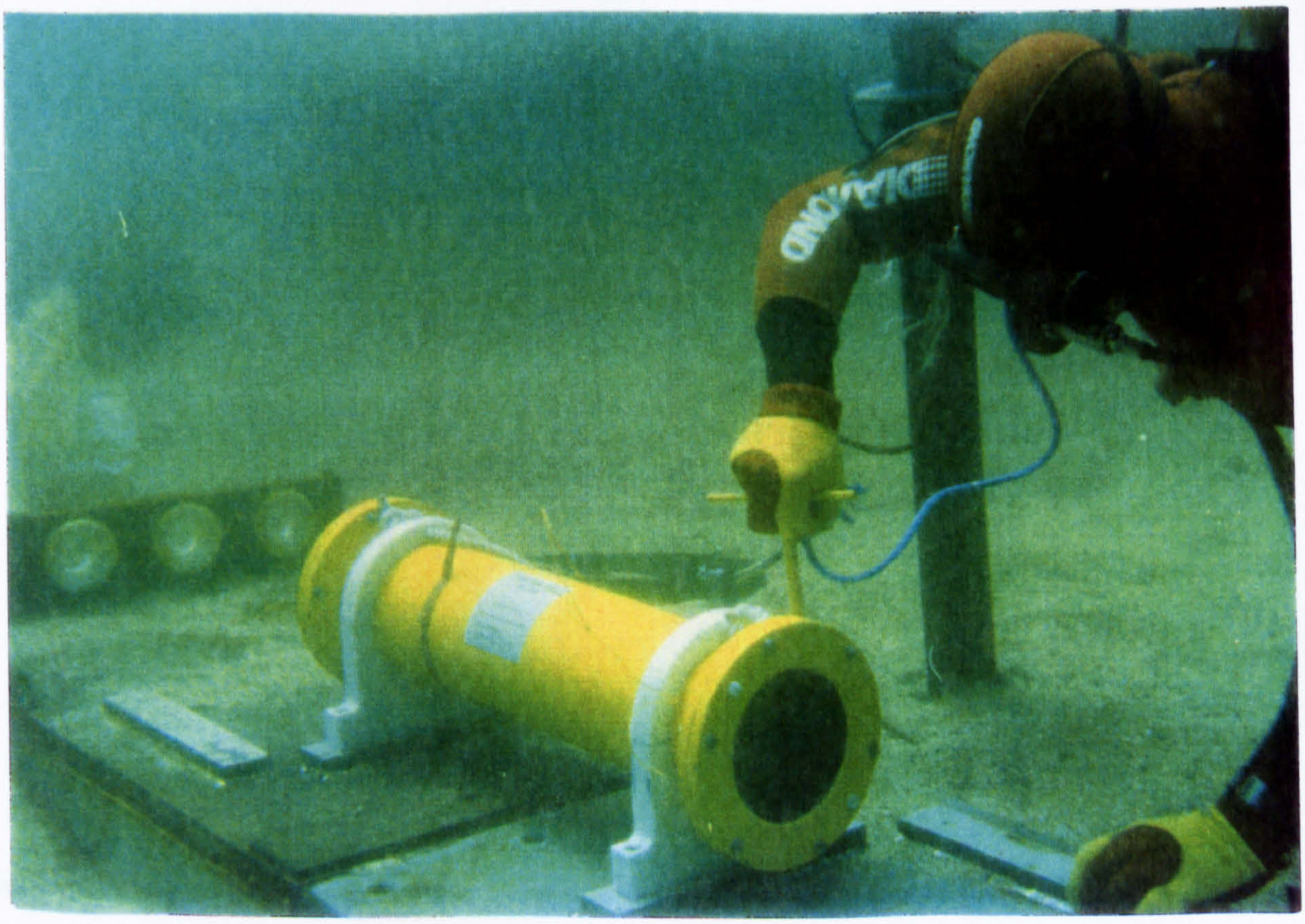

Plate 10 : Diver fixing the wave recorder to its platform

PROJECT		Plymouth Polytechnic	DEPARTMENT OF CIVIL ENGINEERING	
WAVE RECORDER WR1				
SECTION	**date**	**JOB NO.**	**SHEET NO.**	**rev.**
TRANSDUCER VECTORS	26.1.90	WR1-0050	1/1	A (DEP3)

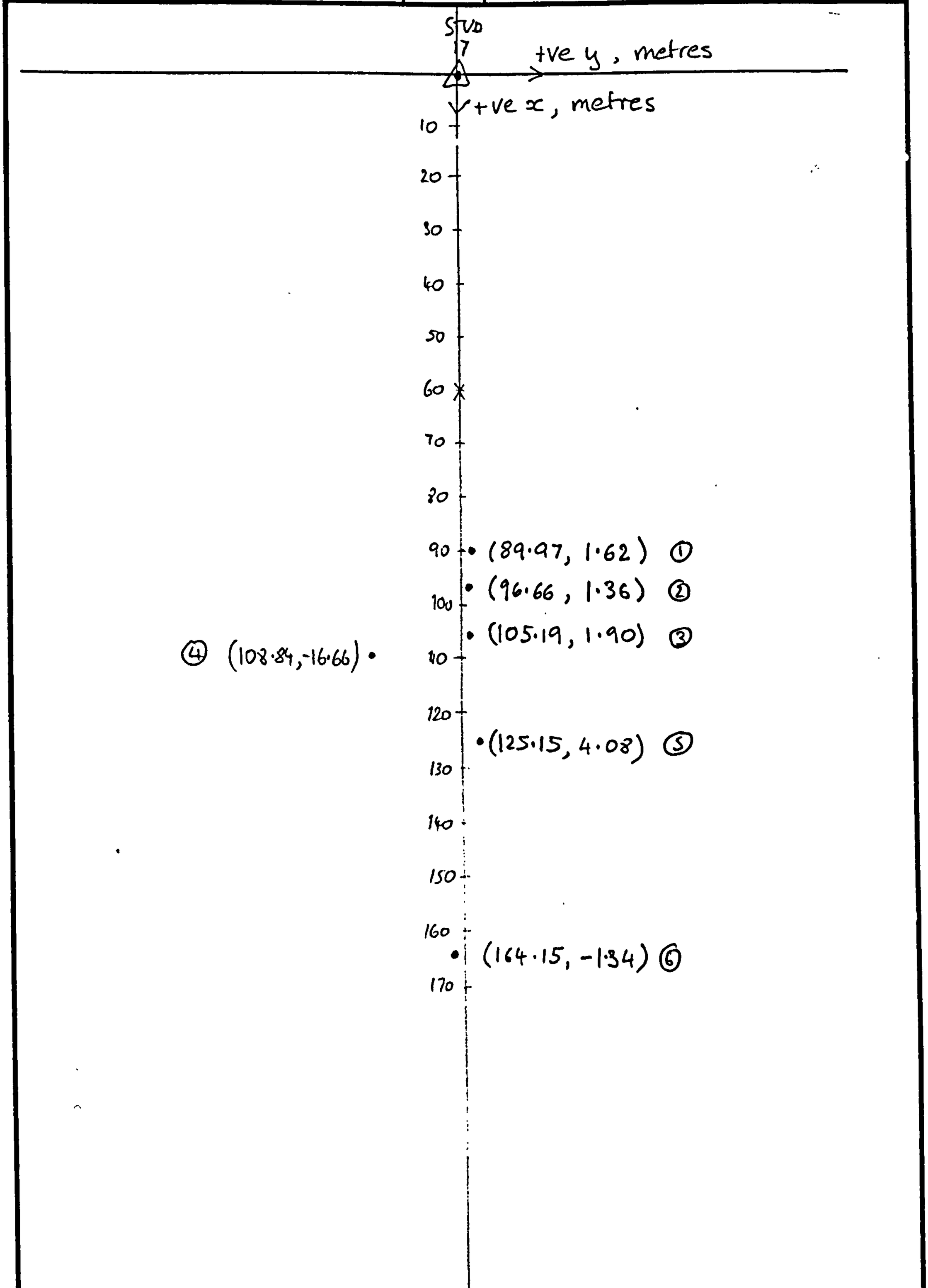

Figure 3.1 : Transducer locations, Plymouth Breakwater

measuring with tapes the distance between selected pairs of transducers, and taking horizontal angles of each location with theodolites. The latter procedure required buoys to be floated above each transducer at slack tide in calm weather. Two theodolites set up at reference stations on the breakwater took horizontal angles for each buoy. Standard surveying software packages processed the measurements from each method to provide coordinates, and these were then compared. It was estimated that the fixes were accurate to within at most 0.5 metres, though the error was probably less.

The jobs of setting out the platforms, fitting the instrumentation and surveying took about a day each, and involved teams of specialists (divers, boat handlers, and surveyors) and careful planning. The recovery procedure was simpler as no surveying operations were involved.

3.3 OPERATION, DATA COLLECTION AND CALIBRATION

The measurement process proceeds in a number of phases; these are described by the following terminology illustrated in Figure 3.2:-

A 'deployment' is the period during which the system is set out on site, normally limited by battery life or operational constraints. In this period the transducer array, the modification standard of the electronic assemblies, and the version of the internal software are fixed. Currently, measurement parameters are also fixed, but future versions will permit changes via the laptop PC.

A 'measurement operation' is defined as the period between two 'start' commands, during which the data store is filled with records taken at fixed intervals after the start time. If the store becomes full before the second start command is received, the wave recorder ceases measurement and remains powered down until the user switches it on to begin a communication session. Existing data is therefore retained.

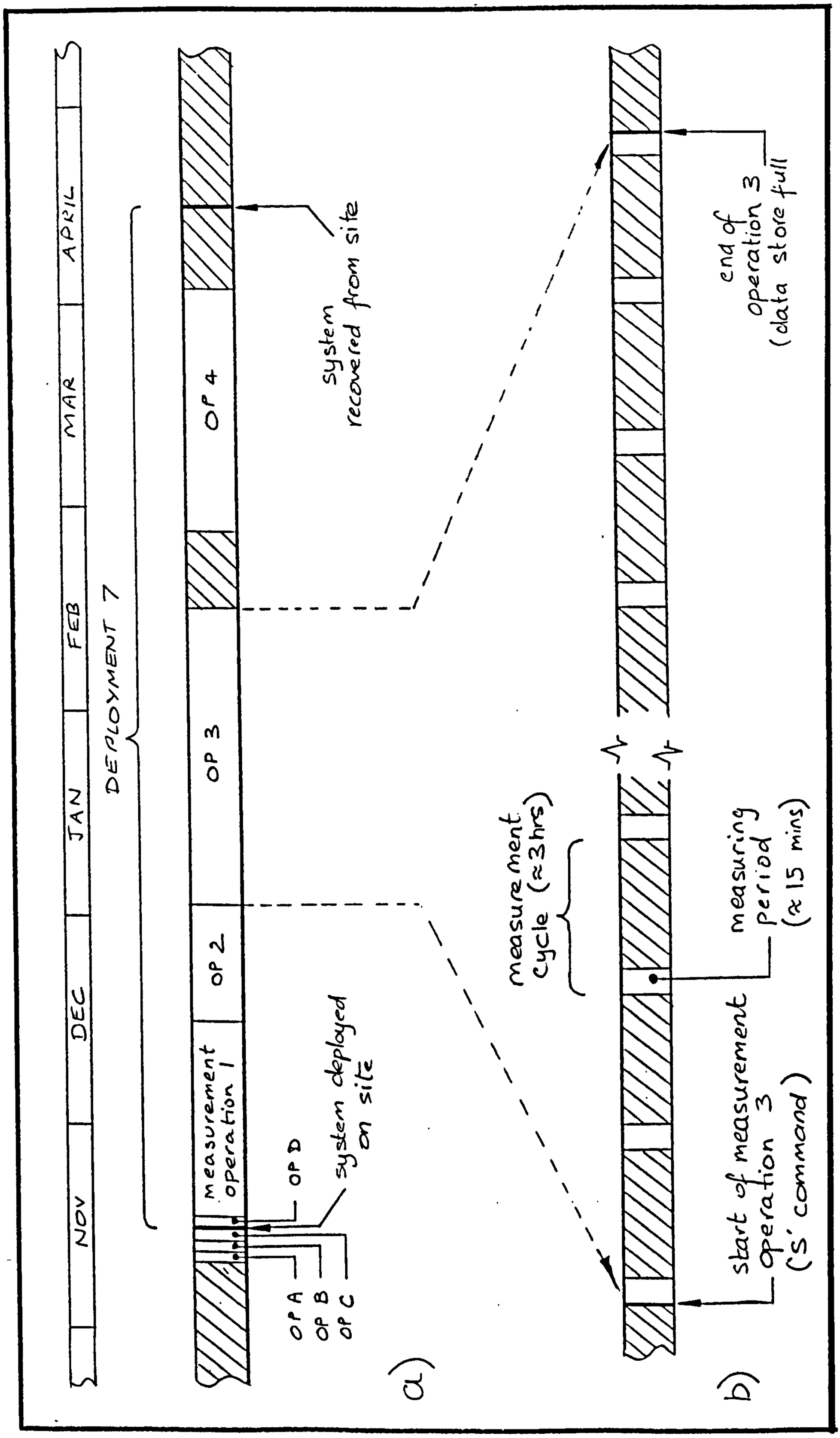

Figure 3.2 : Measurement scheduling (shaded areas denote the wave recorder powered down)

Figure 3.2 shows, for illustration only, a system deployed for the seventh time, in mid November. Short measurement operations in preceding days for checking and calibration are labelled with letters. A similar operation was started immediately after installation at the site to check that all connections had been correctly made. Before leaving the site the start command is again given to commence data collection proper: operation 1. Measurement operations 1 and 2 are shown terminated by the user before the data store was full, possibly to avoid gaps in the data, or to take advantage of good weather, or to recover data from a particularly interesting event as soon as possible. Operations 3 and 4 run on until the data store is full, and so gaps in the data follow. The system is shown recovered in about mid-April, ending deployment 7.

Each operation is composed of a number of 'measuring cycles', lasting typically 3 hours each. In a cycle the wave recorder is switched on for a period of, typically, between 10 and 20 minutes: a 'measuring period'. For the remainder of the cycle it is switched off. The choice of these time intervals is a compromise between the acceptable interruptions to the availability of data and the conservation of battery and data store capacities. The three hours, and 17 minutes, durations are traditional choices (Driver, 1980a). Each record then yields 2048 measurements, a convenient number for the Fast Fourier Transform analysis operation, and records are separated by an interval long enough to allow wave conditions to change. For any given deployment there may be other constraints, such as synchronisation with other measurement apparatus. It may also be an advantage to have a cycle duration of about 3.1 hours so that measurements are taken at similar points in the tidal cycle. There are other considerations that influence choice of duration of the measuring period: the stationarity of the record, and the statistical reliability of spectral estimates that can be derived from it. These are examined in the next chapter. Each measuring period generates a block of data which is stored in the next available page of the rampacks. The block ultimately yields one file of pressure data.

The wave recorder's command list is as follows:

KEY (case sensitive)	FUNCTION
T	WR sends code representing value of its real time clock. This command is used for calibrating the RTC against an accurately set wrist watch.
P	Causes WR to switch off, with real time clock alarm disabled. (WR will not power up again until the 'wake-up' switch is operated.) This command is used before deployment or recovery to prevent power being applied to open connectors.
S	Starts a measurement operation.
0,1,2,or 3	WR dumps data in the specified rampack.
Any other character	WR only echoes the character and sends message 'unrecognised'. (Pressing such a key is a good way of seeing whether the WR is on and the data link is working.)

When the wave recorder's response to any key (except P) is finished it immediately starts a measurement cycle. Measurement records are put into the next free page of data store; only command S causes previous pages of the data store to be overwritten. However the records taken after the communication session will be taken at times referred to the end of the session rather than referred to the operation's original start time.

Calibration

The instrument is calibrated at a number of stages in order to give the greatest possible assurance that the readings obtained are accurate. Before each deployment the recorder and transducers are calibrated separately, the former by applying known voltage sources to the inputs, and the latter by measuring their output voltages over a range of pressures generated by a Budenberg dead-weight tester (Section 2.5.2). An adapter was made to enable the tester to apply pressure to the transducer housings, but in use it turned out to be inconvenient and inadequately repeatable due to the large volume of oil needed and the inclusion of air pockets. Instead the

transducers were calibrated out of their housings, and any changes to the ambient reading after assembly noted.

In the next stage of calibration the system as a whole is set to take a measurement record at ambient pressure, and the results compared to a mercury-in-glass or precision aneroid barometer.

The system and its components were re-calibrated after recovery to check for any drift over time. Other opportunities to cross-check the system's performance were taken as they presented themselves, such as an independent reading of water pressure next to a transducer, or the output of a tide gauge and barometer. However, those measurements tend to be rough checks only as they are likely to be less accurate than the recorder's output. An additional check on the electronic circuits is provided by the internal calibration sources which are measured and recorded at the beginning and end of each measurement period. All calibration data was assessed and combined into correction factors which were incorporated into the data processing software.

In a similar way the accuracy of the real-time clock was assessed during the deployment by using the 'T' command and comparing the recorder's response to the correct current time. A correction factor was then applied by the data processing software.

3.4 DATA PROCESSING

Two programs, written in Fortran and running on either the portable or a desktop PC, convert the coded and compressed dumpfiles into pressure records in standard form (Figure 3.3).

Paginate

The first few lines of a typical dump file are shown in Figure 3.4 . That file is simply an image of one of the wave recorder's rampacks, with each of the

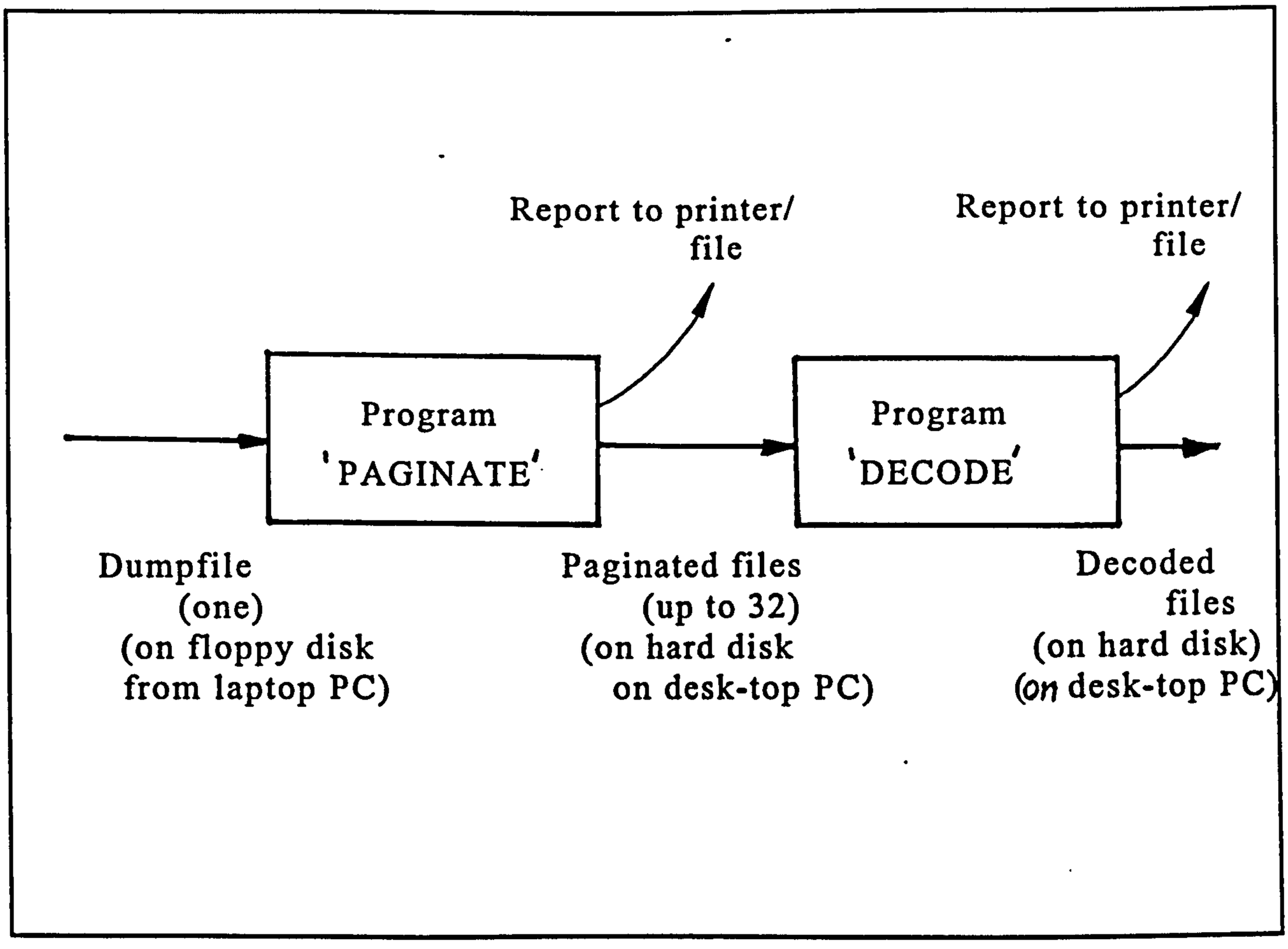

Figure 3.3 : Data processing block diagram

262,144 bytes represented as a pair of hexadecimal characters. The first step is to split the dump file up into files containing one measurement record each. This is done by the program 'Paginate' which also forms six columns of data, one for each transducer. An example of the resulting file is given in Figure 3.5. The first line contains a coded representation of the time the first set of six readings were taken, and the second contains the first six readings in uncompressed form (4 characters each) together with readings of the two calibration sources. These eight readings are taken again at the end of the measurement period. Paginate constructs names for these new files from the name of the dump file in such a way as to enable any processed file to be traced back to its origin in the wave recorder's data store. The correspondence is listed in a report that Paginate sends to the printer, shown in Figure 3.6. The 'format error' column records the result of checks that pages of the dumpfile conform to the expected structure. (F stands for 'false' - no error.)

```
1
dumping rmpk 01

Rampack number : 01   Page number : 00
4003 0115 0401 5900 0000 0000 0000 0000
00CF 0734 03D1 0381 03E6 03B8 0406 03DC
D383 E3B8 07DE D381 E2B7 07E1 D07F E1B8
07E6 CE7D E2B7 05E7 CD7C E0B8 02E5 CC7B
DEBA 02E3 CC7B DDBE 02E1 CB7C E0BF 04DF
CB7D E3BE 05DD CC7E E5BD 05DE CC7D E6BE
01DF CD7E E6BF 02E1 CC7E E4C1 01E3 CA7C
E3C1 02E4 CA7B E3C0 02E2 C97B E2BF 01DF
CA7B E0BD 02DD CC7C DEBA 04DE CC7C DFB7
07E0 CD7C E1B7 09E1 CE7D E1B6 09E1 D07F
E0B5 08E0 D080 DEB5 05E1 CF7F DFB7 04E2
CD7C E1B7 02E2 CB7B E2BB 00E1 C97C E2BC
FDE0 CB7D E2BC FBDE CC7D E3BC FEDF CB7C
E4BD 01E0 CA7B E4BD 03E2 C97C E2BE 05E2
CA7C DFBC 05E1 CC7B DEBB 05E0 CB79 DFBA
07DD CA7A DFBA 08DC CA7A E0B7 09DC CB7B
E0B9 09DD CD7D E0BD 07DF CE7D E0BF 04E1
CD7C E1BD 01E2 CB7B E4BC FFE1 C97B E6B9
FEE2 CA7D E6B9 FEE3 CC7F E3BB FDE3 CD80
E0BB FEE3 D07D E0BA 01E1 CE7C E1B7 04E0
CE7D E1B7 06DD D07F E0B7 07DE D080 E0B7
07DD CF7E E0B8 07E0 CD7D E2B7 06E0 CB7D
E3B8 05E0 C97E E3B9 03E0 CB7D E1BE 03DF
```

Figure 3.4 : First few lines of a 'dump file' (DEP6.4R1)

```
Rampack number : 01   Page number : 00
4003 0115 0401 5900 0000 0000 0000 0000
00CF 0734 03D1 0381 03E6 03B8 0406 03DC
 D3 83 E3 B8 07 DE
 D3 81 E2 B7 07 E1
 D0 7F E1 B8 07 E6
 CE 7D E2 B7 05 E7
 CD 7C E0 B8 02 E5
 CC 7B DE BA 02 E3
 CC 7B DD BE 02 E1
 CB 7C E0 BF 04 DF
 CB 7D E3 BE 05 DD
 CC 7E E5 BD 05 DE
 CC 7D E6 BE 01 DF
 CD 7E E6 BF 02 E1
 CC 7E E4 C1 01 E3
 CA 7C E3 C1 02 E4
 CA 7B E3 C0 02 E2
 C9 7B E2 BF 01 DF
 CA 7B E0 BD 02 DD
 CC 7C DE BA 04 DE
 CC 7C DF B7 07 E0
 CD 7C E1 B7 09 E1
 CE 7D E1 B6 09 E1
 D0 7F E0 B5 08 E0
 D0 80 DE B5 05 E1
 CF 7F DF B7 04 E2
```

Figure 3.5 : First few lines of a 'paginated' file (D6O4R1.P00)

```
Program running :   PAGINATE   Version :                    3.0 1030 16.3.89

Input pathname - A:DEP6.4R1

      LINE 1 OF INPUT PAGE                          O/P FILE              FORMAT ERROR

                                                                              Yes
 Rampack number : 01   Page number : 00   C:\WR1\DATA\D6O4R1.P00              No
 Rampack number : 01   Page number : 01   C:\WR1\DATA\D6O4R1.P01              No
 Rampack number : 01   Page number : 02   C:\WR1\DATA\D6O4R1.P02              No
 Rampack number : 01   Page number : 03   C:\WR1\DATA\D6O4R1.P03              No
 Rampack number : 01   Page number : 04   C:\WR1\DATA\D6O4R1.P04              No
 Rampack number : 01   Page number : 05   C:\WR1\DATA\D6O4R1.P05              No
 Rampack number : 01   Page number : 06   C:\WR1\DATA\D6O4R1.P06              No
 Rampack number : 01   Page number : 07   C:\WR1\DATA\D6O4R1.P07              No
 Rampack number : 01   Page number : 08   C:\WR1\DATA\D6O4R1.P08              No
 Rampack number : 01   Page number : 09   C:\WR1\DATA\D6O4R1.P09              No
 Rampack number : 01   Page number : 0A   C:\WR1\DATA\D6O4R1.P10              No
 Rampack number : 01   Page number : 0B   C:\WR1\DATA\D6O4R1.P11              No
 Rampack number : 01   Page number : 0C   C:\WR1\DATA\D6O4R1.P12              No
 Rampack number : 01   Page number : 0D   C:\WR1\DATA\D6O4R1.P13              No
 Rampack number : 01   Page number : 0E   C:\WR1\DATA\D6O4R1.P14              No
 Rampack number : 01   Page number : 0F   C:\WR1\DATA\D6O4R1.P15              No
 Rampack number : 01   Page number : 10   C:\WR1\DATA\D6O4R1.P16              No
 Rampack number : 01   Page number : 11   C:\WR1\DATA\D6O4R1.P17              No
 Rampack number : 01   Page number : 12   C:\WR1\DATA\D6O4R1.P18              No
 Rampack number : 01   Page number : 13   C:\WR1\DATA\D6O4R1.P19              No
 Rampack number : 01   Page number : 14   C:\WR1\DATA\D6O4R1.P20              No
 Rampack number : 01   Page number : 15   C:\WR1\DATA\D6O4R1.P21              No
 Rampack number : 01   Page number : 16   C:\WR1\DATA\D6O4R1.P22              No
 Rampack number : 01   Page number : 17   C:\WR1\DATA\D6O4R1.P23              No
 Rampack number : 01   Page number : 18   C:\WR1\DATA\D6O4R1.P24              No
 Rampack number : 01   Page number : 19   C:\WR1\DATA\D6O4R1.P25              No
 Rampack number : 01   Page number : 1A   C:\WR1\DATA\D6O4R1.P26              No
 Rampack number : 01   Page number : 1B   C:\WR1\DATA\D6O4R1.P27              No
 Rampack number : 01   Page number : 1C   C:\WR1\DATA\D6O4R1.P28              No
 Rampack number : 01   Page number : 1D   C:\WR1\DATA\D6O4R1.P29              No
 Rampack number : 01   Page number : 1E   C:\WR1\DATA\D6O4R1.P30              No
 Rampack number : 01   Page number : 1F   C:\WR1\DATA\D6O4R1.P31              Yes
Last line of  C:\WR1\DATA\D6O4R1.P31  invalid
```

Figure 3.6 : Paginate Report for D6O4R1.Pnn (The last file is valid, the format error arose because it was not followed by another file)

Decode

This program operates in batch mode on the series of files produced by Paginate, producing for each one a new file with a text header and six columns of pressure data in millibars, Figure 3.7. These new files are automatically given names related to the originals in order to maintain traceablilty. The header contains all the information needed to make use of the file, including start time, references to the modification standard of drawings and software, and the calibration figures applied (by Decode) to the pressure readings. As Decode runs it sends a report to a log file similar to the one in Figure 3.8 which may later be printed.

Decode's function is to work out the actual pressure readings from the compressed values in the Paginated files, applying to those the values of the amplifier gain and offset settings, the ADC transfer function and the pressure transducer characteristic. Corrections are applied to the pressure and the real time clock readings from calibration readings supplied by the user.

The Decode Report forms a convenient summary of the data obtained during a deployment. It also provides a rough indication of wave activity in the file by printing the maximum signal range in millibars of the channels in the record. The internal calibration readings are also presented; in this case the true values were 2000 and 4000 millivolts. (The first pair are from the beginning of the record, and the second from the end.) Excessive deviation is automatically flagged by the 'Cal' column,where F means no error. While evaluating pressure values 'Decode' has to restore the full 12 bit precision of the readings from the least significant 8 bits that are available from the

```
"          Wave recorder : WR1,  System No.2  :                1"
"       Mod standard     :      Deployment 6  :                0"
"           Location     :  Elmer, W. Sussex  :                0"
"  Transducer layout     :    WR1-0079 iss A  :                0"
"  Time/Date 1st rdg     : 06 Jul 92 1734:33  :                0"
"Data element values     : Abs pressures, mb  :                1"
" Data array columns     :     6, ch2 to ch7  :                6"
"    Data array rows     : 1356,sim.rdg sets  :             1356"
"   Reading interval     :           500 ms   :              500"
"Tr. o/s errors used     : 40,-48,33,-2,74,4  :                0"
"    File created by     :          DECODE4   :                0"
"             Version    :  4.1      3.7.92   :                0"


 1408 1415 1437 1425 1428 1416
 1410 1417 1433 1425 1429 1418
 1410 1415 1432 1424 1429 1421
 1407 1413 1431 1425 1429 1427
 1405 1411 1432 1424 1427 1428
 1404 1410 1430 1425 1424 1426
 1403 1409 1428 1427 1424 1423
 1403 1409 1427 1431 1424 1421
 1402 1410 1430 1432 1426 1419
 1402 1411 1433 1431 1427 1417
 1403 1412 1436 1430 1427 1418
 1403 1411 1437 1431 1423 1419
```

Figure 3.7 : First few lines of a 'decoded' file (D6O4R1.A00)

```
 Program running   :  DECODE4
         version   :   4.1        3.7.92
              at   :  29 Jun 93 120S:54

Operation start at:  02 Jul 92 2033:30
RTC error factor   :  1.00000000
```

I/P FILE	O/P FILE	FIRST RDG AT	Prange /mb	ERRORS Rng	ERRORS Cal	CAL VOLTAGES/mV 0,0	0,1	1,0	1,1
C:\WR1\DATA\D6O4R1.P00	.A00	06 Jul 92 1734:33	29	F	F	1999	3995	1999	3996
C:\WR1\DATA\D6O4R1.P01	.A01	06 Jul 92 2034:35	25	F	F	1997	3996	1999	3996
C:\WR1\DATA\D6O4R1.P02	.A02	06 Jul 92 2334:37	12	F	F	1999	3995	1999	3996
C:\WR1\DATA\D6O4R1.P03	.A03	07 Jul 92 0234:39	29	F	F	1998	3995	1999	3995
C:\WR1\DATA\D6O4R1.P04	.A04	07 Jul 92 0534:41	22	F	F	1999	3995	1999	3996
C:\WR1\DATA\D6O4R1.P05	.A05	07 Jul 92 0834:43	27	F	F	1998	3995	1999	3996
C:\WR1\DATA\D6O4R1.P06	.A06	07 Jul 92 1134:45	4	F	F	1999	3995	1999	3996
C:\WR1\DATA\D6O4R1.P07	.A07	07 Jul 92 1434:47	26	F	F	1999	3996	1999	3996
C:\WR1\DATA\D6O4R1.P08	.A08	07 Jul 92 1734:49	41	F	F	1997	3995	1999	3996
C:\WR1\DATA\D6O4R1.P09	.A09	07 Jul 92 2034:51	37	F	F	1999	3995	1999	3996
C:\WR1\DATA\D6O4R1.P10	.A10	07 Jul 92 2334:53	5	F	F	1999	3995	1999	3996
C:\WR1\DATA\D6O4R1.P11	.A11	08 Jul 92 0234:55	24	F	F	1998	3995	1999	3996
C:\WR1\DATA\D6O4R1.P12	.A12	08 Jul 92 0534:57	41	F	F	1997	3995	1999	3996
C:\WR1\DATA\D6O4R1.P13	.A13	08 Jul 92 0834:59	35	F	F	1997	3995	1999	3996
C:\WR1\DATA\D6O4R1.P14	.A14	08 Jul 92 1135:01	8	F	F	1999	3995	1999	3996
C:\WR1\DATA\D6O4R1.P15	.A15	08 Jul 92 1435:03	23	F	F	1999	3995	1999	3996
C:\WR1\DATA\D6O4R1.P16	.A16	08 Jul 92 1735:05	33	F	F	1997	3995	1999	3996
C:\WR1\DATA\D6O4R1.P17	.A17	08 Jul 92 2035:07	36	F	F	1999	3995	1999	3996
C:\WR1\DATA\D6O4R1.P18	.A18	08 Jul 92 2335:09	15	F	F	1999	3995	1999	3996
C:\WR1\DATA\D6O4R1.P19	.A19	09 Jul 92 0235:11	15	F	F	1999	3995	1999	3996
C:\WR1\DATA\D6O4R1.P20	.A20	09 Jul 92 0535:13	30	F	F	1997	3995	1999	3996
C:\WR1\DATA\D6O4R1.P21	.A21	09 Jul 92 0835:15	33	F	F	1999	3995	1999	3996
C:\WR1\DATA\D6O4R1.P22	.A22	09 Jul 92 1135:17	21	F	F	1997	3995	1999	3996
C:\WR1\DATA\D6O4R1.P23	.A23	09 Jul 92 1435:19	18	F	F	1999	3995	1999	3996
C:\WR1\DATA\D6O4R1.P24	.A24	09 Jul 92 1735:21	31	F	F	1999	3995	1999	3996
C:\WR1\DATA\D6O4R1.P25	.A25	09 Jul 92 2035:23	28	F	F	1997	3995	1999	3996
C:\WR1\DATA\D6O4R1.P26	.A26	09 Jul 92 2335:25	25	F	F	1997	3996	1999	3996
C:\WR1\DATA\D6O4R1.P27	.A27	10 Jul 92 0235:27	8	F	F	1997	3995	1999	3996
C:\WR1\DATA\D6O4R1.P28	.A28	10 Jul 92 0535:29	24	F	F	1997	3995	1999	3996
C:\WR1\DATA\D6O4R1.P29	.A29	10 Jul 92 0835:31	19	F	F	1999	3995	1999	3996
C:\WR1\DATA\D6O4R1.P30	.A30	10 Jul 92 1135:33	24	F	F	1998	3995	1999	3995
C:\WR1\DATA\D6O4R1.P31	.A31	10 Jul 92 1435:35	8	F	F	1997	3996	1999	3996

Figure 3.8 : Decode Report for D6O4R1.Ann

datastore. Any errors in this process discovered by the program's checking routines are flagged in the 'Rng' column.

The decoded files form the output of the wave recording system: pressure readings that contain all available calibration corrections and context information. The files are in ASCII, and may therefore be inspected and printed using a text editor or DOS commands. They may also be read into analysis programs written in languages such as Fortran or Basic, or into proprietary analysis packages.

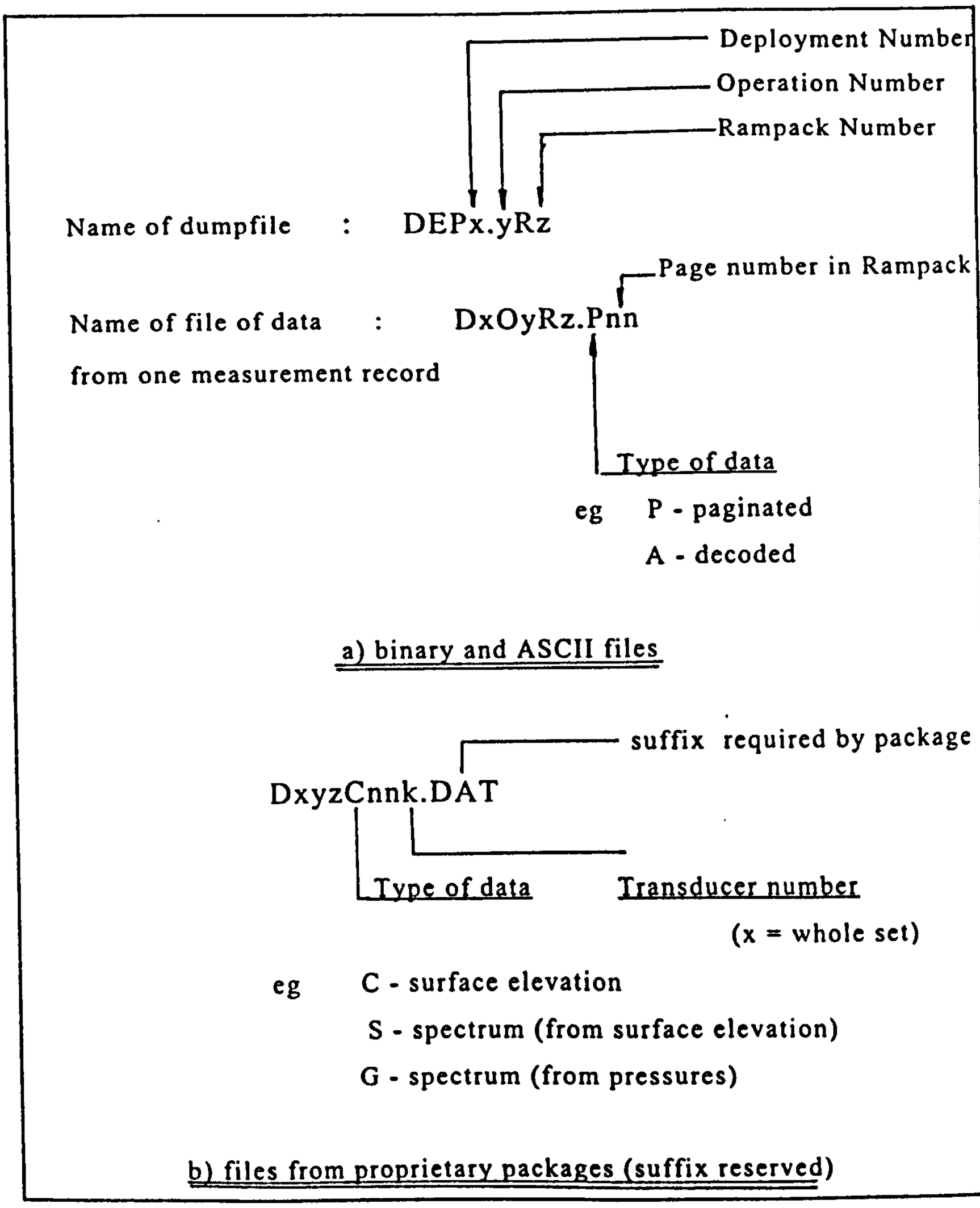

Figure 3.9 : Filename conventions

Managing the data

A typical deployment generates several hundred measurement records, each yielding a paginated file and a decoded pressure file. Further analysis creates many other data sets, such as surface elevations and spectral densities. Applying just the basic analysis steps generates many thousands of files, adding up to many hundreds of megabytes, per deployment. However it is important to be able to connect all related information to the corresponding data files (Driver 1980b). Figure 3.9 indicates how filenames are constructed (within MS DOS constraints) to preserve traceability.

Examples of other information that must be related to the data are:-

i) *Fieldwork notes:* Records of any fieldwork event such as placing platforms, deploying and recovering the system, recovering data. Times and dates, actions, commands and responses, personnel, notes of any difficulties, and special observations are recorded on a 'fieldwork record sheet'.

ii) *Site survey data:* Plans of the site; EDM, levelling and tape survey data; drawings of structure and transducer locations worked up from the data.

iii) *Equipment modification standard:* Drawings of transducer layout, serial numbers and cable numbering, and modification standards of hardware and operating software.

iv) *Calibration and test data:* Records of transducer calibration in the laboratory; printouts and associated calculations for system test data taken in the laboratory; calculations on accuracy of still water level measurements and real time clock value made from field data during deployment; and survey data on transducer positions.

v) *Observations:* Independent measurements or observations of related factors such as tides, wave height and period, direction, atmospheric pressure etc.

REFERENCES

Bird P.A.D. (1992)
University of Plymouth Wave Recording System - Operators Manual
School of Civil and Structural Engineering Report No. SCSE 92-007
Sept '92.

Rendell F. (1989)
Survey of transducer network at Plymouth Breakwater site
Polytechnic South West, Department of Civil Engineering Report, June '89.

Driver J.S. (1980a)
A Guide to sea wave recording
IOS Report No 103, ch 5, 'Data recording'
IOS Wormley, Godalming, UK.

Driver J.S. (1980b)
A Guide to sea wave recording
IOS Report No 103, ch 7, 'Operational techniques'

CHAPTER 4
DATA ANALYSIS

CHAPTER 4
DATA ANALYSIS

4.1 INTRODUCTION

The subject of this chapter is the analysis of the data from measurements already described, with the aim of extracting as much information as possible about the wave conditions and on the properties of the adjacent coastal structure.

The approach taken is governed by the overall measurement objectives:

1) To estimate the incident wave spectrum from pressure records at fixed locations in a reflective wave field.
2) To provide time records showing the movement of individual crests as suitable 'input data' for other measurements, for example of wave impact, loading, aeration and wave transformation, and
3) To estimate the wave reflection properties of the nearby coastal structure.

The measurement of long-term wave statistics is one which could be achieved by the wave recorder, but is less relevant to this study.

The analysis is carried out on complete data sets rather than data arriving in real time, so plenty of processing time on powerful desk-top personal computers was available. Signal processing techniques directed towards optimising processing time are therefore of less interest than those aimed at extracting maximum possible information from the data.

The analysis is implemented using a range of software tools: most routines required the flexibility of a high level language such as Fortran and the functional power of a signal analysis package. (ASYST^R from Keithley Instruments was used initially, and subsequently MATLAB^R from MathWorks Inc.) Interactive packages were more convenient for first examination of records, and quick testing of new ideas before more rigorous coding.

A great deal is known about the behaviour of waves in a deterministic sense from the study of hydrodynamics; the salient results of the wave theories are presented in the next section. This serves to define the nomenclature and conventions adopted, and to present relevant results of theory for convenient reference. In Section 4.3 deterministic wave theory is used to derive water surface elevation records from the sub-sea pressure records. Section 4.4. contains a review of methods for estimating the directional wave spectrum, and in 4.5 an analysis scheme is described that incorporates the most appropriate of these methods.

The selection of the analysis tools and details of the methods of application are as much a matter of engineering judgement as mathematical rigour. Each technique draws out certain features of the data, but each has weaknesses in particular situations. The underlying processes and the overall measurement problem must be carefully idealised or modelled. One way of thinking about the problem is as follows: an unknown, stochastic, input signal (the incident, irregular, wave field) is applied to a system (sea-bed and structure of known geometric form). The system transforms the input in what may or may not be a linear fashion to provide an output, the reflected wave field. The observations available are the time records of surface elevation from the mixture of incident and reflected wave fields, taken at a sample of six locations fixed with respect to the structure. The problem is therefore one of system identification: one wants to know what the system is doing to the input. The experimenter does not have control over the choice of input, although after a long deployment a considerable variety of inputs will have been applied.

Another approach is to attempt to separate incident from reflected waves from the observed data alone, without reference to any knowledge of the structure (Kajima, 1969, Gilbert and Thompson, 1978). It was not clear at the outset to what extent that was possible in the case of an unknown angle of approach.

However, in each case the objective is to analyse or decompose a measured sea state into its components. The whole wave pattern is thus to be expressed in the form of a distribution over frequency and direction: the directional wave spectrum.

4.2 WATER WAVES

Waves on the surface of the sea are caused by wind (wind waves), the pull of the moon and sun (tides), underwater earthquakes and volcanoes (tsunamis), and the motion of ships (wakes). The shortest in period are capillary waves and the longest are the tides. Wind waves have periods within the range of 1 to 30 seconds, although they can undergo processes at the shoreline to produce oscillations of up to several minutes period. Figure 4.1 classifies ocean waves by their period, and gives an indication of the typical amplitudes of each type. The range of period from about 3 to 20

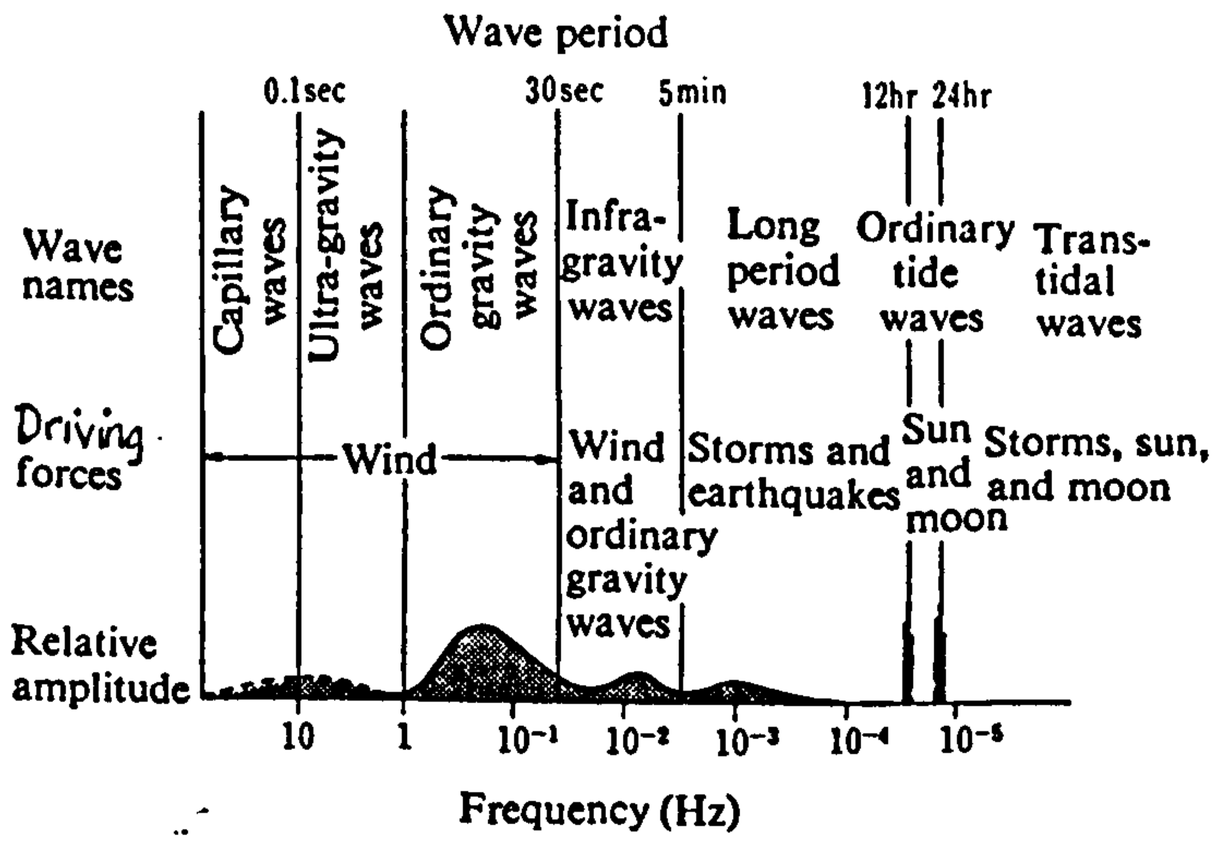

Figure 4.1 : Classification of ocean waves according to wave period (from Horikawa,1978)

seconds is of most interest here. The term gravity waves is also used for these waves from the restoring force that drives them.

The way these waves behave, and the mathematical descriptions of them, are not simple. Propagation is dispersive so that wave speed, and consequently length, are functions of period and depth. Thus in the area of a storm a wide range of wave frequencies is generated creating a confused water surface ('sea'), but at a distant shoreline the longer period waves arrive first so there a more regular wave pattern ('swell') is seen.

As they approach shallower coastal waters waves undergo changes, collectively known as wave transformation. Speed and length decrease and the profile alters from approximately sinusoidal to one of sharper peaks and longer troughs, until in the limit breaking occurs. Speed changes resulting from dispersion in regions of uneven depth lead to refraction. Reflection occurs at obstacles and other discontinuities such as sand bars, and diffraction occurs around them.

4.2.1 Deterministic wave theories

Because of this complex behaviour a complete and general mathematical theory describing waves in all conditions has not yet been devised. The principal difficulty is that one of the boundary conditions, the free surface, is one of the unknowns. So far, a number of theories has been developed, each describing with greater or lesser accuracy waves in particular conditions. All the theories mentioned below assume that water is incompressible and inviscid.

Wave motion may be divided into two main categories: oscillatory, in which there is no net mass transport (except for second order effects), for example wind generated waves, and translatory, for example tidal bores. The former have been sub-divided into small amplitude waves, finite amplitude waves, and long waves. The small amplitude wave equations are linear in wave height enabling superposition of simple components to form more complex

wave patterns. If the assumption of small amplitude is not valid then a better description will be provided by the higher order, non-linear, theories such as those of Stokes, and cnoidal theory. Long wave theory describes the behaviour of tides, and wind waves in very shallow water.

Selection of an appropriate theory to use depends on the relative values of three parameters: wave height H, wave length L and the mean depth d (Fig 4.4). These are combined into wave steepness H/L, relative height H/d, and relative length L/d (or its reciprocal d/L the relative depth). In deep water it is the steepness that matters most: if that is not too great then small amplitude, linear, theory provides good results. The sinusoidal form of 'linear' waves is shown in Figure 4.2 a). From fundamental hydrodynamics the constraint $H/L < 1/16 \tanh 2\pi d/L$ ensures that the non linear terms in H are less than 5% (Komar, 1976, Muir-Wood, 1969). For steeper waves the higher order Stokes equations fit better (Figure 4.2 b). In shallow water relative height is most significant; linear theory applies if that is small, and cnoidal theory if not (Figure 4.2 c). For intermediate depths the Ursell

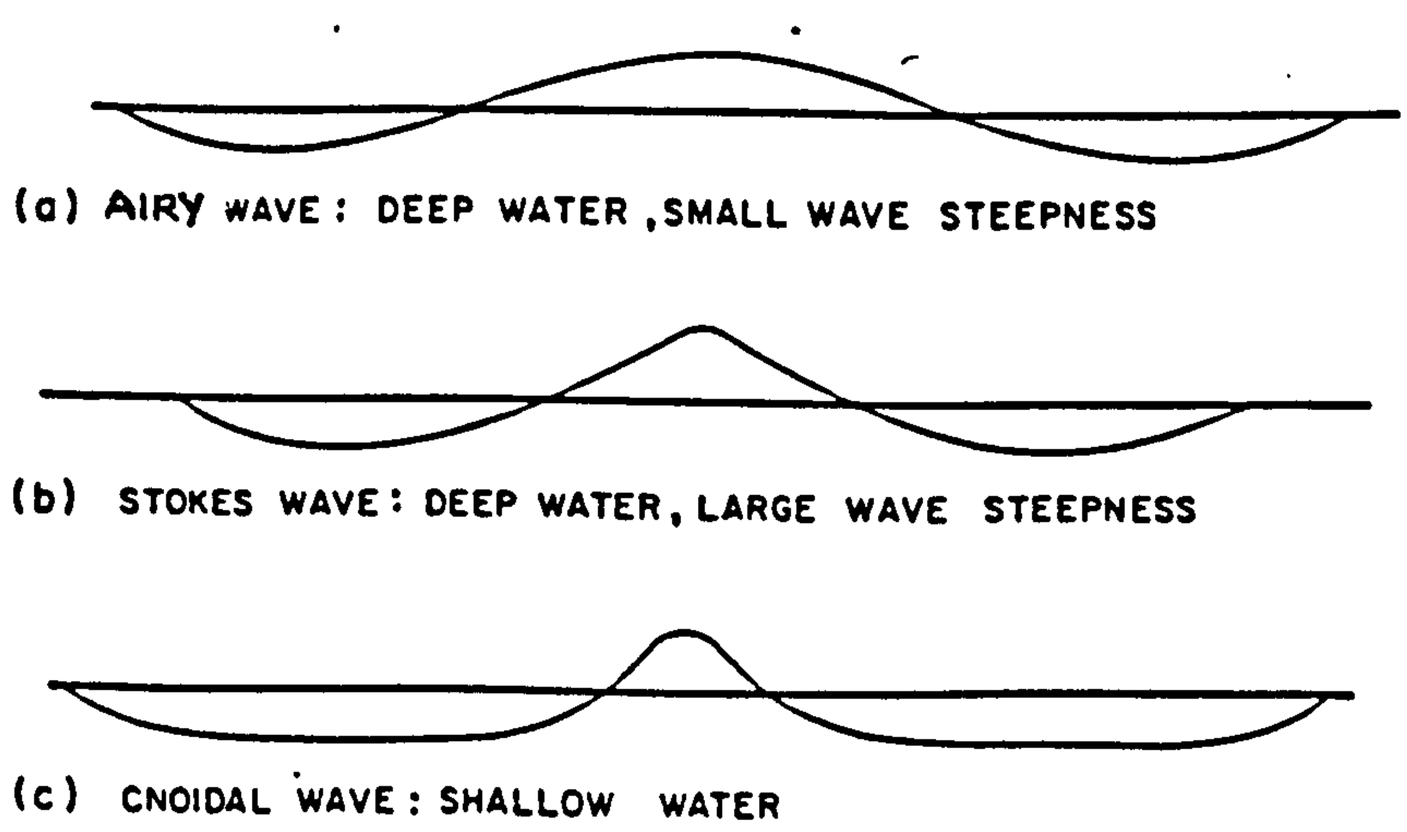

Figure 4.2 : Wave profiles from major wave theories

parameter, U_r, $\frac{1}{2(2\pi)^2}\left(\frac{H}{L}\right)\left(\frac{L}{d}\right)^3$ (of the form steepness x the cube of relative length) is the guide as it is a measure of the relative importance of the type of flow which leads to terms in H^2. Linear theory will produce acceptable results if this parameter is sufficiently small (Ursell, 1953). Longuet-Higgins (1956) quantified this limit suggesting $HL^2/d^3 < 32\pi^2/3$. Long wave theory is not relevant to the data to be analysed in this work.

Much work has been done to estimate the ranges of applicability both experimentally and numerically of the theories (Horikawa 1978, Sarpkaya and Isaacson 1981). The motivation is often to show that linear theory may be applied in particular circumstances since most analysis techniques are founded on the assumption that complex waves are the superposition of independent sinusoidal components. Komar (1976) and LeMehaute (1976) have presented charts that predict theoretically the expected ranges of validity of the theories. Sarpkaya and Isaacson's redrawing of the latter in non-dimensional form is reproduced here in Figure 4.3. Guza and Thornton

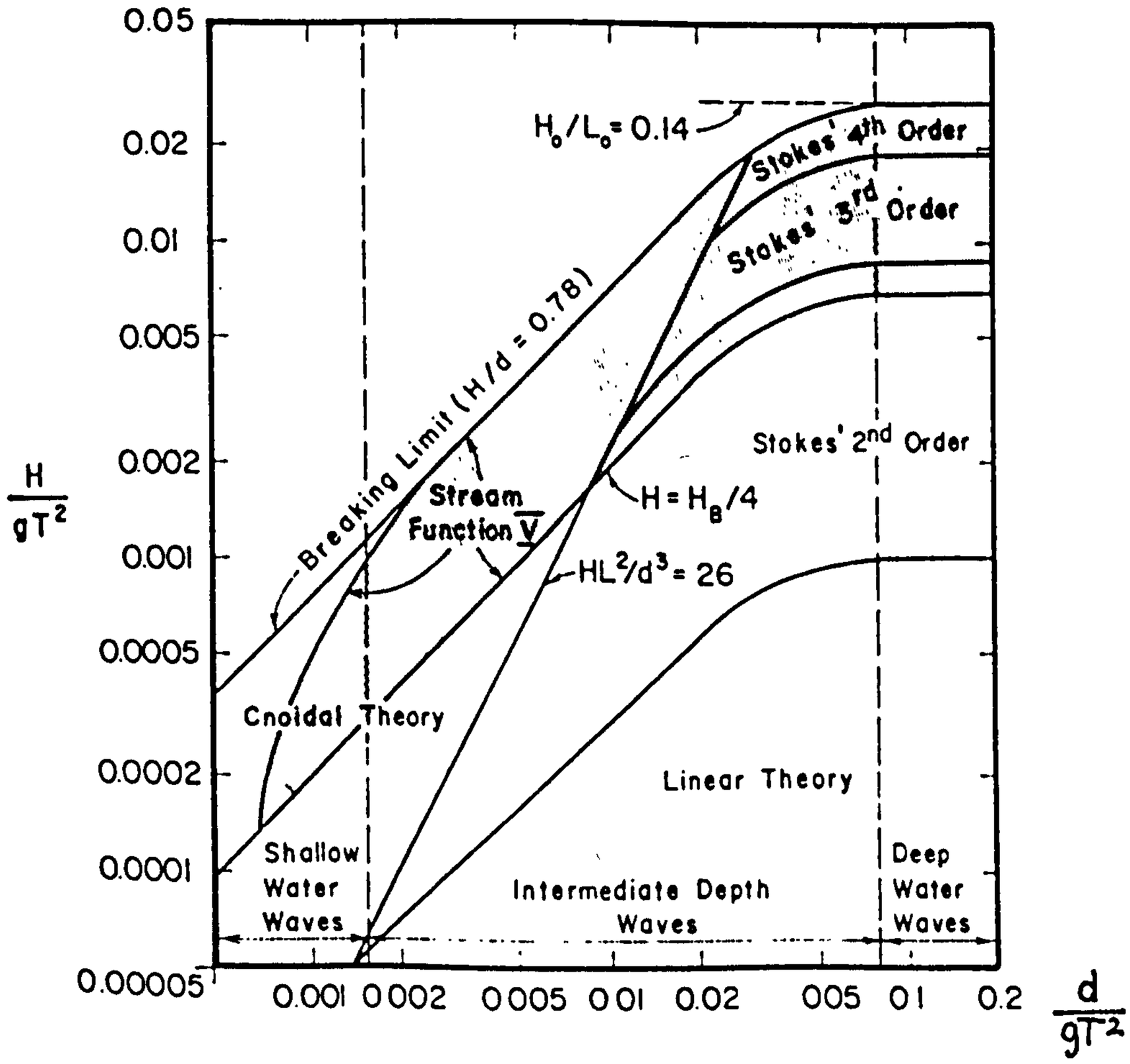

Figure 4.3 : Ranges of suitability of various wave theories (Sarpkaya and Isaacson, 1981)

(1980) investigated the performance of linear theory in a series of measurements of surface elevations, pressures and currents over a beach, from the region of wave breaking to a depth of 10m. Wave frequencies were between 0.05 and 0.3 Hz, and Ursell numbers less than 0.05 in 10m up to numbers much greater than unity in 1m in the area of breaking. At a point, comparison of measured surface elevation to that predicted from sub-surface pressure was reasonably good until close to the region of breaking. Guza and Thornton point out that the accuracy of the theory depends on which of the parameters are compared, and that errors due to any weak non-linearity accumulate over distance as the waves shoal towards the beach.

4.2.2 Small amplitude (linear) wave theory

Developed by George B. Airy in 1845 this theory assumes the wave height to be sufficiently small in comparison to other dimensions that terms in H to the power two or more are negligible. The equations for surface elevation are therefore linear in H and are relatively easy to solve. The principle of superposition applies, and a complex sea state may be modelled as a combination of sinusoidal, long-crested wave trains of different heights and directions of propagation. Linear theory has been used for most of the analysis described in this chapter.

Figure 4.4 defines a coordinate system and the relevant wave parameters. The single period wave component (also known as a 'regular wave') is long-crested: there is no variation in the y direction, all motion is 2-dimensional. The parameters are:-

H	wave height, crest to trough. (Amplitude is therefore $H/2$.)
L	wave length
d	depth, mean water level (MWL) to sea-bed.
η	instantaneous surface elevation relative to MWL.

In addition to those on the diagram are:-

T	wave period

c	wave speed, (also known as celerity and phase velocity). From the definitions of L and T, $c=L/T$.
c_g	group 'velocity' (the speed at which wave groups, and energy, travel).
p	pressure (function of x,z and t).
Φ	velocity potential (function of x,z and t).
V	particle velocity, **V** = -grad Φ.

Some of these parameters are commonly expressed in alternative forms:-

k	wave number = $2\pi/ L$
f	wave frequency = $1/T$
ω	radian frequency = $2\pi f$

so that $c = \omega/k$.

The theory predicts wave speed, length, group velocity, particle velocities and displacements, shape of the free surface, pressures and average energy

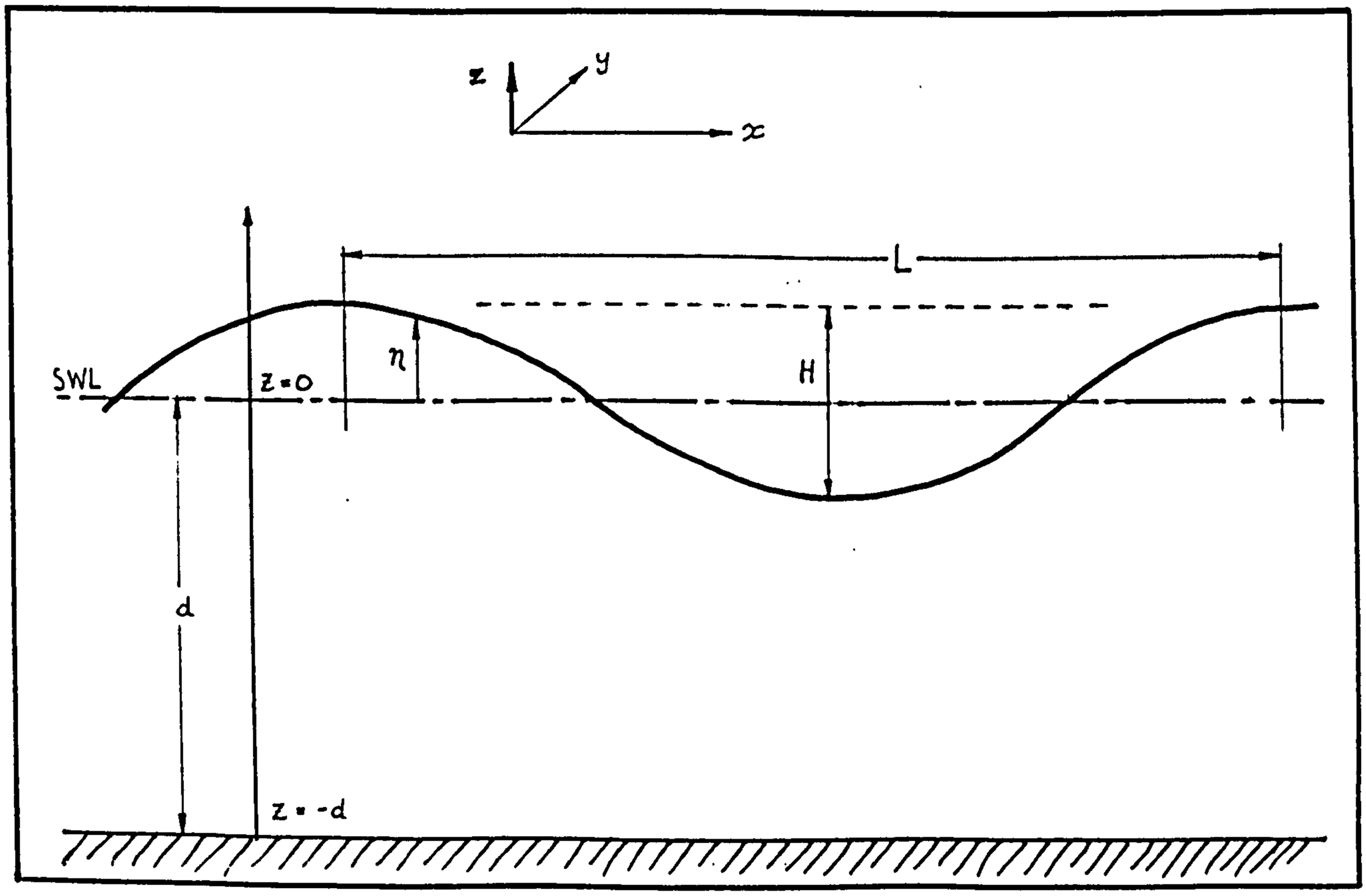

Figure 4.4 : Coordinate system and definition of variables

	Full Expression	Approximation for deep water, $d/L > 0.5$ $(L/d < 2)$	Approximation for shallow water $d/L < 0.05$ $(L/d > 20)$
Free surface	$\eta = \frac{H}{2}\cos(\omega t - kx)$	(relatively short waves) ($\tanh(x) \to +1$)	(relatively long waves) ($\tanh(x) \to (x)$)
Dispersion relation	$\omega^2 = gk\tanh(kd)$		
Wave length	$k = \omega^2/g\tanh(kd)$ or $L = \frac{gT^2}{2\pi}\tanh\left(\frac{2\pi d}{L}\right)$	$L = \frac{gT^2}{2\pi}$	$L = T\sqrt{gd}$
Wave speed (or celerity) $(c = L/T = \omega/k)$	$c^2 = g/k\tanh(kd)$ or $c = \left[\frac{gL}{2\pi}\tanh\left(\frac{2\pi d}{L}\right)\right]^{1/2}$ $= \frac{gT}{2\pi}\tanh\frac{2\pi d}{L}$	$c = \frac{gT}{2\pi}$ (for metres, seconds, $c = 1.56T$)	$c = \sqrt{gd}$
Sub-surface pressure at z	$p = -\rho g z + \frac{\rho g H}{2}\frac{\cosh k(d+z)}{\cosh kd}\sin(\omega t - kx)$	$p = -\rho g z + \rho g \frac{H}{2} e^{kz}\sin(\omega t - kx)$	$p = -\rho g z + \rho g \frac{H}{2}\sin(\omega t - kx)$

flux in terms of the basic parameters *T*, *H*, *L*, and *d*. Each of the resulting expressions may be simplified, both for deep and for shallow water. Table 4.1 gives some of these results in full and simplified forms.

It can be seen that:

i) The shape of the wave profile is sinusoidal.

ii) The function for wave length is implicit, and so has to be solved numerically.

iii) As depth reduces the waves get shorter. Since the period is unchanged they also slow down.

iv) In deep water wave length and speed are functions of period but not depth. This dispersion causes the surface pattern in a complex sea to change as the constituent sinusoidal waves envisaged by the theory move in and out of phase.

v) In shallow water speed is a function of depth but not period. There is no dispersion.

vi) Pressure below the surface has a hydrostatic component proportional to distance below surface, and a component caused by the wave. The latter diminishes in amplitude with increasing depth and wave frequency. Pressure variation at a point is at the same frequency as the wave, and is in phase. (The absence of phase shift is an important property for this work as any phase lag between pressure and surface elevation would have made it difficult to base a directional wave recorder on pressure measurement alone.)

Expressions for more complex sea states formed by adding these sinusoidal components together can be derived using basic trigonometrical identities. For example a standing wave is produced by adding two components equal in size and frequency but travelling in opposite directions, such as occurs with perfect wave reflection. Less perfect reflection produces a partial standing wave. Two similar waves moving in slightly different directions produce a short crested sea, with humps and hollows appearing in a diamond shaped pattern. Two waves of slightly different frequency produce the familiar 'beating' interference pattern at the difference frequency,

resembling a series of groups of waves. Owing to the dispersive nature of wave propagation the groups move more slowly than the wave crests making up the group.

4.2.3 Wave Reflection

When waves meet an obstruction, the part of their energy that is not dissipated (by mechanisms such as wave breaking) or transmitted (through a porous structure or by overtopping) is reflected. The degree of reflection is characterised by a 'reflection coefficient'. In general the reflection coefficient is a strong function of wave frequency, and is also dependent upon the shape, roughness and porosity of the reflecting surface.

For regular waves the reflection coefficient may be defined simply as the ratio of reflected to incident wave height:

$$C_r = H_r / H_i \tag{4.1}$$

For random waves the frequency dependency of the reflection coefficient is acknowledged by the modified definition:

$$C_r = \sqrt{\frac{E_r}{E_i}} \tag{4.2}$$

where E denotes the energy (proportional to H^2) integrated over the frequency band of gravity waves.

Perfect 2D reflection from a wall

A vertical, smooth, non-porous wall rising from a flat sea-bed will reflect all incoming wave energy, and for linear, regular waves produce the classic pattern of nodes and anti-nodes shown in Figure 4.5. This form is derived analytically by adding the incident wave

$$\eta_i = \frac{H_i}{2}\cos(\omega t - kx) \tag{4.3}$$

to the reflected wave

$$\eta_r = \frac{H_r}{2}\cos(\omega t + kx) \tag{4.4}$$

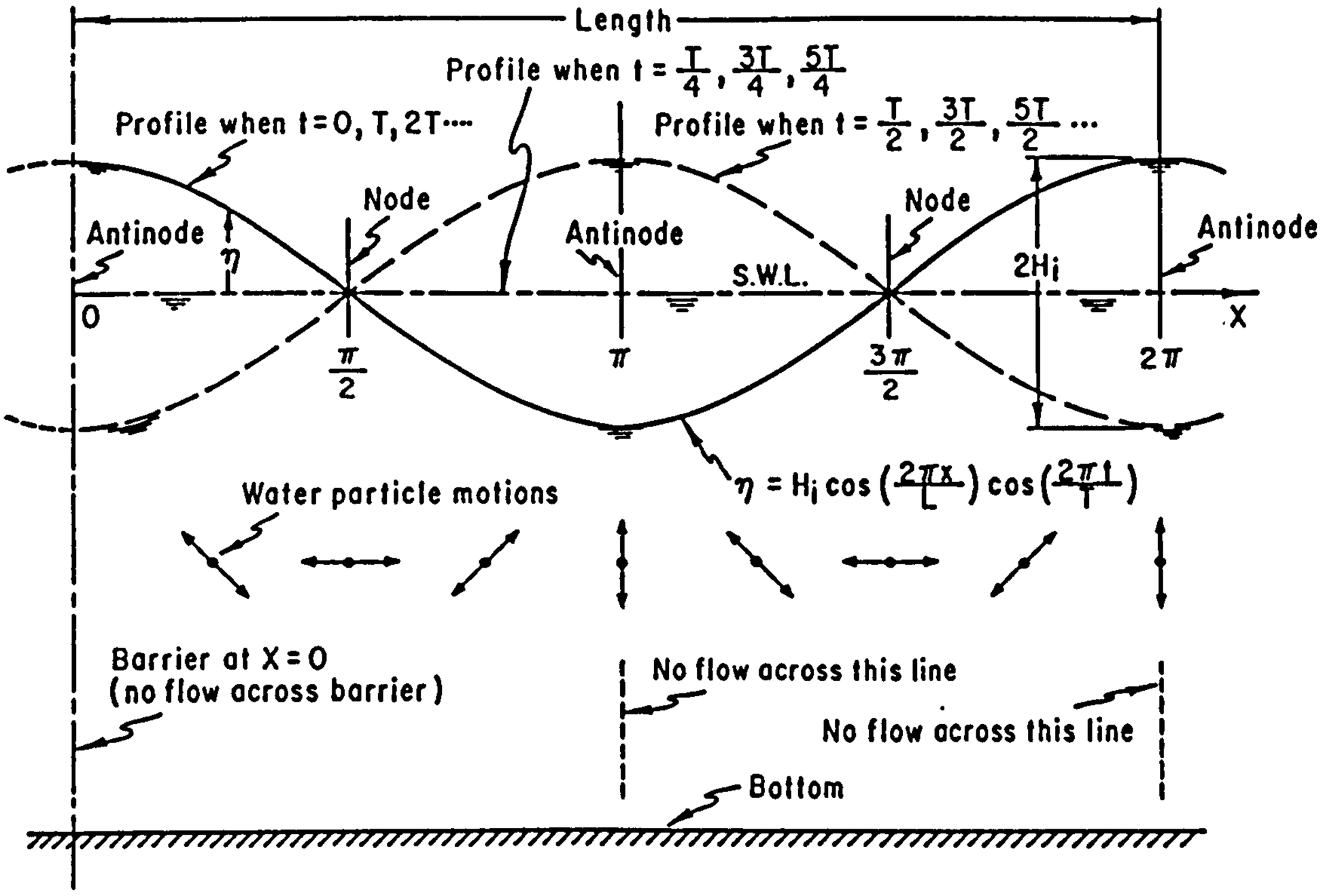

Figure 4.5 : Standing wave system, perfect reflection from a barrier

to give for Hi = Hr

$$\eta = H_i \cos(kx) \cos(\omega t) \tag{4.5}$$

Terms in time and distance are separate so the water surface motion is sinusoidal, and at all places in phase except for the changes of sign between adjacent pairs of nodes.

Perfect 2D reflection from a sloping surface

As has been noted the length and speed of waves decrease as they move into shallower water. Therefore if regular waves encounter a sloping structure such as a beach or a breakwater then the node and antinode positions will be more closely spaced inshore than offshore. In the absence of breaking and other energy dissipating mechanisms the reflection coefficient will be unity.

Lamb (1932) solved the linear long wave equations for this case, and Friedrichs (1948) the linear small-amplitude equations. Both predict a nodal structure which is described in terms of zero-order Bessel functions. Amplitudes are given as a function of offshore distance x by:

$$\eta_{pk} = a J_0\left(2\omega\sqrt{\frac{x}{g\tan\beta}}\right) + b\, Y_0\left(2\omega\sqrt{\frac{x}{g\tan\beta}}\right) \qquad (4.6)$$

where a and b are coefficients with dimension length determined by the boundary conditions. Hotta *et al* (1981) developed a method of predicting nodal structure over a double slope (although their interest was primarily in waves of period greater than 15 seconds). Simultaneous equations for amplitude (of the form in Equation 4.6) and particle velocity on each slope were solved with the constraint that those quantities respectively match across the slope intersection line. Davidson (1993) has extended this solution to more complex slopes, enabling the modelling of breakwaters fronted by a berm.

Partial 2-D reflection

If some of the energy is dissipated or transmitted then the reflection coefficient will be less than unity. The equations describing such water behaviour are complicated and not, in general, linear. However in less extreme conditions it may be possible to consider the overall effect of these mechanisms as a linear process when observed from a distance. That is to say the process may be regarded as a 'black box' which produces an output that is related to its input according to the normal criteria for linearity. If the incident waves are modelled as the sum of sinusoidal components, the linear process applies fixed amplitude and phase changes to each component according to its frequency, and independently of the size of the other components. However, in many cases these simplifications will not apply, and non-linearity must be taken into account in interpreting the data and characterising the performance of the structure.

The amplitude change imposed by the black box is equivalent to the reflection coefficient. For the two-dimensional case, at a sufficient distance

from the structure for linear wave theory to apply, the incident and reflected waves add to form a mixture of standing and progressive waves. There will be regions of lower amplitude waves at partial nodes and enhanced amplitude waves at partial antinodes. To the eye the crests appear to perform a 'swooping' motion as they pass slowly through the antinodes and quickly through the nodes. Combining the incident and reflected waves of Equations 4.3 and 4.4 gives:

$$\eta = H_i \cos(\omega t - kx) + H_r \cos(\omega t + kx) \qquad (4.7)$$

but in this case $H_r < H_i$.

From this it may be shown (Sarpkaya and Isaacson, 1981) that

$$H_{max} = H_i + H_r \qquad (4.8)$$

and $$H_{min} = H_i - H_r \qquad (4.9)$$

so that if H_{max} and H_{min} are estimated (conveniently done in the laboratory by a travelling wave gauge) then H_i and H_r , and hence r, may be found.

The question of whether waves would break or not on a sloping beach was addressed by Miche (1944), who postulated that waves below a critical steepness while in deep water would not break. Reflection in that case would be complete. Waves of greater than the critical steepness would break. Miche envisaged a process of saturation in which reflected wave height increases with the incident wave height until the latter reaches critical steepness. The reflected wave height then stays at that level even as incident wave height and steepness rise further. Miche's critical steepness, a function of beach slope angle β is:

$$\left(\frac{H_o}{L_o}\right)_{crit} = \left(\frac{2}{\pi^3}\right)^{\frac{1}{2}} \tan^{\frac{5}{2}}\beta \qquad (4.10)$$

where the subscript *0* denotes the deep water value.

The Iribarren number is often used as a predictor of the degree of reflection at a slope:

$$I_r = \tan\beta / \left(\frac{H_{i,0}}{L_0}\right)^{\frac{1}{2}} \qquad (4.11)$$

These methods assume substantially monochromatic waves; the position is complicated for waves of two or more components of widely separated frequencies. The tendency of a small wave component to break will be affected by the presence of a larger component of different frequency. Detailed examination of the wave reflection properties of structures is outside the scope of this work.

Non-normal incidence

Waves approaching a vertical structure obliquely reflect from it so that the angle of reflection is equal to the angle of incidence. The corresponding crests and troughs take on a diamond pattern which appears to propagate *along* the structure. The corresponding geometry is described by Silvester (1974), and Sarpkaya and Isaacson (1981, pp254-256). Reflection of oblique waves from gently sloping structures such as beaches is considerably more complex, the description given by Guza and Bowen (1975) involving confluent hypogeometric functions.

The first term is the hydrostatic component, and the second and third are due to the waves, with the third term being the contribution of local kinetic energy. This, being of second order, is usually ignored leaving the signal component (denoted by the prime):

$$p' = \rho \frac{\partial \Phi}{\partial t} \tag{4.13}$$

The profile of a linear progressive wave of height H and radian frequency ω is:

$$\eta(x,t) = \frac{H}{2} \cos(\omega t - kx) \tag{4.14}$$

and the pressure signal becomes:

$$p' = \rho \frac{\partial \Phi}{\partial t} = \frac{\rho \eta \omega^2}{k} \frac{\cosh k(d+z)}{\sinh(kd)} \tag{4.15}$$

Substituting the dispersion relation (Table 4.1)

gives:

$$p' = \rho g \eta \frac{\cosh k(d+z)}{\cosh(kd)} \tag{4.16}$$

or in terms of head of pressure:

$$\frac{p'}{\rho g} = \eta \frac{\cosh k(d+z)}{\cosh(kd)} \tag{4.17}$$

a sinusoid of peak-to-peak magnitude

$$H_p = H \frac{\cosh k(d+z)}{\cosh(kd)} \tag{4.19}$$

The subsurface peak-to-peak pressure head at depth z is therefore equal to wave height multiplied by a factor related to wavenumber k (and hence frequency) and mean water depth z. This factor, termed the 'pressure attenuation factor', is graphed in Figure 4.6 for several mean depths. The severe attenuation of higher frequency waves in depths over about 20 metres imposes limitations on the sensing of waves by sub-surface pressure. In order to predict the wave height from measured pressure head Equation 4.19

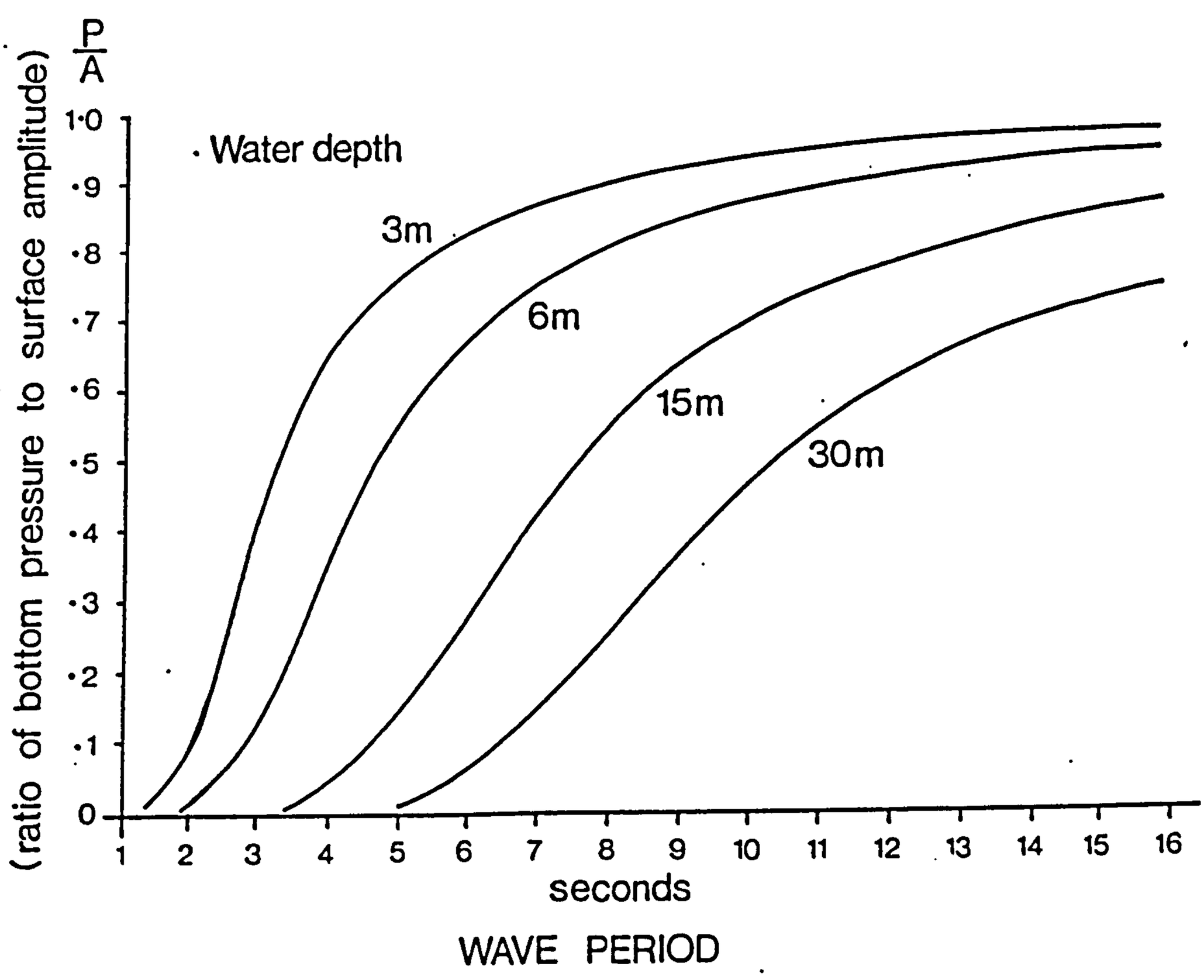

Figure 4.6 : Wave pressure attenuation with frequency and depth (from Driver, 1980)

is transposed to give Equation 4.20 in which the subscript 'a' denotes that the estimate has been obtained with linear (Airy) theory.

$$H_a = H_p \frac{\cosh kd}{\cosh k(d+z)} \tag{4.20}$$

The assumption of linearity enables the pressure attenuation factor (which is derived above for a single sinusoid) to be applied frequency by frequency to a complex sea composed of many such components.

4.3.3 Review of experimental work

Since pressure transducers were first used to sense waves there has been a need to establish the accuracy of conversion of measured pressure to surface conditions. Unfortunately the accuracy was not found to be particularly good in certain cases, and many studies have been carried out since to

determine both the sources of error, and possible methods of correction. Most writers introduce a simple factor to account for all the shortcomings, whatever their causes. Normally designated '*N*' it is the ratio of actual wave height to that predicted by subsurface pressure and linear theory:

$$N = H / H_a \tag{4.21}$$

A value for *N* greater than unity therefore signifies an underestimate of height by the pressure method.

Disagreement on the size of the discrepancy can be gauged from the following comments:

> 'In Japan the value N = 1.3 to 1.35 is normally applied' (Horikawa, 1978)

and

> 'as more evidence has accumulated it is seen that the error can vary in different installations from nothing to as much as 20%, so nowadays the classical formula [Equation 4.20] is usually used to correct for depth attenuation, with the possibility of some error being borne in mind.' (Tucker, 1992).

Hom-ma *et al* (1966) conclude from their measurements that *N* is a function of relative depth *d/Lo*, taking a value of around 1.5 (field) or 1.2 (laboratory) for shallow water (*d/Lo* = 0.1), and reducing to around 0.6 (field and laboratory) for a relative depth of 0.7.

Grace (1978) from field measurements at Honolulu and laboratory measurements in a 100m flume shows a similar trend in *N* with relative depth, although with a smaller deviation from unity.

Cavaleri, Ewing and Smith (1978) carried out a comparison of pressures, velocities and heights taken at an instrumented tower near Venice, and presented the dependency of *N* upon frequency (after spectral analysis of the signals) rather than relative depth. Values for *N* range from 1.25 (at

0.11Hz) to 0.9 (at 0.23 Hz). They also confirm the predicted zero phase shift between pressure and surface.

Crabbe, Driver and Haine (1983) also analysed field results on a spectral basis, using a laser based device for surface elevation at the NMI tower in Christchurch Bay. They found a 10% underestimate (N = 1.1) at 0.6 Hz, falling through N=1 at 0.2 Hz and becoming smaller progressively with higher frequencies. Similar results were found by Lee and Wang (1984) from data obtained during the Atlantic Remote Sensing Land Ocean Experiment (ARSLOE).

Further work carried out by Bishop and Donelan (1987) has N ranging from 0.9 to 1.07, leading to the conclusion (after a careful review of possible sources of error) that '...a well designed pressure transducer system with proper analysis techniques should give estimates of surface wave height to within +/-5%'.

4.3.4 Reasons for a non-exact transformation

The factor N merely signifies that the two sets of measurements which were expected to agree in fact did not. It covers all sorts of imperfections, and all the investigators referred to above speculated on the causes of disagreement.

Measurement and analysis

Possibly receiving less than its full share of the blame is straightforward measurement error. The calibration of the pressure transducers in Grace (1978) showed an average 20% error. Although this was allowed for there was much scatter over the tests which undermines confidence in the corrected results. There have been significant improvements in transducer and signal processing performance since that time. Meniscus error in the surface piercing gauges is thought to lead to a -3mm error in H. Small wave heights at the higher frequencies will be proportionately the most affected, leading to a reduction in N in that region (Bishop and Donelan,

1987). It is interesting that the study using the laser surface gauge produced the smallest values for *N*. The presence of electrical noise will have the same effect: as the pressure signal drops off so markedly with frequency, so does the signal to noise ratio.

Following on from the measurements themselves, the data analysis can contribute small errors: the spectral leakage discussed later in Section 4.5 affects the transformation of the components of the pressure record adjacent to the spectral peaks preferentially, in this case tending to make N larger at higher frequencies.

Hydrodynamic factors

These include all the effects that result in the transducer diaphragm experiencing pressure changes other than those from the second term in Equation 4.12. For example the vertical kinetic energy term $\frac{1}{2}\rho w^2$ will produce such a deviation if the flow is forced to stagnate at the housing. Bishop and Donelan (1978) record a small influence of housing shape on pressure readings. Tucker (1992) draws attention to a consistent feature of the comparative studies: that *N* is nearer unity in tank tests than in the field, and he expresses the view that the local sea bed features are important. Any current present will also have an effect on the transformation due to the Doppler effect (Gabriel and Hedges, 1986).

Theoretical factors

The applicability of linear theory was discussed in Section 4.2. Any non-linearity in the waves will put the classical relationship of Equation 4.16 in error. If operating in significantly non-linear conditions it would be necessary to consider a more complicated conversion. Isaacson (1976) has implemented a numerical solution based on cnoidal theory. A digital filter that incorporates second order corrections, as well as water level changes due to set-up, has been developed by Wang, Lee and Garcia (1986). Fenton (1986) proposed a polynomial method of converting pressure to surface elevation.

In conclusion, the approach to be adopted here will be Tucker's - to assume a perfect linear theory correspondence between pressure and surface, not to apply an arbitrary *N*, but to be aware of the possible errors.

4.4 THE DIRECTIONAL WAVE SPECTRUM

4.4.1 Introduction

Underlying the concept of the directional wave spectrum is the idea that the wave system can be described as the superposition of a number (or in the limit a continuum) of simple free progressive wave components. For this idea to be valid each of the components must be a linear (Airy) wave. It may be specified by amplitude a, wavenumber vector $\mathbf{k}$, frequency ω, and phase (relative to some reference) ε.

A single such component is illustrated in Figure 4.7

The magnitude of the wave number, k, is a 'spatial frequency', with units of radians per metre. Its components along the axes are

$$k_x = k\cos(\theta) \quad \text{and} \quad k_y = k\sin(\theta)\ . \tag{4.25}$$

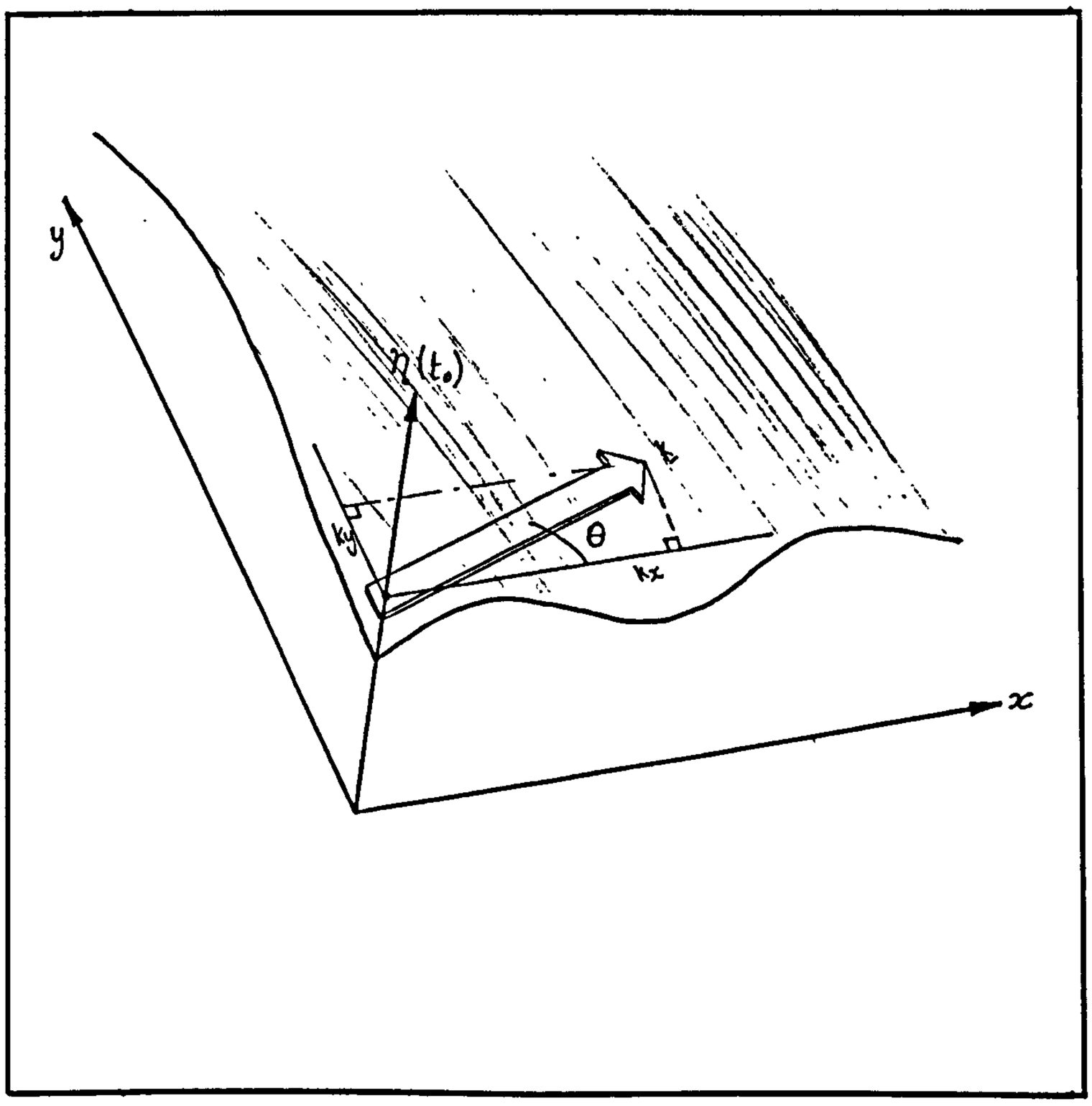

Figure 4.7: Surface elevation at instant t_0 due to single plane wave component $\mathbf{k}$.

For $\theta < 45°$ it can be seen that $k_x > k_y$, but because of the inverse relationship between wavenumber and wavelength, the apparent wavelength along the y axis is greater than that along x. The sum of all such components is:

$$\eta(x,y,t) = \sum_{n=1}^{\infty} a_n \cos(k_n x \cos\theta_n + k_n y \sin\theta_n - \omega t + \varepsilon_n). \qquad (4.26)$$

The set of amplitudes a_n leads to a wavenumber-frequency variance-density spectrum $S(\mathbf{k},\omega)$ such that in a small wavenumber and frequency interval

$$S(\mathbf{k},\omega)\,\Delta\mathbf{k}\,\Delta\omega = \sum_{\mathbf{k}}^{\mathbf{k}+\Delta\mathbf{k}} \sum_{\omega}^{\omega+\Delta\omega} \frac{a_n^2}{2}(\mathbf{k},\omega) \qquad (4.27)$$

In general, with no fixed relationship between $\mathbf{k}$ and ω, or fixed wave speed c, (the case for seismic waves) a wave system can be characterised by plots of variance density against $\mathbf{k}$, with a separate plot needed for each frequency (eg Capon, 1969). For ocean waves the situation is simpler, the dispersion relation fixing the magnitude k for a given frequency. In this case the wavenumber-frequency spectrum simplifies to the directional spectrum:

$$S(\omega,\theta)\,\Delta\omega\,\Delta\theta = \sum_{\omega}^{\omega+\Delta\omega} \sum_{\theta}^{\theta+\Delta\theta} \frac{a_n^2}{2}(\omega,\theta)\,. \qquad (4.28)$$

This may be written as the product of the omni-directional spectrum and a normalised, dimensionless directional distribution for each frequency:

$$S_{dir}(\omega,\theta) = S(\omega)\,G(\theta;\omega) \qquad (4.29)$$

where

$$\int_{-\pi}^{\pi} G(\theta;\omega)\,d\theta = 1 \qquad (4.30)$$

For a sea comprising a single regular wave component, G will be a delta function at the angle corresponding to the wave's direction. Waves in the open sea are not so simple, and the energy is distributed more evenly in direction and

frequency. Cartwright (1963) proposed a 'directional spreading' function of form

$$G(\theta) = F(s)\cos^{2s}\left(\frac{\theta-\theta_m}{2}\right) \qquad (4.31)$$

where θ_m is the mean direction, and the parameter s is chosen to suit particular wave conditions. $F(s)$ is defined in terms of the Gamma function in order to satisfy Equation 4.30. Figure 4.8 (reproduced from Tucker, 1991) illustrates G for several values of s.

The analysis is based upon certain assumptions. The wave system over the array is treated as a stochastic process. Such processes can be envisaged as producing actual time-series outputs which are drawn at random (but according to a particular probability distribution) from an 'ensemble' of possible outputs.

The process is assumed to be:

i) Weakly stationary. The major statistics, such as mean and variance, evaluated for a particular time instant across all possible ensemble

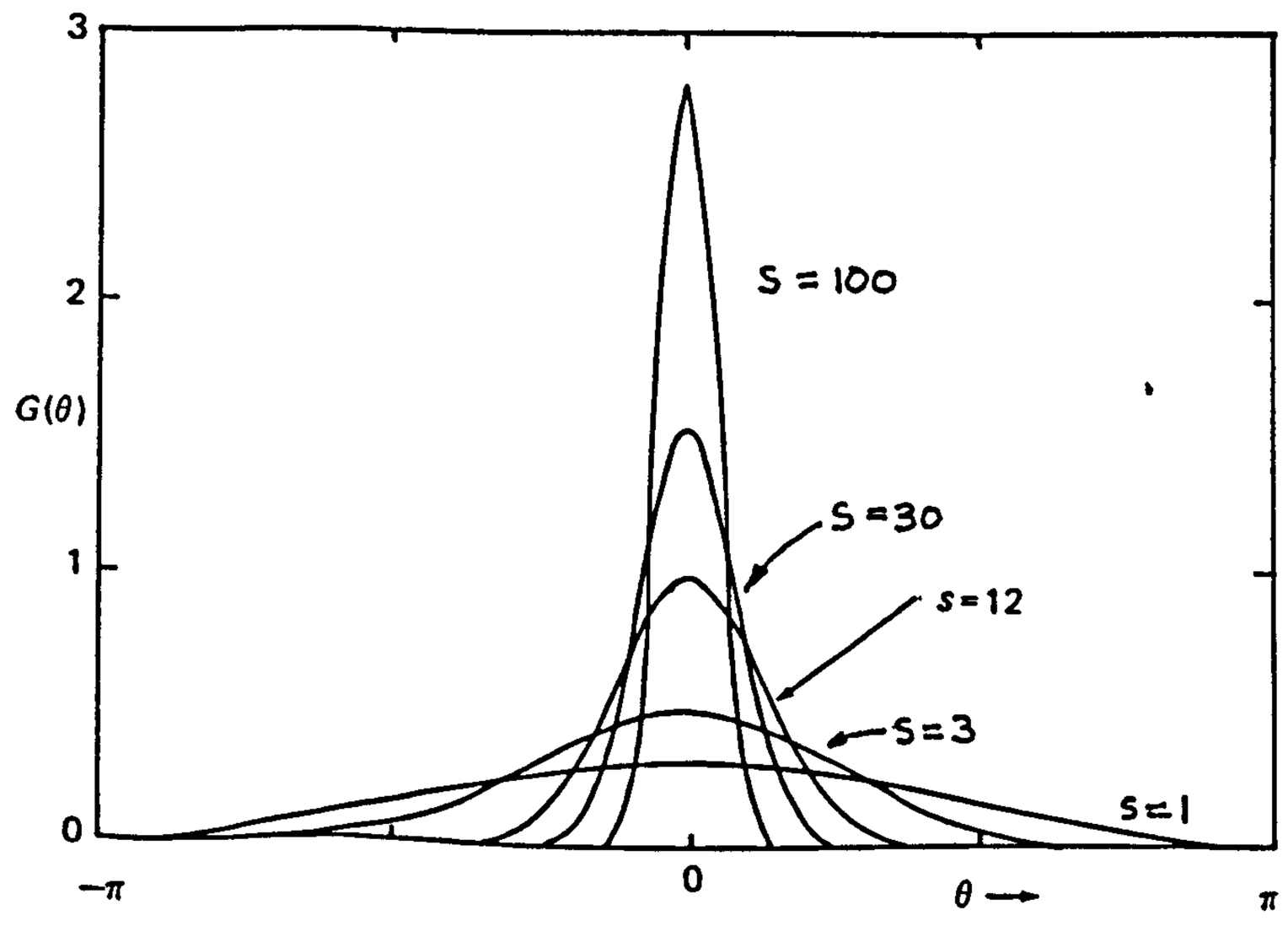

Figure 4.8 : Directional spreading functions
(from Tucker, 1991)

members, are not functions of time. The conceptual problem with this is that no ensemble member other than the measured one is available. In these circumstances a common test for stationarity splits up the available record into segments and checks that the statistics of the later ones are similar to the earlier ones. In fact wave records are usually not even weakly stationary. Tide produces a significant trend in the data, and although that can be removed computationally, the effects of changing mean depth on wave behaviour are not so easily dealt with. Also the non-linear effects of wave groups (surf beat and bound long waves) may have a period of the same order as the wave records.

ii) Homogeneous (in a statistical sense). Each ensemble member possesses similar statistics (when these are evaluated over time for each member). This condition is similarly difficult to test for. A random process that is both stationary and homogeneous is termed ergodic, and has the important property that the expected value of any (future) output is equal to the time average of the available output (which can be measured). These properties are discussed in texts such as Bendat and Piersol (1986) and Jacobs (1969). When space is an independent variable as well as time these definitions become more involved. Jeffreys (1987) takes the property of homogeneity to require that the statistics of any sensor's record should be independent of its position. This precludes any significant phase locking of the components and the attendant nodal structure, of the kind to be discussed in Section 4.4.3.6. He illustrates the importance of ergodicity in both laboratory scale tests and numerical simulation. However, since phase-locking due to reflection imposes a fixed, not random, relationship between locations, it could be argued that such a wave system is still ergodic. It is necessary, of course, that the analysis methods take account of the phase interaction.

Some of the effects of deviations from these assumptions are discussed in Section 4.5.

The wave system is also assumed to be homogeneous in another sense. Individual components of the wave field (as opposed to the combination of components) should not change their characteristics across the area of the sensor array. This implies in practice that the array is set out over a reasonably flat region of sea bed so that shoaling and refraction effects are small. It does not imply that records from each sensor have the same amplitudes: that will depend on the form of any constructive or destructive interference (due to reflection) at each sensor location.

It is considerably easier to extract a frequency distribution from the data than a directional distribution as there are, in the present case, about 1500 time samples available, and only six transducer locations or 'space samples'. Consequently the temporal harmonic analysis for $S(\omega)$ is done first, on each of the records independently, and then $G(\theta)$ is estimated at each frequency of interest. Methods for the former are well established, and detailed discussion is left to Section 4.5 . Techniques of directional analysis are not so well known, and will be described in the remainder of this section before details of implementation are given in Section 4.5 .

There are many approaches to direction finding from spatial arrays, and they come from diverse subject areas such as radar, sonar, acoustics, seismology, radio astronomy and tomography (reviewed in Haykin, 1985) as well as coastal engineering and oceanography. The approaches will be presented in a sequence that is imposed by the degree of prior knowledge of the actual directional distribution, together with the fineness of detail wanted. Thus to start with, a method is described suitable for use in a flume in which waves can only travel in either direction along a line. A range of other methods is then described, ending with a 'data adaptive' technique for high resolution of direction and which can accommodate reflected waves.

Notes on terminology

The term two-dimensional (2D) waves will be used, as is conventional in hydrodynamics, to mean waves propagating in either direction along a straight

line. That is, the particle motion, rather than wave direction, is constrained to two dimensions. Three dimensional (3D) waves can propagate anywhere over the surface. In common with other fields a simple linear wave component will sometimes be referred to as a plane wave, although a water surface wave crest is actually a line rather than a plane.

The variance of a wave system is related to its energy. Wave energy is the sum of potential and kinetic energy associated with the wave field in a certain area of water surface, at an instant in time. The energy per unit area of the component wave of amplitude a_n is:

$$\tfrac{1}{2}\rho g a_n^2 \qquad \text{joules/metre}^2 \tag{4.32}$$

The variance of the sinusoidal surface elevation component of Equation 4.26 is $^1/_2 a_n{}^2$, and the wave system's frequency characteristics may be expressed as the variance density spectrum, or when scaled by the factor ρg, the energy density spectrum.

The power of the component is the rate at which it transports its energy past a line parallel to the crests:

$$\tfrac{1}{2}\rho g a_n^2 c_{gn} \qquad \text{watts/metre crest length} \tag{4.33}$$

where $c_{g\,n}$ is the group velocity for the component at frequency n.

It is common in the field of signal processing is to substitute for the word 'variance' the equivalent appropriate to a signal voltage applied across a 1 ohm resistor. The variance of that signal is the average power over the record, and the energy dissipated (which has no value at an instant) is the time integral of variance. Frequency distributions therefore are often referred to as power density spectra. However, in the case of ocean waves the energy and power spectra are of different form due to the frequency dependency of c_g in Equation 4.33. Hence the term 'power spectrum' will not be applied here to wave-related variables.

4.4.2 Two Dimensional Waves

4.4.2.1 Single frequency (regular) waves constrained to a channel

For the relatively simple case of regular waves constrained to a channel - but which due to reflection are moving in both directions - the common method of establishing the magnitude of incident and reflected waves relies on Equations 4.8 and 4.9 in Section 4.1. At the partial anti-nodes, wave height is $(H_i+H_r)/2$, and at the partial nodes, $(H_i-H_r)/2$ where H_i is the height of the incident wave component, and H_r of the reflected. When the wave system is established a wave gauge fixed to a trolley is moved along the channel so that these maximum and minimum heights can be estimated. The two equations are solved for H_i and H_r.

4.4.2.2 Multiple frequency (random) waves, in a channel or normal to the shore

The above approach is of no use in the field where waves are unlikely to be regular, or where a travelling wave gauge is impractical. However, if waves propagate normal to the reflector the 'frequency response function method' is able to yield the incident and reflected wave components over a spectrum of irregular waves from measurements taken at just two fixed points.

Kajima (1969) showed how the incident and reflected wave spectra can be calculated by the cross-correlation of surface elevation records from two fixed points. Gilbert and Thompson (1978) presented an alternative derivation that calculates the cross-spectrum by means of the fast Fourier transform (FFT). Using the spectra (however calculated) these writers derived for the incident and reflected wave spectra:

$$S_{ii} = \frac{S_{xx} + S_{yy} - 2c\cos(kl) - 2q\sin(kl)}{4\sin^2(kl)} \qquad (4.35)$$

$$S_{rr} = \frac{S_{xx} + S_{yy} - 2c\cos(kl) + 2q\sin(kl)}{4\sin^2(kl)} \tag{4.36}$$

where S_{xx} and S_{yy} are the autospectra of surface elevation measured at sensors X and Y, l is the sensor separation (along the direction of wave travel), c is the co-spectrum (real part of the cross spectrum) and q the quadrature spectrum (imaginary part):

$$S_{xy} = c + jq \tag{4.37}$$

Singularities occur at spacings of integer multiples of half wavelengths, (ie at $kl=n\pi$, $n=1,2,...$) so that in practice three or more unequally spaced sensors are provided to cover the whole spectrum without singularities. Bullock and Murton (1989) describe this analysis method in use in the University of Plymouth's 20 metre wave channel. Davidson (1992) has developed a software routine that takes wave records from three sensors and automatically rejects any pair close to the above spacings for the relevant part of the spectrum.

4.4.2.3 Single frequency (regular,long-crested) waves of unknown direction

If it is known in advance that waves are propagating in one predominant, not necessarily shore-normal, direction then it is possible to estimate that direction with the output of two sensors by, in effect, timing the propagation of the wave profile over the known distance. The propagation delay may be obtained via the cross correlation or the cross spectrum. There is, however, an ambiguity over which side of the line joining the sensors the wave is coming from. The ambiguity can in some cases be resolved by knowledge of the site, or of weather conditions, or by the output of a third sensor.

Using cross-correlation

The simplest method of obtaining predominant wave direction is to evaluate the propagation delay by cross-correlating the record from each sensor. The delay is equal to the number of discrete lags in the cross-correlation function that correspond to the function's maximum value. At the chosen sampling interval of 0.5 seconds it is worth interpolating between time-lags

for greater precision. Linear theory predicts wave speed from period (available from either sensor's record) and mean depth. Angle of propagation is then deduced by simple trigonometry.

Three sensors

As stated above a third sensor resolves the directional ambiguity implicit in any analysis from a line array: the third sensor's output (if it is not in line with the other two) will be consistent with only one of the two possibilities.

In addition the third record may be used to avoid the step of estimating wave speed. Two simultaneous equations, derived from the two pairs of sensors, are solved to eliminate speed and yield the average direction. If desired, a useful check can be made by finding the value of speed from the equations and comparing it with the predictions of linear theory.

4.4.2.4 Multiple frequency (random) waves of unknown direction

The above method is less successful with random wave records if the spectral width is large enough for dispersion to produce a significant variation in wave speed and hence significant variation in wave profile over distance. The problem due to dispersion may be overcome by splitting the records into their component sinusoids by Fourier analysis, and cross-correlating those, one frequency at a time, to obtain propagation delays. The value of speed of propagation must be determined from the dispersion relation for each frequency. However, if it proposed to take the trouble to carry out a harmonic analysis then the phase relationships (and hence propagation delays) can be found more directly from the cross-spectrum.

These relatively simple techniques are not well suited to this project in which reflection is expected, as wave propagation will not be confined to a single predominant direction.

4.4.3 Three dimensional waves

In general two sensors can only provide an estimate of a single direction of wave propagation. If there are wave components from more than one direction then the method gives a 'weighted average' of those present. For example if there are two equal components separated by a certain angle the energy will be ascribed to a direction half way between them - even though there is no energy from that direction at all.

Extra sensors enable resolution of seas with several discrete directional components, and an approximation to a continuous directional spread. The more sensors there are the more components can be uniquely resolved. However, in the general case one does not have prior knowledge of the number of dominant wave components, and so there is an infinite number of possible combinations that could give rise to the measured records. The analysis method is selected to suit the type of sea expected. Some cope well with a few virtually plane wave components, and others manage better with a wide directional spread. A sea including reflections in which some components are phase locked, and therefore correlated with others, is dealt with in Section 4.4.3.6.

Methods fall into two main types: parametric (or 'model fitting') and model independent (Davis and Regier, 1977). If it is known that the directional character of the sea may be adequately described by a mathematical model (such as Cartwright's spreading function, Equation 4.31) then the model parameters - in this case 's' - can be adjusted for a best fit. Examples may be found in Long and Hasselmann (1979) and Hasselmann, Dunckel and Ewing (1980). The danger of this approach is that if an inappropriate model is selected then the method can 'over adjust' the model to force it to fit the data. This leads to an estimate of the directional make-up of the sea which is highly unlikely, although theoretically possible. The common parametric models do not describe the conditions in relatively shallow water close to a structure and so model fitting methods were not used in the present application.

Model independent methods themselves fall into two classes: '*a priori*' and 'data-adaptive'. In principle they all apply a set of phase shifts and weights to the records from each sensor before summing them in order to assess the contribution from a particular direction. Each test direction, (also called 'look direction' and 'target direction', Dudgeon,1977) is examined around the full circle by applying to the signals the set of weights and phase shifts appropriate to that direction. The next methods to be described are of the '*a priori*' type, so called because the phase shifts and weights are fully specified in advance of operating on any data. The 'data adaptive' methods are capable of greater resolution by exploiting particular features of a data set. They cannot be specified fully without reference to the data set under analysis.

4.4.3.1 The delay-and-sum beamformer

The delay-and-sum beamformer (or 'phased array') forms the physical, and conceptual, basis for all the techniques that follow. The method was originally developed by radio and radar engineers to enhance signals received from a known direction, but its application to ocean wave directional analysis is presented here. Rather than for signal enhancement the beamformer is used to assess signal strength from given directions. The following is adapted from Dudgeon (1977), Haykin (1985, ch4) and Haddad and Parsons (1991, ch7).

A line array of equally spaced sensors is set up as in Figure 4.9. In the general case the wave propagating across the array is a non-deterministic function of time. If the signal received by the sensor at the origin is $\eta_0(t)$, then the signals at the other sensors will be delayed versions of this: $\eta_n=\eta_0[t-T_p(n)]$ where $T_p(n)$ is the propagation delay from the origin to sensor n. Referring to Figure 4.9,

$$T_P(n) = \frac{\text{distance of propagation}}{\text{speed of propagation}} = \frac{nD\cos\theta'}{c} \qquad (4.40)$$

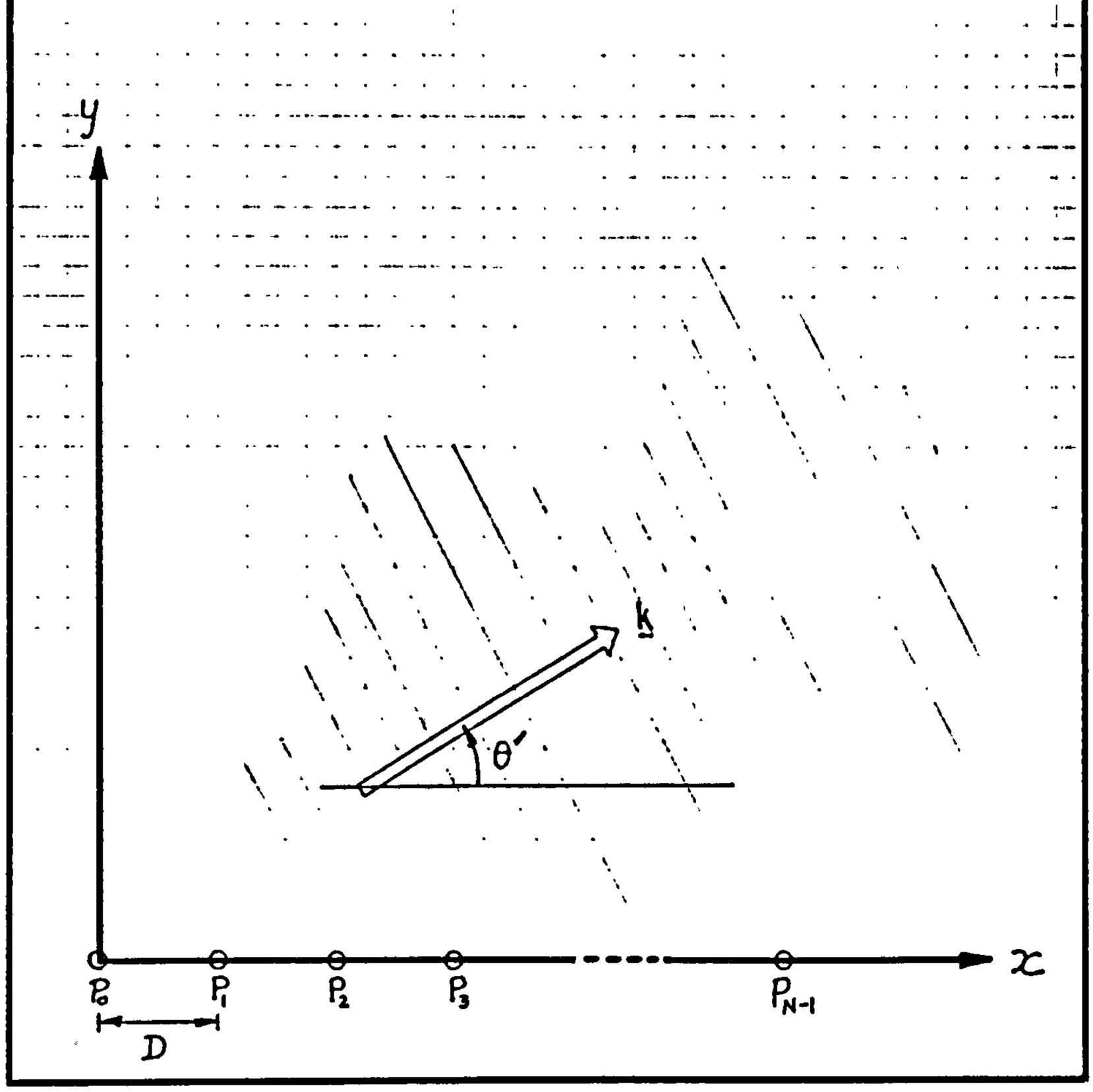

Figure 4.9 : Equi-spaced line array of N sensors

Applying the delay $T_d(n) = T_p(N\text{-}n)$ to each of the signals $\eta(n)$ achieves a 'constructive interference' for wave field components of speed c and direction θ'. Other components will not be enhanced so much, or may interfere destructively.

The beamformer output

$$g(t) = \sum_{n=0}^{N-1} \eta_n(t - T_d(n)) \tag{4.41}$$

which is the sum of the delayed signals, therefore gives some measure of the proportion of the signal moving in that direction. Test directions will be denoted by θ while wave direction by θ'. A directional analyser could be built on this principle by evaluating sets of T_d corresponding to each test direction.

If many frequency components are present, the distortion in the time records due to dispersion will cause errors just as in the cross-correlation method

above. Analysis therefore proceeds one frequency component at a time, and the delays T_d are replaced by phase shifts θ_d. For a particular frequency component

$$c = fL = \frac{\omega}{2\pi} \cdot \frac{2\pi}{k} = \frac{\omega}{k} \tag{4.42}$$

and so the propagation delays and phase shifts are

$$T_p(n) = \frac{nD\cos\theta'}{c} = \frac{knD\cos\theta'}{\omega} \tag{4.43}$$

and $$\phi_p(n) = knD\cos\theta' \tag{4.44}$$

The set of phase shifts that must be applied to bring all the signals from this component into phase alignment is

$$\phi_d(n) = \phi_p(N-n) = k(N-n)D\cos\theta' \text{ where } \theta' = \theta \tag{4.45}$$

Figure 4.10 is a schematic of this process.

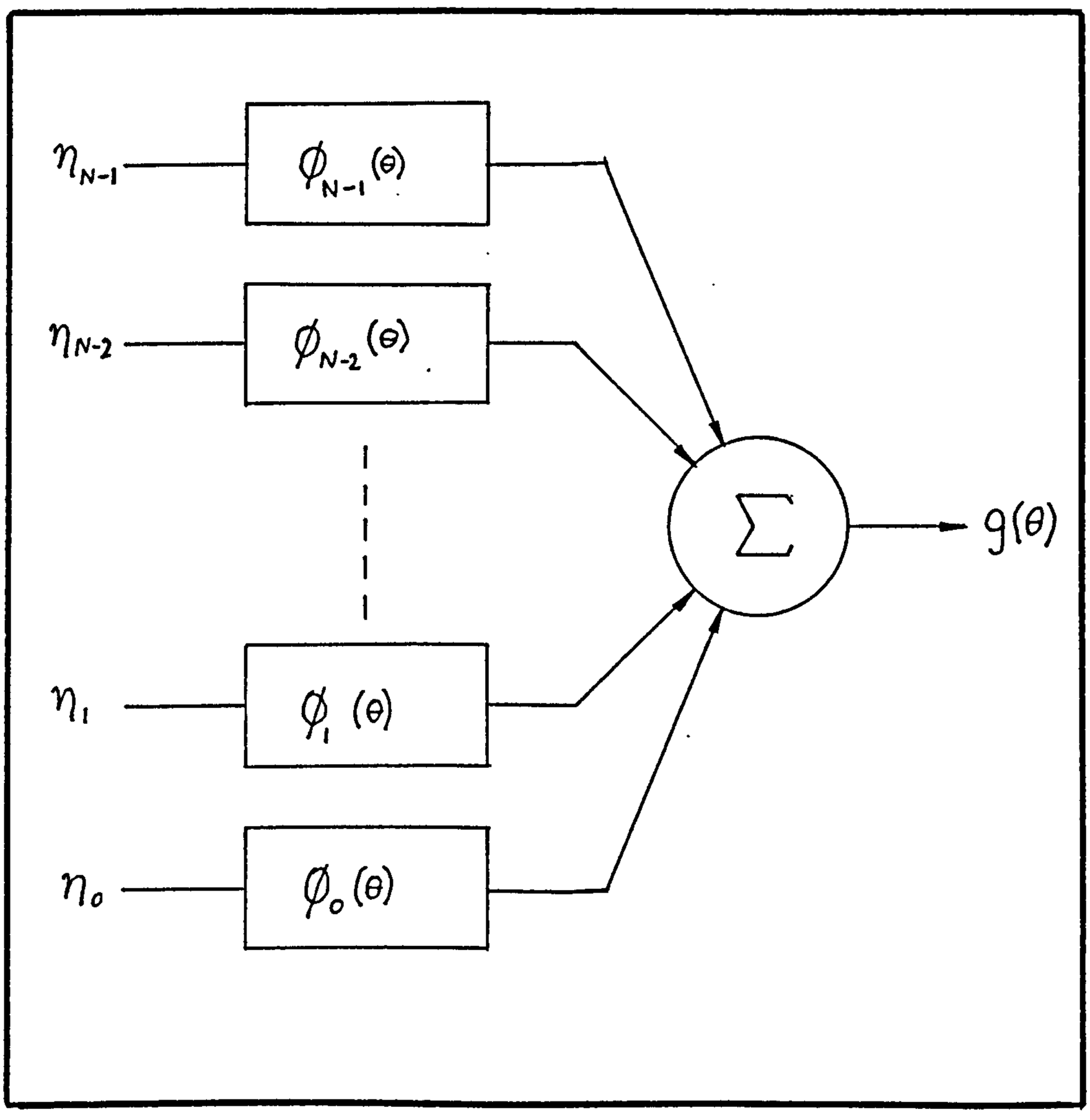

Figure 4.10 : Schematic of the delay-and-sum beamformer

In the present case real time operation is not required and so the wave field is decomposed into a set of sinusoids by Fourier transformation of the whole record.

Consider a wave train of wavenumber vector **k** and height H propagating across the array of Figure 4.9. It gives rise to a surface elevation record at P_0 of

$$\eta_0 = \frac{H}{2}\cos(\omega t + \varepsilon) \tag{4.46}$$

(where ε is an arbitrary phase), and at any other point on the x axis

$$\eta(x) = \frac{H}{2}\cos(\omega t - \mathbf{k}\cdot x\mathbf{i} + \varepsilon) \tag{4.47}$$

where **i** is a unit vector in the direction of the x axis. Therefore at sensor P_n the elevation is

$$\eta_n = \frac{H}{2}\cos(\omega t - knD\cos\theta' + \varepsilon). \tag{4.48}$$

For each test direction θ (typically 0 to 360° in 10° steps) the corresponding set of phase shifts ϕ_d is applied, and $g(\theta)$ evaluated. Thus the required estimate of directional energy distribution is obtained.

Moving to exponential notation by applying Euler's theorem,

$$\cos\alpha = \frac{1}{2}[\exp(j\alpha) + \exp(-j\alpha)] \tag{4.49}$$

Equation 4.48 becomes

$$\eta_n = \frac{H}{4}\exp[j(\omega t - knD\cos\theta' + \varepsilon)] + \frac{H}{4}\exp[-j(\omega t - knD\cos\theta' + \varepsilon)] \tag{4.50}$$

Letting $$a = \frac{H}{4}\exp(j\varepsilon) \tag{4.51}$$

gives $$\eta_n = a\exp(j\omega t)\exp(-jknD\cos\theta')) + a^*\exp(-j\omega t)\exp(jknD\cos\theta') \tag{4.52}$$

which may be thought of as a conjugate pair of phasors of length $\frac{H}{4}$ rotating at angular frequency ω.

Applying the set of phase shifts ϕ_d from Equation 4.45 for a particular test direction θ to the beamformer of Equation 4.41 gives

$$g(\theta) = \sum_{n=0}^{N-1} a \exp[-jknD\cos\theta'] \exp[+jknD\cos\theta] \exp[-jkN\cos\theta] \qquad (4.53)$$

plus conjugate terms. Dropping the exponential independent of n

$$g(\theta) = a \sum_{n=0}^{N-1} \exp[-jknD(\cos\theta' - \cos\theta)] \qquad (4.54)$$

plus conjugate terms.

$$= a.W(v) \qquad (4.55)$$

where $$v = k(\cos\theta' - \cos\theta) \qquad (4.56)$$

and $$W(v) = \sum_{n=0}^{N-1} \exp(-j\, nDv) \qquad (4.57)$$

W is called the window function (or alternatively the radiation pattern, beam pattern, array function, or array pattern). It may be noted that:

i) All the array information (geometry and applied phases) is contained in W.

ii) W acts like a spatial filter, passing some proportion of the signal which depends on its direction. To estimate the directional spectrum $g(\theta)$ is evaluated over an appropriate set of test directions spanning the arc of interest and separated by some convenient interval.

The limit on resolution available is imposed by the array geometry, rather than by the step size chosen for θ. The latter just sets the intervals at which the underlying estimate is evaluated. In order to discover the characteristics of the array, the array function W must be examined. Noticing that W takes the form of a geometric progression, with first term exp[-j0], common ratio exp[+jDv] and N terms, it may be shown that

$$W = \frac{\sin(NvD/2)}{\sin(vD/2)} \exp[j(N-1)vD/2] \qquad (4.58)$$

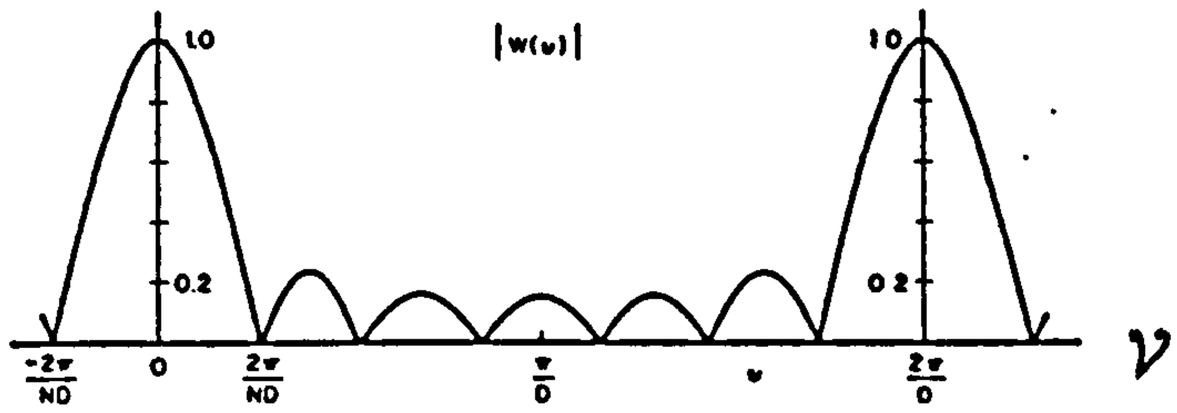

Figure 4.11 : The window function for a delay-and-sum beamformer with $N=7$ (from Dudgeon 197;

The exponential term is merely an overall phase shift arising from the arbitrary choice of origin in the array. The array function is plotted for 7 sensors in Figure 4.11.

The effect of W on the estimate of directional distribution is analogous to the effect that a data window applied to the time record has on the estimated frequency distribution. Figure 4.11 shows that when the beam is 'steered' to the test direction θ the array passes any signal component at that direction, $\theta'=\theta$, together with a certain proportion of any component not travelling in that direction (for which $\theta' \neq \theta$ and so $\nu \neq 0$). The array and associated processing may be thought of as a 'spatial window'. Put in other words one is looking through an imperfect window and seeing only a blurred picture of the true directional distribution.

Turning to the form of the function in Figure 4.11 a number of features are apparent.

i) W is periodic in ν with repeating lobes at integer multiples of $2\pi/D$ (sometimes called 'grating lobes' by analogy with the diffraction grating). Permitting |ν| to take values > $2\pi/D$ produces an angular aliassing effect, placing a maximum value on D of $L/2$ for the measurement of any particular k A given sensor spacing D thus fixes the high end of the working frequency band. Since the analysis is done on one frequency at a time there is no danger of *unexpected* shorter wavelengths aliassing, analogous to the situation in normal harmonic analysis provided the data has been filtered before sampling.

ii) For good resolving power the array function should exhibit a narrow main lobe, or 'beamwidth'. This is a major design objective for a beamformer. Increasing the number of sensors N achieves this, as does lengthening (or increasing the 'aperture') of the array. The former is usually limited by cost, and the latter by angular aliassing considerations. Two wave trains of the same frequency will not be resolved if their directions of propagation differ by less than one standard beamwidth.

iii) Just as with the data window in time, the resolution and leakage properties of this spatial window may be tailored by weighting the data points. This approach will be discussed later.

The beamformer as a Fourier analyser

Comparing Equation 4.54 to the general definition of the Fourier series of a discrete sequence:

$$X(\Omega) = \frac{1}{N} \sum_{n=0}^{N-1} x[n] \exp[-j\Omega n] \qquad (4.59)$$

it is apparent that the beamformer output is similar to a discrete Fourier transform, an *amplitude* spectrum. Haykin (1985, ch4) calls this process the 'Fourier Method', a processing scheme closely related though not the same as that described as the 'Direct Fourier Transform Method' by oceanographic writers and presented later. The signal $x[n]$ is a sequence of N spatial samples of the surface elevation η. The term exp[$-jknD$ cos θ] in 4.54 is equivalent to the basis set exp[$-j\Omega n$]. This term is orthogonal to the signal term for all θ

except $\theta=\theta'$. For an infinite array of sensors the sum (or integral) of the product over n would tend to zero, unless $\theta=\theta'$. The finite array does not behave so well but nevertheless gives some estimate of amplitude distribution over θ.

The directional *energy* spectrum is the sum of the products of the phase shifted signals, which is shown in the next section to be the spatial Fourier transform of the cross spectrum:

$$\hat{S}(\theta) = \sum_{m=1}^{N} \sum_{n=1}^{N} Q_{mn} \exp[j(x_n k\cos\theta - x_m k\cos\theta)] \qquad (4.60)$$

Frequency dependence

The foregoing analysis was developed with one component of a certain height, direction and frequency. The analysis is linear so that it is assumed that a complex sea may be resolved into a directional distribution of simple components, subject to the accuracy of estimating the frequency distribution of each sensor record and to the limitations of the spatial window W. Since k, and hence ν, are functions of frequency (fixed by the dispersion relation) W is also a function of frequency.

4.4.3.2 The direct Fourier transform method (DFT)

The problem of estimating the directional spectrum from a spatial array may be generalised from the linear array to encompass the polygonal array.

The presentation here is based on that of Barber (1963), and the subsequent descriptions in Kinsman (1965) who coined the name for it of 'direct Fourier transform method', and Goda (1985), except that their route to obtaining a variance spectrum via cross-correlation is here re-cast to include the more modern direct multiplication of Fourier series coefficients. Also, vector notation is used instead of the x and y coordinates of wave number and position.

Surface elevation at a position defined by vector **r** from the origin of the frame of reference, and at time t is denoted by $\eta(\mathbf{r},t)$. The signal may be represented by its three-dimensional Fourier transform to give its distribution in frequency ω, and wavenumber **k**, defined as:

$$Z(\mathbf{k},\omega) = \int_{-\infty}^{\infty}\int_{-\infty}^{\infty} \eta(\mathbf{r},t)\,\exp[-j\mathbf{k}\cdot\mathbf{r}]\,\exp[-j\omega t]\,d\mathbf{r}\,dt \qquad (4.61)$$

(where Z is a directional amplitude, not a variance, spectrum.)

As before, since the data is much better sampled in time than in space, the transform with respect to time is done first:

$$z(\mathbf{r},\omega) = \int_{-\infty}^{\infty} \eta(\mathbf{r},t)\,\exp(-j\omega t)\,dt \qquad (4.62)$$

so that

$$Z(\mathbf{k},\omega) = \int z(\mathbf{r},\omega)\,\exp(-j\mathbf{k}\cdot\mathbf{r})\,d\mathbf{r} \qquad (4.63)$$

where $z(\mathbf{r},\omega)$ is the omni-directional amplitude spectrum of surface elevation at any point specified by **r**.

The wavenumber-frequency variance spectrum is the product of the signal's Fourier transform and its conjugate:

$$S(\mathbf{k},\omega) = Z^*(\mathbf{k},\omega)\cdot Z(\mathbf{k},\omega) \qquad (4.64)$$

That is

$$S(\mathbf{k},\omega) = \left[\int z(\mathbf{r},\omega)\,\exp[-j\,\mathbf{k}\cdot\mathbf{r}]\,d\mathbf{r}\right]^* \cdot \left[\int z(\mathbf{r},\omega)\,\exp[-j\mathbf{k}\cdot\mathbf{r}]\,d\mathbf{r}\right]$$

$$= \int z^*(\mathbf{r},\omega)\,\exp[j\,\mathbf{k}\cdot\mathbf{r}]\,d\mathbf{r} \quad \int z(\mathbf{r},\omega)\,\exp[-j\,\mathbf{k}\cdot\mathbf{r}]\,d\mathbf{r}$$

$$= \int\int z^*(\mathbf{r},\omega)\,\exp[j\,\mathbf{k}\cdot\mathbf{r}]\,.\,z(\mathbf{r}',\omega)\,\exp[-j\,\mathbf{k}\cdot\mathbf{r}']\,d\mathbf{r}\,d\mathbf{r}' \qquad (4.65)$$

But $z^*(\mathbf{r},\omega).\,z(\mathbf{r}',\omega)$ is the cross-spectrum between the signals at two points specified by **r** and **r'**. So

$$S(\mathbf{k},\omega) = \int\int Q_{\mathbf{r}\mathbf{r}'}\,\exp[-j\,\mathbf{k}\cdot(\mathbf{r}'-\mathbf{r})]\,d\mathbf{r}\,d\mathbf{r}' \qquad (4.66)$$

The wavenumber-frequency spectrum is seen to be the Fourier transform of the cross-spectrum Q. Q is a complex quantity whose magnitude is constant for any pair of sensor locations m and n (in a homogeneous sea state) and whose argument is a weighted sum of terms such as $\mathbf{k}'.(\mathbf{r}_n-\mathbf{r}_m)$. Compatible with the terminology of the previous section, $\mathbf{k}'$ is the wavenumber of a simple component wave train and $\mathbf{k}$ the general wavenumber variable. Although the Fourier transform of real quantities is more familiar, examination of Equation 4.66 on the Argand diagram shows that $\exp[-j\mathbf{k}.(\mathbf{r}_n-\mathbf{r}_m)]$ is indeed orthogonal to all component waves responsible for Q that are not of wavenumber $\mathbf{k}'$, so that Equation 4.66 acts as a Fourier transform, sifting from Q successive estimates of energy at wavenumber $\mathbf{k}$.

Q is a function of relative position between the sensors rather than a function of the sensors' absolute positions. The domain of relative positions is traditionally known as 'lag-space' from the older practice of evaluating Q from the cross-correlations. With N sensors, Q may be observed at only N^2 points in the lag space. These are not independent as $Q_{mn}=Q_{nm}^*$.

Barber's estimate of the directional spectrum therefore becomes

$$\hat{S}(\mathbf{k},\omega)=\sum_m\sum_n Q_{mn}(\omega)\exp\left[-j\,\mathbf{k}\cdot(\mathbf{r}_n-\mathbf{r}_m)\right] \qquad (4.67)$$

the circumflex over the spectrum indicating that the latter is only an estimate of the true spectrum, since Q_{mn} is only a sampled version of the continuous Q. A program has been written to evaluate $\hat{S}(\mathbf{k},\omega)$ using Equation 4.67, the direct Fourier transform method, although its performance is much inferior to the schemes described below.

Array design

The directional resolving power of a particular array of sensors is most easily assessed by examining its window function, although that is determined by the subsequent processing method as well as by the array itself. One of the major contributions of the aforementioned paper by Barber (1963) was a method for predicting the window function of an irregular polygonal (as opposed to a uniformly spaced linear) array with DFT processing. For the data adaptive methods to be described later it is not possible to predict the beam pattern independently of the data, but it seems reasonable that an array geometry which performs well for the DFT will also be suitable for other processing methods. Barber's method is presented here, again re-cast to avoid using the now superseded route to obtaining spectra via 'correlograms', and with some reference to image processing techniques, from for example Haddad (1991). It will then be applied to the transducer array used for measurements at Plymouth Breakwater.

It is convenient to resolve the wavenumber vector into its x and y components, k_x and k_y. Also the cross-spectrum is a function of the relative position between two points rather than of the absolute position of those points with respect to some coordinate frame. These relative-position independent variables will be denoted by X and Y.

If there are N sensors at positions (x_n, y_n), $n=1,2,\ldots,N$, then there are N^2 pairs of sensors, with relative positions (X_{mn}, Y_{mn}) where $X_{mn} = x_n - x_m$ and $Y_{mn} = y_n - y_m$, $m=1,2,\ldots,N$ and $n=1,2,\ldots,N$. It is possible to calculate the cross-spectrum $\underline{Q}$ only for these N^2 shifts

$$\underline{Q}_{mn} = \underline{Q}(X_{mn}, Y_{mn}) \qquad (4.68)$$

Since there are only $N(N-1)/2$ independent pairs (because $\underline{Q}_{mn} = \underline{Q}_{nm}^*$) there are only $N(N-1)/2+1$ distinct samples of $\underline{Q}$.

The non-ideal window function is a consequence of knowledge of the continuous $Q(X,Y)$ being limited to samples at a number of discrete relative

positions. Q_{mn} may be modelled as the product of Q and a two-dimensional sampling function $w(X,Y)$

$$Q_{mn} = Q(X,Y)\, w(X,Y,m,n) \quad \text{(dropping } \omega \text{ for simplicity)} \tag{4.69}$$

where w is a set of unit impulses located at those values of X and Y for which Q is available (the 'bed of nails' function):

$$w(X,Y,m,n) = \sum_{m=1}^{N} \sum_{n=1}^{N} \delta(X - X_{mn}, Y - Y_{mn}) \tag{4.70}$$

Our estimate $\hat{S}$ of the true spectrum S is therefore the spatial transform of the product Qw (Equation 4.67). By the convolution theorem this is equal to the convolution of their transforms:

$$\hat{S} = F.T.\{Q(X,Y)\} ** F.T.\{w(X,Y)\} \tag{4.71}$$

$$= S(\mathbf{k}) ** W(k_x, k_y) \tag{4.72}$$

The Fourier transform of w is

$$W(k_x,k_y) = \int_{X=-\infty}^{\infty} \int_{Y=-\infty}^{\infty} w \exp(-j k_x X) \exp(-j k_y Y)\, dX\, dY \tag{4.73}$$

which by the sifting property of the delta function reduces to:

$$W(k_x,k_y) = \sum_{m=1}^{N} \sum_{n=1}^{N} \exp[-j(k_x X_{mn} + k_y Y_{mn})] \tag{4.74}$$

Noting that $X_{mn} = -X_{nm}$ and applying Euler's theorem

$$W(k_x,k_y) = 1 + 2 \sum_m \sum_n \cos(k_x X_{mn} + k_y Y_{mn}). \tag{4.75}$$

As in the harmonic analysis of time series, the convolution may be visualised as a filtering and a summing operation. Making an estimate of the energy at k_x, k_y contained in spatial variable $Q(X,Y)$ can be visualised as placing the origin of a plot of W over the point k_x, k_y on a plot of the true spectrum of the signal. The estimate will consist as it should of energy at k_x, k_y, but will also include all the

other components in the true spectrum weighted by the corresponding values of W. This smearing or loss of resolution is due to the spectral leakage arising from the limited extent, or aperture, of the array. Further, W is periodic in k_x and k_y. If there are components in the true spectrum greater than half the periodic spacing from the estimated wavenumber k_x, k_y the 'filter' will collect them into the estimate with full weighting. This aliasing effect is due to the spectral leakage that arises from sample points in w (ie the sensors) being too widely spaced. The description of the linear, equi-spaced beamformer's window function (Equations 4.55 to 4.58) is a special case of the above.

From this it is evident that it is the relative, rather than the absolute, positions of the transducers that are important, and that in general one should aim at an even coverage of the X Y space. Consequently it is helpful to examine the 'co-array' of shifts X Y instead of the sensor positions themselves. Davies and Regier (1977) give the illustration reproduced in Figure 4.12.

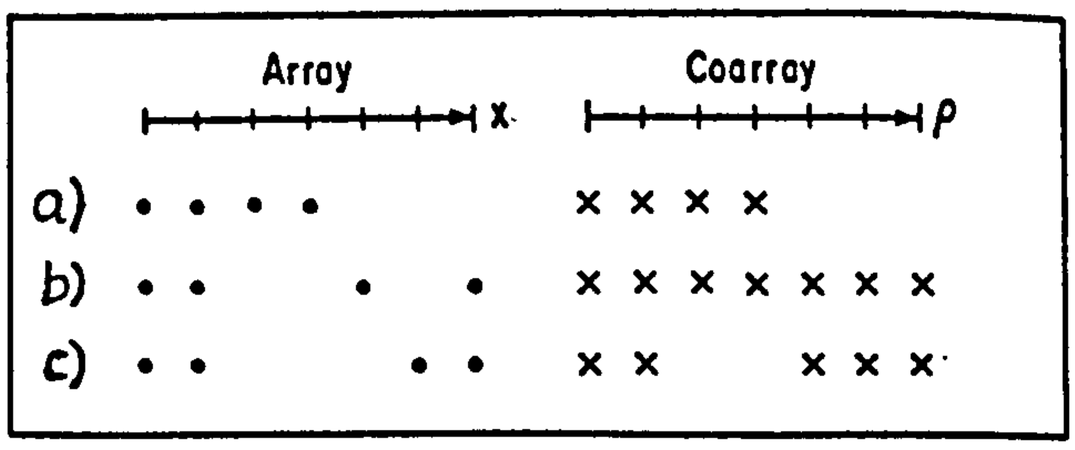

Figure 4.12 : Linear arrays and their associated co-arrays
(from Davis and Regier, 1977)

The regularly spaced linear array a) contains several redundant separations, and does not produce good coverage of the X Y space, while b) uses the same number of sensors to much greater effect. Davis and Regier comment that an array that looks regular to the eye is likely to have a poor co-array.

For this project the recommendation of Isobe and Kondo (1984) was followed: a linear array of exponentially increasing spacings, with values chosen to suit the range of wavelengths expected. In addition, one extra sensor was placed off-line to resolve the linear array's implicit semi-circular ambiguity. A plot of sensor positions (surveyed) for the Plymouth Breakwater deployment is shown

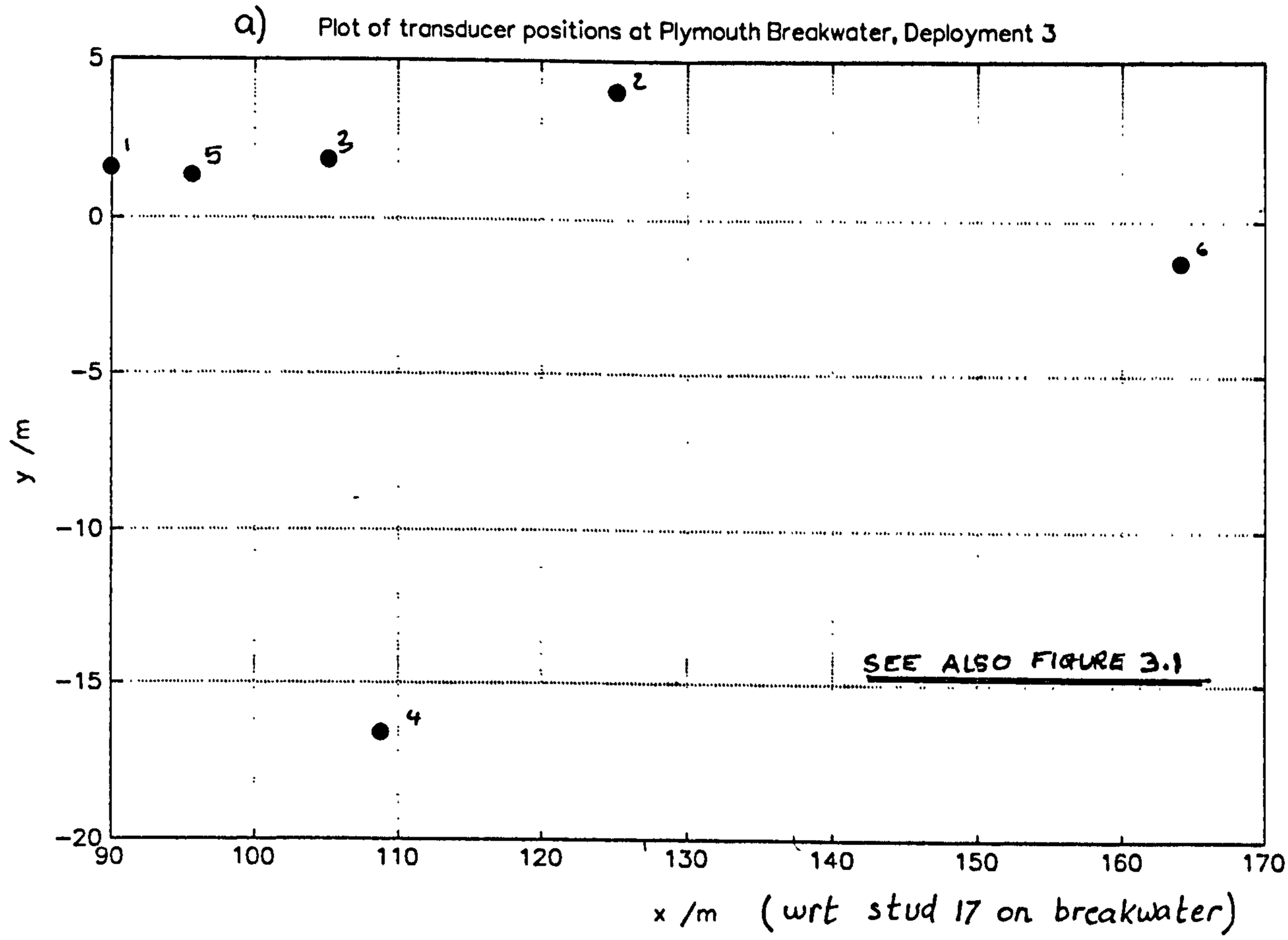

Figure 4.13 : Transducer positions at Plymouth Breakwater, Deployment 3
a) surveyed co-ordinates of the array b) corresponding co-array.

in plan in Figure 4.13a). The actual positions indicated are more irregular than those designed because of placement error. This is no bad thing (provided the survey of the actual positions is accurate) as it increases the coverage of the co-array. The equivalent co-array is given in Figure 4.13b). Figure 4.14 illustrates the beam pattern for this array, spanning a range in k_x and k_y of +/- 0·6 radians/m from the central peak. To give a better view of the magnitudes, cross sections along the k_x and k_y axes are plotted in Figures 4.15a) and b). The lack of a single sharp peak results in poor directional resolution. For sea waves the phenomenon of dispersion mitigates the position somewhat. For a given (temporal) frequency, energy should exist only in a small range of the magnitude of **k**. On a plot of the directional spectrum this corresponds to a narrow annulus of radius k. Therefore in evaluating the directional distribution of the energy in a particular frequency component the important feature of the beam pattern is its cross section around a circle whose radius is k, and which is located on the beam pattern plot (Figure 4.14) so that the line from its centre to the point (k_x=0,k_y=0) is the vector **k**, the wavenumber for which energy is being estimated.

Even with a relatively extensive array of six transducers the beam pattern does not give good resolution. The simpler arrays in Barber's paper are even worse. These results provide a motivation to seek more sophisticated methods of directional analysis.

4.4.3.3 Other *a priori* methods

The estimate of Equation 4.67 would seem to be a logical adaptation of the true relationship of Equation 4.66 to the real situation, in which only a limited number of sensors is available. However it is not the only one. A more general form is

$$\hat{S}(\mathbf{k},\omega) = \sum_{mn} \alpha_{mn}(\mathbf{k},\omega)\, Q_{mn}(\omega) \qquad (4.76)$$

which differs from Equation 4.67 in that the weights α may have a non-unity magnitude. Davis and Regier (1977) show how the weights α_{mn} may be optimised with respect to particular criteria, such as the resolution of wave components, or the rejection of noise (either measurement or statistical). They

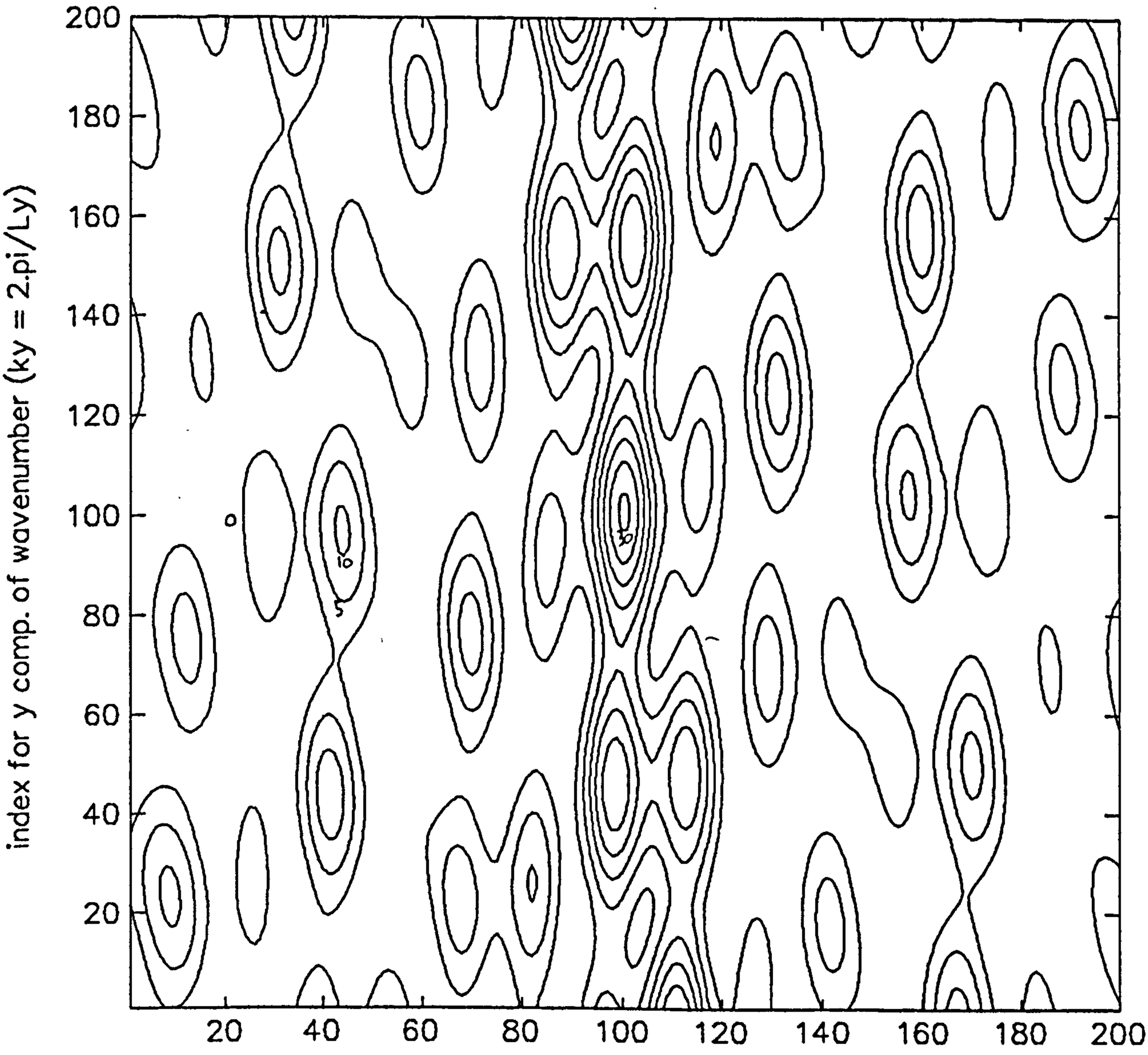

(k_x and k_y range from -0.6 to +0.6 radians per metre in 200 points)

Figure 4.14 : Beam pattern for Plymouth Breakwater array

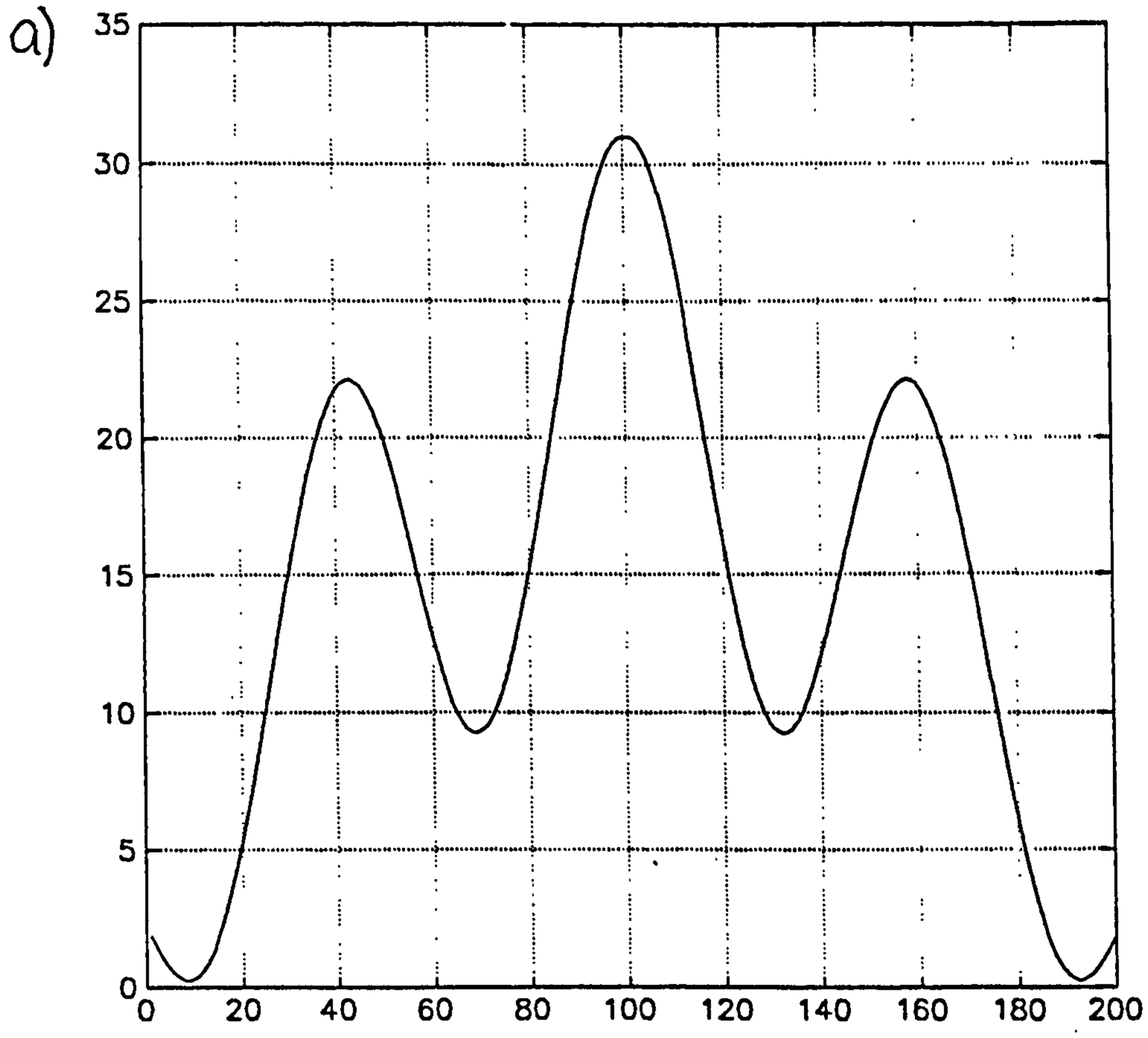

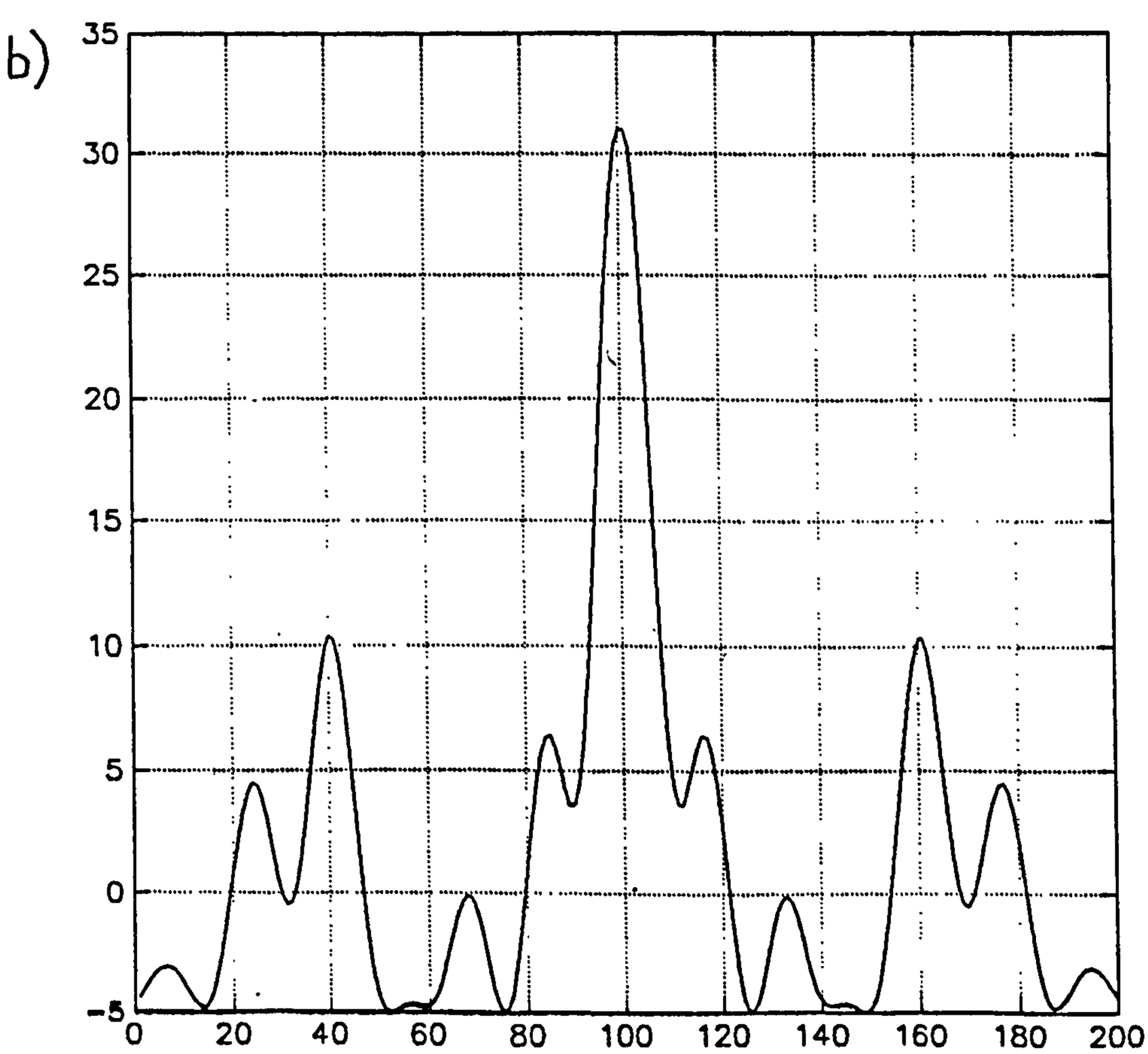

Figure 4.15 : Cross sections through the beam pattern
a) along the k_y axis, b) along the k_x axis.

conclude that Barber's estimate, whilst not truly optimal (for example total energy must be obtained afterwards by normalising from the autospectra) does have reasonable resolution and noise rejection. Moreover it is computationally relatively simple. Davis and Regier describe two alternative scheme, both of which give an improved performance over a particular range of k at the expense of a degradation if signals are present of k outside that range. The methods are therefore appropriate for analysis of waves in a medium with a fixed dispersion relationship. The first, the omni-directional *a priori* (OAP) scheme makes no assumption about wave angle, whereas the second, the steered *a priori* (SAP) method, uses weights that perform better on data sets with waves confined to certain ranges of direction. Both schemes include parameters that the user can adjust to optimise noise and resolving power based on his assumptions about the wave field under analysis. It can be seen from the results of trials with numerically generated data (reproduced in Figure 4.16) that none of the *a priori* schemes (DFT, OAP or SAP) has particularly high resolution when presented with a simple wave train.

This is particularly so for the longer period, 0.1 Hz , wave. At 0.3 Hz spurious peaks occur. Simulated wave fields with greater directional spread are handled more accurately (b,c,d). Interestingly, only the SAP correctly renders the rather extreme, isotropic, case in f). The array geometry used for these simulations was that of the floating spar buoy 'FLIP', consisting of six sensors arranged approximately along the arms of a 'V' of height 15m, oriented so that the apex pointed into the predominant wave direction.

The data adaptive methods

The limitations in performance of the DFT method were seen in the last section to be expressible in terms of its poor wavenumber window. A desirable window would (as in the case of analysis of time records) have a narrow passband and small sidelobes that do not extend far from the centre. The OAP and SAP processing schemes bring some improvement, but major enhancements are possible if the window shapes itself automatically to suit the data as well as being defined by the array geometry. The estimate of the power in a particular direction is adjusted so as to be least disturbed by the energy present in others.

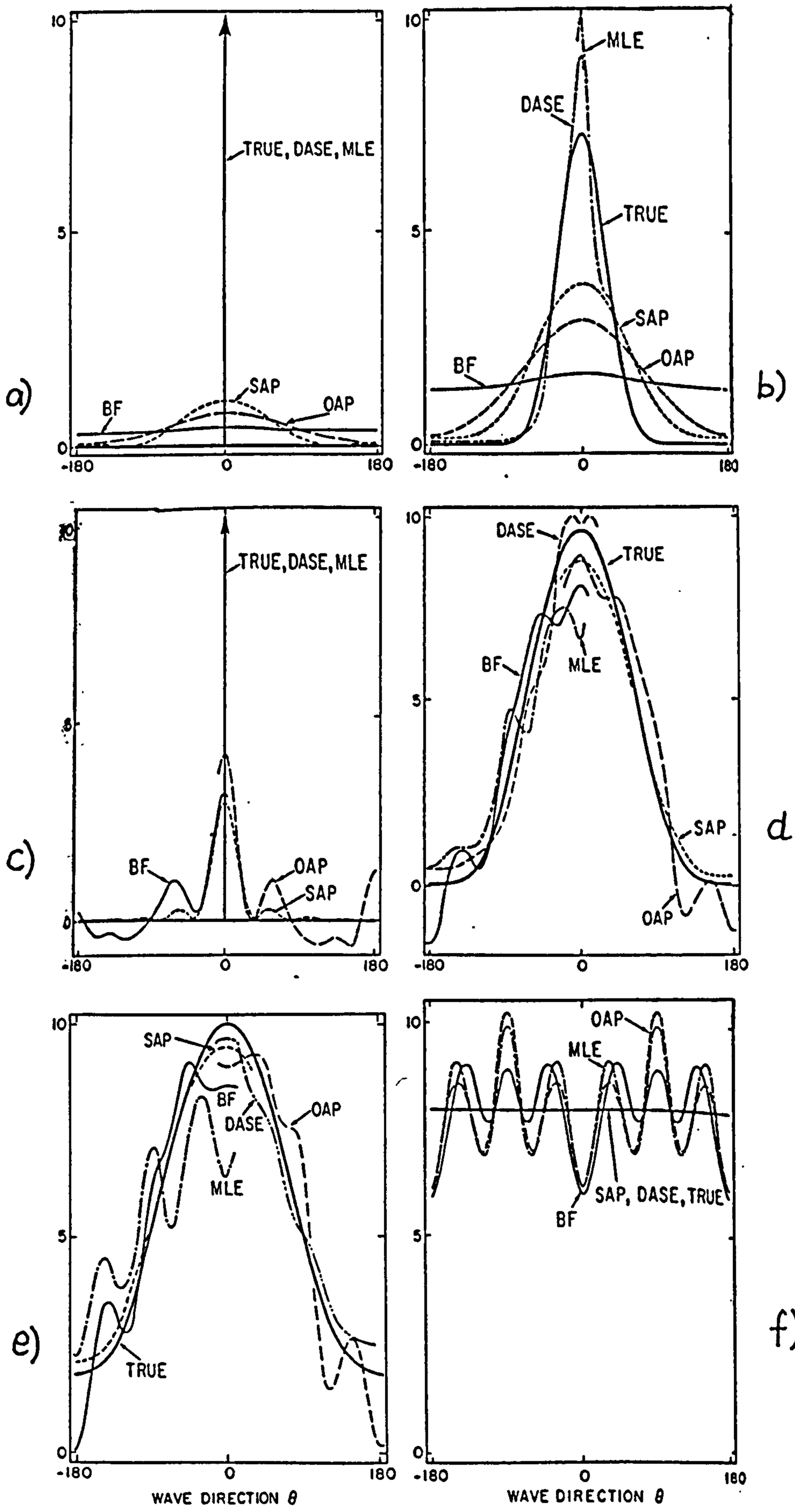

Figure 4.16 : Estimated directional spectra compared with the true (numerically generated spectra). a) 0.1Hz, plane wave b) 0.1Hz, $\cos^{16}(\theta/2)$ spread c) 0.3Hz, plane wave d) 0.3Hz, $\cos^{4}(\theta/2)$ spread e) 0.3Hz, $\cos^{16}(\theta/2) + 0.18\cos^{2}(\theta-\pi)/2$ f) 0.3Hz, isotropic. From Davies and Regier (1977).

The effective window function is thus adapted to the data being analysed, and such a method is called 'data adaptive' by Lacoss (1971).

Two techniques that achieve this are the Maximum Likelihood Method and the Maximum Entropy Method.

4.4.3.4 Maximum likelihood method (MLM)

This data adaptive technique was proposed by Capon (1969) for the determination of wavenumber-frequency spectra of the seismic waves detected by the Large Aperture Seismic Array in Montana, USA. A very marked improvement is demonstrated over the conventional DFT method. To develop the theory Capon envisaged a tuneable 'maximum likelihood ' filter whose job was to make an estimate of signal energy at a particular wavenumber.

Two specifications are made for the filter:

i) If its input consists only of a signal at wavenumber **k** then its output power should equal the input power.

ii) Inputs of any other wavenumber, and of noise, must make a minimum contribution to the output.

(In view of (ii) some writers refer to this as the 'minimum variance method, for example Kay (1981). Capon himself merely calls it the high-resolution method.)

Most writers describe the derivation in the form in which it is applied to finding the frequency spectrum of evenly discretised time-series data, and then indicate its extension to the wavenumber spectrum of unequally sampled spatial data. That approach will be followed here, adapting the presentation of Lacoss (1971), Haddad (1991) and Huntley (personal communication).

Let $x(n)$ be a uniformly sampled time record whose spectrum $S(\omega)$ is to be estimated. It may consist of a sinusoid at frequency ω, as well as others at different frequencies (which are therefore uncorrelated) and uncorrelated noise. These others are collectively denoted by $q(n)$.

$$x(n) = Ae^{j\omega n} + q(n) \tag{4.77}$$

If x is applied to a non-recursive filter with N coefficients $a_0, a_1, \ldots, a_{N-1}$ the output will be

$$y(n) = \sum_{k=0}^{N-1} a_k \, x(n-k) \tag{4.78}$$

where here k stands for a sample index and not a wavenumber. Substituting Equation (4.77):

$$y(n) = \sum_{k=0}^{N-1} a_k \, [A \exp(j\omega(n-k)) + q(n-k)] \tag{4.79}$$

From requirement i) above, if $q(n) = 0$, then

$$y(n) = x(n)$$

that is

$$\sum_{k=0}^{N-1} a_k [A \exp(j\omega(n-k))] = A \exp(j\omega n) \tag{4.80}$$

and so

$$\sum_{k=0}^{N-1} a_k \exp(-j\omega k) = 1 \tag{4.81}$$

Requirement ii) in conjunction with requirement i) implies that with noise and other spectral components in the input, the output power should be as close to the input power as possible. Since these other components are uncorrelated with the signal we are looking for at ω, it follows that the output power P should be as small as possible subject to its containing at least the input power at ω, that is

$$P = \langle y^2(n) \rangle \tag{4.82}$$

and P is to be minimised subject to the constraint of Equation (4.81).
The brackets denote the expectation value over record length.

$$P = \left\langle \sum_{k=0}^{N-1} a_k x(n-1) \sum_{k'=0}^{N-1} a^*_{k'=0} x^*(n-k') \right\rangle$$

$$= \sum_{k} \sum_{k'} a_k a^*_{k'} \langle x(n-k) x^*(n-k') \rangle \tag{4.83}$$

But the expression $\langle x(n-k) x^*(n-k') \rangle$ is the value of the autocorrelation function of x at a lag of $(k'-k)$, $r_{k'-k}$. So

$$P = \sum_{k} \sum_{k'} a_k \, a^*_{k'} \, r_{k'-k} \tag{4.84}$$

From this point matrix notation becomes more concise.

Letting $\mathbf{a} = [\, a_0 \;\; a_1 \;\; a_2 \ldots \; a_{N-1} \,]^T$

and $\mathbf{e} = [\;\; 1 \;\; e^{j\omega} \;\; e^{j2\omega} \;\; \ldots \;\; e^{j(N+1\omega)} \;\;]^T$

where T indicates transposition.

Equation (4.81) becomes

$$\mathbf{e}^{*T} \mathbf{a} = 1 \tag{4.85}$$

and (4.84):

$$P = \mathbf{a}^{*T} \mathbf{R} \, \mathbf{a} \tag{4.86}$$

where **R** is the autocorrelation matrix, element R_{ik} being the autocorrelation function at lag *ik*: r_{ik}.

To minimise P in Equation (4.86) subject to the constraint in Equation (4.85) the method of Lagrangian multipliers is used, and it is found that

$$\mathbf{a} = \frac{\mathbf{R}^{*-1} \mathbf{e}}{\mathbf{e}^{*T} \mathbf{R}^{-1} \mathbf{e}} \tag{4.87}$$

The coefficients of the (imaginary) filter are functions of frequency (in **e**) and of the data itself (in **R**) - a 'data adaptive' filter.

The filter's output is therefore

$$P = \mathbf{a}^{*T} \mathbf{R} \mathbf{a} = \frac{1}{(\mathbf{e}^{*T} \mathbf{R}^{-1} \mathbf{e})^2} \mathbf{e}^{*T} \mathbf{R}^{-1} \mathbf{R} \mathbf{R}^{-1} \mathbf{e} \tag{4.88}$$

but $\mathbf{R}.\mathbf{R}^{-1} = \mathbf{I}$, the identity matrix, so

$$P = \frac{1}{\mathbf{e}^{*T} \mathbf{R}^{-1} \mathbf{e}} \tag{4.89}$$

This is the spectral estimate $S(\omega)$ of the filter for the frequency ω in x. Reverting to normal notation,

$$S(\omega) = \frac{1}{\mathbf{e}^{*T}\,\mathbf{R}^{-1}\,\mathbf{e}} = \frac{1}{\sum_{ik} r_{ik}^{-1}\,\exp[-j(i-k)\omega]} \tag{4.90}$$

To apply this method to the analysis of spatial data the underlying independent variable is the position vector $\mathbf{r}$ rather than time t, and the signal $x(n)$ is replaced by the Fourier coefficient of surface elevation, z:

$$z(\mathbf{r},\omega) = F.T.\{\eta(\mathbf{r},t)\} \tag{4.91}$$

Temporal frequency ω in Equation 4.90 is replaced by spatial frequency $\mathbf{k}$ (reverting to its previous meaning). An ω remains in 4.91 as all these quantities are functions of frequency, but it is the distribution over $\mathbf{k}$ that is of interest here. The equivalent of $\langle x^*(n-i)\,x(n-k)\rangle$ is the cross-spectral component

$$Q_{ik} = z_i^*\,z_k \tag{4.92}$$

where i and k now identify sensors, and the spectral estimate is:

$$S(\mathbf{k},\omega) = \frac{1}{\sum_{ik} Q^{-1}(\omega)\,\exp[-j\,\mathbf{k}\cdot(\mathbf{r}_i - \mathbf{r}_k)]} \tag{4.93}$$

Somewhat surprisingly after all this development Equation (4.93) shows that the computation needed to evaluate the MLM is little more than that for the DFT, being only the inversion of the cross-spectral density matrix Q.

Oakley and Lozow (1977) give an expression for the window function of the MLM for a given array, which in this terminology becomes:

$$W(\mathbf{k},\mathbf{k}') = \frac{\sum_{mn} \exp[-j\,\mathbf{k}'\cdot\mathbf{r}_m]\,Q_{mn}^{-1}\,\exp[j\,\mathbf{k}\cdot\mathbf{r}_n]}{\sum_{mn} \exp[-j\,\mathbf{k}\cdot\mathbf{r}_m]\,Q_{mn}^{-1}\,\exp[j\,\mathbf{k}\cdot\mathbf{r}_n]} \tag{4.94}$$

where $\mathbf{k}'$ is the wavenumber of the signal, and $\mathbf{k}$ the wavenumber being estimated. As expected it includes (in Q) terms dependent on the data itself.

In view of the relatively high resolution that the MLM offers it was chosen (subject to a modification for reflection, Section 4.4.3.6) for the analysis of wave records in this project.

Data adaptive spectral estimator

Referring back to Figure 4.16, the MLM (labelled MLE - maximum likelihood estimator - by Davis and Regier) is successful in picking out a plane wave, but tends to 'over-focus' wider directional spreads. Davies and Regier proposed a modification in which constraint (i) is changed so that it is the integral of output over some (user specified) wavenumber region that is set to unity. Labelled the DASE in the figure, it does show some improvement for the wider-spread seas.

4.4.3.5 Maximum Entropy Method (MEM)

This method is philosophically quite different to the ones described above. The Fourier transform is based on the assumption that the original signal is infinite in duration. In the real case only a limited portion is available for analysis. The application of various windows to the measured signal attempts to reduce the unwanted consequences of a limited data set. Outside the available range the data is assumed either to be zero or made up of endless repetitions of the segment that does exist. As a consequence the estimate is degraded by spectral leakage.

Burg (1972,1975) rejected this approach and made no assumptions about the data outside its actual range. The requirement for his (notional) spectral estimation filter is that its output assumes as little as possible of the unknown region (and so has maximum uncertainty, or entropy) while being consistent with the data that is known.

The form of Burg's maximum entropy spectral estimator is, for discrete time data (Haddad, 1991):

$$S(\omega) = \left[\sum_{n=-p}^{p} q_n \exp(-j\omega n l) \right]^{-1} \tag{4.95}$$

where p defines the extent of the known data. Finding the coefficients q, which include the data itself, is by no means straightforward. Use is made of the theory of linear prediction and the auto-regressive process (Parzen, 1969).

A key parameter is the order of the auto-regressive process by which the MEM models the data. Too low an order fails to resolve close spectral components, the optimum order can show excellent resolution, but too high a value causes a spurious splitting of the true spectral lines. Without prior knowledge of the input choice of order is difficult: Akaike (1969) has proposed criteria for the choice, and Alvarez and Louriero (1986) demonstrate the influence of order on the analysis of Waverider buoy records. Lacoss (1971) compared the

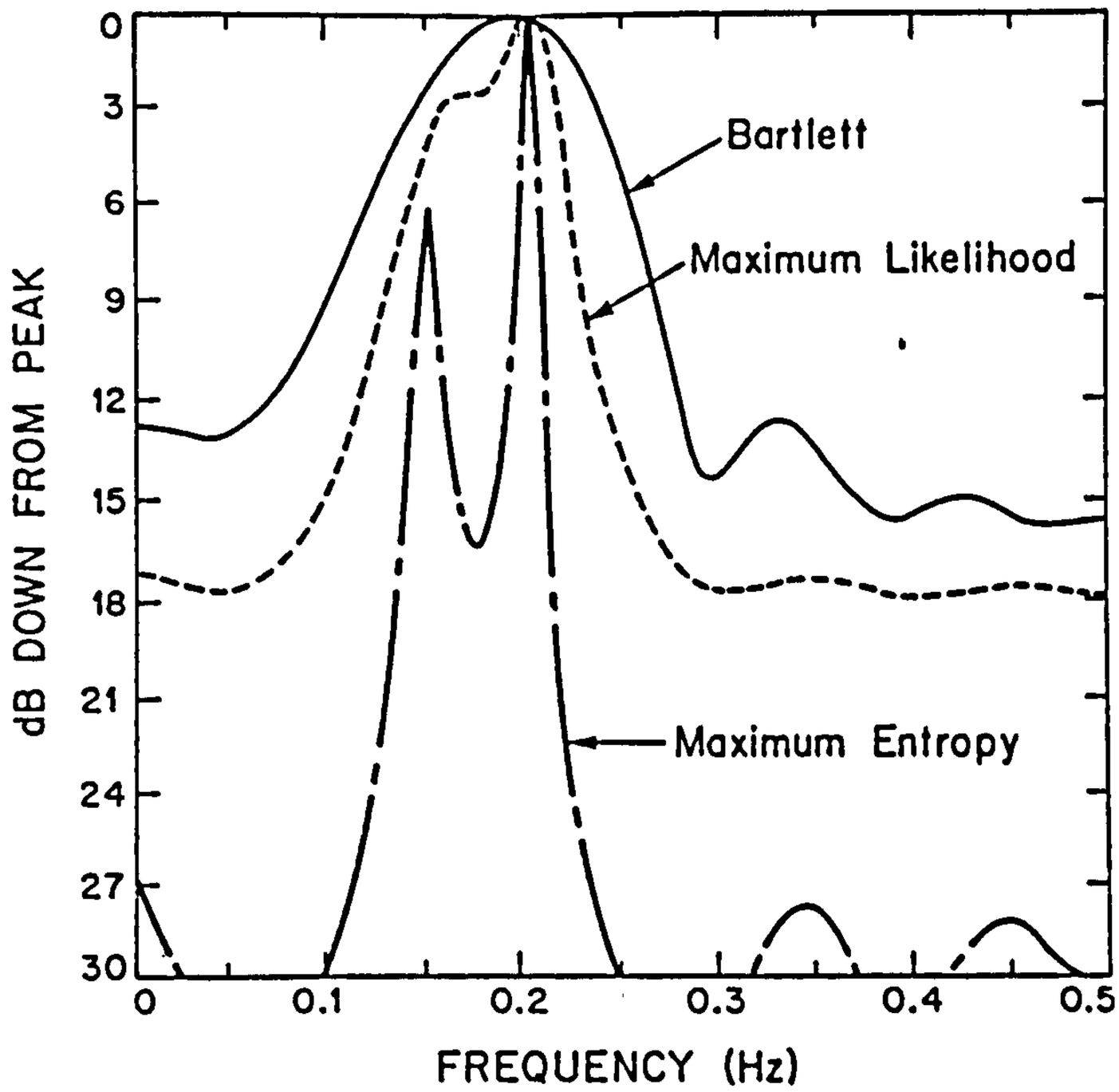

Figure 4.17 : Spectra obtained from correlation function
$\rho_n = 1 + 5.33 \cos(0.3\pi n) + 10.66 \cos(0.4\pi n)$, n=0,1,...10. (from Lacoss, 1977)

conventional DFT, MLM and MEM methods in computing the spectra of short time series. An example is produced in Figure 4.17.

Clearly the resolution of the MEM can be very good. For spatial data Burg noted that it is very difficult to apply the method to unevenly spaced arrays. (McDonough, 1974, describes its application to equally-spaced arrays.) Another complication is that the MEM's peaks represent the square of spectral density rather than spectral density itself. Consequently the MEM was not selected for use in this project, and so a more detailed description is not given here.

4.4.3.6 Including reflected waves

So far in the analysis of the 3D wave system the assumption has been made that the sea state is homogeneous: amplitudes of the frequency components are the same at all locations. Under these conditions the auto-spectra, and the

magnitudes of the cross-spectra, are independent of sensor location. In addition, the phases of the cross-spectra from any pair of sensors with a certain vector separation are independent of the absolute position of the pair. Whilst the time records at the locations may not look the same, due to dispersion, the average powers will be identical. This is the state of affairs that exists when no two wave components are correlated, so that their products averaged over time tends to zero, and the total power is the sum of the two components. The frequencies of the components may be similar but are not identical, and their phase relationship is not fixed over time.

However, that assumption is not valid in wave conditions near a partially reflecting barrier, since the reflected components will be 'phase locked' to their incident counterparts. Power at a point is not the sum of the powers of the components and a structure of partial nodes and antinodes is observed. For the present case those were the conditions in which waves were to be measured, and so it was necessary to use a processing scheme that took account of any phase interaction between wave components.

Isobe and Kondo (1984) modified the MLM to include phase-locked reflected waves. The 'modified maximum likelihood method' - MMLM - gives an estimation of the spectrum covering two cases. In the derivation of the MLM spectral estimator (Section 4.4.3.4) the signal $x(n)$ was modelled as a sinusoid whose magnitude was to be determined, together with uncorrelated noise and signals at different frequencies. Because of the lack of correlation (ie phase locking) the expected value products containing those components was zero. Isobe and Kondo made the modification of setting the signal equal to the elevation from an incident plane wave component and its reflection, together with uncorrelated signals and noise.

If $\mathbf{k}'$ is the wavenumber vector of the reflected wave (so that its magnitude $k'=k$, and its angle is such that the angle of incidence equals the angle of reflection) then, in the notation of Sections 4.4.3.1 and 4.4.3.2,

$$\eta_n = a(\omega)\exp[j(\omega t - \mathbf{k}\cdot\mathbf{r}_n)] + C_r a \exp[j(\omega t - \mathbf{k}'\cdot\mathbf{r}_n)] \qquad (4.96)$$

where C_r is the reflection coefficient. After applying some geometry this becomes

$$\eta_n = a(\omega)\exp[j(\omega t - \mathbf{k}\cdot\mathbf{r}_n)] + C_r a \exp[j(\omega t - \mathbf{k}\cdot\mathbf{r}'_n)] \qquad (4.97)$$

where $\mathbf{r}_n'$ (designated $\mathbf{r}_{nr}$ below) is the position vector to the image of the point n in the reflection line, that is (in the coordinate system of Section 4.5) the point with the same y coordinate as n but the negative of the x coordinate.

Carrying out the steps of the MLM's derivation on this modified signal gives the following result. For any test direction that indicates a spurious negative, or zero, reflection coefficient the estimated directional spectrum is the same as the MLM (Equation 4.93):

$$\hat{S}(\mathbf{k},\omega) = \frac{\kappa}{\sum_m \sum_n Q^{-1}_{mn} \exp[j\,\mathbf{k}\cdot(\mathbf{r}_n - \mathbf{r}_m)]}$$

but for a positive reflection coefficient:

$$\hat{S}(\mathbf{k},\omega) = \kappa \quad \div$$

$$\left[\sum_m \sum_n Q^{-1}_{mn} \exp[j\,\mathbf{k}\cdot(\mathbf{r}_n - \mathbf{r}_m)] \quad - \quad \frac{\left\{\sum_m \sum_n Q^{-1}_{mn}(\omega)\{\exp[j\,\mathbf{k}\cdot(\mathbf{r}_n - \mathbf{r}_{mr})] + \exp[j\,\mathbf{k}\cdot(\mathbf{r}_{mr} - \mathbf{r}_m)]\}\right\}^2}{4\sum_m \sum_n Q^{-1}_{mn}(\omega)\exp[j\,\mathbf{k}\cdot(\mathbf{r}_{mr} - \mathbf{r}_{mr})]}\right] \qquad (4.98)$$

the extra term in the denominator being called the 'phase interaction term'.

The proportionality constant κ is set so that the resulting estimated directional spectrum, when integrated over angle, agrees with the auto-spectra at any of the locations:

$$Q_{mm}(\omega) = \int_{\mathbf{k}_i} [\hat{S}(\mathbf{k}_i,\omega) + 2\sqrt{\hat{S}(\mathbf{k}_i,\omega)\hat{S}(\mathbf{k}_r,\omega)\cos[\mathbf{k}_r\cdot(\mathbf{x}_m - \mathbf{x}_{mr})]} + \hat{S}(\mathbf{k}_r,\omega)]\,d\mathbf{k}_i \qquad (4.99)$$

the subscript i specifying the incident range of $\mathbf{k}$, and r the reflected, so that

$$\hat{S}(\mathbf{k}_r, \omega) = C_r^2 \hat{S}(\mathbf{k}_l, \omega) \tag{4.100}$$

Isobe and Kondo present the results of tests on their method using numerically generated, simulated, wave data, based on the Cartwright/Mitsuyasa spreading model of Equation (4.31). Their findings may be summarised:

i) The effects of phase interaction diminish with distance (as a proportion of wavelength) from the reflection line. The rate of fall is faster for seas of wide directional spread, and for wave directions off the shore normal line.

ii) Resolution is greatly improved by increasing the number of sensors. Isobe and Kondo test arrays of between two and five sensors.

ii) Array shape is less critical than it is for DFT processing.

iv) The method is sensitive to noise (as is the MLM), with sharpness of resolution falling quite markedly for only 1% noise level, but stabilising quickly with more, so that there is little difference between 10 and 20% noise.

v) The MMLM sometimes generates spurious peaks in the directional distribution, and may split the peak of a uni-modal distribution into two. This appears to be the result of spatial aliassing. Isobe and Kondo indicate that this will not occur if the shoreward sensor is $< 0.2L$ from the reflection line, and state that if present these artifacts should not be difficult to identify.

vi) Minimum and maximum sensor separations are recommended to be $0.2L$ and $1.5L$.

vii) The method does not constrain the reflection coefficients to be constant for all frequencies (since the directional analysis is done on each frequency separately) nor for all angles. The accuracy of the reflection coefficient estimate declines as wave direction deviates from the shore-normal.

The MMLM was much the most suitable published method for the present application.

4.5 ANALYSIS SCHEME

4.5.1 Overview

The implementation of these data analysis procedures to the measured wave records is now described. Figure 4.18 shows the overall scheme in four main stages:

I Data preparation

II Removing the tidal trend and mean level

III Calculating the (omni-directional) spectra

IV Calculating the directional spectrum.

At each stage additional files of plots and statistics are produced. With many hundreds of records (as well as the simulated data records) together with the associated information on sensor positions and site topography, and the calibration data, care is needed to maintain the correct association between files. This is done by applying a logical file-naming and directory structure. Also the files contain, as far as possible, all the variables needed for a complete interpretation without reference to information kept elsewhere.

Most of the 25 or so programs that carry out these functions were written in the mathematical analysis language MATLAB®, and the others are in FORTRAN. Examples of the output will be found in Chapter 5.

4.5.2 Stage I : Data preparation

Chapter 3 described the decoding of wave recorder 'dump' files so that each measurement record of pressure readings ended up with its own file, in standard ASCII form, with all the instrument calibration information applied. The next step is converting the sub-surface pressures into surface heights above the sea bed. Equation 4.20 is implemented in a program described by Davidson (1992). The user supplies the applicable atmospheric pressure value for the record, and a list of transducer heights above the sea bed. A typical water density (1025 kg/m^2) is assumed. Mean depth is found

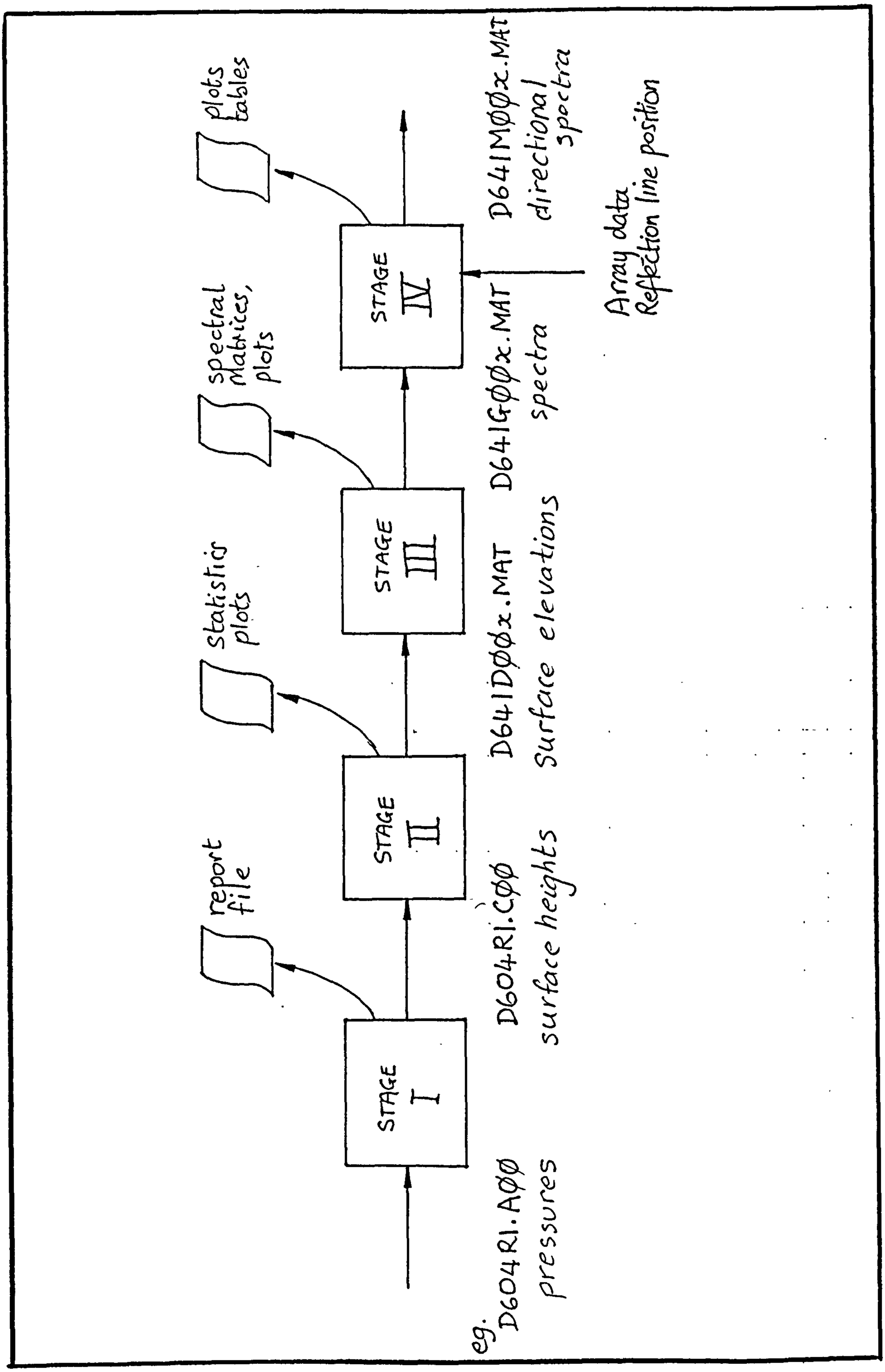

Figure 4.18 : Main stages in the analysis

from the data and the inverse factor for the pressure head attenuation, for each frequency (or rather its corresponding wavelength), is evaluated iteratively. This gain function is then applied, as a digital filter in the frequency domain, to the Fourier transform of the pressure record. Phases remain unchanged. The resulting record is inverse transformed and the mean added back in to give a time record of surface heights.

(Previously a non-recursive, time domain, filter had been used, but this lost more data than the frequency domain filter due to its inferior impulse response , and its advantage of ability to work in real-time was not relevant here.)

Whilst the magnitude response is dictated by Equation 4.20, the higher frequencies cannot be amplified without limit. Referring to Fig. 4.6 a 4-second wave (chosen as the highest frequency of interest) will require multiplication by 1.43 (ie 1/0.7) if occurring in three metres of water, but 20 (ie 1/.05) in 15m. A judgement must be made on the degree of amplification permissible, and that will depend on the signal to noise ratio of the measurement. Noise sources comprise contributions from all the amplifiers, as well as 'hydrodynamic noise': any pressure fluctuation appearing at the transducer diaphragm not related to the passage of waves. Other effects such as dead band and hysteresis errors in the transducers and quantisation noise from the A/D converter also contribute. An overall calculation may be made along the lines of the error calculations in Appendix F, choosing the appropriate signal paths from Figure 2.8. However this lengthy process can be circumvented by examining the actual performance of the system, in the laboratory and using selected field data sets. That shows that quantisation noise dominates, as had been hoped at the instrument planning stage (Section 2.2.2) in which a (possibly conservative) maximum amplitude of 10 was envisaged.

The files of surface heights are, at this stage, self-contained. That is, instrument settings, calibration data and physical variables have all been applied to the data. The file header identifies the drawing number of the

transducer layout, and one remaining instrument setting - the sampling interval. The file header also identifies the site, time and date of record start, and the units of the data in the file.

Numerical simulations

A program was written to construct files of simulated surface heights for use in assessing the performance of the analysis procedures. These are fairly simple, allowing the user to specify a number of components of different frequencies and directions, with associated reflection coefficients. The files are used mainly for fault-finding rather than for a thorough validation, for which more complex and realistic simulations would be required.

Site information

The directional analysis programs (as well as the simulation program if it is to include reflection) must be supplied with the position vectors of the transducers with respect to the apparent reflection line. The location of this line is a variable that depends on tide level and the slopes of the structure, and possibly (it is hoped to a small extent) on the wave angle. This is discussed in Section 4.5.5.

4.5.3 Stage II : Removing the tidal trend and mean level

Most records of surface height show a strong trend due to the tide. This, and the mean water level, are removed to leave surface elevations from the still-water level. Since linear waves are assumed, the results have a zero mean value. To remove a trend Bendat and Piersol (1986) (Section 11.1) recommend fitting a polynomial to the data set by the least squares method, and then subtracting it from the data. This was done here with a second order polynomial.

In addition to the surface elevation records the output file contains: a vector of sampling instants (in seconds after the record start time) which corresponds row for row with the data array, and a vector of quality flags,

one for each column (ie. transducer). This enables the user to earmark data from any malfunctioning, or non-existent, sensor. subsequent programs use the flags to size arrays automatically and conduct all calculations on the good data only. The file also carries with it the mean depth that was removed from the surface heights.

4.5.4 Stage III : Calculating the spectra

One of the purposes of producing auto- and cross- spectra for each record is to provide the directional analysis programs with estimates of signal magnitude and phase for each frequency value of a distribution. These must be as reliable as possible because errors here can upset the much more complicated directional analysis procedures. Spectra are obtained in the normal way by taking the fast Fourier transform (Cooley and Tukey, 1965) and multiplying it by its conjugate. This supercedes the equivalent route used earlier of transforming the signal's autocorrelation function (summarised in Blackman and Tukey, 1959). For the cross-spectrum the Fourier transform of one signal is multiplied by the conjugate of the Fourier transform of the other of the pair.

The practical problems of carrying this out on sets of random data of limited length are well known (see for example Lynn and Fuerst, 1989, Bendat and Piersol, 1986, or Harris, 1978). Firstly the sampling process introduces a spurious periodicity into the transform which causes the aliasing of any frequency in the input greater than half the sampling frequency. This is dealt with by anti-aliasing filters, Section 2.5.3.3.

Secondly, the limited duration of 'window' through which the data is viewed imposes a limit to the frequency resolution in the transform (no matter how fast the sampling rate). It also introduces a 'leakage' of energy from other frequencies in the input to the one being estimated. This can be thought of as a result of the implicit repetition of the windowed data set - if there are large jumps in data values at the joins in the repetitions then spectral leakage will be severe (Harris, 1978). Tapering the ends of the window

reduces these discontinuities (and their derivatives) and reduces the leakage, but at the cost of frequency resolution, and of losing some of the data.

Thirdly, the *number* of time samples in the record determines the number of frequency samples in the transform. The true Fourier transform of a sampled data sequence is a continuous function of frequency. The FFT yields only samples of the continuous function. If a spectral line in the underlying transform lies between two samples its power will be shared between adjacent samples, and therefore difficult to discern. This is the so-called 'picket-fence' effect (Haddad and Parsons, 1991, Section 7.2). Zero-padding either end of the windowed data set increases the number of frequency samples, though not the underlying resolution. Zero padding, and the application of any window other than the rectangular, require an appropriate scaling in amplitude to preserve total power in the signal.

Finally, for random data, there is the question of statistical reliability. It was stated in Section 4.4.1 that the physically realised (and measured) record is modelled as only one outcome of many possibilities, the others of which did not actually occur: one member of an ensemble with common statistics. But if the members' time records are different then their Fourier transforms will also be different. In many studies the general characteristics of a wave field are of more interest than the detailed forms and timings of the wave trains. Similarly, in the frequency domain the form of the spectrum of the underlying random process would be of interest, not the spectrum of any particular record. In these circumstances an assessment is made of the statistical significance of measured spectra. The null hypothesis is made: that the time series is completely random and contains no particular dominant frequencies. Each of the Fourier coefficients is assumed to be a Gaussian random variable. The significance of a certain number of observations of this coefficient is assessed and expressed as a confidence band around an expected value. The method is presented in texts such as Jenkins and Watt (1968) and also by Huntley (1992). It turns out that if only one measurement of a Fourier coefficient is available then the standard

deviation will be as great as the expected value. Even if twelve are available, then the confidence band is still very wide, extending from 0.6 to 1.8 times the expected value. In practice it is often difficult or impossible (due to lack of stationarity) to acquire data of adequate duration for that many independent Fourier transforms.

However, the main interest to date in using the wave recorder has been to measure the reflection performance of coastal structures, and not the general characteristics of the wave field. The pessimistic conclusions of the above analysis would apply if it were possible to measure incident and reflected wave characteristics only at different times, then to compare spectral peaks to deduce reflection coefficient. That is not the case here. Any particular wave record contains both the (incident) input to the wave-structure system and the (reflected) output. The fact that the input wave conditions were drawn at random from a set of possibilities is less important than whether the system's output is well correlated with its input.

Some non-deterministic elements do remain, such as instrument noise, and imperfections in the analysis. The standard methods of improving statistical significance will be used, but the level of confidence in the spectrum of a particular record is higher than in the spectrum of a general sea state.

There are three standard methods:

i) Neighbouring frequency estimates are split into groups and averaged.

ii) Neighbouring frequency estimates are smoothed with, for example, a moving-average low pass filter.

iii) Block- (or ensemble-) averaging. A single time record is split into segments which are individually transformed, and the corresponding frequency estimates from the spectrum of each segment are averaged.

All methods result in a loss of frequency resolution.

Procedure for obtaining omni-directional spectra

Method (iii) ('the Welch method', Oppenheim and Schafer, 1975, p556) was adopted as it allows more flexibility in the way the window is applied to the

data. The time series of about 1350 samples were sectioned into nine partially overlapping blocks, then windowed, transformed and averaged. Overlapping the blocks brings the advantage that data which would have been attenuated in the tails of a window is included in the neighbouring block. Careful choice of the overlap ratio results in the loss of only a few data points while permitting block lengths to be integer powers of 2 (in this case 256) to suit the FFT. (Zero padding, or the use of a Winograd Fourier transform algorithm (eg Press *et al*, 1989, Chapter 12) are other ways of retaining the computational efficiency of the FFT and not losing data). One wants as many independent blocks as possible for maximum statistical reliability, but a minimum block size is set by the required frequency resolution. That in turn is limited by the errors caused in the MMLM from the range in wavelength contained within the frequency 'bins'. The compromise chosen was a block size of 256 half-second samples giving a frequency bin width of 1/128, or 0.0078, Hz. Tests were done to assess the errors arising from spectral leakage into adjoining bins. The effect is that the MMLM produces spurious peaks as the phases in Q do not agree with the wavelength assumed from the incorrect frequency. These peaks were found to be acceptably small for the block size chosen.

Many data windows have been developed. Harris (1978) defines a number of performance criteria and compares over twenty common windows. Selection of an appropriate window requires a judgement of how its various characteristics will affect the type of data to be analysed. The Hanning window was chosen as a reasonable compromise between close-in resolution and leakage from frequencies distant from the central lobe. (This choice is reasonable but may not be the optimum; more work is needed.)

Stage III produces an output file containing the auto-spectra of each transducer's wave record, cross-spectral density matrices Q_{mn} for all transducer pairs (one matrix for each frequency bin), coherence matrices, a vector of frequency values to enable the matrices to be interpreted as spectra, and the quality flags copied through from Stage II. That constitutes

all the measured (as opposed to site) information that the directional analysis programs need.

4.5.5. Stage IV: Calculating the directional spectrum

Equations 4.93, 4.98 and 4.99 define the modified maximum likelihood method (MMLM). The general procedure is, for each frequency bin:

i) evaluate the cross-spectral matrix **Q** (Section 4.5.4)
ii) invert it (necessary only once per frequency)
iii) for each test direction in steps of 10° around the circle:
    iv) evaluate the four matrices of phase shifts, ie $\exp[j\mathbf{k}.(\mathbf{r}_n-\mathbf{r}_m)]$ etc
    v) apply these phase shifts, element by element, to $\mathbf{Q}^{-1}$
    vi) combine the terms in the denominator of Equation 4.98
vii) reciprocate and scale by evaluating k with Equation 4.99.

In practice there can be a number of difficulties in following this procedure.

Inverting the cross-spectral matrix

In some cases the matrix **Q** can be singular or nearly singular, and therefore impossible to invert. With real, measured, wave data the matrix is usually well-conditioned, but with simulated data of a few components and no added noise the coherences are unity, and **Q** singular. To overcome this **Q** is perturbed by increasing the elements of the leading diagonal by one part per million - small compared to the error specification of the measurements, but large compared to the precision of computation.

Locating the apparent reflection line

The MMLM assumes that reflection occurs at a long vertical barrier of a certain, not necessarily unity, reflection coefficient. Whilst this is true of some sea walls and breakwaters it is not true for coastal structures with compound, inclined slopes. However, as observed from the transducer array, the wave field of interacting incident and reflected components can be equivalent to such an idealised case. The problem is to find the position of

this equivalent idealised barrier relative to the transducers. Davidson (1993) has implemented in software, and extended, the solutions of Hotta *et al* (1981) and Suhayda (1974) evaluating the complex nodal structure (envelope of wave height versus cross-shore distance) near a multi-slope reflecting barrier. A cross-correlation technique predicts from this amplitude profile the location of the apparent reflection line. The theoretical basis relies on the shallow water approximation to linear wave theory (Table 4.1). Application is therefore limited to the lower frequency end of the wind wave range.

Additional information was gained from model tests carried out in the University of Plymouth's wave channel (Hiscock, 1992). Also, for shore normal waves it is proposed to adapt the frequency response method to give distance to the reflection line.

This work is continuing: it is hoped to build up a picture of how the reflection line location at a structure is influenced by tide height, wave frequency and spectral form, wave height, and angle of approach. This will both advance the understanding of the reflection process, and provide the necessary input to the MMLM with more confidence than is presently possible.

REFERENCES

Airy G.B. (1845)
Tides and waves
Encyc. Metrop., Art. **192** 241-396.

Akaike H. (1969)
Fitting autoregressive models for prediction
Ann. Inst. Stat. Math. **21** 243-247.

Alvarez J.C. and Louriero A.M. (1986)
Maximum entropy spectral estimation for wind waves
Proc ASCE Conf on Coastal Engineering.

Barber N.F. (1963)
The directional resolving power of an array of wave detectors
in *Ocean wave spectra* Prentice Hall, Englewood Cliffs, New Jersey, USA,pp137-150.

Blackman R.B. and Tukey J.W. (1959)
The measurement of power spectra from the point of view of communications engineers
Dover Press, New York, USA.

Bullock G.N. and Murton G.J. (1989)
Wave testing of coastal structures
in *Advances in water modelling and measurement* Ed. M.H. Palmer, ch25, pp353-366, BHRA, UK.

Bendat J.S. and Piersol A.G. (1986)
Random data: analysis and measurement procedures
2nd ed. John Wiley and Sons, New York, USA.

Burg J.P. (1972)
The relationship between maximum entropy spectra and the maximum likelihood spectra
Geophysics **37** April 1972, 375-376.

Burg J.P. (1975)
Maximum entropy spectral analysis
PhD dissertation, Stanford University, USA.

Cartwright D.E (1963)
The use of directional spectra in studying the output of a wave recorder on a moving ship
in *Ocean wave spectra* Prentice Hall, Englewood Cliffs, New Jersey, USA, pp203-218.

Cavaleri L. Ewing J.A. Smith N.D. (1978)
Measurement of the pressure and velocity field below surface waves
in *Turbulent Fluxes through the sea surface, wave dynamics, and prediction*
Eds: A. Favre and K. Hasselmann. Plenum Press New York. pp257-272.

Cooley J.W. and Tukey J.W. (1965)
An algorithm for the machine calculation of complex Fourier Series
Mathematics of computing **19** 297-301.

Crabbe J.A. Driver J.S. Haine R.A. (1983)
An intercomparison between six wave recorders at NMI Tower, Christchurch Bay
IOS Deacon Laboratory Report No 154.

Davidson M.A. (1992a)
Development and implementation of a software routine for the analysis of the reflection processes associated with random and monochromatic waves
Research Report No. SCSE 92-003, School of Civil and Structural Engineering, University of Plymouth, Plymouth, UK.

Davidson M.A. (1992b)
Implementation of linear wave theory in the frequency domain for the conversion of sea bed pressure to surface elevation
Research Report No. SCSE 92-008, School of Civil and Structural Engineering, University of Plymouth, Plymouth, UK.

Davidson M A , Bird P A D , Bullock G N and Huntley D A. (1993)
A mathematical solution for standing, shallow water waves over a multiple component sloping sea bed.
Research Report No SCSE 93-001, School of Civil and Structural Engineering, University of Plymouth, UK

Davis R.E. and Regier L.A. (1977)
Methods for estimating directional wave spectra from multi-element arrays
Jnl Mar. Res. **35** 453-477.

Dudgeon D.E. (1977)
Fundamentals of digital array processing
Proc IEEE **65** (6) 898-904.

Fenton J. (1986)
Polynomial approximation and water waves
Proc. 20th Coastal Engineering Conf.,Taiwan, pp193-207.

Friedrichs K.O. (1948)
Water waves on a shallow sloping beach
Commun. Pur & Appl. Maths. **1** 109-134.

Gabriel D.W. and Hedges T.S (1986)
Effects of current on interpretation of sub-surface pressure spectra
Coastal Engineering, Elsevier, Amsterdam, **10** 309-323.

Gilbert G. and Thompson D.M. (1978)
Reflections in random waves: the frequency response method
Report No.IT173, Hydraulics Research Station, Wallingford, Oxford, UK.

Goda Y. (1985)
Random seas and the design of maritime structures
University of Tokyo Press, Tokyo, Japan.

Grace R. (1978)
Surface wave heights from pressure records
Coastal Engineering, Elsevier, Amsterdam, **2** 55-67.

Guza R.T. and Bowen A.J. (1975)
The resonant instabilities of long waves obliquely incident on a beach
Jnl. Geographical Reseach **80** (33) 4529-4534.

Guza R.T. and Thornton E.B. (1980)
Local and shoaled comparisons of sea surface elevations, pressures and velocities
Jnl. Geophys. Res. **85** (C3) 1524-1530, Mar 1980.

Haddad A. and Parsons W. (1991)
Digital signal processing
W.H.Freeman and Company, New York, USA and Oxford, UK.

Hasselmann D.E. Dunckel M. and Ewing J.A. (1980)
Directional wave spectra observed during JONSWOP 1973
Jnl Physical Oceanog. **10** 1264-1280 (Aug 1980)

Harris F.J. (1978)
On the use of windows for harmonic analysis with the discrete Fourier transform
Proc. IEEE **66** (1) Jan 1978.

Haykin S. (ed) (1985)
Array signal processing
Prentice Hall, Englewood Cliffs, New Jersey, USA, pp203-218.

Hiscock B. (1992)
Plymouth Breakwater: reflection characteristics
BEng Project Report, Department of Civil and Structural Engineering, University of Plymouth, UK.

Hom-ma M. Horikawa K. and Komori S. (1966)
Response characteristics of underwater wave gauge
Proc 10th Conf on Coastal engineering, pp99-114.

Horikawa K. (1978a)
Coastal Engineering
University of Tokyo Press, pp34-35, 1978.

Horikawa K. (1978b)
Coastal Engineering
University of Tokyo Press, pp291-3.

Hotta S. Mizuguchi M. Isobe M. (1981)
Observations of long period waves in the nearshore zone
Coastal Engineering in Japan, **24** 41-76.

Huntley D.A. (1992)
Spectral analysis
Seminar notes, University of Plymouth, UK.

Isaacson M. (1976)
The second approximation to mass transport in cnoidal waves
J. Fluid Mechs. **78** 445-457.

Isobe M. and Kondo K. (1984)
Method for estimating directional wave spectrum in incident and reflected wave field
Proc ASCE Conf on Coastal Engineering, Houston, Texas pp467-483.

Jacobs O.L.R (1969)
Introduction to random processes
in *Modern control theory*, Eds D. Bell and A.W.J. Griffin , McGraw-Hill, London.

Jeffreys E.R. (1987)
Directional seas should be ergodic
Applied Ocean Research **9** (4) 186-191

Jenkins G.M. and Watts D.G. (1968)
Spectral analysis and its applications
Holden Day, SanFrancisco and London.

Kajima R. (1969)
Estimation of incident wave spectrum under the influence of reflection
Coastal Engineering in Japan **12** 9-16.

Kay S.M. and Marple S.L. Jnr. (1981)
Spectrum analysis - a modern perspective
Proc IEEE **69** (11) Nov 1981 1380-1419.

Kinsman B. (1965)
Wind waves
Prentice Hall, Englewood Cliffs, New Jersey, USA.

Komar P.D. (1978)
Beach processes and sedimentation
Prentice Hall Inc, New Jersey, p62.

Lacoss R.T. (1971)
Data adaptive spectral analysis methods
Geophysics **36** (4) 661-675 (Aug 1971)

Lamb H.
Hydrodynamics
Cambridge University Press, 1932.

Lee D-Y. Wang H. (1984)
Measurement of surface waves from subsurface gage
Proc19th Coastal Engineering Conf, Houston, pp270-286.

Le Mehaute B. (1976)
An introduction to hydrodynamics and water waves
Springer-Verlag p205.

Long R.B. and Hasselmann K. (1979)
A variational technique for extracting directional spectra from multi-component wave data
Jnl Physical Oceanog. **9** 373-381 (Mar 1979)

Longuet-Higgins M.S. (1956)
The refraction of sea waves in shallow water
Jnl. Fluid Mech. **1** 164-76.

Lynn P.A. and Fuerst W. (1989)
Introductory digital signal processing
John Wiley and Sons, Christchurch, UK.

McDonough R.N. (1974)
Maximum entropy spatial processing of wave data
Geophysics **39** 843-857.

Miche R. (1944)
Undulatory movements of the sea in constant and decreasing depth
Ann. de Ponts et Chaussees pp25-78, 131-164, 270-292 resp.

Muir-Wood A.M. (1969)
Coastal hydrodynamics
Macmillan, London, 187pp.

Munk W.H. (1951)
Origin and generation of waves
Proc. 1st Conf on Coastal Engineering pp1-4.

Oakley O.H. and Lozow J.B. (1977)
Directional spectra measured by small arrays
Proc 9th Offshore Technology Conf, May 2-5, 1977, Houston, Texas, USA.

Oppenheim A.V. and Schafer R.W. (1975)
Digital signal processing
Prentice Hall, Englewood Cliffs, New Jersey, USA.

Parzen E. (1969)
Multiple time series modelling
in *Multivariate Analysis II*, Ed P.R. Krishnaiah, Academic Press, New York, USA.

Press W.H. Flannery B.P. Teutolski S.A. and Vetterling W.T. (1989)
Numerical recipes: the art of scientific computing
Cambridge University Press, Cambridge, UK.

Sarpkaya T. and Isaacson M. (1981)
Mechanics of wave forces on offshore structures
Van Nostrand Reinhold Co. pp215-224.

Silvester R. (1974)
Coastal Engineering
Elsevier Scientific Publishing Co., 1 186-191.

Suhayda J.N. (1974)
Standing waves on beaches
Jnl Geophys Res **79** (21) 3065-3071

Tucker M.J. (1992)
Waves in ocean engineering
Ellis Horwood, pp60-63.

Ursell F. (1953)
The long wave paradox in the theory of gravity waves
Proc. Cambridge Phil. Soc. **49** (4) 685-94.

Wang H. Lee D-Y. and Garcia A. (1986)
Time series surface-wave recovery from pressure gage
Coastal Engineering (Elsevier, Amsterdam) **10** 379-393.

BIBLIOGRAPHY

Barber N.F. 'Water Waves' Wykeham Publications (London) Ltd., 1969.

Bendat J.S. and Piersol A.G. (1986)
Random data: analysis and measurement procedures
2nd ed. John Wiley and Sons, New York, USA.

British Standards Institution 'BS6349:1984 British Standard Code of Practice for the design of Maritime Structures'

Dean R.G. and Dalrymple R.A. 'Water Wave Mechanics for Engineers and Scientists'Prentice-Hall, New Jersey, 1984.

Goda Y. 'Random seas and the design of maritime structures' University of Tokyo Press, 1985.

Haddad A. and Parsons W. (1991)
Digital signal processing
W.H.Freeman and Company, New York, USA and Oxford, UK.

Haykin S. (ed) (1985)
Array signal processing
Prentice Hall, Englewood Cliffs, New Jersey, USA, pp203-218.

Horikawa K. 'Coastal Engineering' University of Tokyo Press, 1978.

Kinsman B. 'Water Waves: their generation and propagation on the ocean surface' Prentice-Hall, New Jersey, 1965.

Komar P.D. 'Beach processes and sedimentation' Prentice Hall Inc, New Jersey, 1976.

Le Mehaute B. 'An introduction to hydrodynamics and water waves' Springer-Verlag, 1976.

Muir-Wood A.M. and Fleming C.A. 'Coastal Hydraulics' Macmillan, London, 1981.

Sarpkaya T. and Isaacson M. 'Mechanics of wave forces on offshore structures' Van Nostrand Reinhold Co., 1981.

Silvester R. 'Coastal Engineering' Elsevier Scientific Publishing Co., v1, 1974.

Tucker M.J. 'Waves in Ocean Engineering' Ellis Horwood, 1991.

US Army Corps of Engineers 'Shore Protection Manual', v1 and 2, Coastal Engineering Research Centre, Washington DC, 1984.

Weigel R.L. 'Oceanographical Engineering' Prentice Hall Inc., 1978.

PAGE NUMBERING AS ORIGINAL

CHAPTER 5
RESULTS

CHAPTER 5
RESULTS

5.1 INTRODUCTION

At the time of writing (Spring 1993) two wave recording systems had been manufactured, and measurements made at four sites. This chapter describes two of these sites, and presents in detail four measurement records from the many hundreds obtained (Table 5.1). The measurements at the other two sites - Bovisand Bay near Plymouth and Felpham near Bognor Regis - were carried out to provide data in support of separate research programmes; reflection of waves was low. The breakwaters at Plymouth and Elmer were of more relevance to this study.

5.2 FIELD SITES

5.2.1 Plymouth Breakwater

Built by Rennie between 1811 and 1842 to protect the naval port of Plymouth, this armoured rubble-mound breakwater is founded on a rock shoal at the entrance to Plymouth Sound (Figure 5.1 and Plate 11). It is nearly two kilometres long and consists of about four million tonnes of limestone taken from local quarries (Rennie, 1848). The upper sections are surfaced with dovetailed granite paving. Since the 1920's rectangular concrete blocks ranging in weight from 25 to 100 tonnes have been placed on the berm in an attempt to dissipate the force of the waves. The seaward side is made up of sections of different gradients (Figure 5.2). The unusual shape and the considerable width of the base are partly due to shifting and settlement of the material over the long construction period. Though very stable, these gradients would be considered uneconomical today.

DEPLOYMENT NO.	SITE	NO. OPS	PERIOD	NO. MEASUREMENT RECORDS	
1	Plymouth BW	1	19.5.88	1	(Trial only)
2	Plymouth BW	1	24.10.88 - 31.10.88	58	
3	Plymouth BW	4	26.1.88 - 8.3.89	236	
4	Plymouth BW	1	6.12.89 - 10.1.90	12	(Malfunction /damage)
5	Bovisand, Plymouth	1	31.3.92 - 29.4.92	127	
6	Elmer, W.Sussex	7	4.6.92 - 17.8.92	586	
7	Felpham, W.Sussex	?	11.2.93 -		

Table 5.1 Summary of wave recorder measurements

Penlee Point to the west of the Sound and Renney Point, Wembury to the east restrict incident waves to those from bearings of 140° to 235°. Longer wave components are limited to an even smaller range due to refraction. The area in front of the breakwater is reasonably flat so that waves do not shoal noticeably over the array. The depth, at about 8 metres below chart datum, was convenient for diving operations. Moreover that was deep enough for linear wave theory to be a reasonable approximation, while not so deep that pressure fluctuations at the sea bed would be unacceptably attenuated. The transducer layout is shown in Figure 5.3. The separations shown on brackets are the design values; actual surveyed values are in Figure 3.1.

5.2.2 Elmer, West Sussex

In 1990 the authority with responsibility for the frontage, Arun District Council, constructed two 'rock island' breakwaters to the design of consultants Robert West and Partners (1991) to protect the village of Elmer (near Bognor Regis) from flooding by storm waves overtopping the sea wall. Each of the structures was 90m long, and constructed from 10,000 tonnes of 6 to 8 tonne rocks. They were located on the foreshore 130m from the sea wall (Figures 5.4 and 5.5 and Plate 12). The seaward face had the unusually steep slope of 1:1.1. That was partly experimental: the 1990 work was an intermediate step for 'emergency' protection; modification was envisaged for 1992. Apart from providing a partial barrier to incident waves these breakwaters cause a shoreward build up of beach material. During the summer of 1991 over 11,000 m^3 of sand and shingle had accumulated.

The flat foreshore around the structure ensured wave homogeneity over the transducer array, and allowed placement close-in to what was expected to be a barrier of high reflectivity. The depth, however, was less than ideal. At 1.5 m below Ordnance Datum the site dried out at low water spring tides. That resulted in the equipment being situated in the surf-zone. Extra precautions against storm damage were therefore taken: new transducer mounting blocks and wave recorder platform were designed to enclose the units completely in steel plate, except for the faired top plates of the

Plate 11 : Plymouth Breakwater from the east

Plate 12 : Rock Island Breakwater at Elmer, West Sussex

transducers. The blocks and platform were dug into the chalk bed with the aid of a mechanical excavator. Bearing in mind that the expected intensity of the wave climate was lower than that at Plymouth it was hoped no damage would occur. This has in fact been the case.

The restricted depth had implications also for the analysis. The assumption of linear theory would hold less well. Also tide would cause a greater fractional depth change over a record, leading to a loss of stationarity. On the other hand, shallow water measurement did bring the benefit of smaller pressure attenuation. The transducer layout is shown in Figure 5.6.

5.3 DESCRIPTION OF SELECTED DATA SETS

Two records from the January - March 1989 deployment at Plymouth breakwater and two from the Elmer deployment of 1992 are selected for presentation here. The first from Plymouth consists of a long swell, and the second is of a storm. Visual observations were taken at the same time as the latter record and provide a rough check on the measurement and directional analysis. The first from Elmer is a low-intensity swell, in which the waves would not have been breaking, and the second contains the largest waves of the deployment.

5.3.1 Plymouth - long period swell (Figures 5.7 to 5.19)

The first and last parts of the file of measured pressures are shown in Figure 5.7. The six columns are arranged in the order of the electronic channel numbers in the wave recorder. Unfortunately, for deployments 3 and 4 it was not possible (for reasons of underwater connector compatibility) to match this order to the location numbers on the transducer layout plan (Figure 5.5). The plan does, however, show the correspondence between locations and channels: numbers 1 and 5 are interchanged. The appropriate correction is carried out in a later stage of the analysis. The rows contain

the pressure readings in millibars, taken simultaneously, each row separated by 0.5 seconds. The text header provides further information.

When corrected to surface heights by frequency domain filtering (where the 'surface height' is the dimension in metres from sea bed - not transducer sensing level - to the instantaneous water surface) the file in Figure 5.8 results. (The version of the program carrying this out did not modify the text header correctly.) The next step, for the Plymouth data, is to swap columns 1 and 5 so that from that point the column numbers correspond to transducer location numbers.

The pressure readings of Figure 5.7 are plotted in Figure 5.9, and the surface elevations (surface heights with means removed) in 5.10. The correspondence between these two is seen more clearly in the shorter section in Figure 5.11. To make the comparison pressures have been converted to surface elevations using the simple hydrostatic relationship, that is with no allowance for attenuation with depth (full line). Calculated surface elevations, applying Airy wave theory, are shown in the dotted line. As expected, the higher frequency components in the pressure record have been amplified substantially, but the phases remain unaltered. The erroneous points at the beginning and end due to the impulse response of the filter have been deleted, losing nine seconds at each end.

The program that de-trends and de-means these files also produces tables of statistics, and these are given in Figures 5.12 and 5.13 for pressures and surface heights respectively. Significant wave height is fairly low, in the region of 0.75 metres. The differences between mean surface height in each column show the variation in sea-bed level over the array. Maximum excursions are displayed in standard deviations as well as the base units to indicate any outliers that may require checking.

Frequency distributions of both pressures and heights (taking the form of periodograms rather than spectral densities, units: mb^2 and m^2) are given in Figures 5.14 and 5.15: the action of the pressure-to-surface filter can again

be seen. The frequency range plotted is 0 to 0.4 Hz. Plots at the appropriate vertical scale of the full range up to the Nyquist frequency of 1 Hz show no energy above 0.4 Hz.

The cross-spectral matrices for some of the higher-energy frequency 'bins' are tabulated in Figure 5.16, and the corresponding coherences in 5.17. The cross spectral matrices are the 'raw material' for the directional analysis that follows. The leading diagonals are the auto spectra. In a sea with no phase locking these would be of similar magnitude. A large disparity (as in frequency bin 8) suggests a high degree of reflection: some of the transducers are close to the partial nodes for that particular frequency, and others close to the partial anti-nodes.

The output of directional analysis by the modified maximum likelihood method (MMLM, Chapter 4) is shown in Figure 5.18 as a contour plot, with the directional distribution of the most energetic frequency bin in 5.19. The angle scale in the MMLM refers to the direction of wave propagation with 0° directly offshore from the breakwater and increasing positive anticlockwise, Figure 5.20. Incident waves therefore occupy the range of angle from 90° to 270° (the centre section of the direction axis of the plots) and reflected waves 0° to 90° and 270° to 360°. In this record reflection is quite marked, as would be expected from the long period and low height of the swell.

5.3.2 Plymouth - storm (Figures 5.21 to 5.32)

Results are presented in the same form for the remaining three records. This one is of a storm in which large waves were breaking on the structure. Most of the energy was dissipated and very little reflected. The wave system appears to consist of two predominant frequencies, the higher energy one at 190° and the lower at 160°.

5.3.3 Elmer - low intensity swell (Figures 5.33 to 5.45)

The array diagram for the Elmer deployment is shown in Figure 5.6. The dimensions are smaller than at Plymouth as the expected wave periods and lower mean depth result in shorter wavelengths. This record is of long-period waves which are too small to break. Given also the steep gradient of the breakwater a high degree of reflection was expected.

The comparison of measured pressure and calculated surface height, Figure 5.37, displays the closer correspondence appropriate to the smaller depth of pressure measurement.

5.3.4 Elmer - moderate sea (Figures 5.46 to 5.57)

With a significant wave height of around 0.75 metres these were the largest waves from the Elmer deployment. As in the last example, high reflection is evident.

5.4 COMPARISON WITH OTHER OBSERVATIONS

The ideal validation of the wave recording system would be a comparison over the full range of input conditions to another wave recorder, possibly working on a completely different principle but in whose performance one had full confidence. That ideal was impractical; had such a system existed it would not have been necessary to develop a new one. However, opportunities were taken whenever practical to assess performance against other measurements in the field, and against calibration standards. The process was necessarily piecemeal: different facets of both measurement and analysis were checked in a number of independent ways, and confidence in the system gradually built up.

The calibration procedures for pressure sensors alone, electronic sections alone, and of the two together, were described in Chapter 3. Additional checks were made from time to time against tide data, divers' depth gauges and similar information as the opportunities arose. In general those sources

were not as accurate as the wave recorder and so did not count as true calibration.

The process of which there was least experience was the directional analysis. Simulated wave data files were used during development, but as these were highly idealised versions of a real sea they provided only checks for gross errors. However, it was possible to make two important checks on the directional analysis of some of the data sets: predominant wave direction compared to visual observation, and conformity with the theoretically predicted nodal structure in a reflective sea, and with the same measured on a laboratory model. These are described below.

5.4.1 Visual observation

At the time of the storm record from Plymouth (0900 hrs, 24.2.89) it was possible to observe the sea conditions from a vantage point just north of Heybrook Bay (Bullock 1989). The main crest lines were estimated to be at an angle about half way between those of the centre section and the western arm of the breakwater, corresponding to a direction of wave propagation of about 7° to the east of the normal line, 173° on Figure 5.20. No great accuracy could be claimed for the observation as the viewpoint's elevation angle was low, and visibility during the storm poor. The direction, nevertheless, agrees reasonably well with the results in Figures 5.31 and 5.32.

5.4.2 Theoretical models

Inspection of the auto-spectra (leading diagonals) for certain of the records, eg Figures 5.16 and 5.42, reveals the considerable variation in wave height between locations expected in a reflective wave system. Two methods of 2D analysis were applied to these data sets, and the results found to be reasonable and consistent. They thus provide a check and increase confidence in the analysis, although they do not constitute a true calibration.

5.4.2.1 Frequency response function method

The method was described in Chapter 4, and a computer program written to implement it by Davidson (1992). Applying it to the data in D3O3R3.C01, long period swell at Plymouth, gives the incident and reflected spectra in Figure 5.58 a). The result is substantially the same whichever of the three possible pairs of locations is chosen. The reflection coefficient (Figure 5.58 b) is calculated to be a reasonable 50% at 0.05Hz (20s wave period), decreasing slowly with increasing wave frequency as expected. Furthermore, values of reflection coefficient are similar for all the frequencies processed (above 0.04Hz) even for frequencies of very low signal level - the greatest energy component, at 0.057Hz, corresponds to an incident wave height of only 0.2m.

The same features are seen in the first of the records from Elmer, Figure 5.59 a) and b). The reflection coefficient is higher, around 70%, due to the steeper slope. The harmonic analysis procedure used in this method was similar but not identical to that producing Figure 5.41. The latter did not resolve the dip at 0.125Hz so clearly. Further work is needed to determine the optimum window for this type of data.

5.4.2.2 Theoretical prediction of nodal structure

The technique of Davidson (1993, and mentioned in Chapter 4) for calculating the magnitude of the wave envelope as a function of position from the reflective barrier gives, for the geometry of Plymouth Breakwater, the profile in Figure 5.60, and for the Elmer breakwater that in Figure 5.61. The theory assumes linear waves and the shallow water approximation, as well as an absence of loss mechanisms such as wave breaking or friction so that the reflection coefficient is unity. The shallow water approximation is only valid for lower frequencies, and the theory has not been applied to cases were the resulting error would be greater than 5%

The envelope magnitudes at the antinodes decay with cross-shore distance over the structure until a level sea bed is reached. The measured signal levels are superimposed as shaded squares.

This analysis is at an early stage. The vertical scaling is arbitrary, and in the measured sea, unlike the theoretical model, reflection is not perfect. However it can be seen qualitatively that lower and higher signal strengths occur at approximately the distances predicted. Agreement is better at Elmer where reflection was greater and the sensor array was closer to the reflection line.

5.4.3 Physical model

A model at scale 1:15 was constructed and tested in the University of Plymouth's 20m wave channel (Hiscock, 1992, Bullock and Murton 1989). The wave envelopes for certain discrete frequencies were measured at points over the model, and are plotted in Figure 5.62. The theoretical curves from the method of Section 5.4.2 are superimposed and agree well, except for some wave set-up of the model waves. By extension, the full scale results agree qualitatively with those from the physical model.

Hiscock also measured the model's reflection coefficient for a range of wave conditions. For those equivalent to the data set of Figure 5.58, long-period (0.055Hz scaled), low height swell with no breaking, he recorded approximately 66%. The result in the figure from the field data shows about 56% at the peak frequency. Since the model was idealised (smooth and regular slopes with no armouring blocks, monochromatic waves) the results appear to agree quite well.

REFERENCES

Bullock G.N. and Murton G.J. (1989)
Performance of a wedge type absorbing wavemaker
Jnl of Waterway,Port,Coastal and Ocean Engineering **115** (1) (Jan '89)
ASCE USA.

Bullock G N (1989)
Personal communication

Davidson M.A. (1992)
Development and implementation of a software routine for the analysis of the reflection processes associated with random and monochromatic waves
Research Report No. SCSE 92-003, School of Civil and Structural Engineering, University of Plymouth, Plymouth, UK.

Davidson M A , Bird P A D , Bullock G N and Huntley D A. (1993)
A mathematical solution for standing, shallow water waves over a multiple component sloping sea bed.
Research Report No SCSE 93-001, School of Civil and Structural Engineering, University of Plymouth, UK

Hiscock B. (1992)
Plymouth Breakwater: reflection characteristics
BEng Project Report, Department of Civil and Structural Engineering, University of Plymouth, UK.

Rendell F (1989)
Survey of transducer network at Plymouth Breakwater site
Research Report, School of Civil and Structural Engineering, University of Plymouth, UK

Rennie Sir J. (1848)
An historical, practical and theoretical account of the breakwater in Plymouth Sound
Henry G. Bohn, London.

Robert West and Partners (1991)
Joint coastal defence study, Elmer - West Sussex
Report for Arun District Council and National Rivers Authority
(Robert West and Partners, Orpington, Kent, UK.)

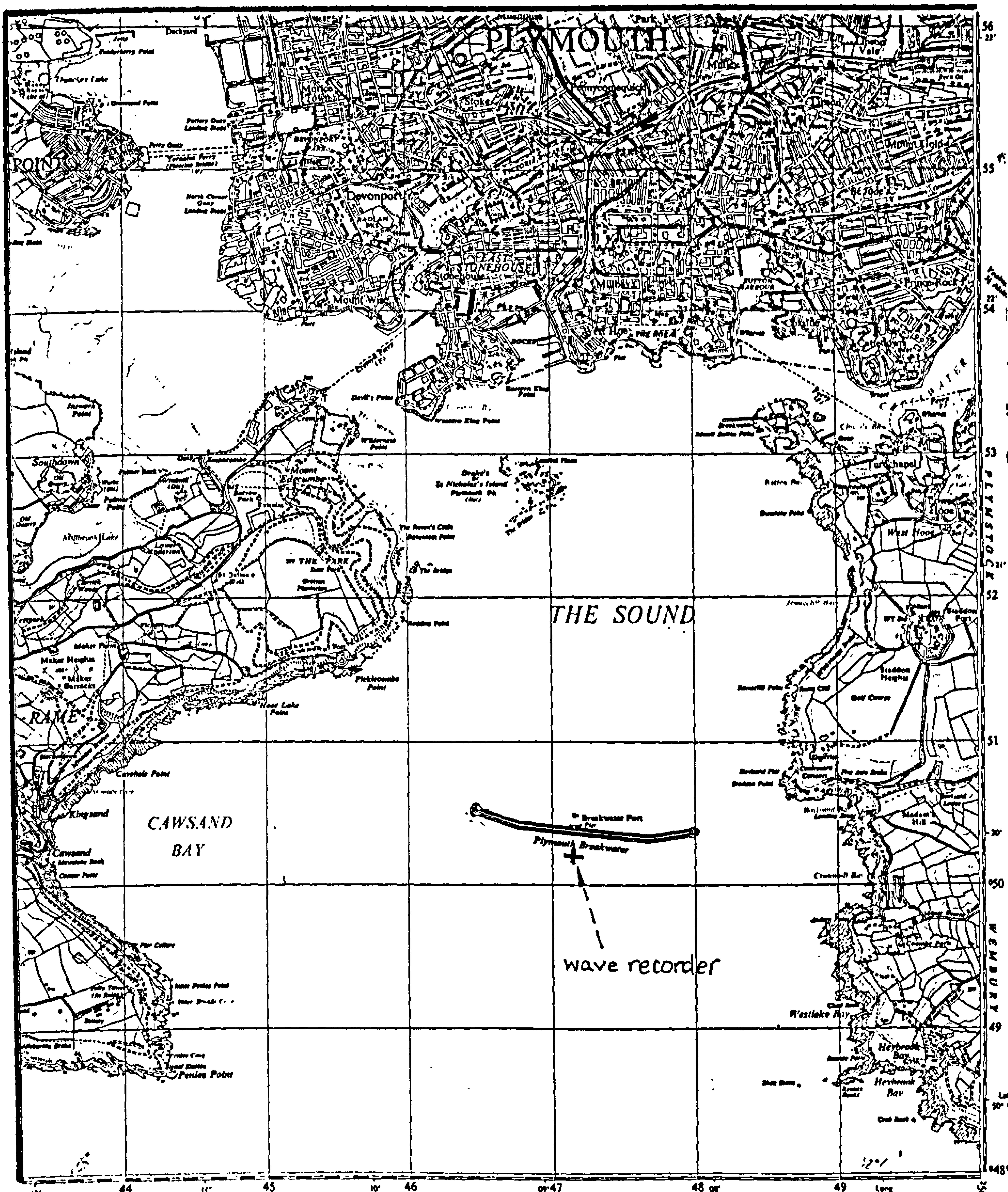

Figure 5.1 Plymouth Sound and the Breakwater

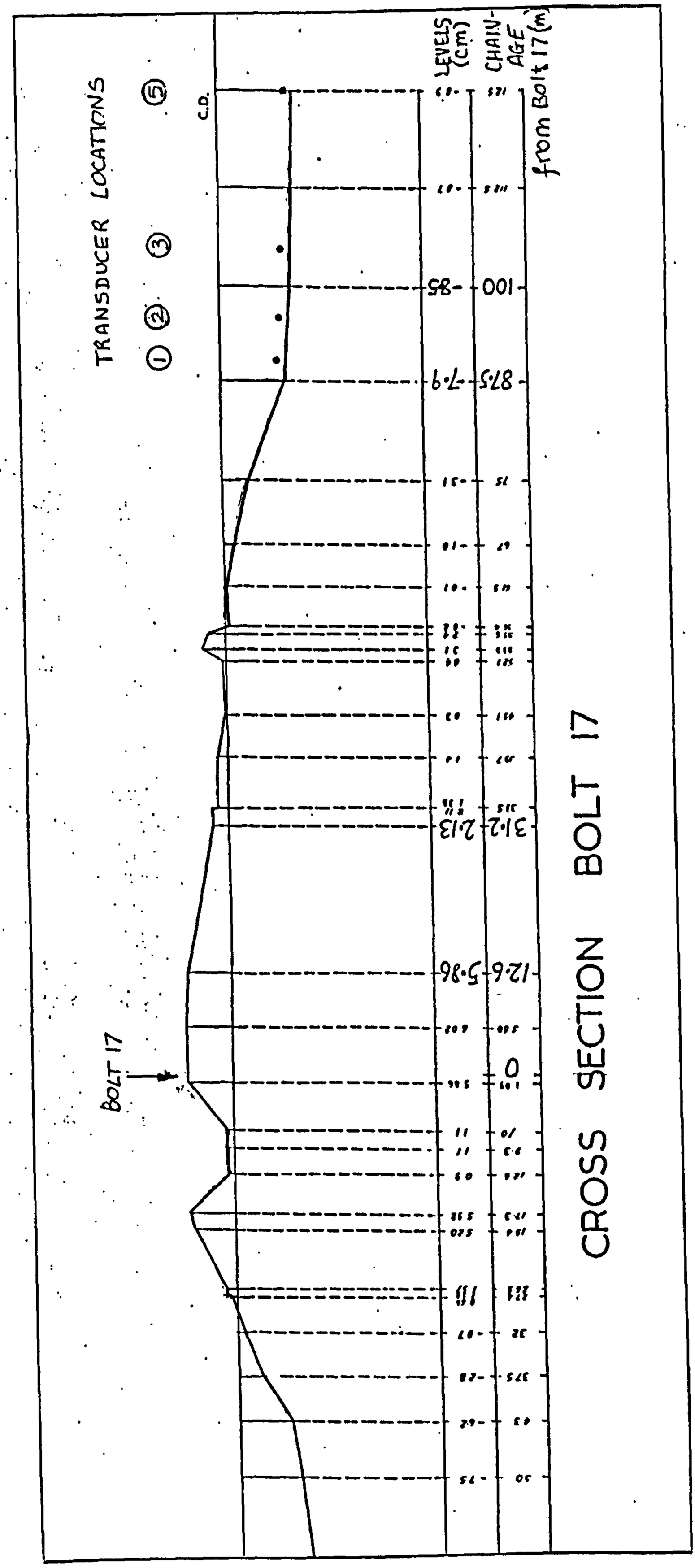

Figure 5.2 Plymouth Breakwater - cross section at the centre

PROJECT	made	Plymouth Polytechnic	DEPARTMENT OF CIVIL ENGINEERING		
WAVE RECORDER WR1	PB				
SECTION	**date**	**JOB NO.**	**SHEET NO.**	**rev.**	
TRANSD. ARRAY DIAGRAM	11-1-89	WR1-0049	1/1	B 30-11-89 VEP3	

LOCATION	TRANSD. ASSY Nº	TRANSD. S/Nº	CABLE			WR PORT Nº	WR CHANNEL Nº	
			Nº	TYPE	LENGTH (m)			
1	1	256 585	1	A	20	5	Ø6	
2	2	144 360 (?)	2	NA	15	2	ø3	
3	3	144 756 (?)	3	NA	10	3	ø4	
4	4	256 588	4	A	25	4	ø5	
5	5	144 359	5	NA	25	1	ø2	
6	6	256 587	6	A	65	6	ø7	

NOTES

1) 'A' = armoured 'NA' = non-armoured

2) 'A' cables go with TR Nºs 1, 4, 6 & WR PORT Nºs 4, 5, 6.
'NA' " " " " 2, 3, 5 " " " 1, 2, 3
To be made interchangeable after next major deployment.

3) See Departmental Research Report F. Rendell, 'Survey of the transducer network at Plymouth Breakwater site' for exact positions

LOCATION Nºs

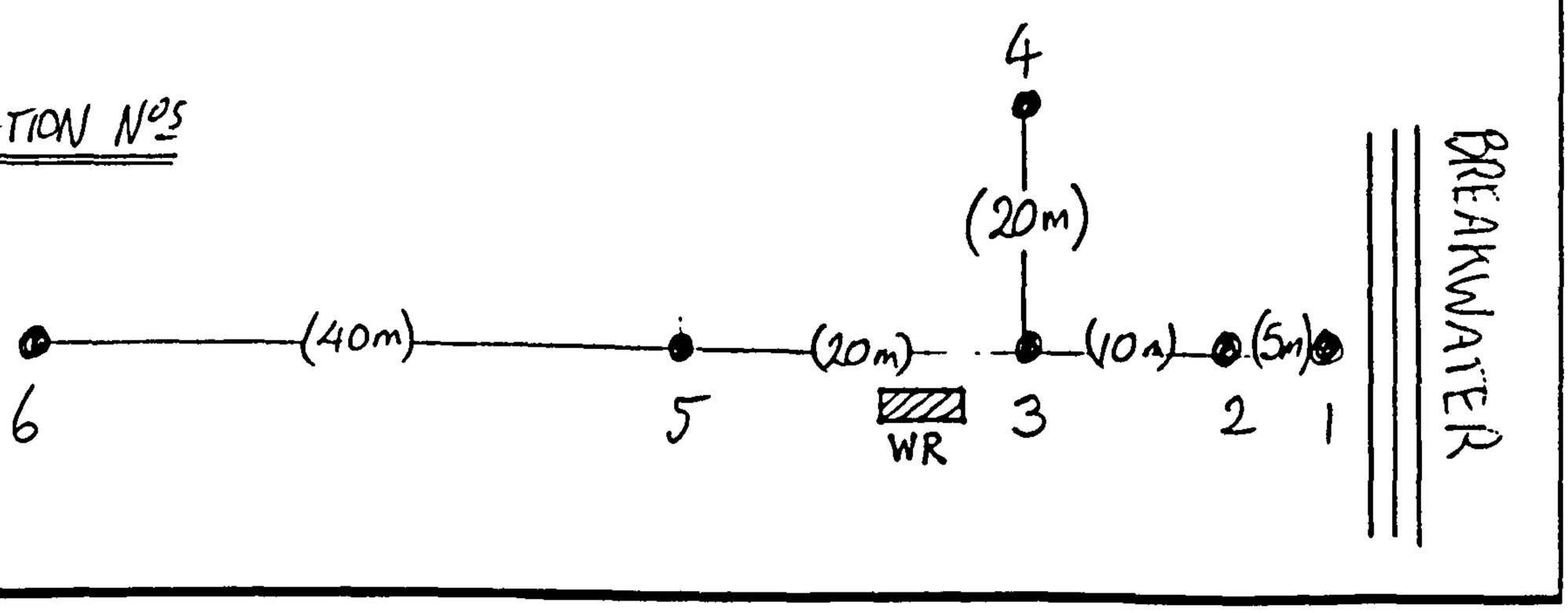

Figure 5.3 Transducer layout drawing - Plymouth Breakwater

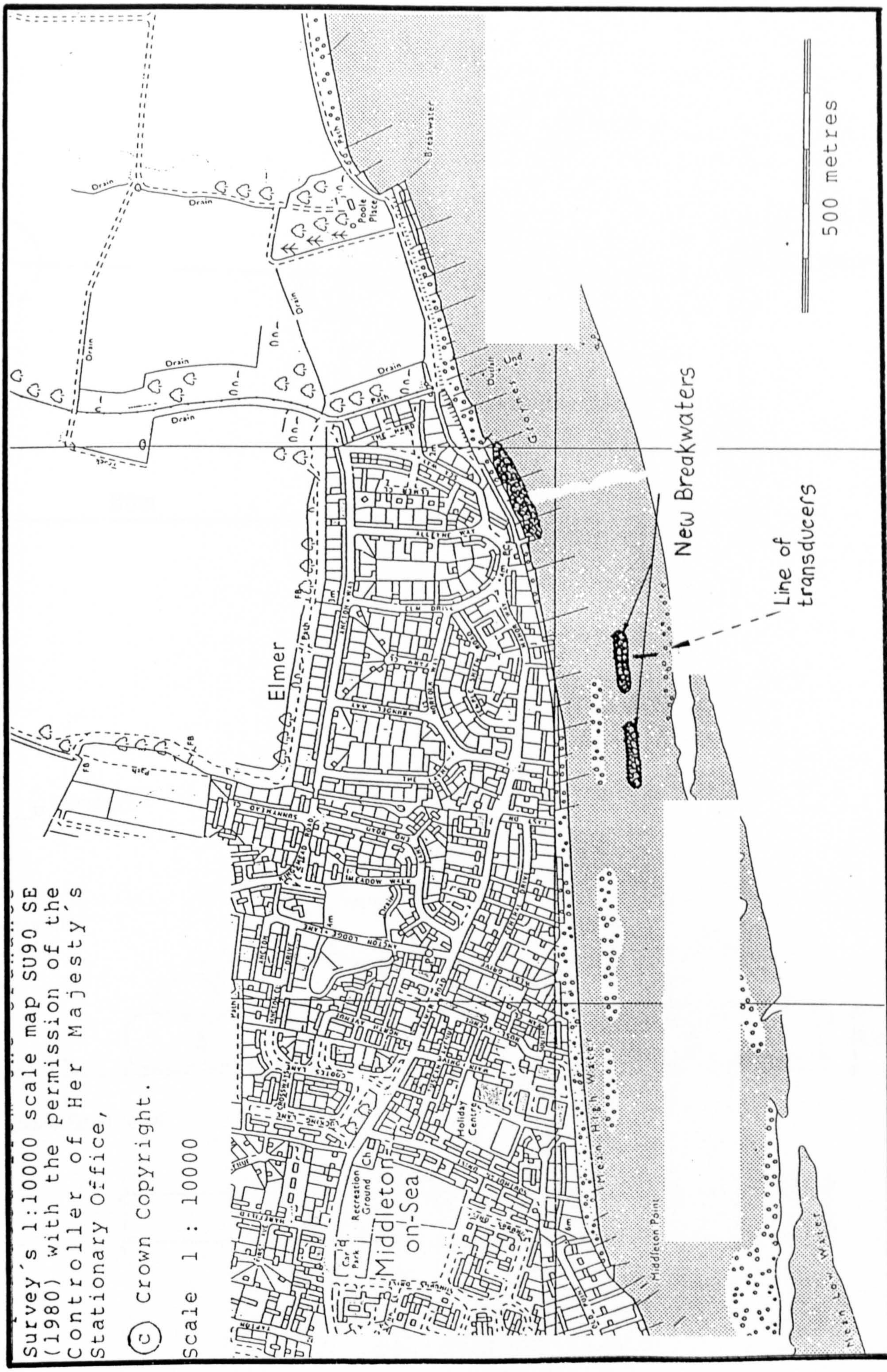

Figure 5.4 Elmer, West Sussex - rock island breakwater, site plan

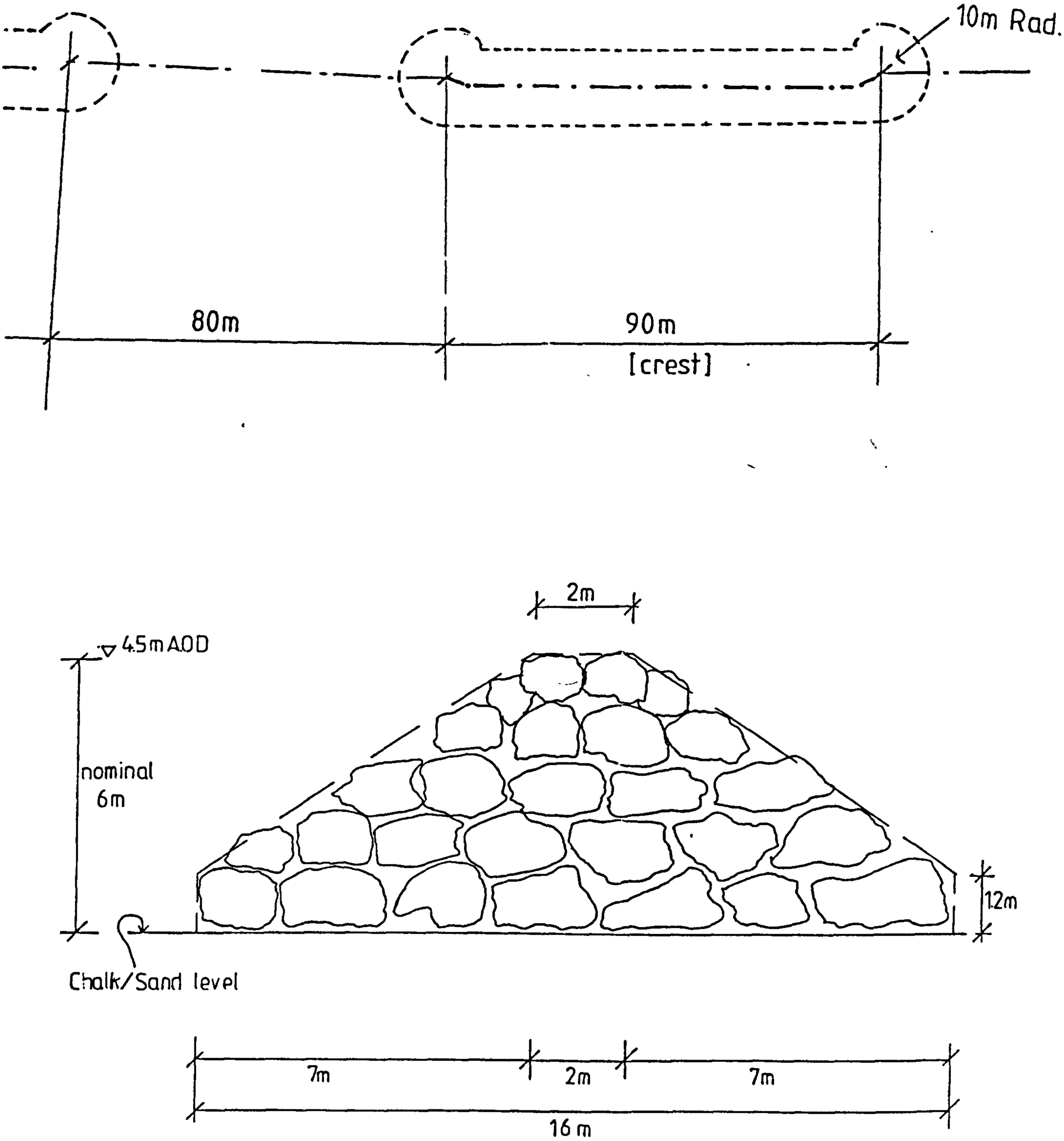

Revised Optimum profile
Scale - 1:100

Figure 5.5 Elmer - proposed plan and section

LOC N	STAND Nº	TRANSD MKG	TRANSD S/Nº	CABLE		WR PORT MARKING	WR PORT NO.	WR CHANNEL Nº
				MKG	LENGTH			
1	-	201	469191	1	17 m	1	1	2
2	-	202	469189	2	13 m	2	2	3
3	-	203	469197	3	10 m	3	3	4
4	-	204	469176	4	15 m	4	4	5
5	-	205	466906	5	47 m	5	5	6
6	-	206	469174	6	22 m	6	6	7

NOTES

1) All cables are to drawing number WRI-0046 iss C (Armoured)

LOCATION Nºs (nominal spacings (m) in brackets)

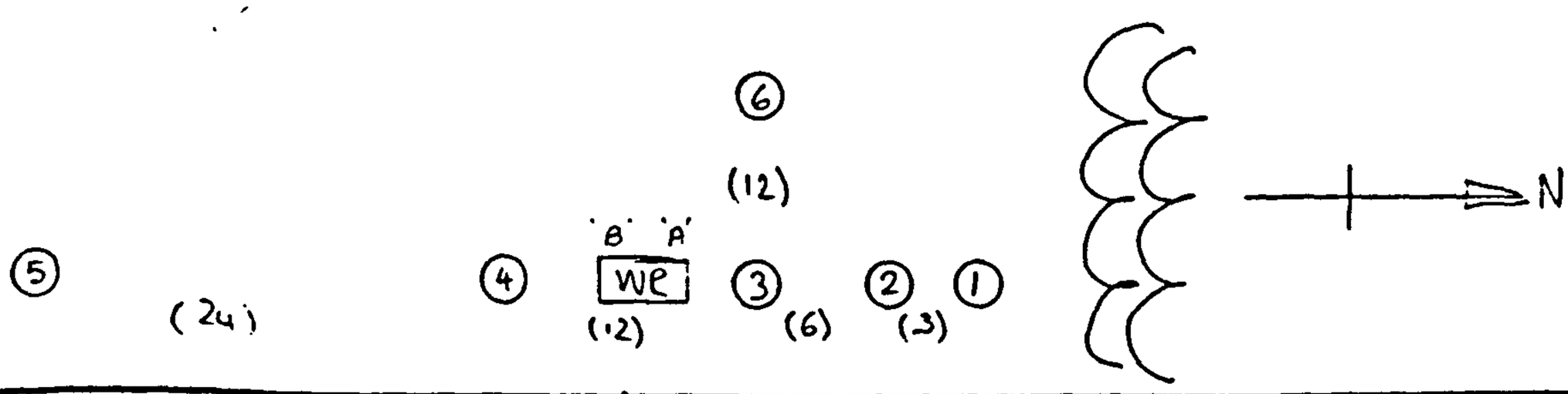

				POLYTECHNIC SOUTH WEST Department of Civil and Structural Engineering Palace Court, Palace Street, Plymouth, PL1 2DE Tel (0752) 232644	WAVE RECORDER
					TRANSDUCER ARRAY DIAGRAM - ELMER
A	Elmer May/June 92	-	10.6.92		WRI-0079
Iss	Change	C/N	Date		

Figure 5.6 Transducer layout drawing - Elmer

```
"       Wave recorder :                 WR1  :                    1"
"        Mod standard :                DEP3  :                    0"
"            Location :  Plymouth Bkwater  :                    0"
"  Transducer layout  :    WR1-0049 iss A  :                    0"
"  Time/Date 1st rdg  : 12 Feb 89 1200:05  :                    0"
"Data element values  :     Abs pressures  :                    1"
" Data array columns  :     6, ch2 to ch7  :                    6"
"    Data array rows  : 1354,sim.rdg sets  :                 1354"
"   Reading interval  :              500 ms  :                  500"

"    File created by  :                DECODE  :                 0"
"             Version :  3.0 1120 20.3.89  :                    0"

 2288 2237 2258 2294 2202 2267
 2293 2240 2261 2295 2205 2262
 2295 2241 2264 2296 2207 2260
 2295 2244 2266 2297 2210 2260
 2293 2246 2268 2299 2214 2263
 2288 2250 2269 2300 2217 2266
 2281 2254 2270 2300 2222 2269
 2274 2258 2271 2298 2226 2269
 2268 2260 2271 2294 2229 2268
 2264 2261 2270 2290 2231 2264
 2264 2260 2268 2286 2230 2258
 2267 2258 2264 2286 2228 2250
 2273 2254 2261 2288 2224 2242
 2279 2249 2258 2293 2220 2236
 2284 2243 2257 2299 2215 2230
 2288 2239 2258 2304 2211 2226
 2288 2237 2261 2307 2207 2223
   |    |    |    |    |    |
   |    |    |    |    |    |
   |    |    |    |    |    |
 2264 2227 2246 2263 2185 2228
 2264 2226 2247 2263 2184 2226
 2264 2226 2247 2262 2183 2224
 2264 2226 2247 2261 2182 2224
 2265 2227 2247 2259 2183 2224
 2263 2227 2246 2257 2184 2226
 2261 2228 2245 2253 2186 2228
 2258 2229 2244 2249 2187 2229
 2255 2228 2242 2245 2187 2231
 2251 2226 2240 2242 2187 2232
 2249 2223 2238 2240 2182 2234
 2250 2219 2237 2241 2178 2236
```

Figure 5.7 Plymouth, 1200 12.2.89 - file of pressures, D3O3R3.A01 (first and last few lines)

```
"       Wave recorder :                  WR1  :                    1"
"        Mod standard :                 DEP3  :                    0"
"            Location :  Plymouth Bkwater  :                    0"
"  Transducer layout :     WR1-0049 iss A  :                    0"
"  Time/Date 1st rdg : 12 Feb 89 1200:05  :                    0"
"Data element values :      Abs pressures  :                    1"
" Data array columns :      6, ch2 to ch7  :                    6"
"    Data array rows : 1354,sim.rdg sets  :                 1354"
"   Reading interval :               500 ms  :                  500"

"    File created by :
"   Input created by :          DECODE
```

13.106	12.261	12.765	13.439	12.094	12.378
13.044	12.338	12.920	13.389	12.042	12.298
12.974	12.544	13.031	13.241	12.087	12.253
12.885	12.780	13.046	13.024	12.223	12.303
12.755	12.944	12.946	12.816	12.413	12.464
12.599	12.985	12.780	12.699	12.580	12.684
12.461	12.899	12.622	12.674	12.644	12.891
12.391	12.702	12.507	12.675	12.568	13.039
12.420	12.440	12.427	12.652	12.378	13.104
12.535	12.195	12.377	12.616	12.121	13.062
12.666	12.040	12.363	12.590	11.851	12.911
12.742	11.990	12.361	12.578	11.638	12.699
12.758	12.015	12.331	12.590	11.551	12.524
12.769	12.072	12.278	12.655	11.602	12.478
12.610	12.125	12.491	12.569	11.781	12.692
12.799	12.157	12.552	12.637	11.708	12.635
12.985	12.254	12.552	12.744	11.720	12.567
13.120	12.371	12.530	12.885	11.797	12.504
13.177	12.452	12.537	13.022	11.903	12.454
13.132	12.467	12.595	13.092	12.002	12.424
13.005	12.431	12.707	13.068	12.066	12.424
12.867	12.401	12.857	12.988	12.069	12.443
12.774	12.436	12.985	12.897	12.036	12.460
12.729	12.557	13.010	12.807	12.035	12.470
12.716	12.711	12.898	12.716	12.119	12.491
12.735	12.799	12.701	12.645	12.252	12.523
12.781	12.767	12.515	12.610	12.346	12.545
12.815	12.630	12.412	12.608	12.333	12.543
12.803	12.442	12.412	12.631	12.211	12.530
12.759	12.251	12.483	12.682	12.023	12.517
12.724	12.123	12.575	12.752	11.835	12.494
12.729	12.125	12.651	12.809	11.713	12.456

```
THE SOURCE DATA FILE IS CALLED :- C:\WR1\DATA\DEP3\D3O3R3.A01
THIS DATA FILE IS CALLED       :- C:\WR1\DATA\DEP3\D3O3R3.C01
```

Figure 5.8 Plymouth, 1200 12.2.89 - file of surface heights, D3O3R3.C01

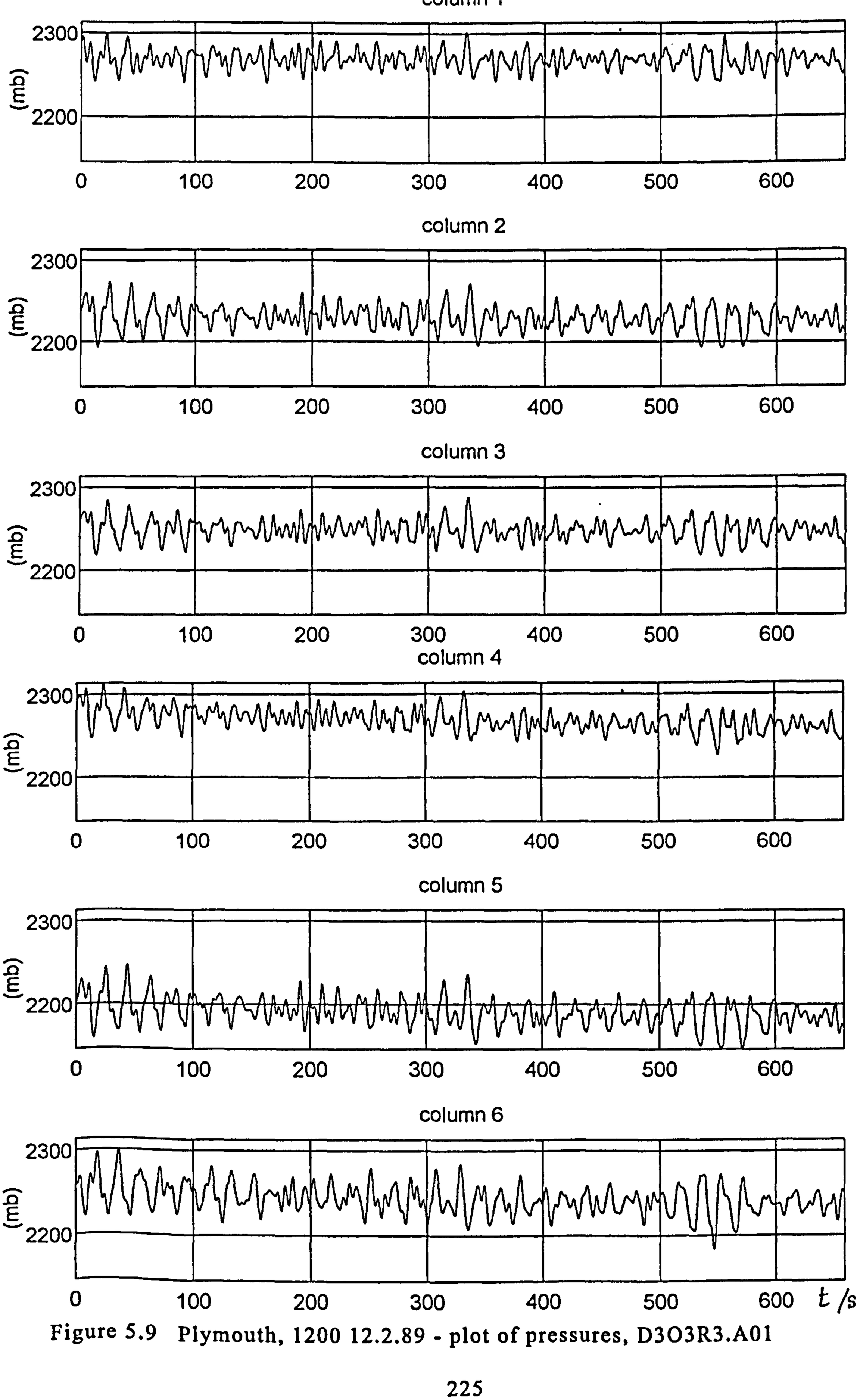

Figure 5.9 Plymouth, 1200 12.2.89 - plot of pressures, D3O3R3.A01

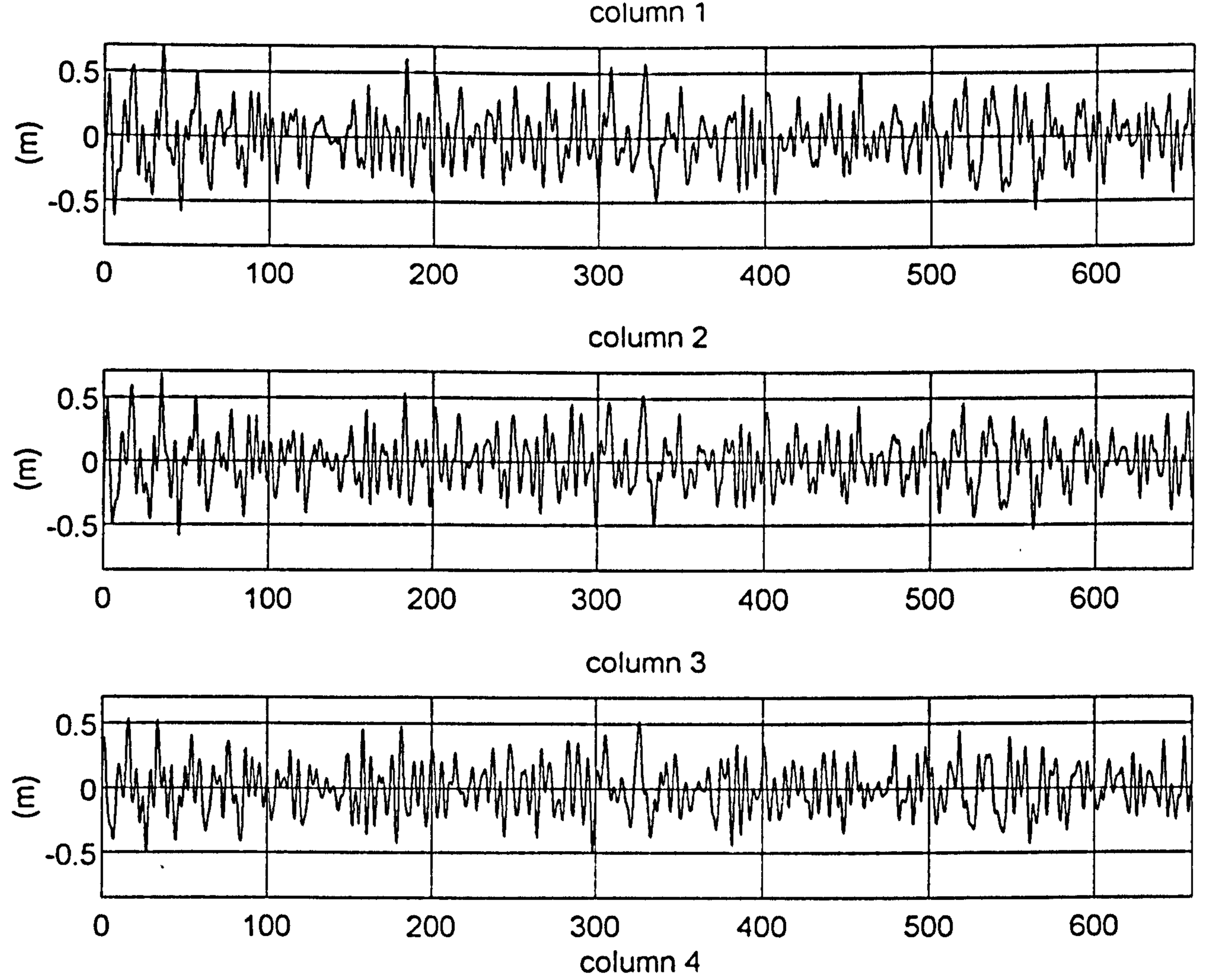

Figure 5.10Plymouth, 1200 12.2.89 - plot of surface elevation D3O3R3.C01

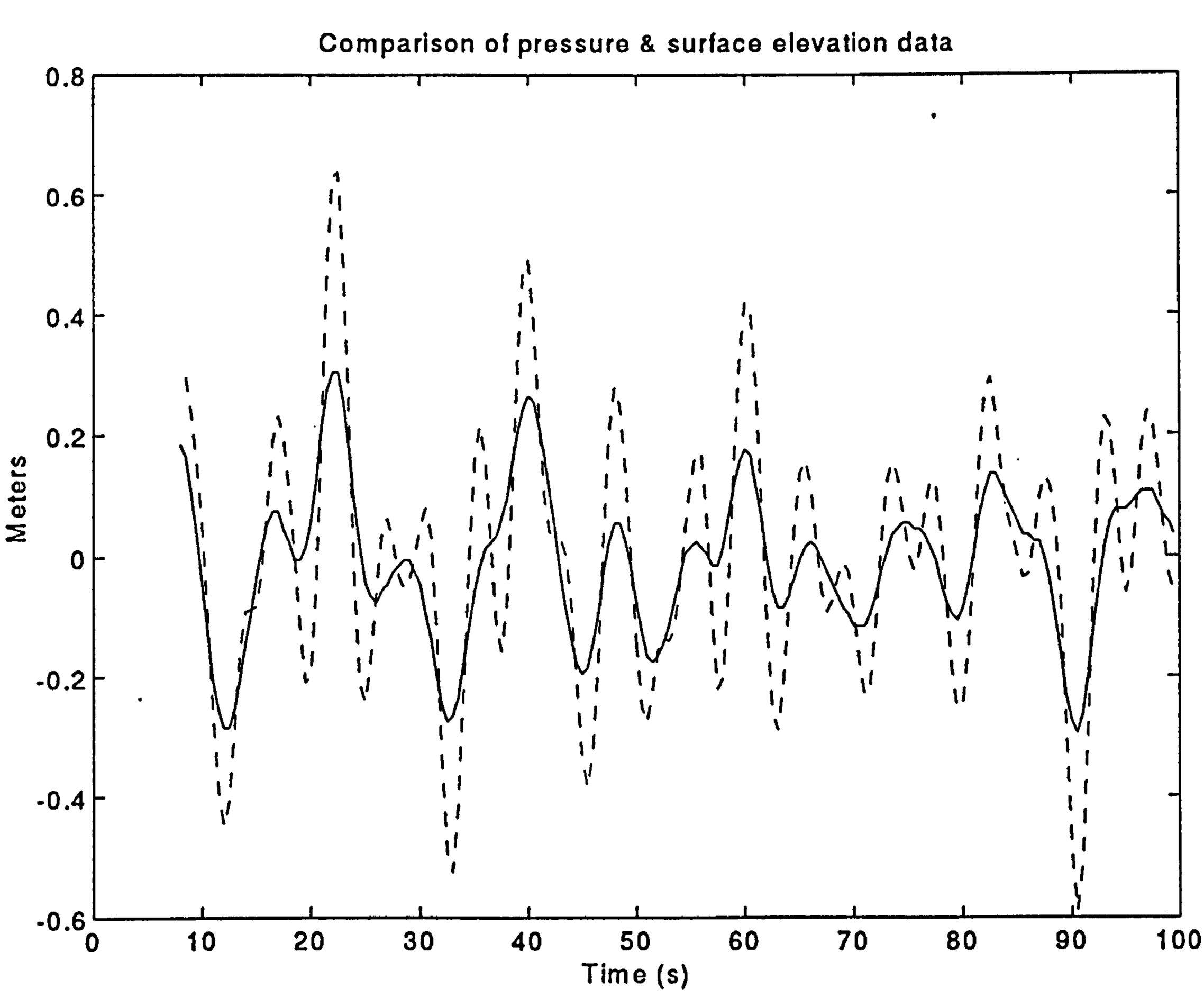

Figure 5.11 Plymouth, 1200 12.2.89 - comparison of pressure and surface records. Full line - elevation from pressure with no allowance for depth attenuation. Dotted line - elevation from pressure using Airy theory.

STATISTICS FROM FILE D303R3.A01

No. rows in press.dat		1356					
first data points (press)		2202	2237	2258	2294	2288	2267
first data points (pwave)		-1.7	2.5	6.2	11.4	18.4	9.7
means	(mb)	2191.2	2229.7	2248.6	2268.9	2268.0	2243.3
means (relative)	(mb)	0.0	38.5	57.4	77.7	76.8	52.1
tidal changes	(mb)	-20.5	-8.5	-6.1	-23.4	-4.8	-20.7
range (de-trended)	(mb)	89.8	82.9	72.2	69.7	63.1	98.1
max pressure excn	(mb)	45.9	42.6	39.5	34.9	33.6	44.9
max press. exc.(std-devs)		3.0	3.1	3.4	3.2	3.1	2.9
min pressure excn	(mb)	-44.0	-40.3	-32.7	-34.8	-29.5	-53.2
min press. exc.(std-devs)		-2.9	-2.9	-2.8	-3.2	-2.7	-3.4
std devs (de-trended)	(mb)	15.2	13.9	11.6	10.9	10.9	15.4
vars (de-trended)	(mb^2)	230.6	192.8	134.8	117.9	118.9	238.5
Q_flags		1	1	1	1	1	1

Figure 5.12 Plymouth, 1200 12.2.89 - statistics from pressure record

STATISTICS FROM FILE D303R3.C01

No. rows in surf.dat		1320					
first data points (surf)		12.094	12.261	12.765	13.439	13.106	12.378
first data points (wave)		-0.077	-0.219	0.107	0.478	0.271	-0.348
Hs	(m)	0.85	0.81	0.73	0.69	0.73	0.85
means	(m)	12.066	12.449	12.638	12.840	12.831	12.587
tidal changes	(m)	-0.186	-0.071	-0.050	-0.214	-0.035	-0.197
means (relative)	(mm)	0	383	572	774	765	521
range (de-trended)	(m)	1.324	1.268	1.036	1.107	1.216	1.473
max wave excn	(m)	0.706	0.681	0.542	0.608	0.639	0.621
max wave excn (std-devs)		3.3	3.4	3.0	3.5	3.5	2.9
min wave excn	(m)	-0.618	-0.587	-0.493	-0.500	-0.577	-0.852
min wave excn (std-devs)		-2.9	-2.9	-2.7	-2.9	-3.2	-4.0
std devs (de-trended)	(m)	0.213	0.203	0.182	0.173	0.182	0.213
vars (de-trended)	(m^2)	0.045	0.041	0.033	0.030	0.033	0.045
refl. coeff. >		0.102					
Q_flags		1	1	1	1	1	1

Figure 5.13 Plymouth, 1200 12.2.89 - statistics from surface height record D3O3R3.C01

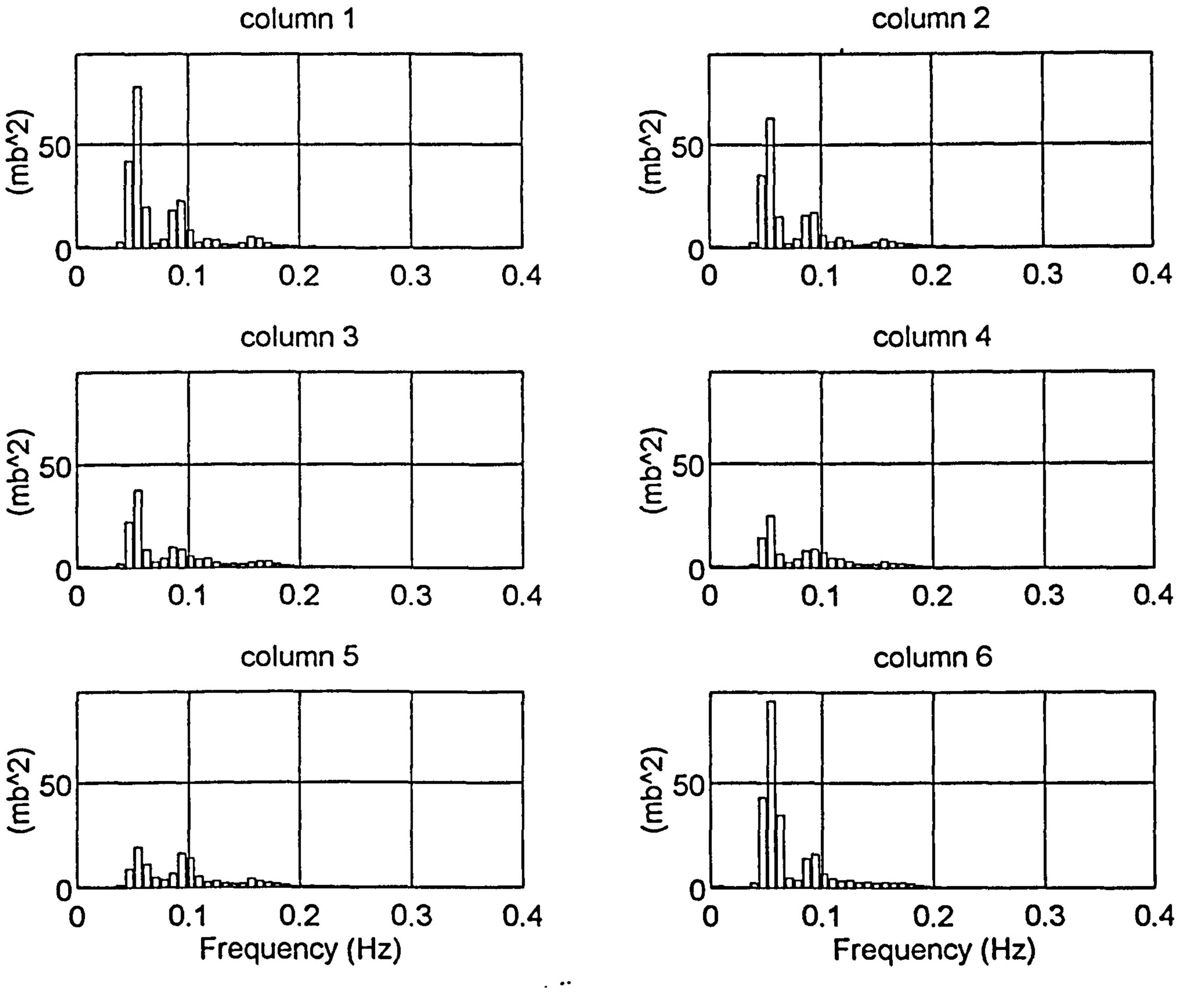

Figure 5.14 Plymouth, 1200 12.2.89 - frequency distribution of variance from pressure record D3O3R3.A01

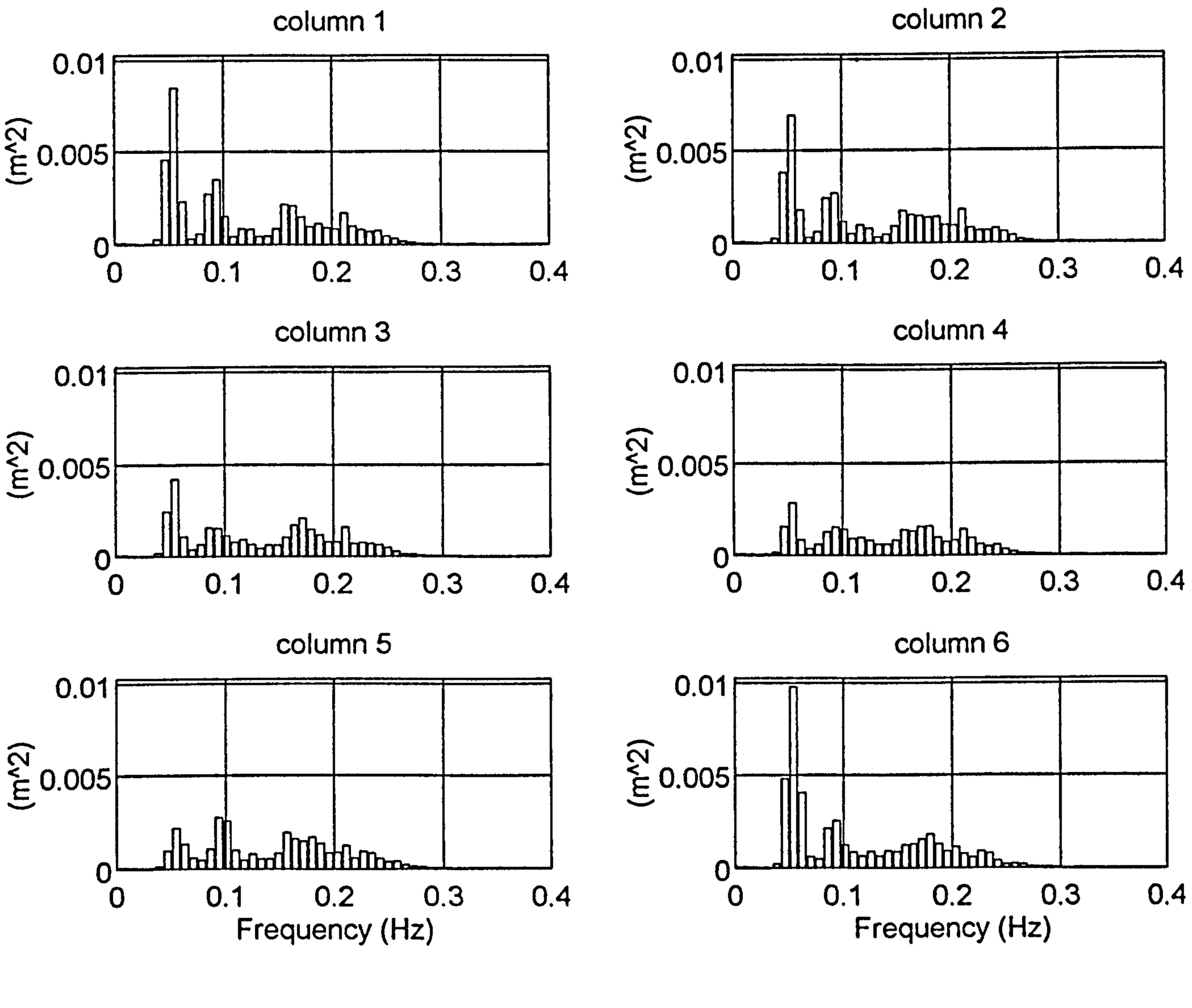

Figure 5.15 Plymouth, 1200 12.2.89 - frequency distribution of variance from surface height record D3O3R3.C01

CROSS-SPECTRAL DENSITY MATRICES FROM: D303R3.C01
XSD_f(i,j)

frequency: 0.039Hz frequency index: 6
magnitude /(10^-6 m^2): phase /degrees:

269	255	223	193	151	199	0	3	12	27	39	131
255	243	213	184	146	187	-3	0	8	23	35	126
223	213	189	166	134	160	-12	-8	0	15	25	113
193	184	166	149	121	133	-27	-23	-15	0	9	96
151	146	134	121	110	123	-39	-35	-25	-9	0	71
199	187	160	133	123	225	-131	-126	-113	-96	-71	0

frequency: 0.047Hz frequency index: 7
magnitude /(10^-5 m^2): phase /degrees:

455	416	332	264	201	452	0	4	14	33	62	146
416	381	305	243	185	414	-4	0	10	30	58	142
332	305	244	195	149	329	-14	-10	0	19	48	131
264	243	195	158	120	261	-33	-30	-19	0	28	112
201	185	149	120	97	207	-62	-58	-48	-28	0	80
452	414	329	261	207	479	-146	-142	-131	-112	-80	0

frequency: 0.055Hz frequency index: 8
magnitude /(10^-5 m^2): phase /degrees:

850	767	591	477	376	873	0	4	16	40	73	149
767	693	537	435	343	785	-4	0	12	36	68	144
591	537	422	345	277	604	-16	-12	0	24	53	130
477	435	345	285	229	488	-40	-36	-24	0	28	106
376	343	277	229	217	430	-73	-68	-53	-28	0	70
873	785	604	488	430	977	-149	-144	-130	-106	-70	0

frequency: 0.063Hz frequency index: 9
magnitude /(10^-5 m^2): phase /degrees:

229	201	144	118	122	276	0	6	25	53	100	162
201	178	132	109	109	238	-6	0	18	46	88	153
144	132	107	93	93	172	-25	-18	0	28	56	127
118	109	93	83	86	144	-53	-46	-28	0	23	94
122	109	93	86	132	206	-100	-88	-56	-23	0	54
276	238	172	144	206	403	-162	-153	-127	-94	-54	0

frequency: 0.070Hz frequency index: 10
magnitude /(10^-6 m^2): phase /degrees:

298	292	298	292	341	378	0	14	40	70	81	163
292	293	310	307	353	354	-14	0	25	55	62	146
298	310	352	354	427	367	-40	-25	0	29	32	112
292	307	354	364	439	366	-70	-55	-29	0	2	80
341	353	427	439	594	511	-81	-62	-32	-2	0	67
378	354	367	366	511	602	-163	-146	-112	-80	-67	0

Figure 5.16 Plymouth, 1200 12.2.89 - cross-spectral matrices for the most energetic frequency bins from D3O3R3.C01

COHERENCE MATRICES FROM: D303R3.C01
COH_f(i,j)

frequency: 0.039Hz frequency index: 6

1.000	0.998	0.977	0.926	0.767	0.656
0.998	1.000	0.986	0.940	0.790	0.640
0.977	0.986	1.000	0.974	0.864	0.603
0.926	0.940	0.974	1.000	0.884	0.530
0.767	0.790	0.864	0.884	1.000	0.614
0.656	0.640	0.603	0.530	0.614	1.000

frequency: 0.047Hz frequency index: 7

1.000	0.999	0.994	0.973	0.916	0.939
0.999	1.000	0.997	0.977	0.924	0.938
0.994	0.997	1.000	0.984	0.942	0.927
0.973	0.977	0.984	1.000	0.939	0.904
0.916	0.924	0.942	0.939	1.000	0.925
0.939	0.938	0.927	0.904	0.925	1.000

frequency: 0.055Hz frequency index: 8

1.000	0.998	0.973	0.941	0.768	0.917
0.998	1.000	0.985	0.957	0.785	0.911
0.973	0.985	1.000	0.985	0.835	0.883
0.941	0.957	0.985	1.000	0.849	0.855
0.768	0.785	0.835	0.849	1.000	0.873
0.917	0.911	0.883	0.855	0.873	1.000

frequency: 0.063Hz frequency index: 9

1.000	0.990	0.847	0.731	0.496	0.827
0.990	1.000	0.910	0.809	0.504	0.792
0.847	0.910	1.000	0.974	0.614	0.684
0.731	0.809	0.974	1.000	0.674	0.621
0.496	0.504	0.614	0.674	1.000	0.800
0.827	0.792	0.684	0.621	0.800	1.000

frequency: 0.070Hz frequency index: 10

1.000	0.974	0.844	0.789	0.658	0.798
0.974	1.000	0.932	0.885	0.717	0.710
0.844	0.932	1.000	0.981	0.871	0.635
0.789	0.885	0.981	1.000	0.892	0.613
0.658	0.717	0.871	0.892	1.000	0.730
0.798	0.710	0.635	0.613	0.730	1.000

Figure 5.17 Plymouth, 1200 12.2.89 - coherence matrices for the most energetic frequency bins from D3O3R3.C01

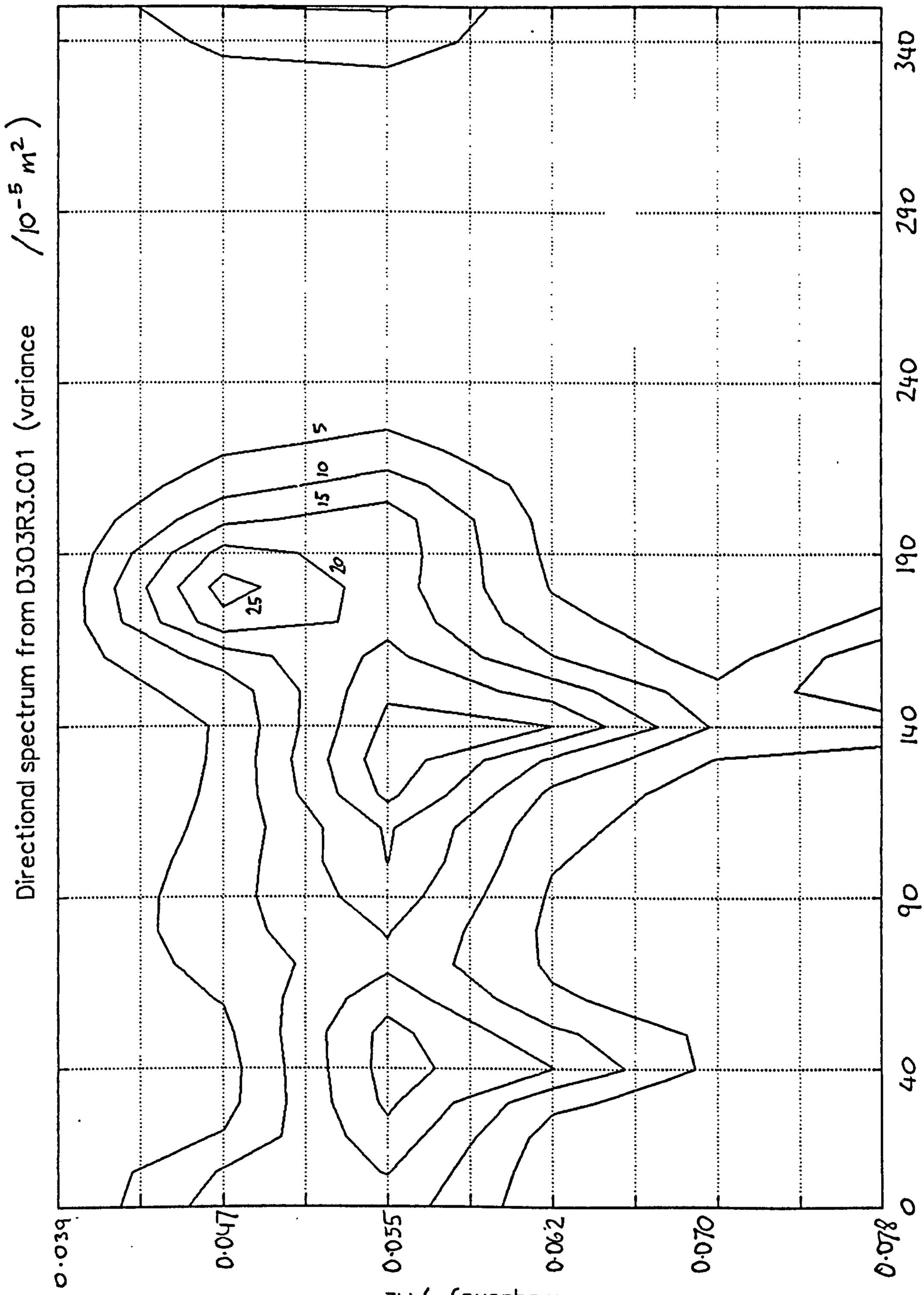

Figure 5.18 Plymouth, 1200 12.2.89 - directional wave spectrum from D3O3R3.C01 as a contour plot

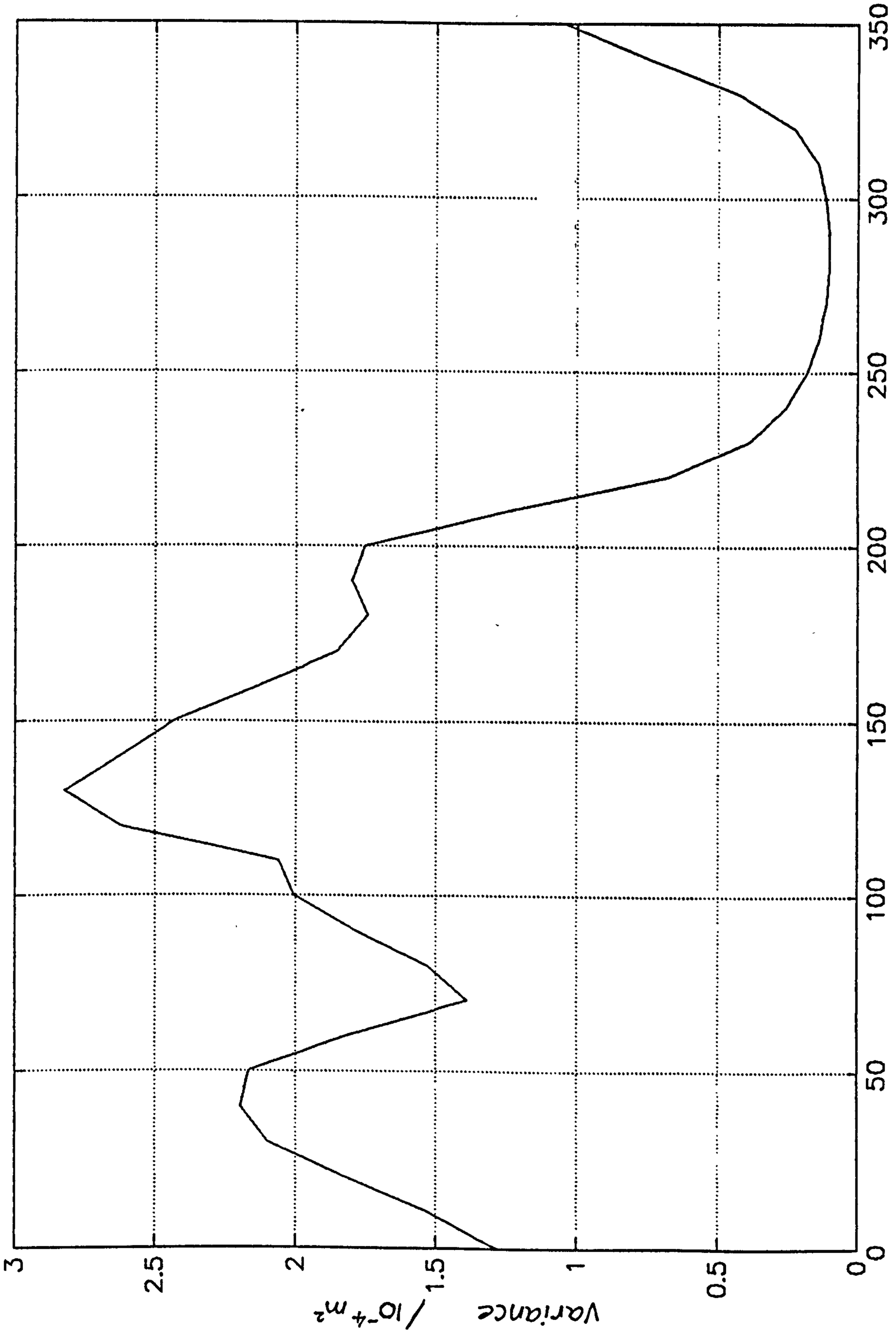

Figure 5.19 Plymouth, 1200 12.2.89 - directional wave distribution from D3O3R3.C01 : 0.055 Hz

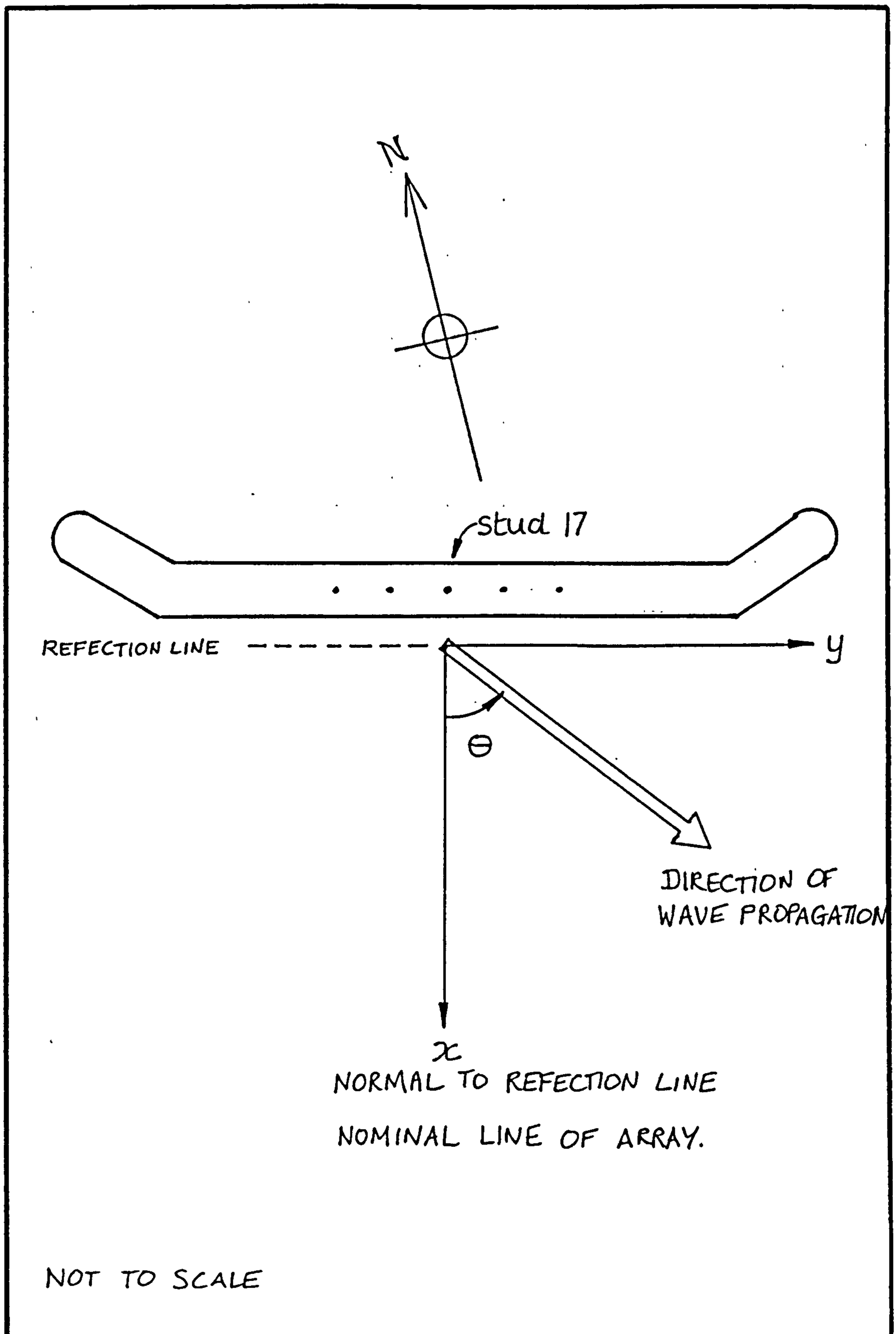

Figure 5.20 Definition of angle of wave propagation

```
"       Wave recorder :                 WR1  :                1"
"        Mod standard :                DEP3  :                0"
"            Location :  Plymouth Bkwater  :                0"
"  Transducer layout  :    WR1-0049 iss A  :                0"
"  Time/Date 1st rdg  : 24 Feb 89 0858:09  :                0"
"Data element values  :     Abs pressures  :                1"
" Data array columns  :     6, ch2 to ch7  :                6"
"    Data array rows  : 1354,sim.rdg sets  :             1354"
"   Reading interval  :              500 ms  :              500"

"    File created by  :               DECODE  :              0"
"             Version :  3.0 1120 20.3.89  :                0"



 2343 2350 2356 2376 2320 2284
 2334 2346 2341 2359 2319 2286
 2328 2338 2327 2346 2315 2292
 2324 2328 2315 2336 2308 2302
 2320 2317 2307 2327 2299 2314
 2314 2306 2303 2321 2288 2329
 2308 2297 2303 2318 2276 2343
 2303 2292 2305 2318 2266 2356
 2303 2290 2307 2320 2259 2367
 2308 2290 2308 2325 2255 2374
 2321 2291 2307 2332 2253 2376
 2339 2290 2306 2341 2252 2376
 2358 2289 2306 2350 2252 2373
 2374 2287 2309 2360 2251 2367
 2386 2286 2316 2371 2251 2358
 2394 2288 2326 2383 2251 2343
 2394 2296 2339 2396 2255 2325
 2387 2309 2353 2406 2264 2304
 2378 2325 2364 2413 2278 2285
 2366 2339 2368 2414 2293 2272



 2353 2246 2272 2326 2212 2265
 2365 2241 2285 2334 2199 2275
 2368 2244 2301 2341 2193 2292
 2363 2255 2319 2344 2195 2311
 2351 2272 2335 2341 2208 2328
 2334 2293 2344 2333 2228 2339
 2315 2311 2344 2319 2250 2342
 2300 2323 2336 2305 2271 2340
 2292 2325 2319 2296 2285 2330
 2295 2319 2298 2292 2290 2318
 2307 2303 2279 2295 2283 2305
 2327 2284 2268 2304 2268 2296
 2349 2267 2271 2320 2250 2291
 2366 2258 2284 2338 2234 2290
 2375 2261 2305 2356 2222 2291
 2374 2273 2330 2372 2221 2290
 2366 2292 2351 2385 2231 2288
 2355 2313 2365 2391 2246 2285
 2343 2331 2370 2389 2265 2280
 2335 2341 2364 2380 2282 2277
 2332 2342 2351 2365 2295 2275
```

Figure 5.21 Plymouth, 0858 24.2.89 - file of pressures, D3O4R2.A00 (first and last few lines)

```
"        Wave recorder :                  WR1  :                    1"
"         Mod standard :                 DEP3  :                    0"
"             Location :  Plymouth Bkwater  :                    0"
"   Transducer layout  :    WR1-0049 iss A  :                    0"
"   Time/Date 1st rdg  : 24 Feb 89 0858:09  :                    0"
"Data element values   :     Abs pressures  :                    1"
" Data array columns   :     6, ch2 to ch7  :                    6"
"     Data array rows  : 1354,sim.rdg sets  :                 1354"
"    Reading interval  :              500 ms  :                  500"

"     File created by :
"    Input created by :          DECODE
```

```
14.777   13.417   14.299   14.517   12.969   13.958
14.548   13.846   14.635   14.920   13.148   13.519
14.353   14.271   14.796   15.317   13.476   13.168
14.195   14.571   14.775   15.527   13.860   12.967
14.076   14.685   14.622   15.429   14.191   12.934
14.009   14.611   14.371   14.983   14.364   13.086
13.979   14.400   14.062   14.236   14.334   13.415
13.938   14.136   13.775   13.393   14.147   13.849
13.850   13.888   13.594   12.767   13.895   14.286
13.720   13.693   13.535   12.596   13.655   14.636
13.586   13.559   13.550   12.875   13.446   14.848
13.497   13.477   13.589   13.413   13.256   14.903
13.490   13.429   13.633   13.987   13.095   14.820
13.582   13.402   13.678   14.440   13.002   14.644
13.793   13.386   13.710   14.687   12.997   14.425
14.129   13.382   13.727   14.731   13.035   14.208
14.539   13.406   13.745   14.680   13.049   14.034
14.912   13.464   13.797   14.679   13.037   13.927
15.172   13.555   13.916   14.807   13.064   13.879



14.356   13.665   14.187   14.429   13.032   13.569
14.613   13.788   14.135   14.215   13.146   13.606
14.816   13.874   14.032   14.014   13.282   13.605
14.878   13.920   13.941   13.927   13.417   13.523
14.753   13.930   13.929   13.976   13.540   13.382
14.455   13.900   14.028   14.068   13.624   13.263
14.044   13.857   14.198   14.106   13.631   13.287
13.626   13.871   14.341   14.085   13.584   13.540
13.319   13.979   14.370   14.063   13.556   13.970
13.186   14.128   14.260   14.053   13.597   14.376
13.199   14.209   14.032   14.002   13.678   14.550
13.302   14.148   13.730   13.868   13.724   14.426
13.469   13.941   13.415   13.688   13.687   14.046
13.691   13.634   13.163   13.550   13.565   13.490
13.948   13.303   13.029   13.540   13.357   12.898
14.229   13.014   13.033   13.687   13.046   12.519
14.522   12.805   13.170   13.963   12.647   12.588
14.776   12.702   13.434   14.294   12.258   13.120

THE SOURCE DATA FILE IS CALLED :- C:\WR1\DATA\DEP3\D304R2.A00
THIS DATA FILE IS CALLED       :- C:\WR1\DATA\DEP3\D304R2.C00
```

Figure 5.22 Plymouth, 0858 24.2.89 - file of surface heights, D3O4R2.C00 (first and last few lines)

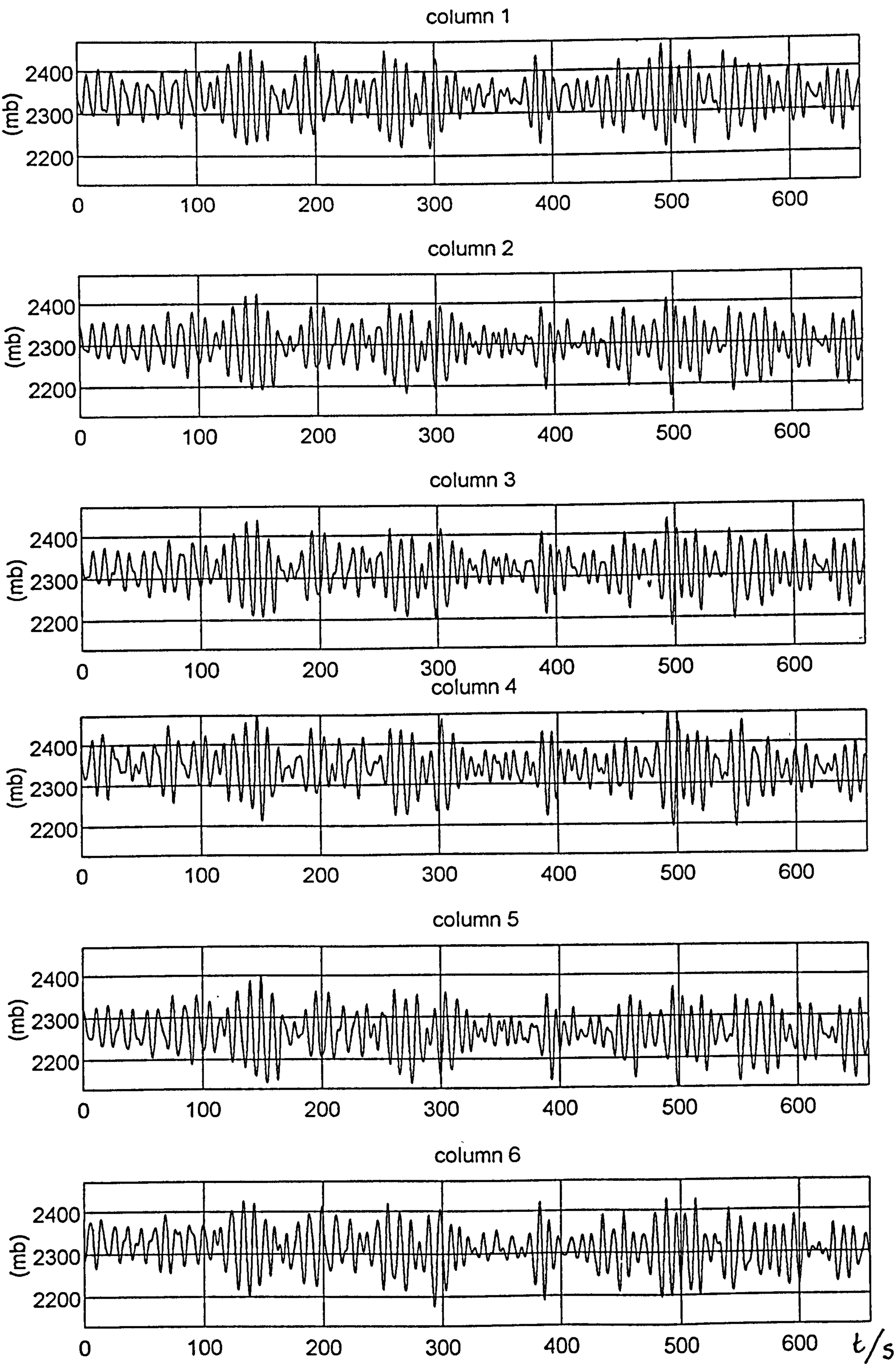

Figure 5.23 Plymouth, 0858 24.2.89 - plot of pressures, D3O4R2.A00

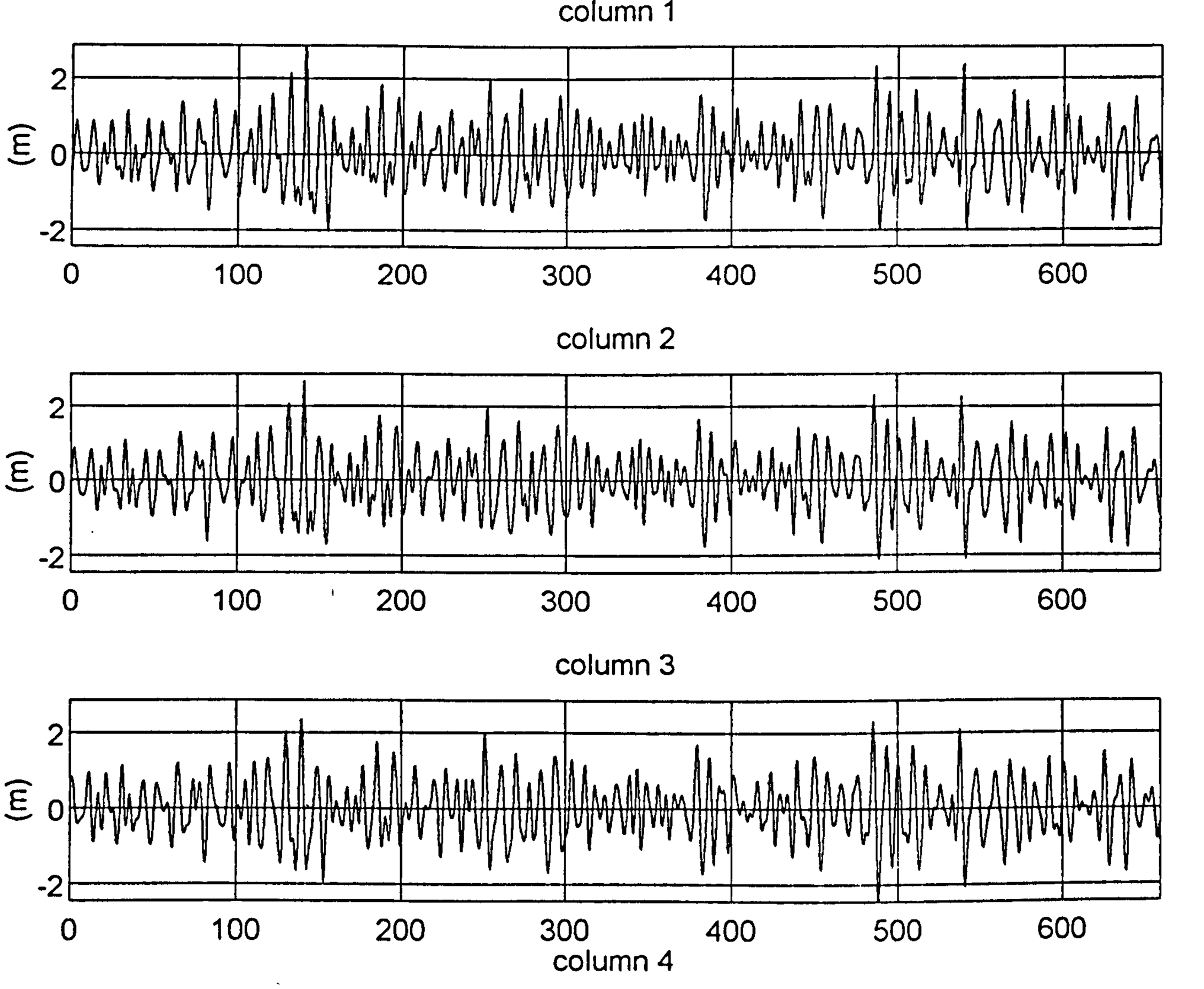

Figure 5.24 Plymouth, 0858 24.2.89 - plot of surface elevationD3O4R2.C00

FROM FILE D304R2.A00

No. rows in press.dat		1356					
first data points (press)		2320	2350	2356	2376	2343	2284
first data points (pwave)		45.0	43.2	33.6	21.6	2.5	-46.5
means	(mb)	2261.8	2298.7	2316.8	2339.8	2336.4	2311.4
means (relative)	(mb)	0.0	36.9	55.0	78.0	74.6	49.6
tidal changes	(mb)	-23.0	-13.7	-9.7	-23.7	-8.7	-29.0
range (de-trended)	(mb)	253.9	245.7	256.0	274.8	246.6	257.2
max pressure excn	(mb)	127.8	121.5	121.6	134.1	125.5	121.9
max press. exc.(std-devs)		2.7	2.7	2.7	2.9	2.7	2.7
min pressure excn	(mb)	-126.1	-124.2	-134.4	-140.6	-121.1	-135.2
min press. exc.(std-devs)		-2.7	-2.8	-3.0	-3.0	-2.6	-3.0
std devs (de-trended)	(mb)	46.6	45.2	44.7	47.0	46.1	45.0
vars (de-trended)	(mb^2)	2173.1	2039.6	1999.4	2207.9	2121.8	2025.0
Q_flags		1	1	1	1	1	1

Figure 5.25 Plymouth, 0858 12.2.89 - statistics from pressure record D3O4R2.A00

STATISTICS FROM FILE D304R2.C00

No. rows in surf.dat		1320					
first data points (surf)		12.969	13.417	14.299	14.517	14.777	13.958
first data points (wave)		-0.506	-0.378	0.345	0.244	0.650	-0.046
Hs	(m)	3.01	3.00	3.00	3.21	3.08	2.99
means	(m)	13.348	13.714	13.893	14.122	14.089	13.837
tidal changes	(m)	-0.219	-0.141	-0.116	-0.250	-0.091	-0.279
means (relative)	(mm)	0	366	546	775	741	489
range (de-trended)	(m)	4.924	4.814	4.815	4.404	4.720	4.625
max wave excn	(m)	2.858	2.672	2.365	2.464	2.456	2.312
max wave excn (std-devs)		3.8	3.6	3.2	3.1	3.2	3.1
min wave excn	(m)	-2.067	-2.142	-2.450	-1.940	-2.264	-2.313
min wave excn (std-devs)		-2.7	-2.9	-3.3	-2.4	-2.9	-3.1
std devs (de-trended)	(m)	0.752	0.749	0.751	0.801	0.771	0.747
vars (de-trended)	(m^2)	0.566	0.561	0.564	0.642	0.594	0.558
refl. coeff. >		0.035					
Q_flags		1	1	1	1	1	1

Figure 5.26 Plymouth, 0858 24.2.89 - statistics from surface height record D3O4R2.C00

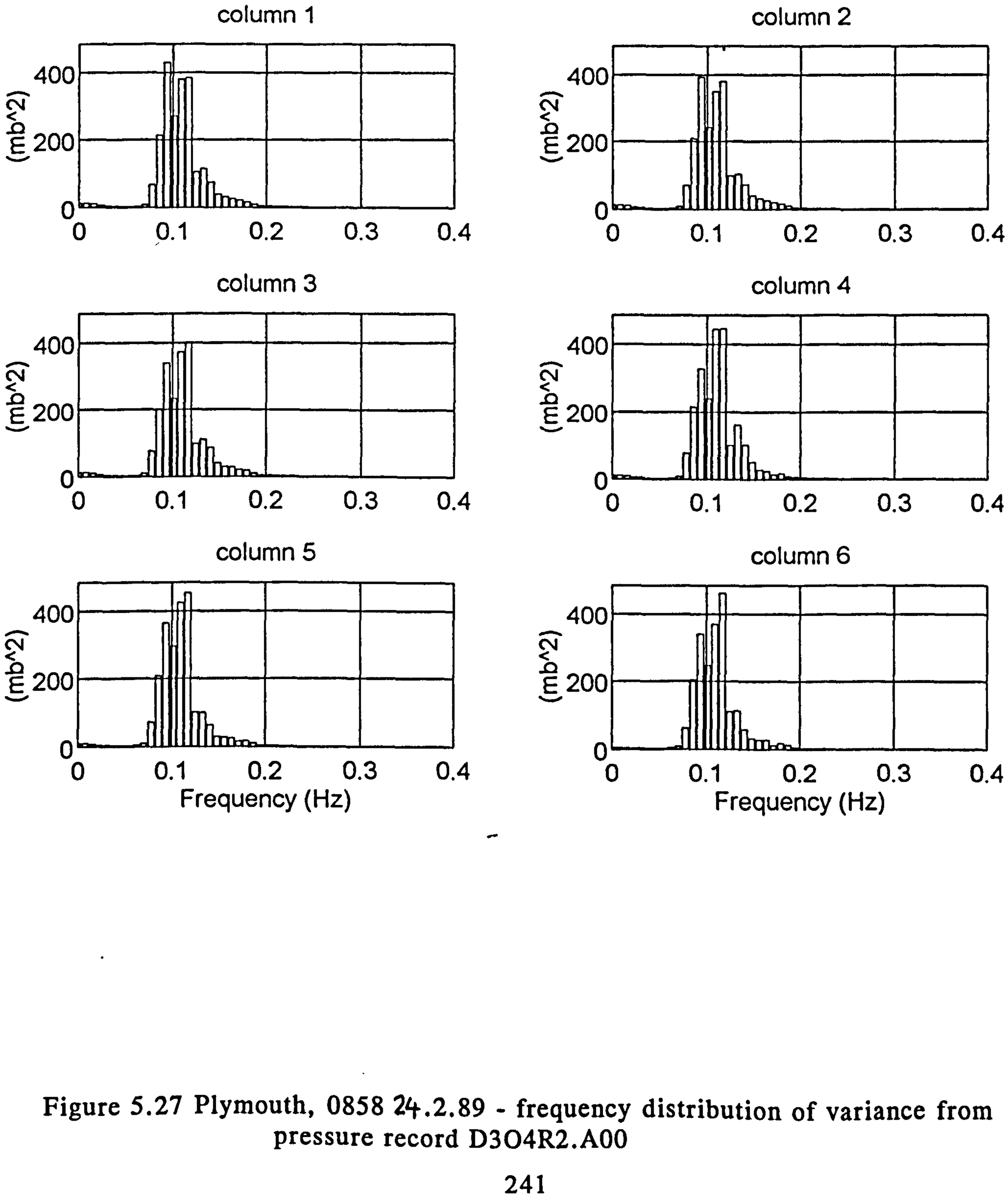

Figure 5.27 Plymouth, 0858 24.2.89 - frequency distribution of variance from pressure record D3O4R2.A00

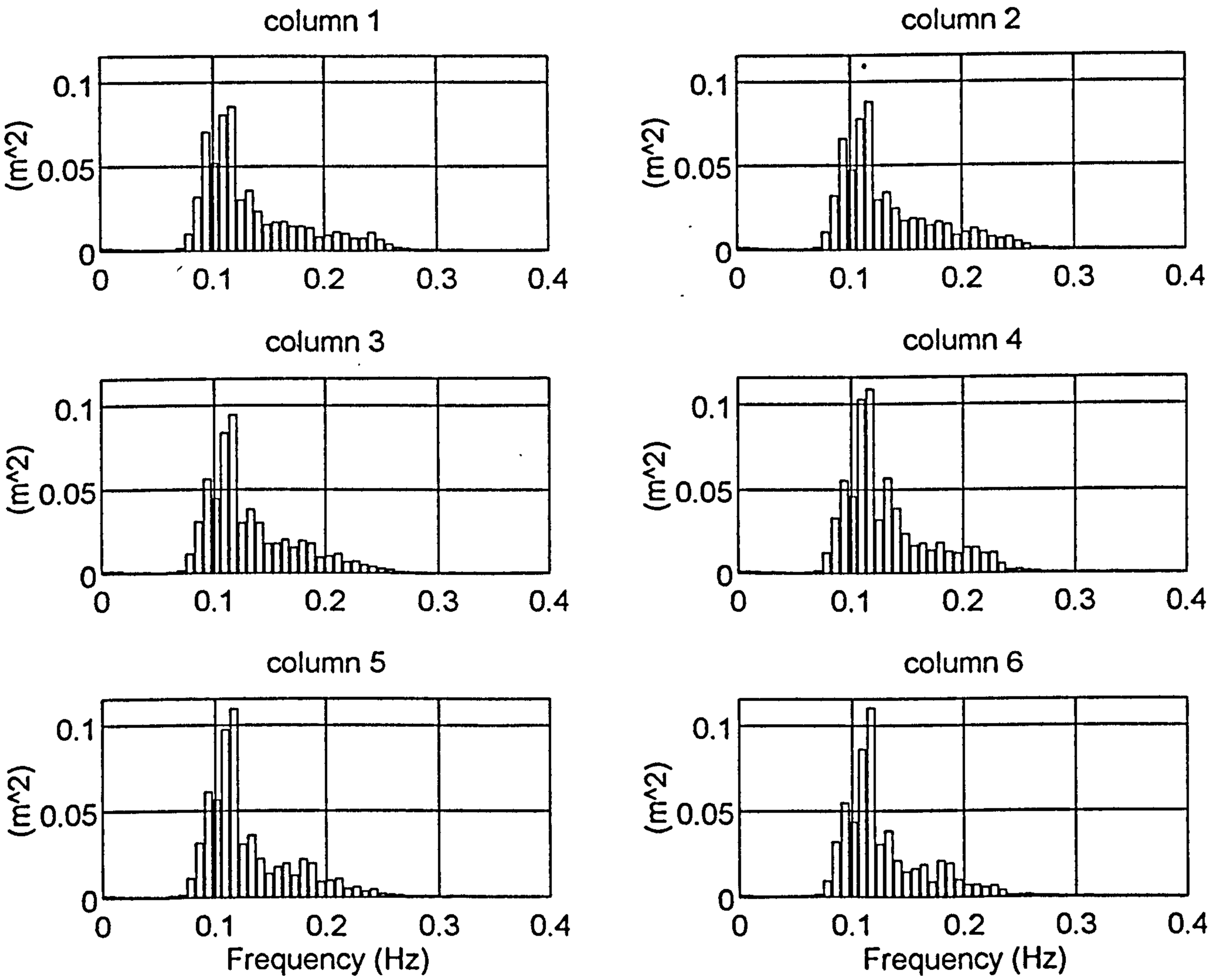

Figure 5.28 Plymouth, 0858 24.2.89 - frequency distribution of variance from surface height record D3O4R2.A00

CROSS-SPECTRAL DENSITY MATRICES FROM: D304R2.C00
XSD_f(i,j)

frequency: 0.094Hz frequency index: 13
magnitude /(10^-4 m^2): phase /degrees:

702	677	621	612	626	563	0	14	41	82	98	-153
677	655	604	594	609	550	-14	0	27	68	84	-167
621	604	565	554	575	521	-41	-27	0	40	55	165
612	594	554	555	566	510	-82	-68	-40	0	15	124
626	609	575	566	607	552	-98	-84	-55	-15	0	109
563	550	521	510	552	543	153	167	-165	-124	-109	0

frequency: 0.102Hz frequency index: 14
magnitude /(10^-4 m^2): phase /degrees:

521	494	472	447	531	418	0	18	54	96	115	-109
494	471	454	427	508	406	-18	0	36	77	97	-128
472	454	445	419	497	405	-54	-36	0	40	60	-164
447	427	419	458	469	388	-96	-77	-40	0	20	158
531	508	497	469	565	460	-115	-97	-60	-20	0	135
418	406	405	388	460	436	109	128	164	-158	-135	0

frequency: 0.109Hz frequency index: 15
magnitude /(10^-4 m^2): phase /degrees:

805	789	815	857	868	779	0	22	61	97	124	-87
789	775	802	841	852	768	-22	0	39	74	101	-110
815	802	838	880	892	811	-61	-39	0	34	62	-150
857	841	880	1028	933	891	-97	-74	-34	0	28	179
868	852	892	933	971	888	-124	-101	-62	-28	0	148
779	768	811	891	888	859	87	110	150	-179	-148	0

frequency: 0.117Hz frequency index: 16
magnitude /(10^-4 m^2): phase /degrees:

853	864	894	896	952	921	0	22	60	84	131	-79
864	876	909	914	965	935	-22	0	39	62	109	-101
894	909	946	957	1005	978	-60	-39	0	23	70	-140
896	914	957	1083	1009	1051	-84	-62	-23	0	47	-163
952	965	1005	1009	1095	1069	-131	-109	-70	-47	0	150
921	935	978	1051	1069	1100	79	101	140	163	-150	0

frequency: 0.125Hz frequency index: 17
magnitude /(10^-4 m^2): phase /degrees:

302	298	294	262	297	235	0	22	63	91	137	-59
298	296	295	267	297	243	-22	0	41	68	114	-82
294	295	298	277	301	259	-63	-41	0	26	73	-123
262	267	277	316	282	282	-91	-68	-26	0	46	-151
297	297	301	282	309	271	-137	-114	-73	-46	0	163
235	243	259	282	271	305	59	82	123	151	-163	0

Figure 5.29 Plymouth, 0858 24.2.89 - cross-spectral matrices for the most energetic frequency bins from D3O4R2.C00

COHERENCE MATRICES FROM: D304R2.C00
COH_f(i,j)

frequency: 0.094Hz frequency index: 13

1.000	0.997	0.973	0.960	0.921	0.833
0.997	1.000	0.986	0.970	0.933	0.850
0.973	0.986	1.000	0.979	0.966	0.884
0.960	0.970	0.979	1.000	0.952	0.862
0.921	0.933	0.966	0.952	1.000	0.925
0.833	0.850	0.884	0.862	0.925	1.000

frequency: 0.102Hz frequency index: 14

1.000	0.994	0.960	0.838	0.957	0.769
0.994	1.000	0.982	0.846	0.968	0.803
0.960	0.982	1.000	0.863	0.982	0.844
0.838	0.846	0.863	1.000	0.850	0.754
0.957	0.968	0.982	0.850	1.000	0.858
0.769	0.803	0.844	0.754	0.858	1.000

frequency: 0.109Hz frequency index: 15

1.000	0.997	0.983	0.886	0.964	0.878
0.997	1.000	0.992	0.888	0.966	0.886
0.983	0.992	1.000	0.900	0.978	0.914
0.886	0.888	0.900	1.000	0.873	0.901
0.964	0.966	0.978	0.873	1.000	0.946
0.878	0.886	0.914	0.901	0.946	1.000

frequency: 0.117Hz frequency index: 16

1.000	0.998	0.991	0.870	0.972	0.904
0.998	1.000	0.996	0.880	0.970	0.907
0.991	0.996	1.000	0.894	0.976	0.919
0.870	0.880	0.894	1.000	0.859	0.927
0.972	0.970	0.976	0.859	1.000	0.949
0.904	0.907	0.919	0.927	0.949	1.000

frequency: 0.125Hz frequency index: 17

1.000	0.994	0.961	0.717	0.943	0.599
0.994	1.000	0.983	0.759	0.968	0.656
0.961	0.983	1.000	0.816	0.987	0.736
0.717	0.759	0.816	1.000	0.817	0.828
0.943	0.968	0.987	0.817	1.000	0.782
0.599	0.656	0.736	0.828	0.782	1.000

Figure 5.30 Plymouth, 0858 24.2.89 - coherence matrices for the most energetic frequency bins from D3O4R2.C00

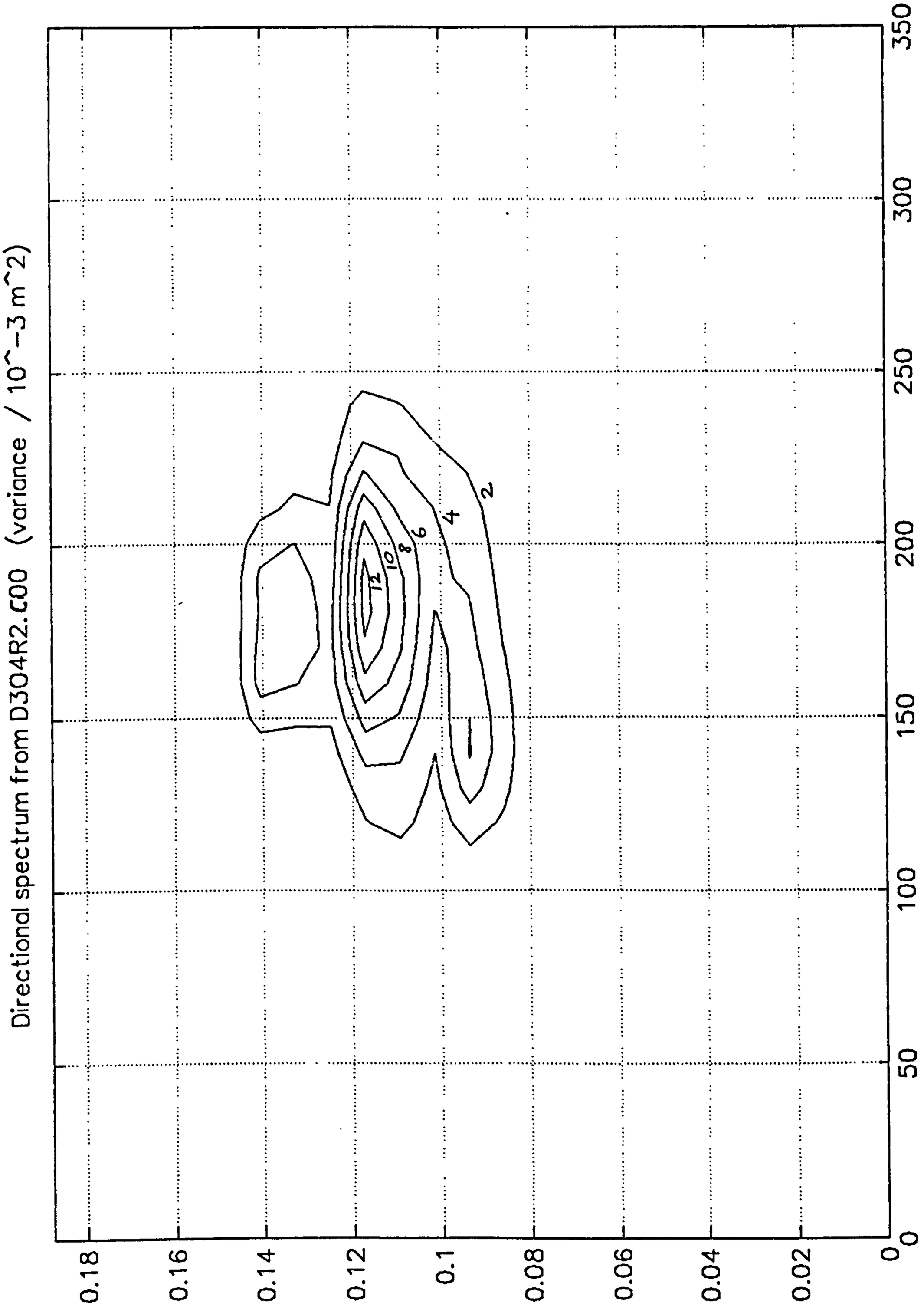

Figure 5.31 Plymouth, 0858 24.2.89 - directional wave spectrum from D3O4R2.C00 as a contour plot

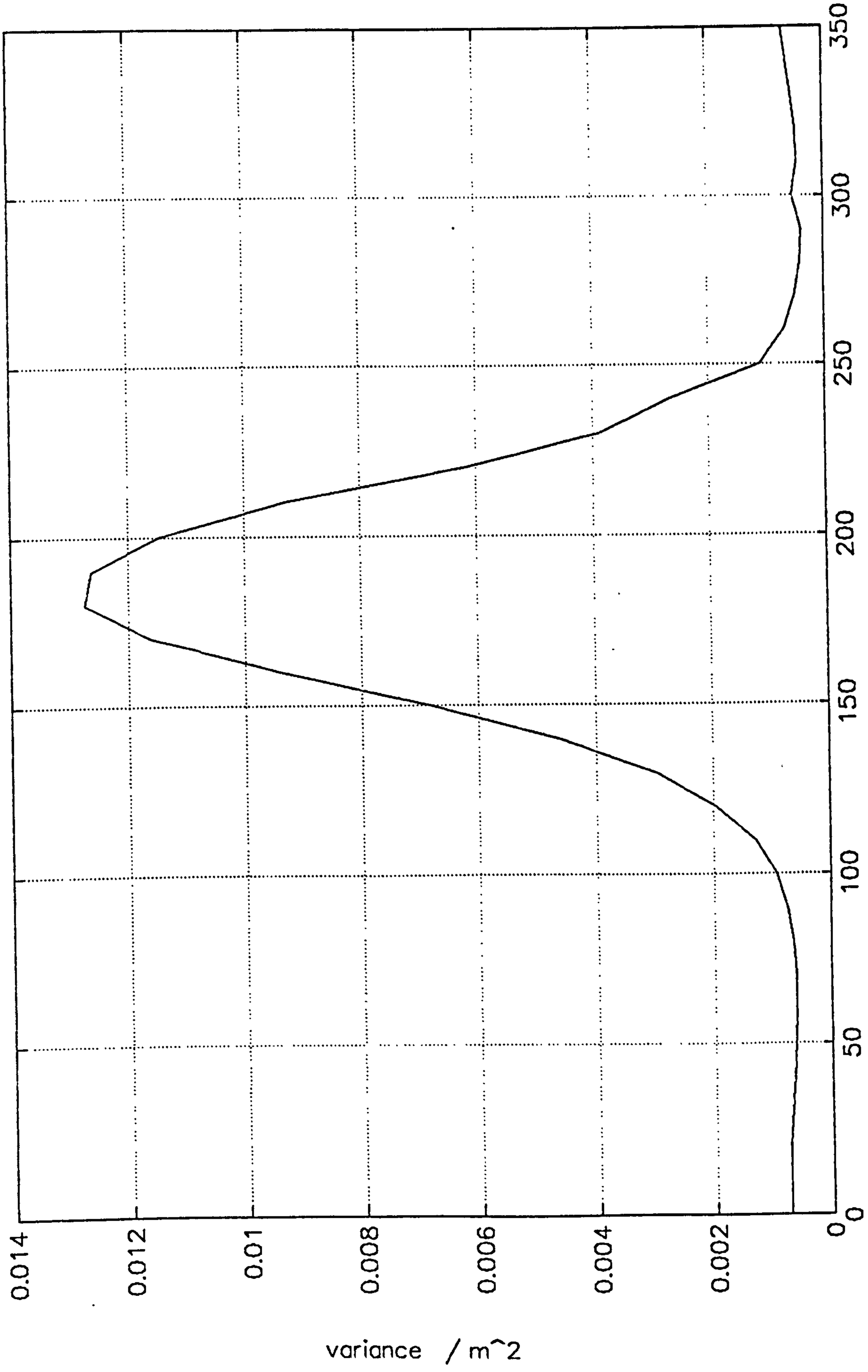

Figure 5.32 Plymouth, 0858 24.2.89 directional wave distribution from D3O4R2.C00 : 0.117 Hz

```
"       Wave recorder : WR1,  System No.2  :                1"
"        Mod standard :       Deployment 6  :                0"
"            Location :  Elmer, W. Sussex  :                0"
"  Transducer layout  :    WR1-0079 iss A  :                0"
"  Time/Date 1st rdg  : 05 Jul 92 0233:15  :                0"
"Data element values  : Abs pressures, mb  :                1"
" Data array columns  :     6, ch2 to ch7  :                6"
"    Data array rows  : 1356,sim.rdg sets  :             1356"
"   Reading interval  :              500 ms  :              500"
"Tr. o/s errors used  : 40,-48,33,-2,74,4  :                0"
"    File created by  :           DECODE4   :                0"
"             Version  :  4.1    ·   3.7.92  :               0"



 1411 1420 1445 1432 1427 1436
 1413 1421 1443 1431 1428 1433
 1414 1421 1441 1431 1429 1430
 1415 1421 1438 1431 1432 1427
 1417 1421 1436 1430 1432 1424
 1416 1420 1434 1430 1434 1422
 1414 1418 1434 1431 1435 1421
 1413 1417 1434 1434 1436 1422
 1409 1415 1436 1436 1435 1421
 1407 1415 1438 1439 1434 1424
 1406 1415 1438 1440 1433 1426
 1405 1414 1440 1441 1432 1429
 1404 1414 1441 1442 1432 1431
 1403 1413 1443 1441 1432 1433
 1402 1414 1444 1438 1433 1432
 1402 1415 1443 1437 1434 1429
 1404 1416 1440 1434 1433 1427
 1406 1415 1437 1432 1433 1423
 1409 1415 1431 1430 1433 1421
 1410 1414 1430 1429 1433 1421



 1416 1423 1446 1457 1434 1435
 1418 1423 1445 1456 1431 1435
 1419 1424 1446 1455 1430 1436
 1421 1426 1448 1452 1430 1438
 1424 1429 1452 1448 1430 1442
 1427 1435 1455 1446 1431 1445
 1430 1437 1458 1442 1434 1447
 1432 1439 1459 1439 1437 1449
 1431 1439 1459 1436 1440 1448
 1432 1438 1457 1434 1443 1444
 1430 1436 1455 1434 1446 1441
 1427 1432 1451 1433 1449 1437
 1424 1429 1446 1432 1452 1434
 1421 1426 1440 1432 1452 1430
 1419 1423 1438 1433 1451 1427
 1417 1420 1436 1435 1450 1426
 1413 1417 1434 1440 1447 1424
 1409 1414 1436 1445 1444 1424
 1404 1413 1438 1452 1441 1427
 1402 1414 1441 1456 1437 1430
 1402 1414 1446 1460 1437 1435
```

Figure 5.33 Elmer, 0233 5.7.92 - file of pressures, D6O4R0.A19 (first and last few lines)

```
"        Wave recorder : WR1,  System No.2  :                1"
"         Mod standard :       Deployment 6  :                0"
"             Location :  Elmer, W. Sussex  :                0"
"   Transducer layout  :    WR1-0079 iss A  :                0"
"   Time/Date 1st rdg  : 05 Jul 92 0233:15  :                0"
"Data element values   : Abs pressures, mb  :                1"
" Data array columns   :     6, ch2 to ch7  :                6"
"     Data array rows  : 1356,sim.rdg sets  :             1356"
"    Reading interval  :              500 ms  :              500"
"Tr. o/s errors used   : 40,-48,33,-2,74,4
"     File created by  :
"    Input created by  :       DECODE4
```

```
4.257   4.527   4.589   4.532   4.650   4.422
4.295   4.511   4.527   4.535   4.647   4.415
4.308   4.481   4.493   4.517   4.662   4.424
4.294   4.460   4.488   4.475   4.677   4.422
4.275   4.468   4.500   4.437   4.674   4.401
4.272   4.496   4.518   4.434   4.650   4.383
4.294   4.529   4.537   4.469   4.620   4.398
4.325   4.550   4.567   4.515   4.598   4.452
4.344   4.556   4.611   4.543   4.587   4.523
4.335   4.554   4.664   4.551   4.582   4.575
4.306   4.554   4.709   4.558   4.580   4.593
4.279   4.556   4.730   4.587   4.577   4.587
4.276   4.563   4.720   4.629   4.572   4.576
4.302   4.571   4.690   4.657   4.567   4.567
4.338   4.579   4.659   4.644   4.571   4.553
4.361   4.578   4.642   4.597   4.594   4.524
4.356   4.561   4.635   4.547   4.637   4.482
4.331   4.534   4.624   4.527   4.686   4.437
4.305   4.512   4.593   4.536   4.725   4.404
```

```
4.391   4.668   4.840   4.669   4.760   4.712
4.456   4.707   4.798   4.631   4.792   4.683
4.487   4.711   4.730   4.592   4.797   4.623
4.491   4.681   4.659   4.548   4.791   4.533
4.487   4.638   4.611   4.513   4.797   4.440
4.482   4.611   4.592   4.506   4.814   4.386
4.467   4.609   4.594   4.536   4.831   4.397
4.437   4.616   4.603   4.590   4.840   4.464
4.396   4.611   4.620   4.639   4.847   4.547
4.353   4.588   4.654   4.657   4.856   4.606
4.319   4.566   4.707   4.639   4.860   4.631
4.294   4.562   4.769   4.610   4.846   4.635
4.279   4.579   4.811   4.609   4.810   4.634
4.280   4.601   4.807   4.655   4.764   4.628
4.299   4.610   4.757   4.731   4.724   4.610
4.332   4.599   4.689   4.796   4.694   4.576
4.363   4.578   4.640   4.815   4.666   4.545
4.380   4.562   4.633   4.790   4.637   4.533
```

```
THE SOURCE DATA FILE IS CALLED :- C:\WR1\DATA\DEP6\D604R0.A19
THIS DATA FILE IS CALLED       :- C:\WR1\DATA\DEP6\D604R0.C19
```

Figure 5.34 Elmer, 0233 5.7.92 - file of surface heights, D6O4R0.C19 (first and last few lines)

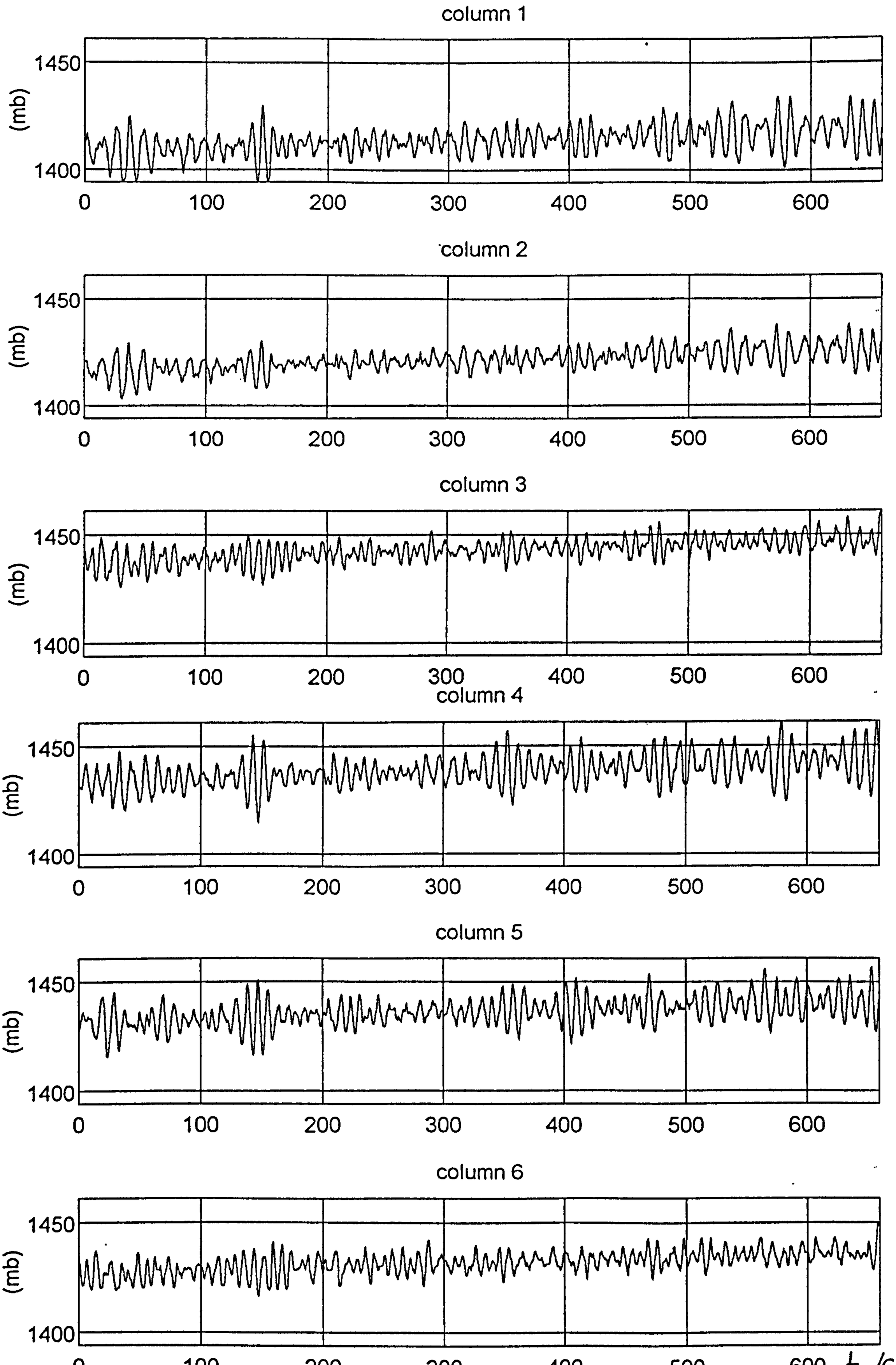

Figure 5.35 Elmer, 0233 5.7.92 - plot of pressures, D6O4R0.A19

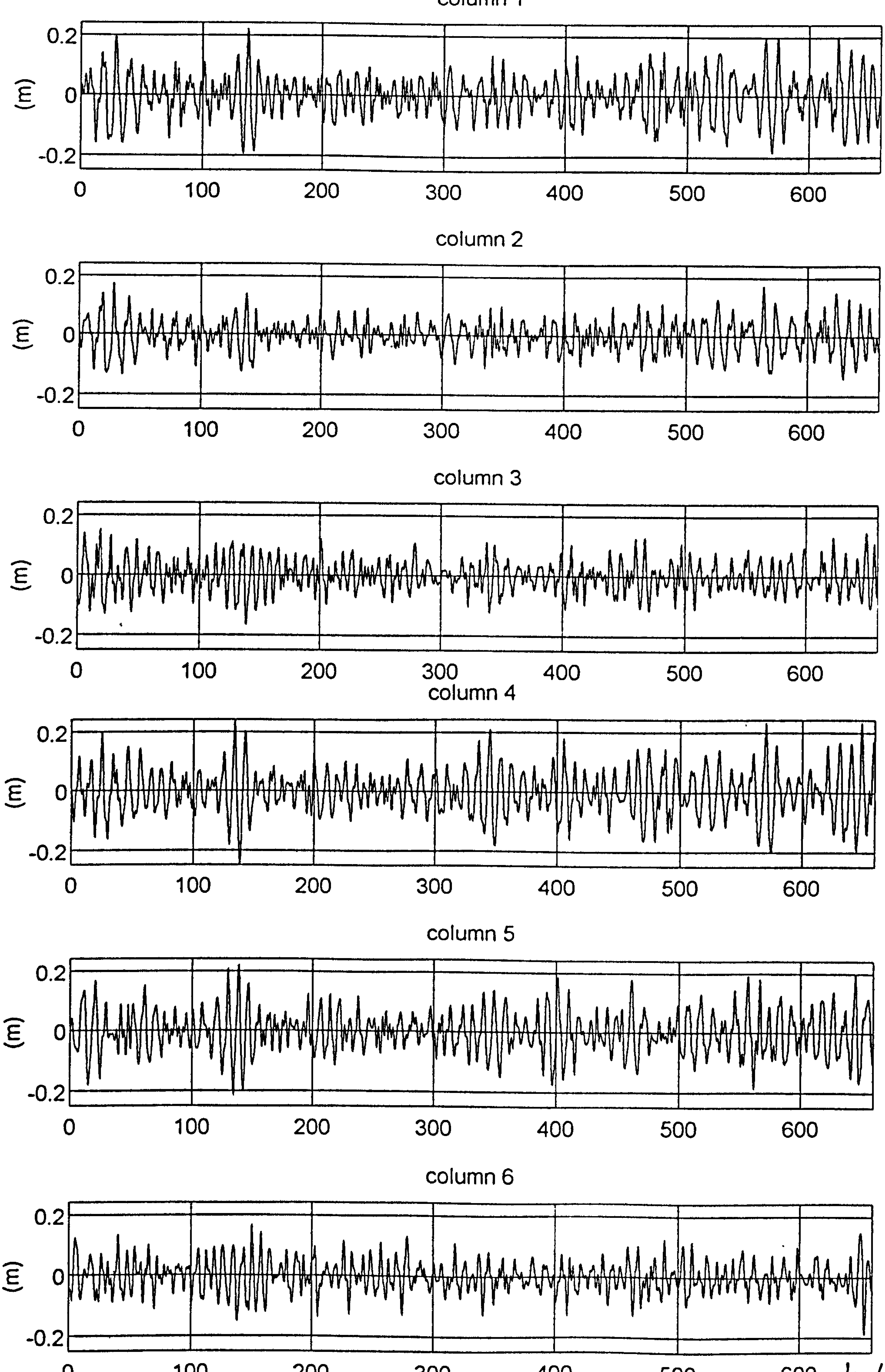

Figure 5.36 Elmer, 0233 5.7.92 - plot of surface elevations
D6O4R0.C19

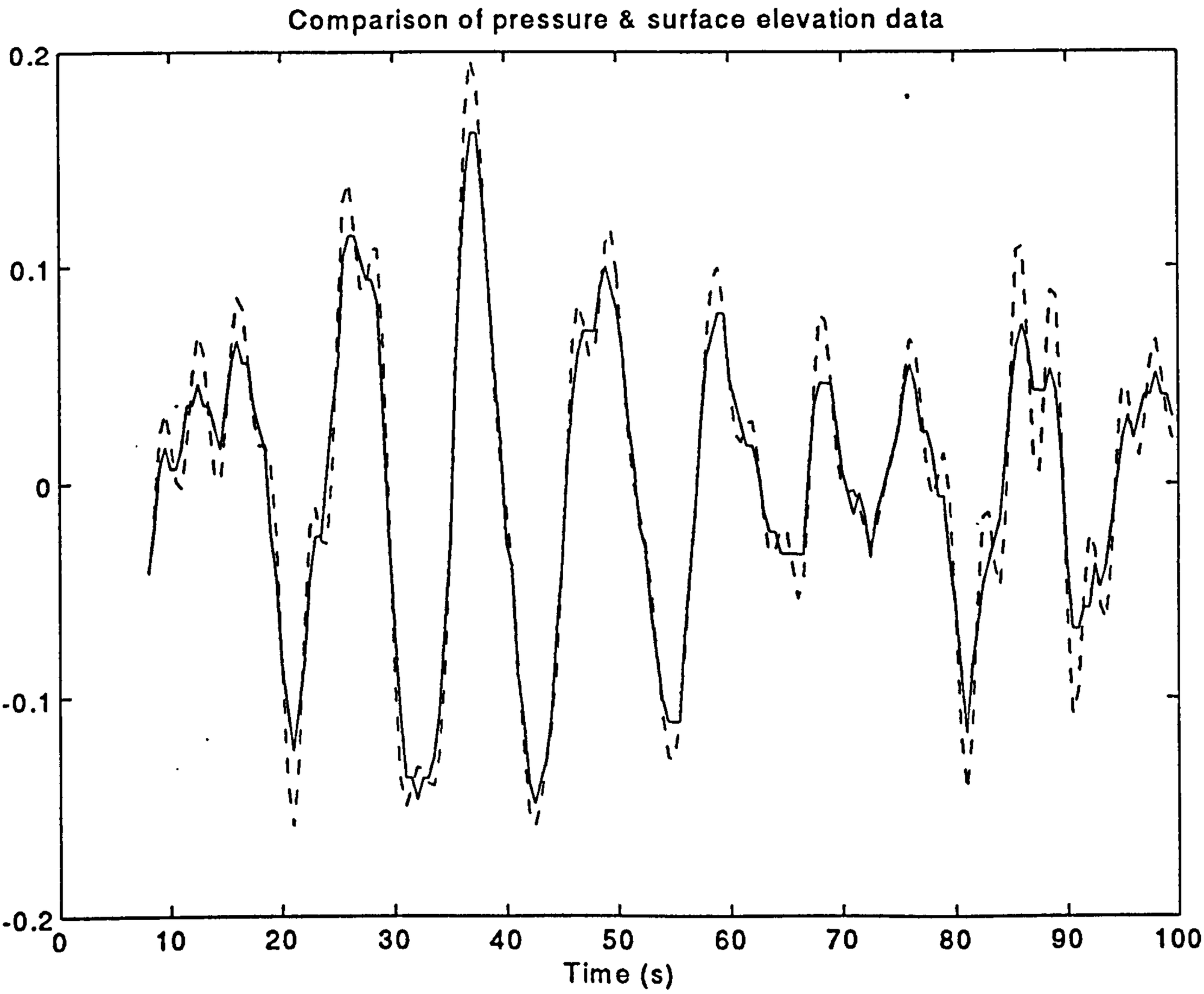

Figure 5.37 Elmer, 0233 5.7.92 - comparison of pressure and surface records. Full line - elevation from pressure with no allowance for depth attenuation. Dotted line - elevation from pressure using Airy theory.

STATISTICS FROM FILE D604R0.A19

No. rows in press.dat		1356					
first data points (press)		1411	1420	1445	1432	1427	1436
first data points (pwave)		2.9	4.4	8.2	-0.8	-3.6	10.4
means	(mb)	1414.0	1421.3	1443.0	1438.6	1436.3	1431.7
means (relative)	(mb)	0.0	7.4	29.0	24.6	22.3	17.7
tidal changes	(mb)	11.2	10.6	11.1	10.7	10.9	11.0
range (de-trended)	(mb)	36.4	26.3	26.2	41.1	35.1	27.0
max pressure excn	(mb)	19.2	13.1	12.2	19.5	17.8	13.6
max press. exc.(std-devs)		3.2	3.0	2.9	3.0	3.0	3.2
min pressure excn	(mb)	-17.3	-13.2	-14.0	-21.5	-17.3	-13.4
min press. exc.(std-devs)		-2.9	-3.0	-3.3	-3.3	-3.0	-3.2
std devs (de-trended)	(mb)	6.0	4.4	4.2	6.5	5.8	4.2
vars (de-trended)	(mb^2)	36.5	19.4	17.8	42.7	34.1	17.8
Q_flags		1	1	1	1	1	1

Figure 5.38 Elmer, 0233 5.7.92 - statistics from pressure record

STATISTICS FROM FILE D604R0.C19

No. rows in surf.dat		1320					
first data points (surf)		4.257	4.527	4.589	4.532	4.650	4.422
first data points (wave)		-0.017	0.019	0.001	-0.006	0.014	-0.045
Hs	(m)	0.27	0.21	0.21	0.30	0.28	0.20
means	(m)	4.332	4.565	4.651	4.596	4.694	4.528
tidal changes	(m)	0.108	0.103	0.111	0.107	0.107	0.108
means (relative)	(mm)	0	233	319	265	362	196
range (de-trended)	(m)	0.415	0.318	0.318	0.490	0.437	0.358
max wave excn	(m)	0.222	0.175	0.151	0.241	0.221	0.169
max wave excn (std-devs)		3.2	3.4	2.9	3.2	3.2	3.3
min wave excn	(m)	-0.194	-0.143	-0.167	-0.249	-0.216	-0.189
min wave excn (std-devs)		-2.8	-2.8	-3.2	-3.3	-3.1	-3.7
std devs (de-trended)	(m)	0.069	0.051	0.052	0.075	0.069	0.051
vars (de-trended)	(m^2)	0.005	0.003	0.003	0.006	0.005	0.003
refl. coeff. >		0.191					
Q_flags		1	1	1	1	1	1

Figure 5.39 Elmer, 0233 5.7.92 - statistics from surface height record D6O4R0.C19

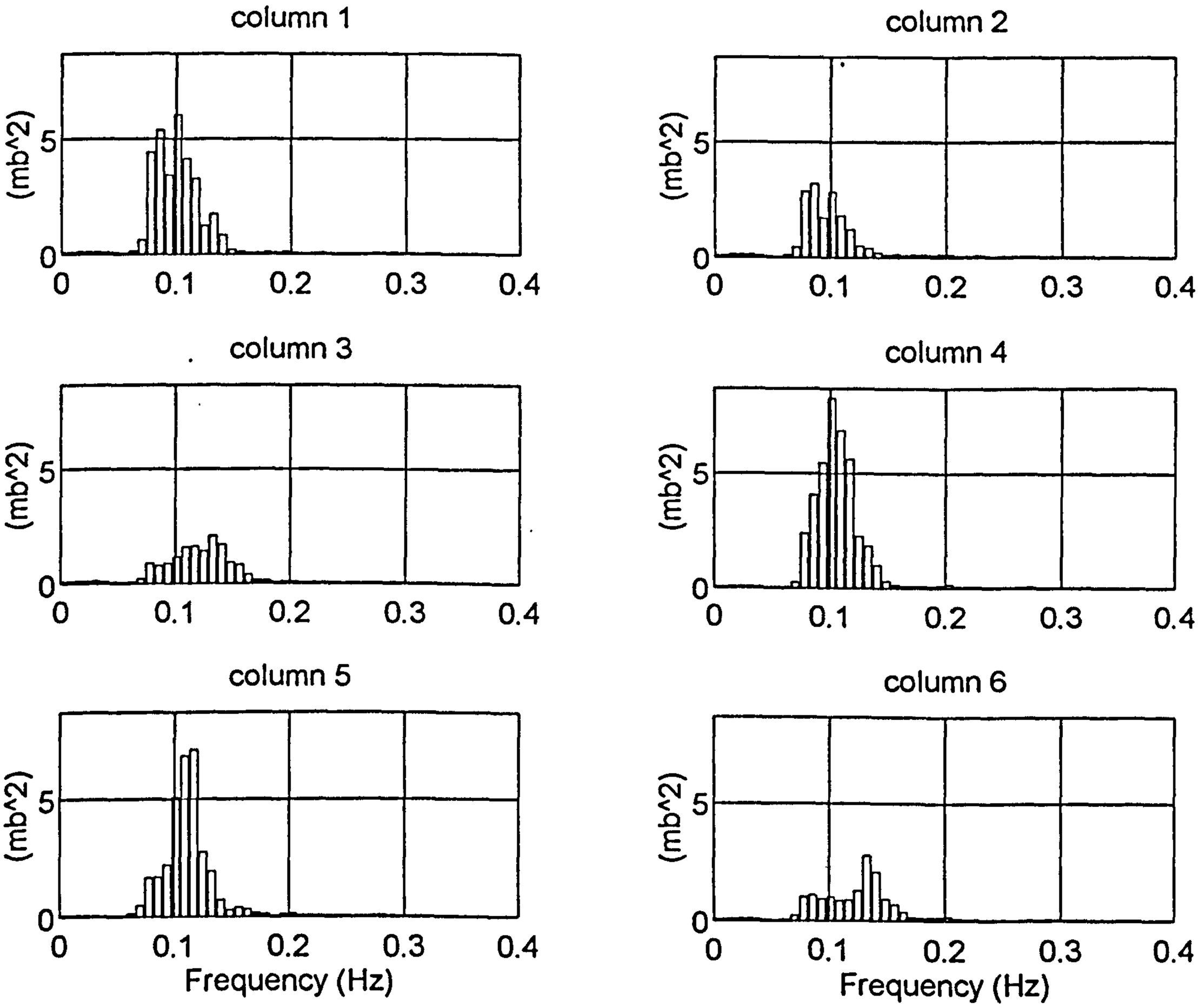

Figure 5.40 Elmer, 0233 5.7.92 - frequency distribution of variance from pressure record D6O4R0.A19

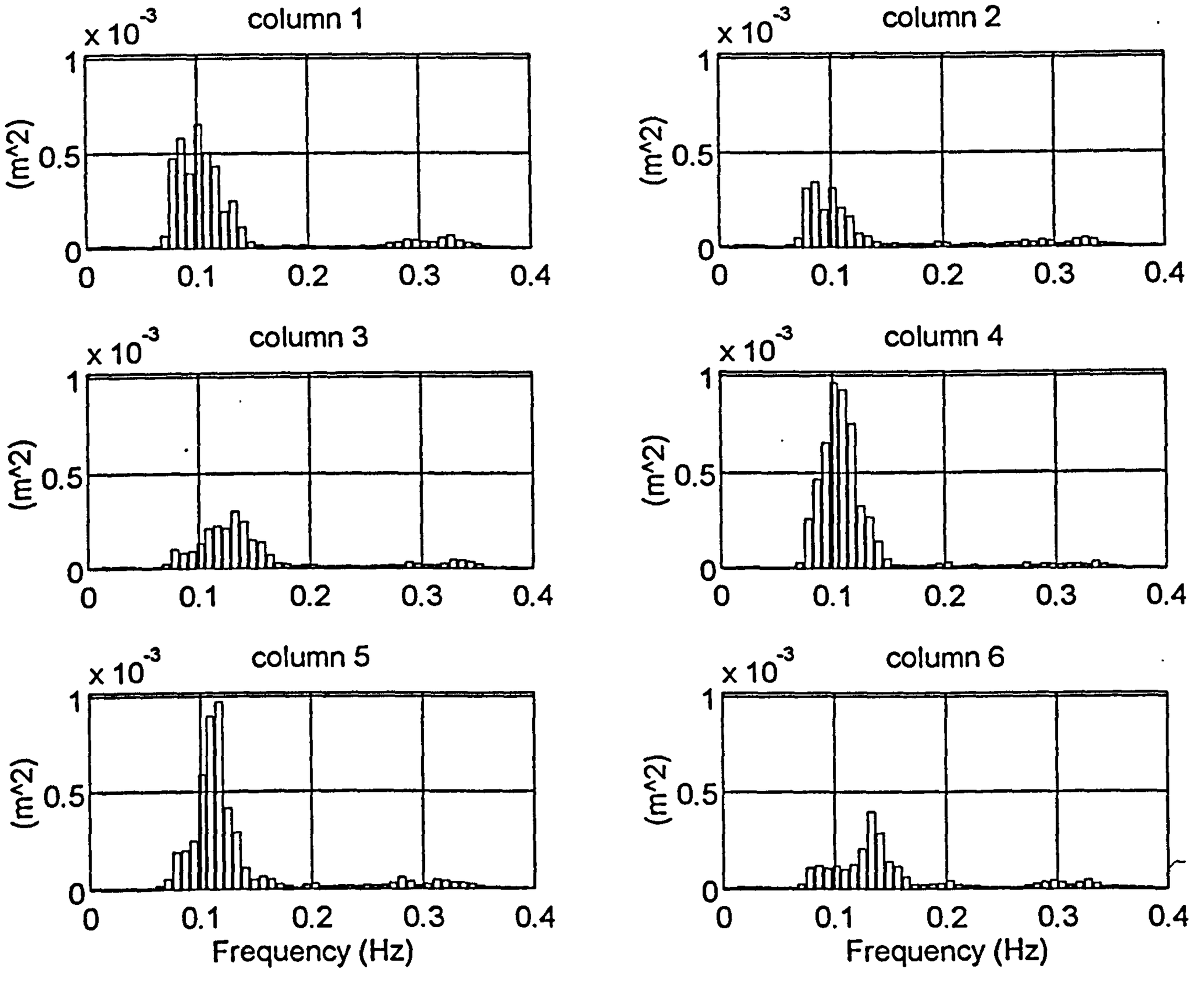

Figure 5.41 Elmer, 0233 5.7.92 - frequency distribution of variance from surface height record D6O4R0.C19

CROSS-SPECTRAL DENSITY MATRICES FROM: D604R0.C19
XSD_f(i,j)

frequency: 0.102Hz frequency index: 14
magnitude /(10^-6 m^2): phase /degrees:

655	446	209	706	569	144	0	10	93	163	-38	91
446	312	149	452	382	96	-10	0	75	151	-49	70
209	149	132	286	203	104	-93	-75	0	50	-136	-17
706	452	286	961	609	242	-163	-151	-50	0	159	-60
569	382	203	609	589	151	38	49	136	-159	0	139
144	96	104	242	151	118	-91	-70	17	60	-139	0

frequency: 0.109Hz frequency index: 15
magnitude /(10^-6 m^2): phase /degrees:

506	321	274	628	648	144	0	16	112	156	-31	133
321	211	176	381	406	80	-16	0	89	137	-49	110
274	176	207	413	382	111	-112	-89	0	37	-145	5
628	381	413	924	835	242	-156	-137	-37	0	173	-27
648	406	382	835	895	206	31	49	145	-173	0	162
144	80	111	242	206	100	-133	-110	-5	27	-162	0

frequency: 0.117Hz frequency index: 16
magnitude /(10^-6 m^2): phase /degrees:

433	261	282	551	639	188	0	20	119	157	-28	146
261	162.	170	324	383	114	-20	0	94	135	-49	121
282	170	222	389	433	151	-119	-94	0	34	-148	29
551	324	389	751	826	251	-157	-135	-34	0	175	-7
639	383	433	826	972	290	28	49	148	-175	0	175
188	114	151	251	290	122	-146	-121	-29	7	-175	0

frequency: 0.125Hz frequency index: 17
magnitude /(10^-6 m^2): phase /degrees:

196	114	187	239	270	182	0	31	123	161	-21	137
114	72	109	138	159	106	-31	0	85	127	-54	101
187	109	210	249	275	198	-123	-85	0	36	-144	15
239	138	249	327	363	223	-161	-127	-36	0	180	-22
270	159	275	363	419	248	21	54	144	-180	0	159
182	106	198	223	248	205	-137	-101	-15	22	-159	0

frequency: 0.133Hz frequency index: 18
magnitude /(10^-6 m^2): phase /degrees:

248	108	250	246	251	302	0	34	144	175	-10	153
108	57	105	106	116	125	-34	0	99	137	-46	114
250	105	301	268	261	335	-144	-99	0	31	-151	9
246	106	268	270	271	300	-175	-137	-31	0	178	-22
251	116	261	271	292	298	10	46	151	-178	0	163
302	125	335	300	298	400	-153	-114	-9	22	-163	0

Figure 5.42 Elmer, 0233 5.7.92 - cross-spectral matrices for the most energetic frequency bins from D6O4R0.C19

COHERENCE MATRICES FROM: D604R0.C19
COH_f(i,j)

frequency: 0.102Hz frequency index: 14

1.000	0.973	0.503	0.792	0.839	0.269
0.973	1.000	0.541	0.684	0.793	0.247
0.503	0.541	1.000	0.647	0.529	0.686
0.792	0.684	0.647	1.000	0.654	0.515
0.839	0.793	0.529	0.654	1.000	0.325
0.269	0.247	0.686	0.515	0.325	1.000

frequency: 0.109Hz frequency index: 15

1.000	0.962	0.720	0.844	0.928	0.411
0.962	1.000	0.707	0.743	0.872	0.302
0.720	0.707	1.000	0.893	0.788	0.592
0.844	0.743	0.893	1.000	0.844	0.635
0.928	0.872	0.788	0.844	1.000	0.471
0.411	0.302	0.592	0.635	0.471	1.000

frequency: 0.117Hz frequency index: 16

1.000	0.970	0.831	0.935	0.970	0.672
0.970	1.000	0.800	0.860	0.929	0.654
0.831	0.800	1.000	0.908	0.871	0.846
0.935	0.860	0.908	1.000	0.934	0.686
0.970	0.929	0.871	0.934	1.000	0.709
0.672	0.654	0.846	0.686	0.709	1.000

frequency: 0.125Hz frequency index: 17

1.000	0.928	0.847	0.893	0.889	0.820
0.928	1.000	0.792	0.807	0.843	0.761
0.847	0.792	1.000	0.907	0.861	0.911
0.893	0.807	0.907	1.000	0.963	0.744
0.889	0.843	0.861	0.963	1.000	0.715
0.820	0.761	0.911	0.744	0.715	1.000

frequency: 0.133Hz frequency index: 18

1.000	0.823	0.837	0.903	0.870	0.917
0.823	1.000	0.640	0.725	0.805	0.690
0.837	0.640	1.000	0.887	0.775	0.935
0.903	0.725	0.887	1.000	0.933	0.835
0.870	0.805	0.775	0.933	1.000	0.760
0.917	0.690	0.935	0.835	0.760	1.000

Figure 5.43 Elmer, 0233 5.7.92 - coherence matrices for the most energetic frequency bins from D6O4R0.C19

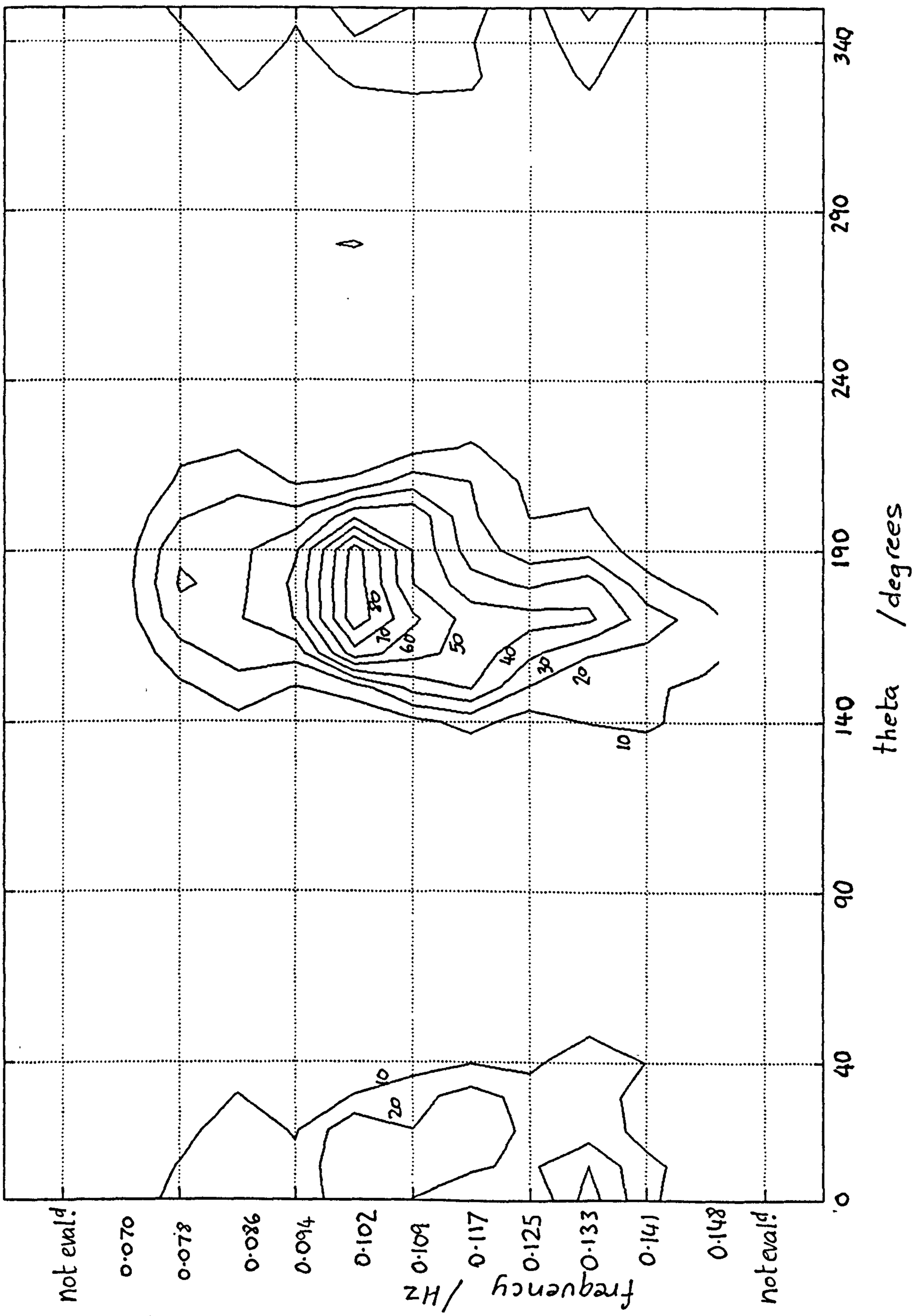

Figure 5.44 Elmer, 0233 5.7.92 - directional wave spectrum from D6O4R0.C19 as a contour plot

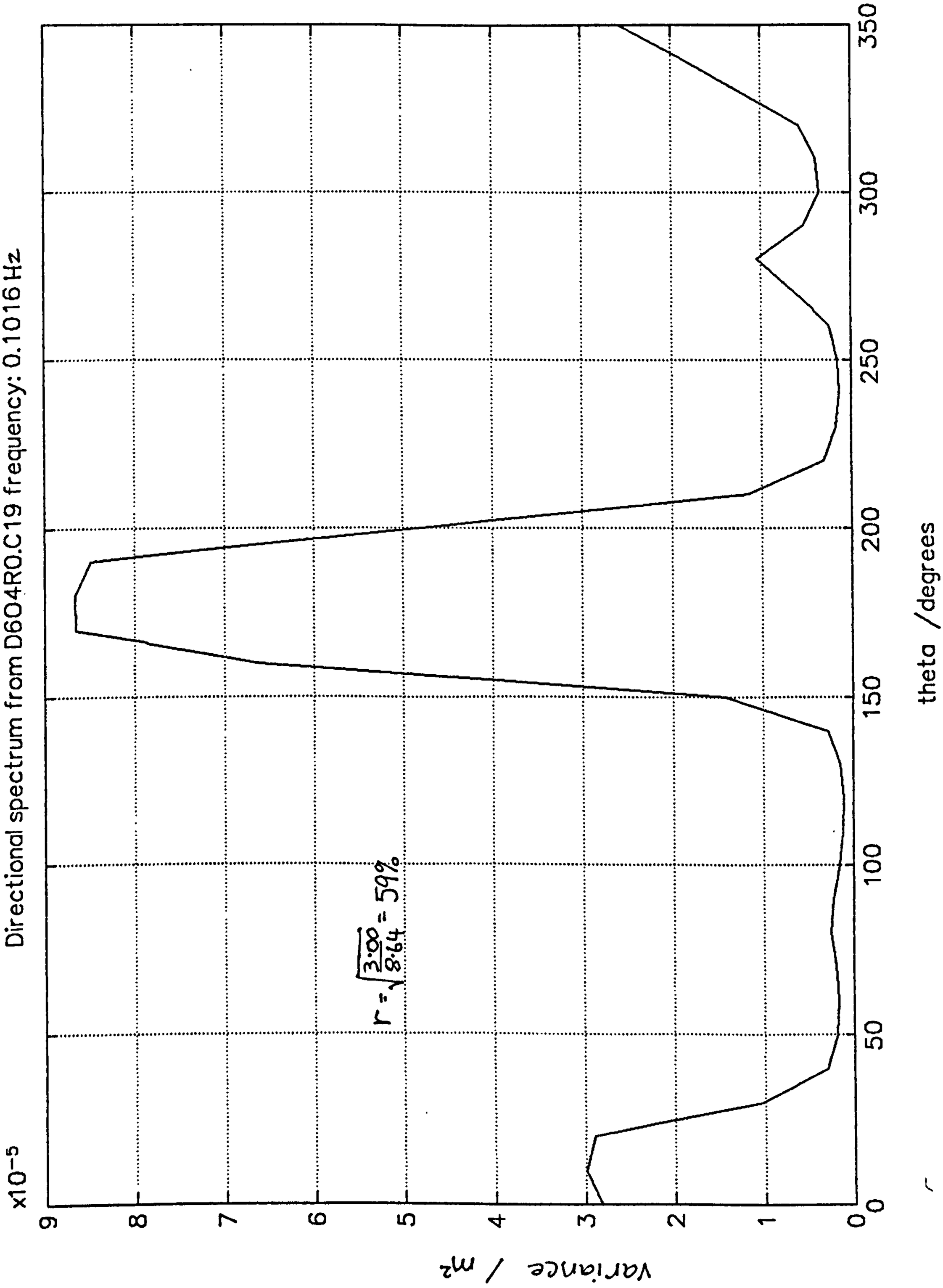

Figure 5.45 Elmer, 0233 5.7.92 - directional distribution from D604R0.C19 : 0·102 Hz

```
"       Wave recorder : WR1,  System No.2  :                1"
"        Mod standard :       Deployment 6  :                0"
"            Location :  Elmer, W. Sussex  :                0"
"  Transducer layout  :    WR1-0079 iss A  :                0"
"  Time/Date 1st rdg  : 13 Jul 92 2332:09  :                0"
"Data element values  : Abs pressures, mb  :                1"
" Data array columns  :     6, ch2 to ch7  :                6"
"    Data array rows  : 1356,sim.rdg sets  :             1356"
"   Reading interval  :              500 ms  :              500"
"Tr. o/s errors used  : 40,-48,33,-2,74,4  :                0"
"    File created by  :            DECODE4  :                0"
"             Version :  4.1       3.7.92  :                0"
```

```
1368 1375 1400 1427 1402 1403
1362 1371 1412 1424 1415 1428
1357 1372 1426 1404 1414 1433
1357 1381 1433 1379 1405 1416
1366 1396 1427 1368 1400 1390
1378 1406 1410 1364 1403 1368
1390 1403 1391 1369 1406 1354
1397 1387 1373 1383 1404 1346
1385 1364 1357 1404 1392 1344
1359 1344 1348 1424 1377 1353
1348 1340 1358 1427 1366 1372
1350 1353 1387 1418 1362 1397
1351 1372 1421 1403 1364 1423
1354 1389 1446 1394 1376 1444
1358 1400 1450 1393 1397 1451
1366 1408 1443 1398 1418 1443
1379 1409 1429 1397 1432 1411
1390 1397 1412 1395 1435 1373
1393 1383 1400 1387 1426 1347
1387 1374 1389 1379 1409 1343
```

```
1391 1377 1373 1410 1400 1372
1379 1364 1378 1401 1412 1371
1373 1363 1389 1390 1422 1382
1370 1370 1399 1385 1425 1389
1372 1383 1406 1389 1421 1395
1374 1394 1410 1396 1410 1398
1377 1399 1411 1403 1396 1400
1380 1398 1416 1408 1384 1404
1381 1392 1415 1411 1375 1407
1374 1381 1413 1414 1370 1407
1369 1373 1413 1420 1367 1403
1363 1371 1413 1426 1372 1395
1367 1380 1412 1424 1385 1390
1374 1393 1409 1418 1403 1387
1384 1400 1405 1403 1416 1392
1393 1397 1403 1382 1420 1400
1394 1392 1408 1365 1419 1407
1382 1385 1410 1361 1415 1408
1379 1387 1407 1370 1412 1402
1384 1395 1399 1386 1405 1389
1388 1395 1390 1407 1402 1381
```

Figure 5.46 Elmer, 2332 13.7.92 - file of pressures, D6O4R2.A26 (first and last few lines)

```
"       Wave recorder : WR1,  System No.2  :          1"
"        Mod standard :       Deployment 6 :          0"
"            Location :  Elmer, W. Sussex  :          0"
"  Transducer layout  :    WR1-0079 iss A  :          0"
"  Time/Date 1st rdg  : 13 Jul 92 2332:09  :          0"
"Data element values  : Abs pressures, mb  :          1"
" Data array columns  :     6, ch2 to ch7  :          6"
"    Data array rows  : 1356,sim.rdg sets  :       1356"
"   Reading interval  :              500 ms  :        500"
"Tr. o/s errors used  : 40,-48,33,-2,74,4
"    File created by  :
"   Input created by  :       DECODE4
```

```
4.090   4.303   4.299   4.388   4.850   3.852
4.151   4.166   4.236   4.187   4.717   3.489
4.135   4.088   4.161   3.854   4.451   3.435
4.069   4.061   3.999   3.663   4.173   3.613
3.998   4.059   3.803   3.808   4.006   3.856
3.950   4.070   3.705   4.214   4.008   4.037
3.925   4.088   3.796   4.592   4.143   4.137
3.897   4.098   4.050   4.680   4.302   4.214
3.837   4.079   4.362   4.478   4.375   4.326
3.740   4.041   4.627   4.229   4.332   4.471
3.645   4.042   4.787   4.177   4.242   4.591
3.626   4.145   4.823   4.336   4.213   4.608
3.737   4.340   4.732   4.501   4.283   4.487
3.957   4.516   4.530   4.472   4.392   4.265
4.184   4.542   4.278   4.252   4.445   4.032
4.300   4.386   4.062   4.024   4.409   3.883
4.262   4.158   3.952   3.951   4.349   3.853
4.130   4.018   3.949   4.016   4.353   3.903
4.006   4.037   4.005   4.079   4.438   3.962
```

```
4.125   4.206   4.154   4.123   4.871   4.111
4.094   4.042   4.163   3.868   4.688   4.065
4.042   4.014   4.163   3.770   4.417   4.001
3.997   4.124   4.140   3.845   4.268   3.901
3.992   4.286   4.114   4.009   4.307   3.820
4.025   4.374   4.099   4.188   4.426   3.836
4.053   4.310   4.087   4.365   4.474   3.975
4.008   4.116   4.077   4.526   4.383   4.179
3.866   3.907   4.118   4.609   4.233   4.361
3.680   3.823   4.282   4.534   4.140   4.469
3.561   3.938   4.567   4.305   4.153   4.500
3.600   4.212   4.844   4.048   4.217   4.466
3.800   4.501   4.912   3.937   4.246   4.370
4.063   4.645   4.665   4.051   4.208   4.211
4.253   4.565   4.210   4.295   4.153   4.022
4.276   4.309   3.814   4.475   4.166   3.874
4.143   4.019   3.703   4.446   4.290   3.831
3.949   3.840   3.891   4.228   4.487   3.905
```

```
THE SOURCE DATA FILE IS CALLED :- C:\WR1\DATA\DEP6\D604R2.A26
THIS DATA FILE IS CALLED       :- C:\WR1\DATA\DEP6\D604R2.C26
```

Figure 5.47 Elmer, 2332 13.7.92 - file of surface heights, D6O4R2.C26 (first and last few lines)

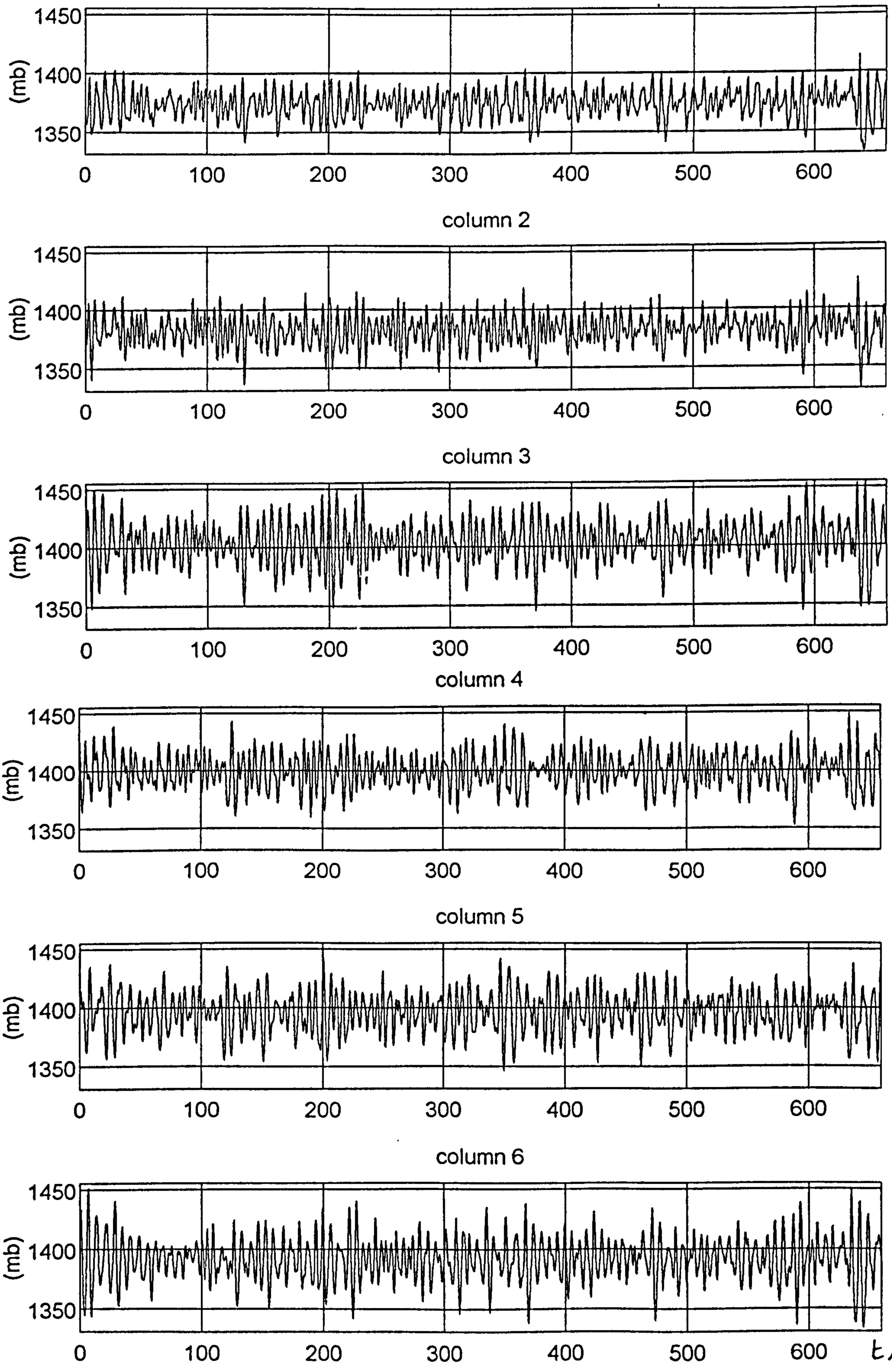

Figure 5.48 Elmer, 2332 13.7.92 - plot of pressures, D6O4R2.A26

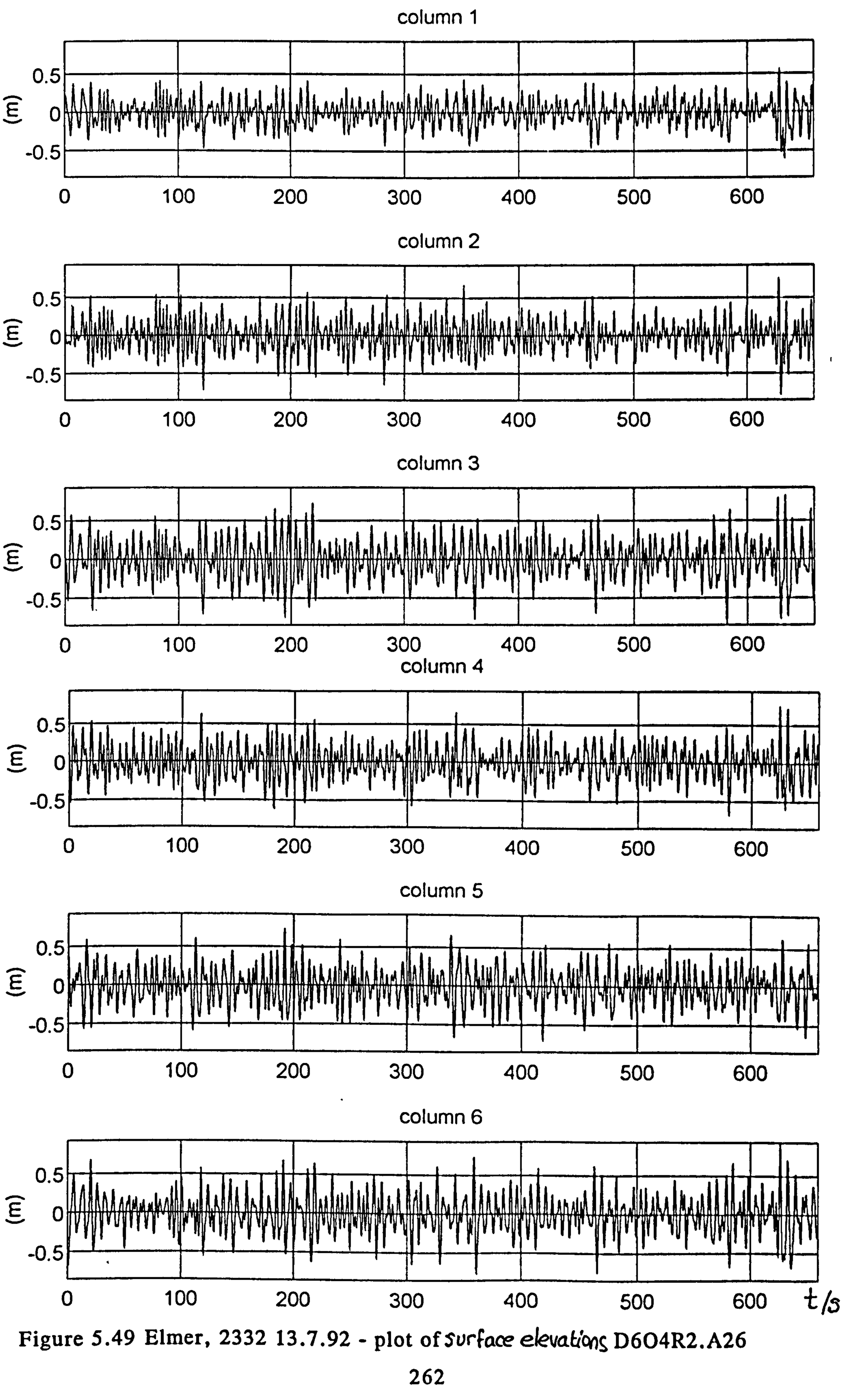

Figure 5.49 Elmer, 2332 13.7.92 - plot of surface elevations D604R2.A26

STATISTICS FROM FILE D604R2.A26

No. rows in press.dat		1356					
first data points (press)		1368	1375	1400	1427	1402	1403
first data points (pwave)		-5.0	-7.0	-3.3	27.5	5.4	10.9
means	(mb)	1373.8	1382.3	1403.5	1399.8	1396.6	1392.1
means (relative)	(mb)	0.0	8.5	29.6	26.0	22.7	18.2
tidal changes	(mb)	1.5	1.2	1.0	0.7	1.0	0.9
range (de-trended)	(mb)	81.0	95.0	110.8	96.0	97.1	117.7
max pressure excn	(mb)	39.5	43.0	50.8	47.9	46.7	58.9
max press. exc.(std-devs)		3.3	3.3	2.7	3.1	2.7	3.2
min pressure excn	(mb)	-41.5	-52.0	-60.0	-48.1	-50.3	-58.9
min press. exc.(std-devs)		-3.5	-4.0	-3.2	-3.1	-2.9	-3.2
std devs (de-trended)	(mb)	11.9	13.1	18.6	15.5	17.1	18.3
vars (de-trended)	(mb^2)	141.7	172.0	347.0	239.4	292.9	333.1
Q_flags		1	1	1	1	1	1

Figure 5.50 Elmer, 2332 13.7.92 - statistics from pressure record

FROM FILE D604R2.C26

No. rows in surf.dat		1320					
first data points (surf)		4.090	4.303	4.299	4.388	4.850	3.852
first data points (wave)		0.163	0.135	0.054	0.182	0.556	-0.265
Hs	(m)	0.67	0.84	1.03	0.90	0.97	1.00
means	(m)	3.928	4.172	4.251	4.207	4.294	4.127
tidal changes	(m)	0.007	0.008	0.010	0.008	0.006	0.012
means (relative)	(mm)	0	243	323	278	365	199
range (de-trended)	(m)	1.170	1.549	1.685	1.429	1.458	1.708
max wave excn	(m)	0.560	0.760	0.831	0.744	0.737	0.929
max wave excn (std-devs)		3.4	3.6	3.2	3.3	3.1	3.7
min wave excn	(m)	-0.611	-0.789	-0.854	-0.685	-0.721	-0.779
min wave excn (std-devs)		-3.7	-3.7	-3.3	-3.0	-3.0	-3.1
std devs (de-trended)	(m)	0.167	0.211	0.258	0.226	0.241	0.249
vars (de-trended)	(m^2)	0.028	0.045	0.067	0.051	0.058	0.062
refl. coeff. >		0.216					
Q_flags		1	1	1	1	1	1

Figure 5.51 Elmer, 2332 13.7.92 - statistics from surface height record D6O4R2.C26

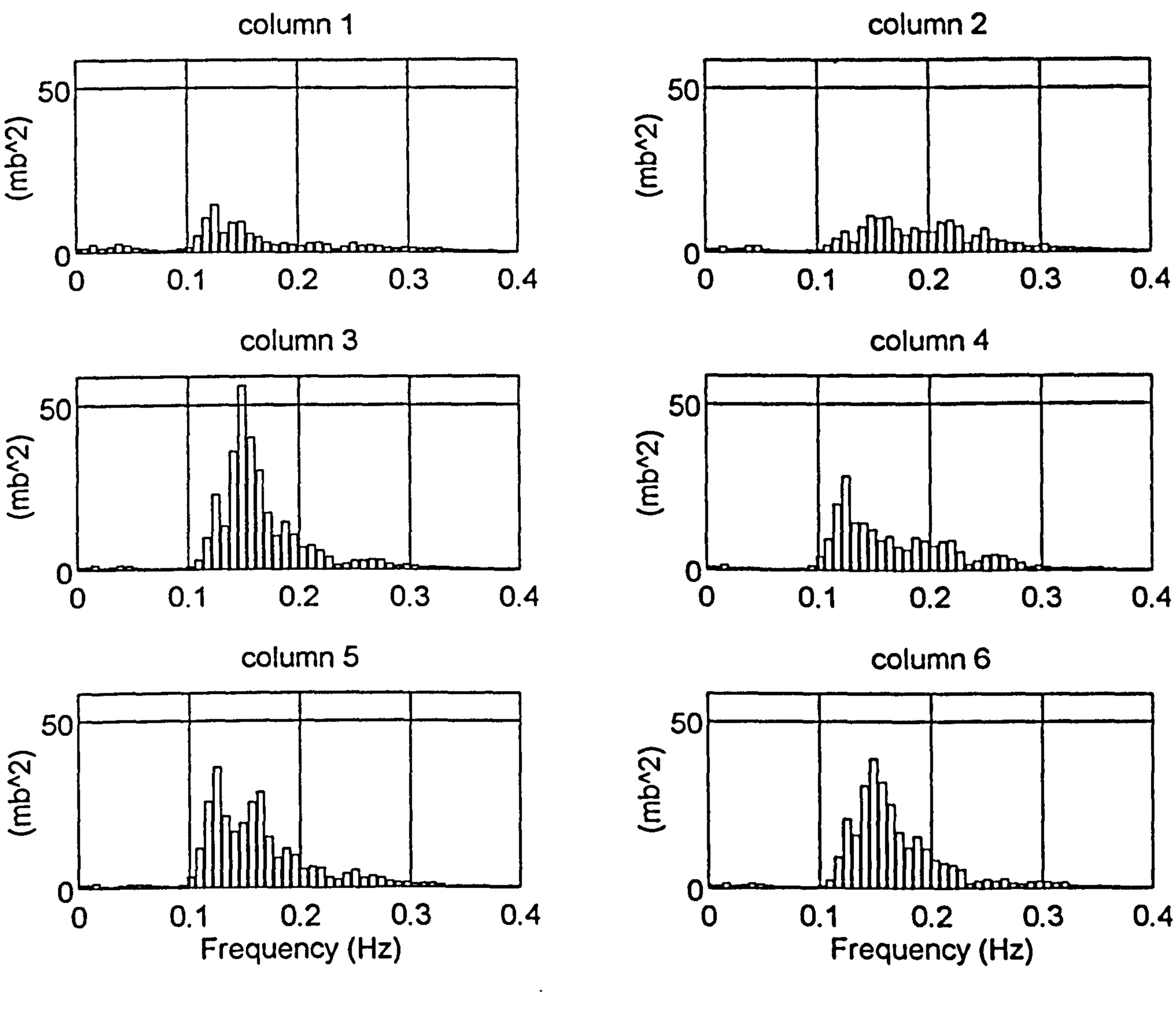

Figure 5.52 Elmer, 2332 13.7.92 - frequency distribution of variance from pressure record D6O4R2.A26

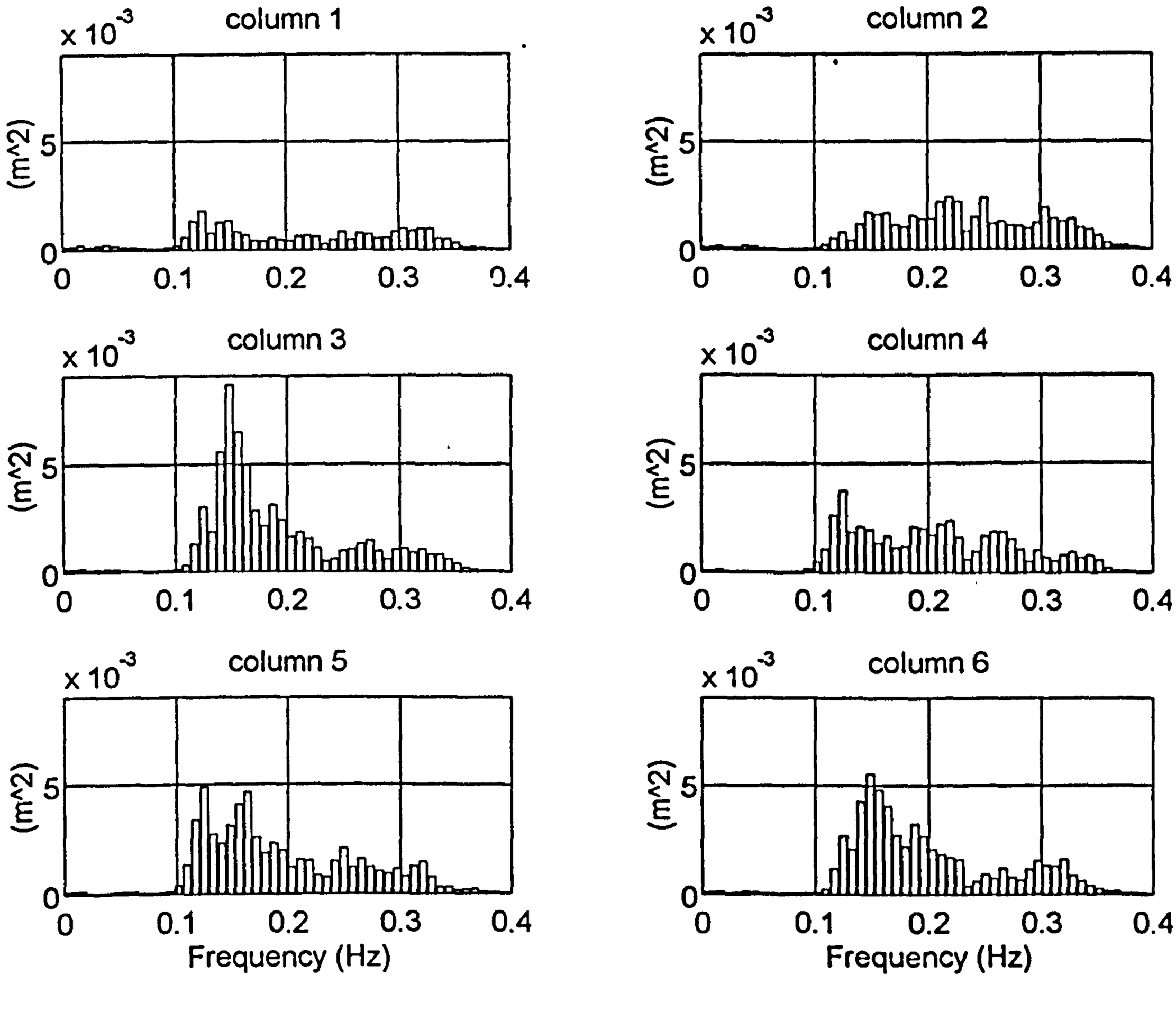

Figure 5.53 Elmer, 2332 13.7.92 - frequency distribution of variance from surface height record D6O4R2.C26

CROSS-SPECTRAL DENSITY MATRICES FROM: D604R2.C26
XSD_f(i,j)

frequency: 0.141Hz frequency index: 19

magnitude /(10^-5 m^2):						phase /degrees:					
125	114	250	148	126	224	0	72	128	-175	39	149
114	115	245	150	143	199	-72	0	51	112	-31	74
250	245	556	323	292	454	-128	-51	0	61	-79	18
148	150	323	210	200	251	175	-112	-61	0	-146	-39
126	143	292	200	228	206	-39	31	79	146	0	100
224	199	454	251	206	425	-149	-74	-18	39	-100	0

frequency: 0.148Hz frequency index: 20

magnitude /(10^-5 m^2):						phase /degrees:					
132	145	329	151	164	258	0	82	126	-163	76	146
145	170	378	174	209	287	-82	0	43	117	-4	60
329	378	861	384	444	667	-126	-43	0	73	-45	17
151	174	384	196	223	284	163	-117	-73	0	-127	-55
164	209	444	223	312	318	-76	4	45	127	0	59
258	287	667	284	318	554	-146	-60	-17	55	-59	0

frequency: 0.156Hz frequency index: 21

magnitude /(10^-5 m^2):						phase /degrees:					
83	113	228	98	168	189	0	81	119	-136	97	142
113	161	322	142	248	258	-81	0	37	144	16	57
228	322	649	282	494	532	-119	-37	0	107	-21	20
98	142	282	136	228	221	136	-144	-107	0	-131	-89
168	248	494	228	410	399	-97	-16	21	131	0	38
189	258	532	221	399	478	-142	-57	-20	89	-38	0

frequency: 0.164Hz frequency index: 22

magnitude /(10^-5 m^2):						phase /degrees:					
70	106	184	102	173	157	0	72	110	-122	97	134
106	168	287	163	277	240	-72	0	37	168	25	58
184	287	498	274	472	427	-110	-37	0	131	-12	21
102	163	274	167	271	220	122	-168	-131	0	-144	-111
173	277	472	271	466	394	-97	-25	12	144	0	31
157	240	427	220	394	404	-134	-58	-21	111	-31	0

frequency: 0.172Hz frequency index: 23

magnitude /(10^-5 m^2):						phase /degrees:					
43	67	106	64	100	88	0	68	104	-118	99	136
67	111	175	108	165	152	-68	0	34	176	31	63
106	175	281	167	260	245	-104	-34	0	141	-4	30
64	108	167	114	165	138	118	-176	-141	0	-144	-118
100	165	260	165	259	218	-99	-31	4	144	0	32
88	152	245	138	218	270	-136	-63	-30	118	-32	0

Figure 5.54 Elmer, 2332 13.7.92 - cross-spectral matrices for the most energetic frequency bins from D6O4R2.C26

COHERENCE MATRICES FROM: D604R2.C26
COH_f(i,j)

frequency: 0.141Hz frequency index: 19

1.000	0.895	0.895	0.828	0.554	0.943
0.895	1.000	0.938	0.929	0.779	0.805
0.895	0.938	1.000	0.895	0.671	0.873
0.828	0.929	0.895	1.000	0.833	0.706
0.554	0.779	0.671	0.833	1.000	0.440
0.943	0.805	0.873	0.706	0.440	1.000

frequency: 0.148Hz frequency index: 20

1.000	0.939	0.952	0.887	0.650	0.909
0.939	1.000	0.977	0.914	0.823	0.876
0.952	0.977	1.000	0.874	0.735	0.933
0.887	0.914	0.874	1.000	0.814	0.744
0.650	0.823	0.735	0.814	1.000	0.587
0.909	0.876	0.933	0.744	0.587	1.000

frequency: 0.156Hz frequency index: 21

1.000	0.956	0.969	0.849	0.835	0.900
0.956	1.000	0.990	0.919	0.932	0.865
0.969	0.990	1.000	0.896	0.915	0.912
0.849	0.919	0.896	1.000	0.932	0.749
0.835	0.932	0.915	0.932	1.000	0.813
0.900	0.865	0.912	0.749	0.813	1.000

frequency: 0.164Hz frequency index: 22

1.000	0.955	0.961	0.886	0.910	0.860
0.955	1.000	0.982	0.946	0.979	0.850
0.961	0.982	1.000	0.899	0.961	0.906
0.886	0.946	0.899	1.000	0.943	0.715
0.910	0.979	0.961	0.943	1.000	0.824
0.860	0.850	0.906	0.715	0.824	1.000

frequency: 0.172Hz frequency index: 23

1.000	0.936	0.931	0.853	0.904	0.678
0.936	1.000	0.981	0.912	0.943	0.771
0.931	0.981	1.000	0.867	0.929	0.790
0.853	0.912	0.867	1.000	0.922	0.622
0.904	0.943	0.929	0.922	1.000	0.681
0.678	0.771	0.790	0.622	0.681	1.000

Figure 5.55 Elmer, 2332 13.7.92 - coherence matrices for the most energetic frequency bins from D6O4R2.C26

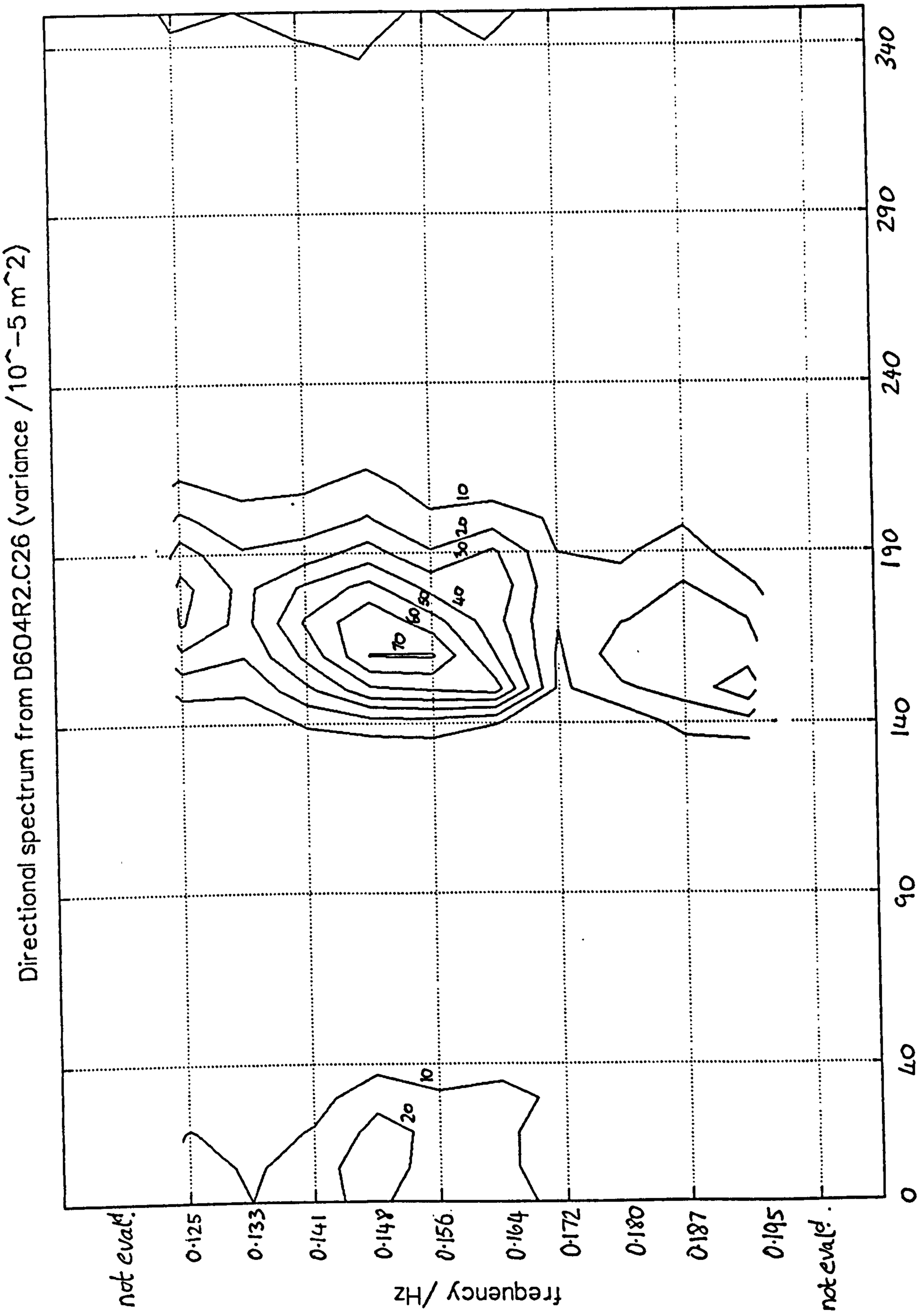

Figure 5.56 Elmer, 2332 13.7.92 - directional wave spectrum from D6O4R2.C26 as a contour plot

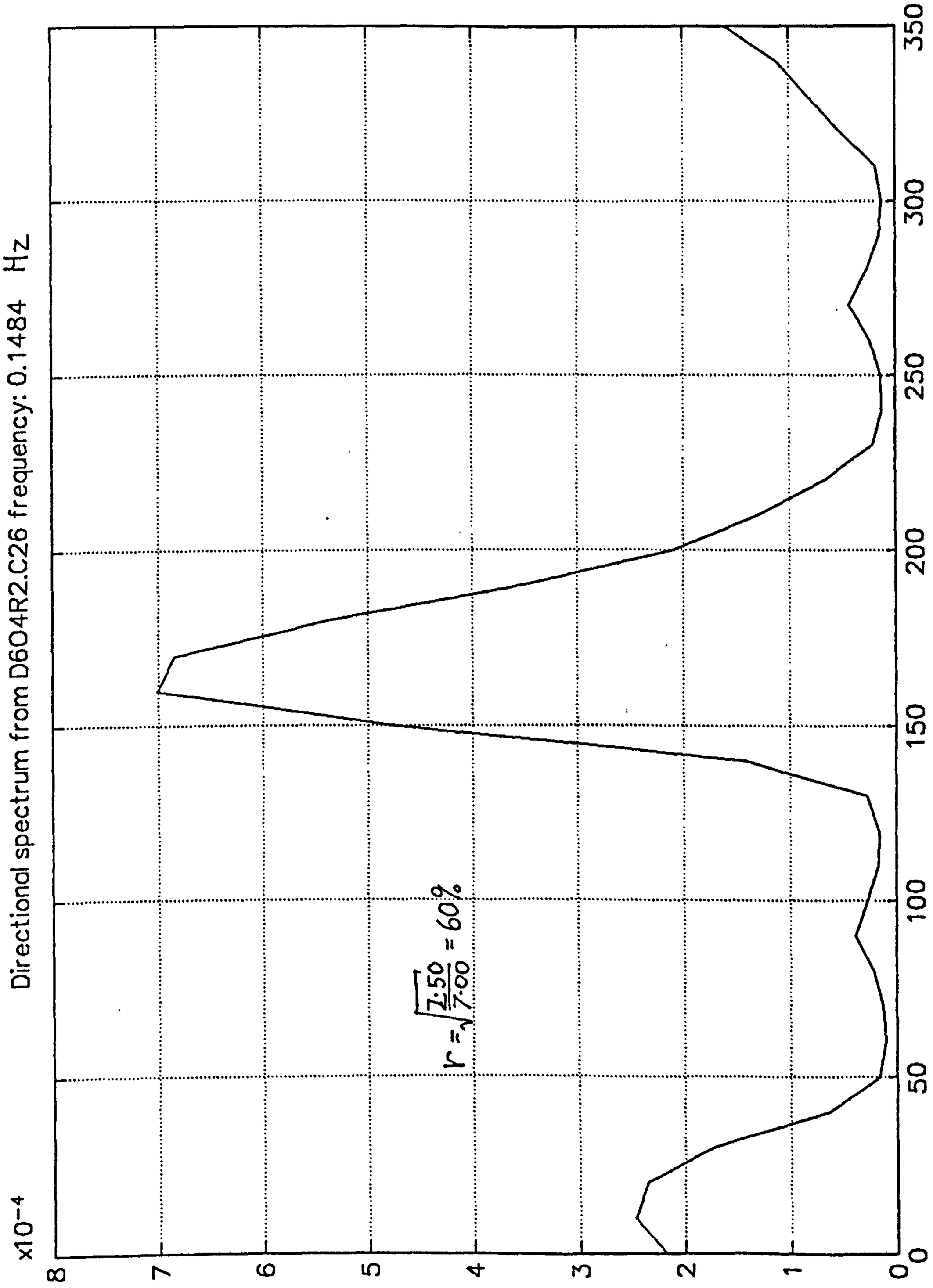

Figure 5.57 Elmer, 2332 13.7.92 - directional distribution .. from D6O4R2.C26 : 0·148Hz

a) INCIDENT & REFLECTED WAVE SPECTRA COMPUTED FROM 3 SENSOR PAIRS.

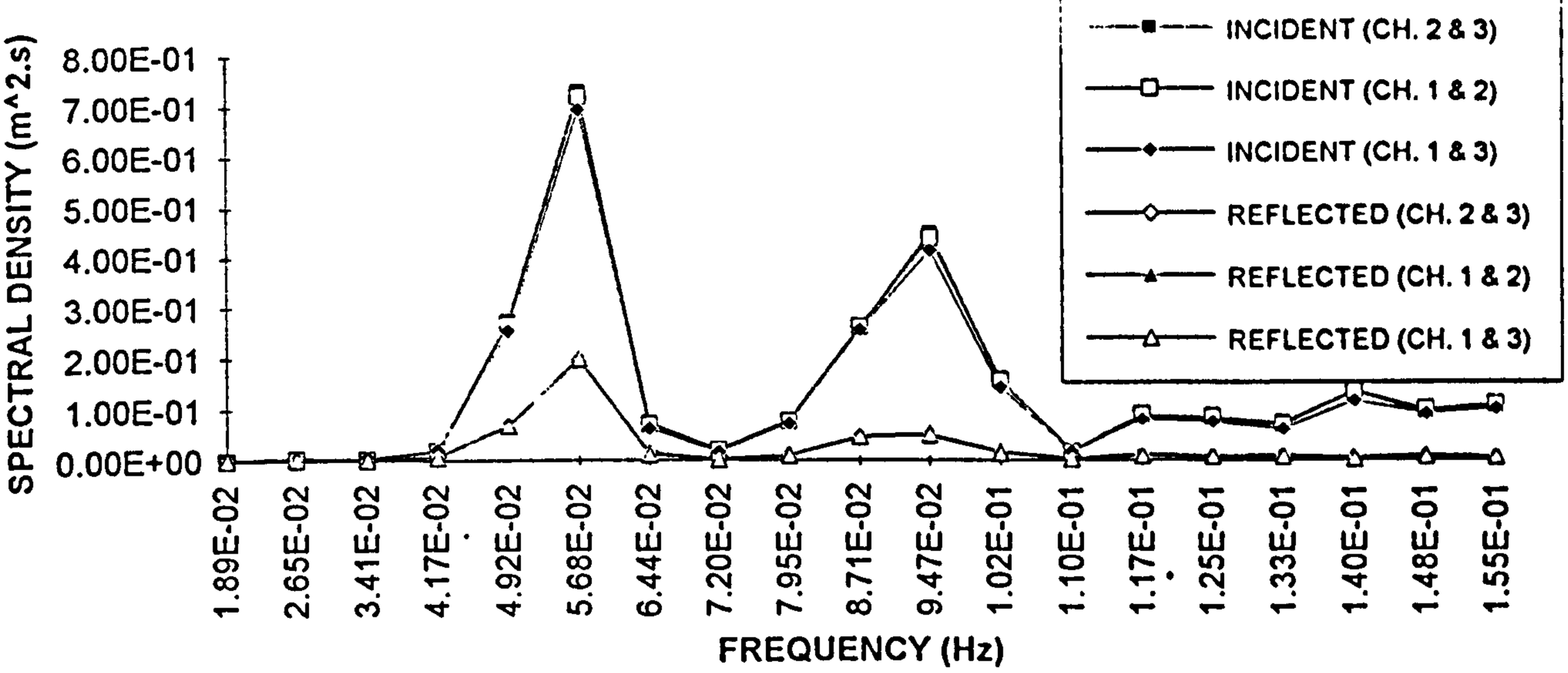

b) REFLECTION COEFFICIENT DERIVED FROM 3 SENSOR PAIRS.

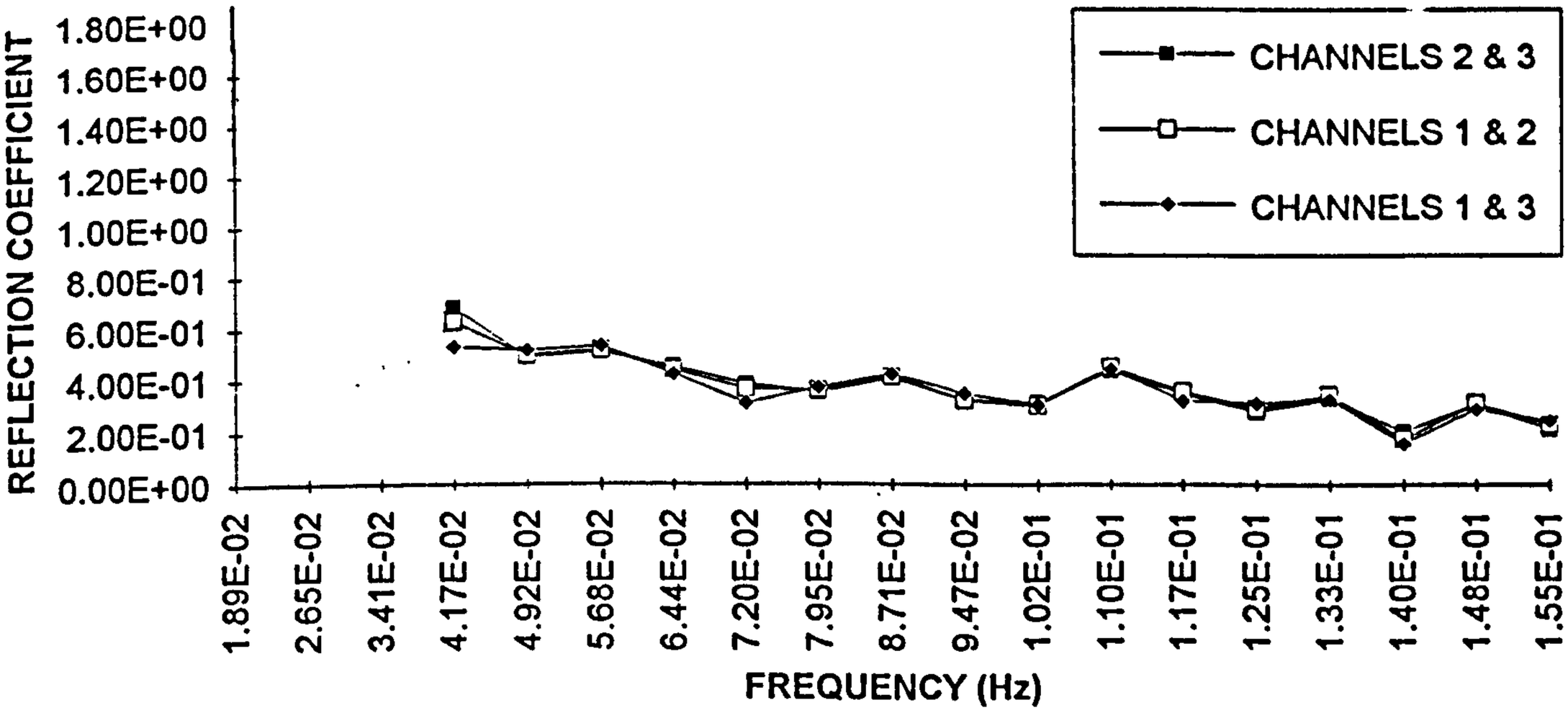

Figure 5.58 Plymouth, 1200 12.2.89 a) Decomposition of incident and reflected wave spectra b) Frequency dependent reflection coefficient (erratic coefficients at frequencies of weak signal are not plotted). (From Davidson, 1992).

a)

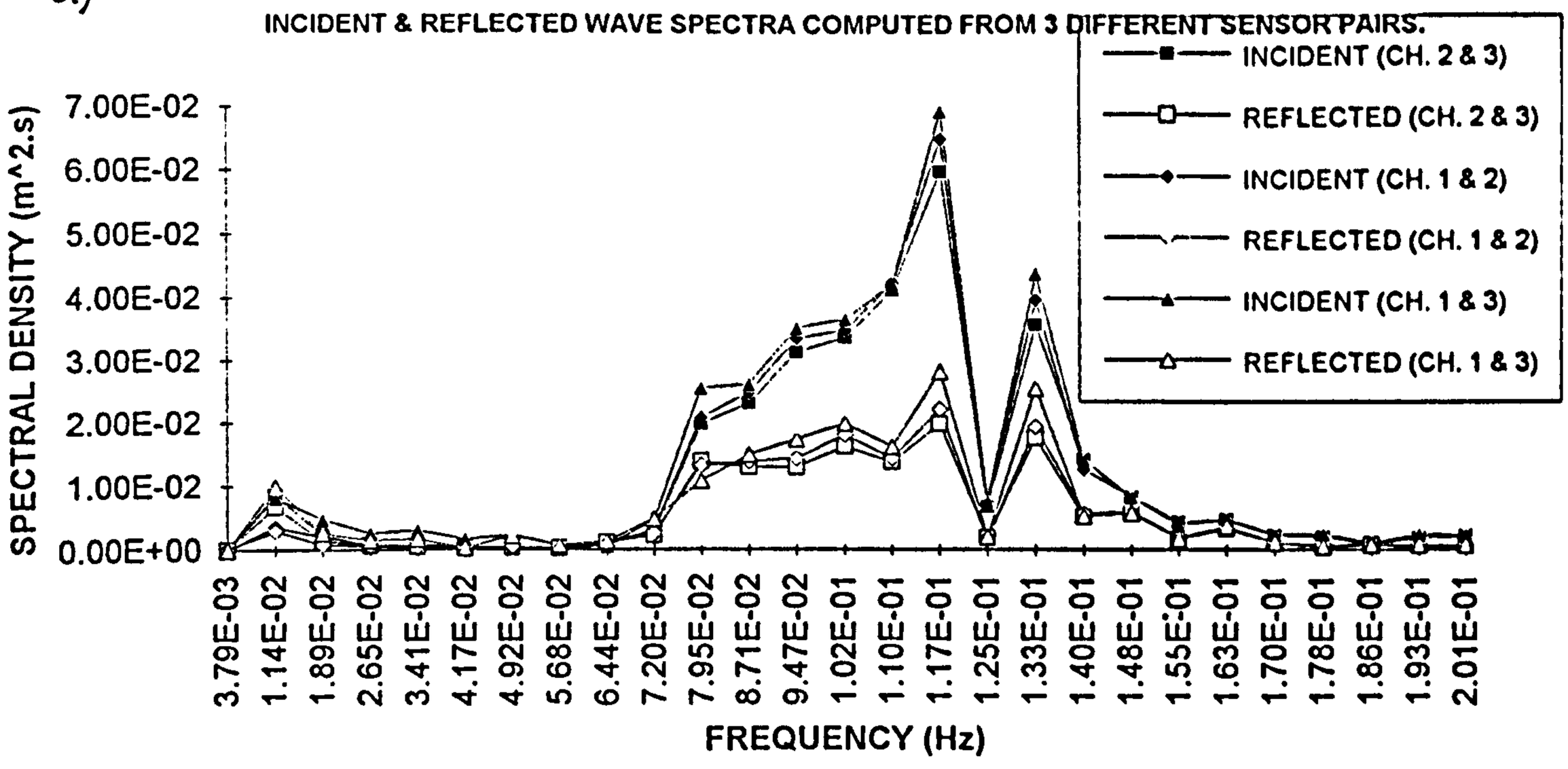

b)

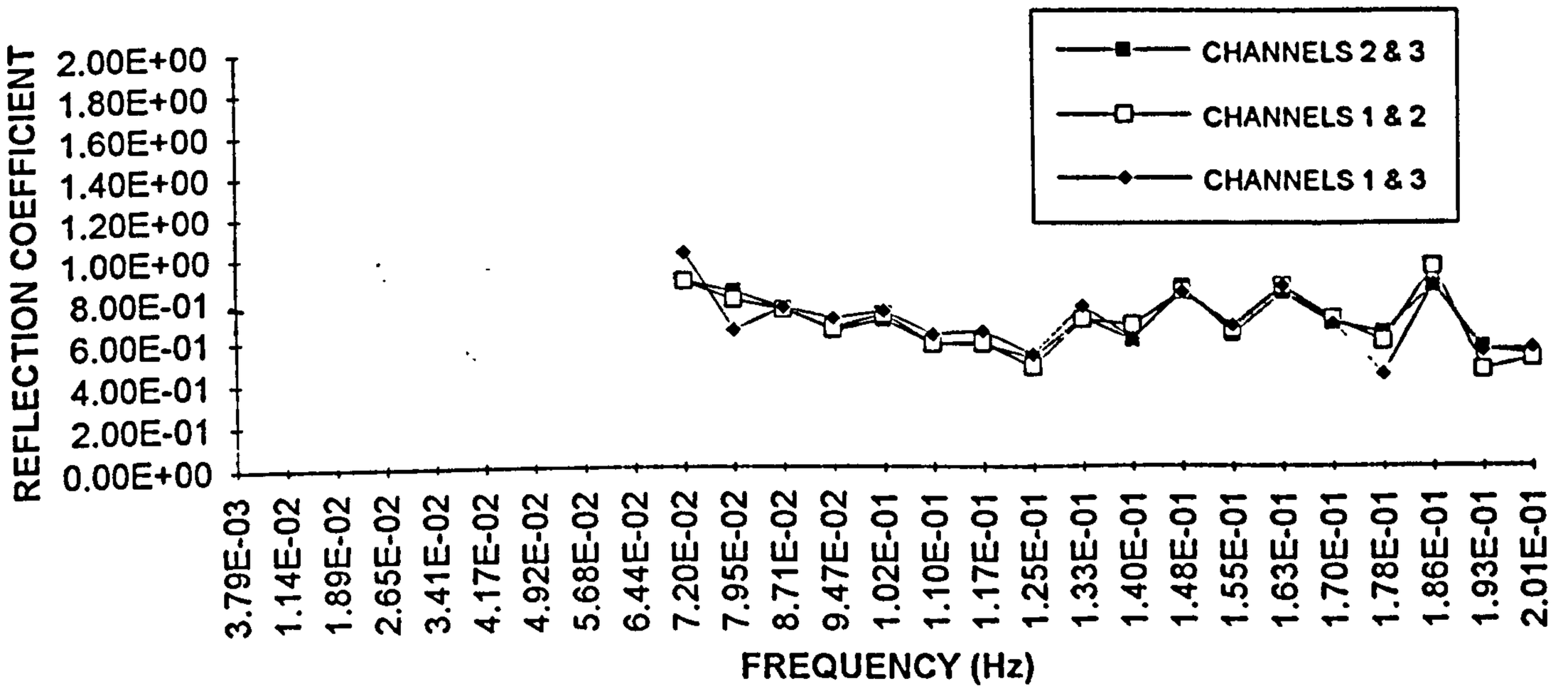

Figure 5.59 a) Elmer, 0233 5.7.92 Decomposition of incident and reflected wave spectra b) Frequency dependent reflection coefficient (erratic coefficients at frequencies of weak signal are not plotted). (From Davidson, 1992).

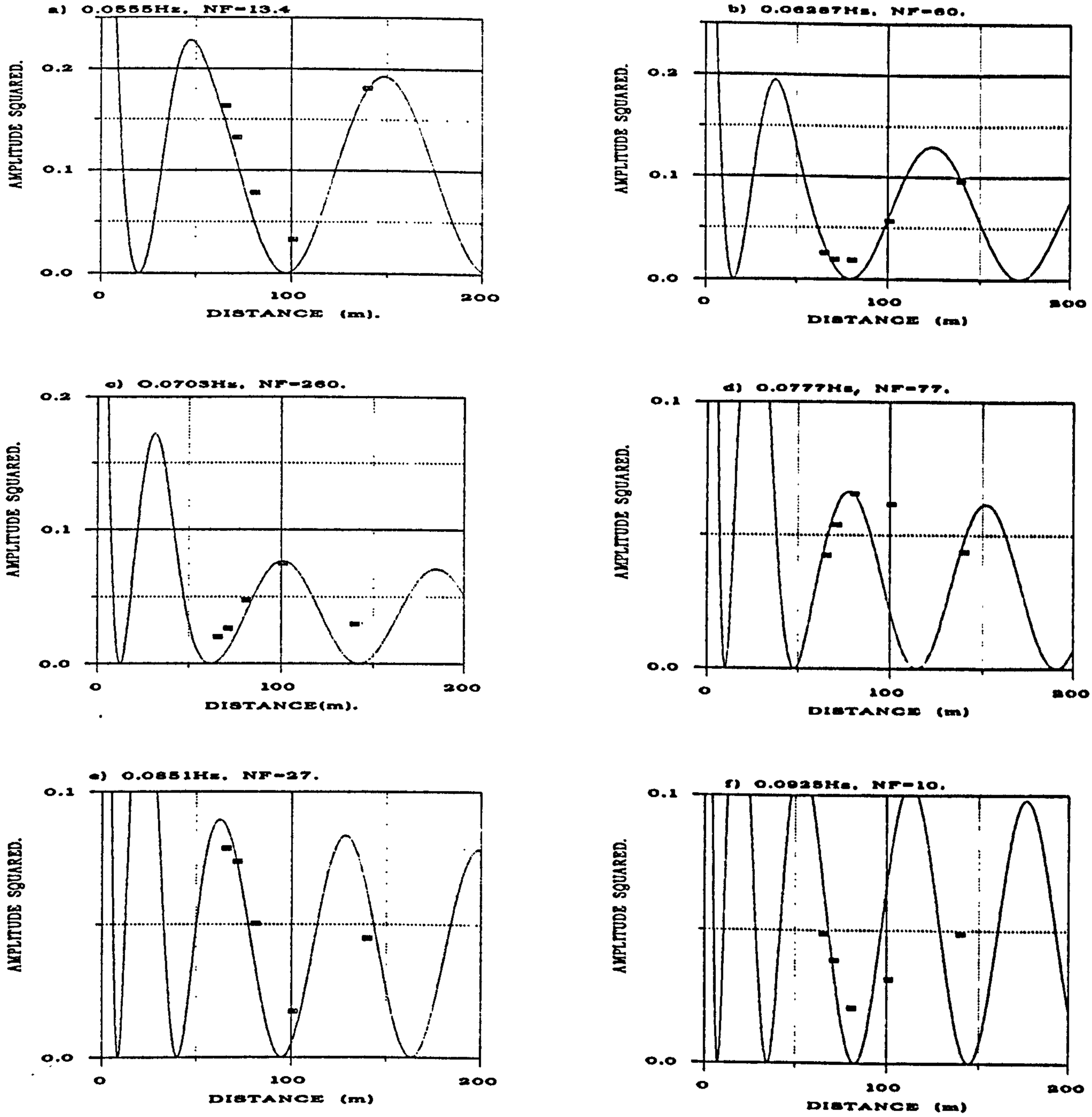

Figure 5.60 Plymouth, 1200 12.2.89 - Comparison between measured data and theory for different freqency bands. NF is the normalisation factor

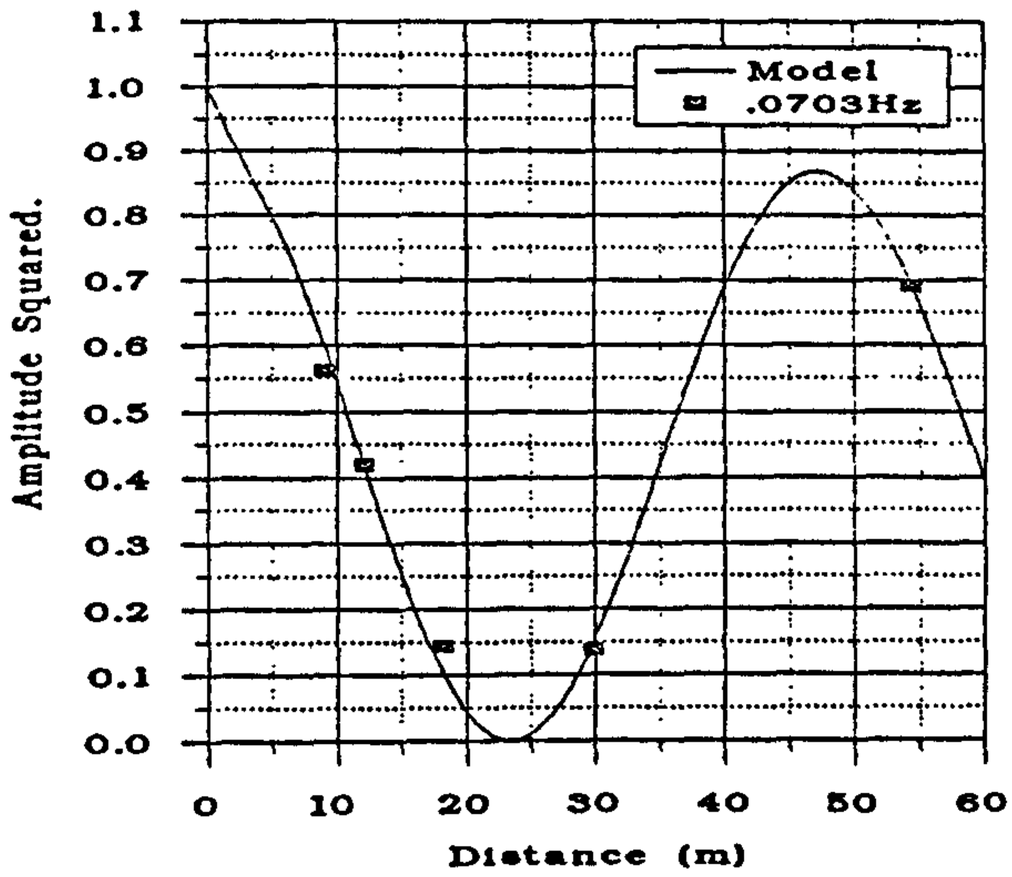

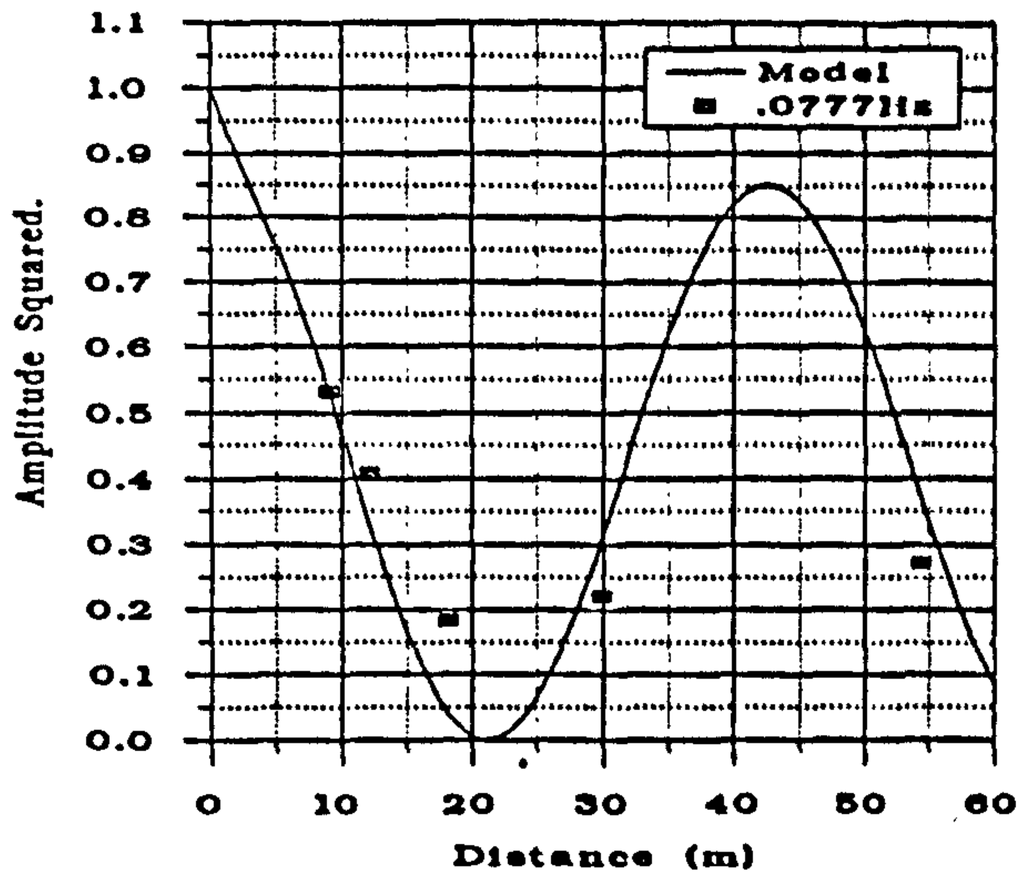

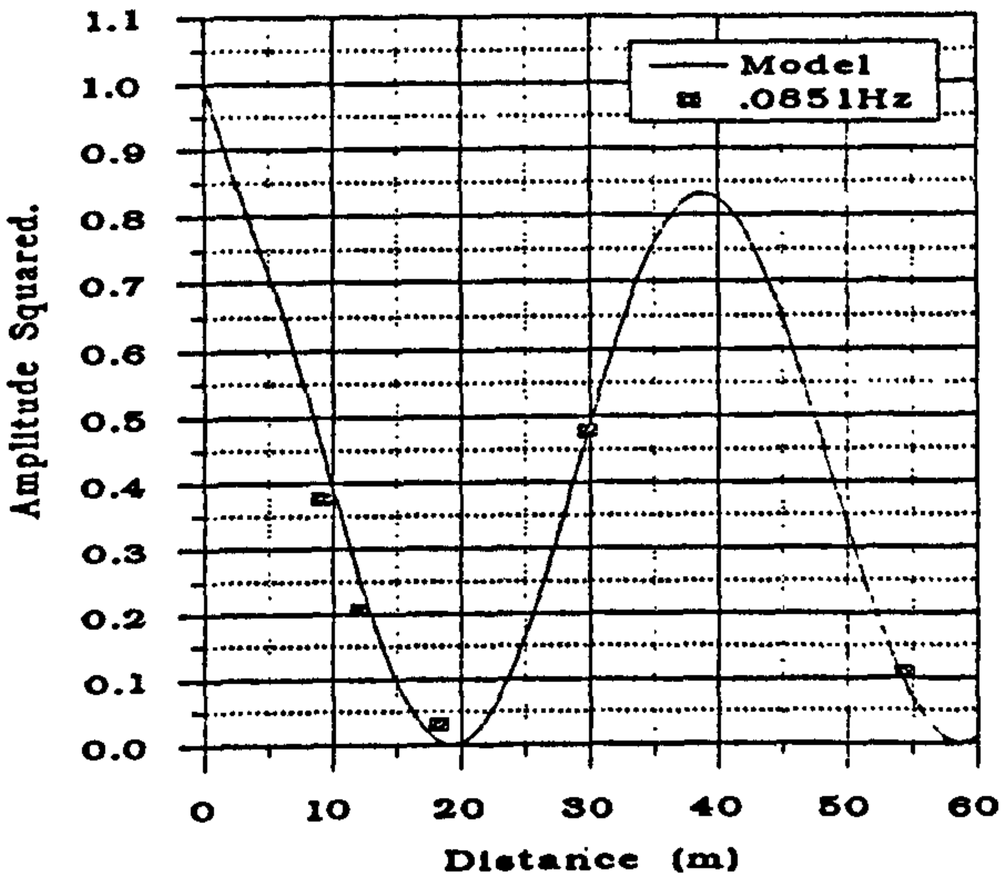

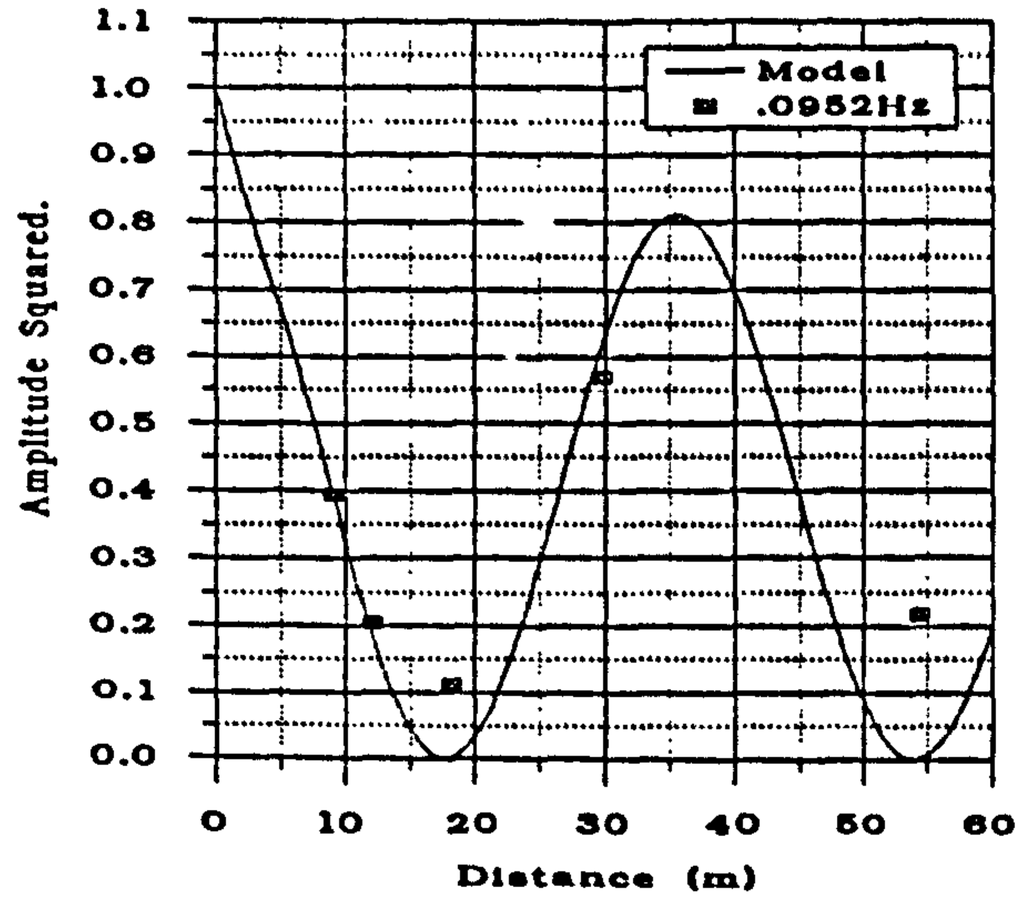

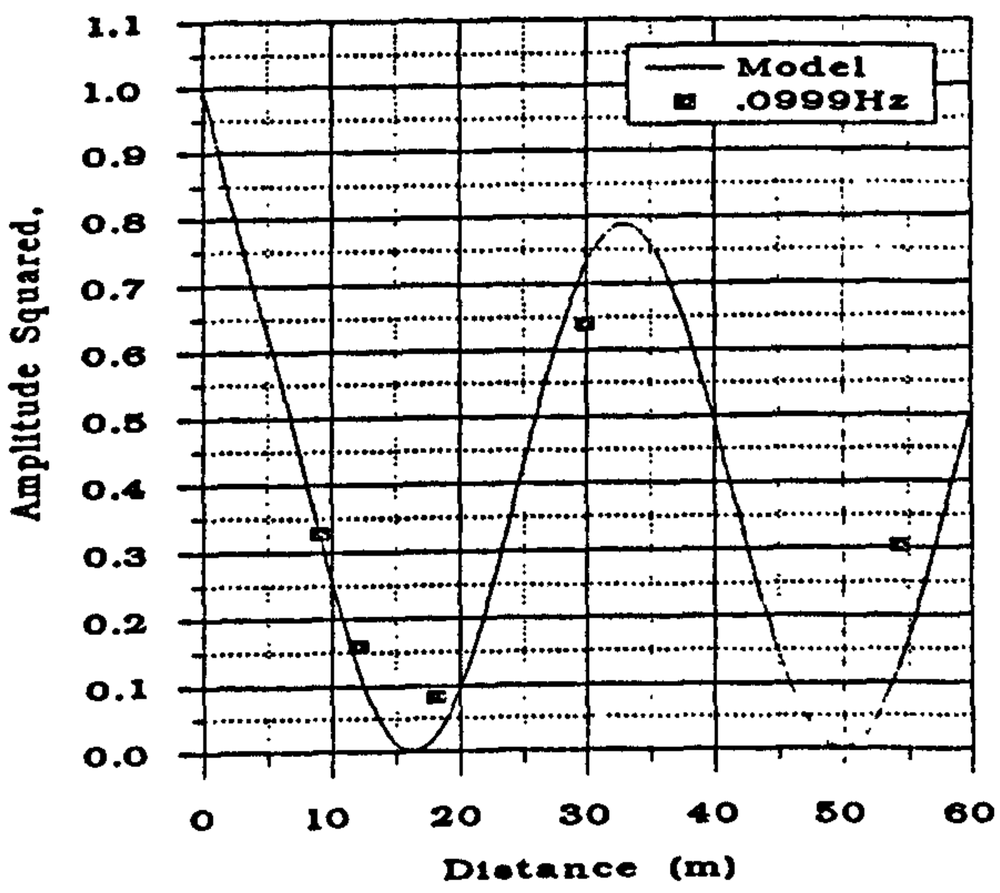

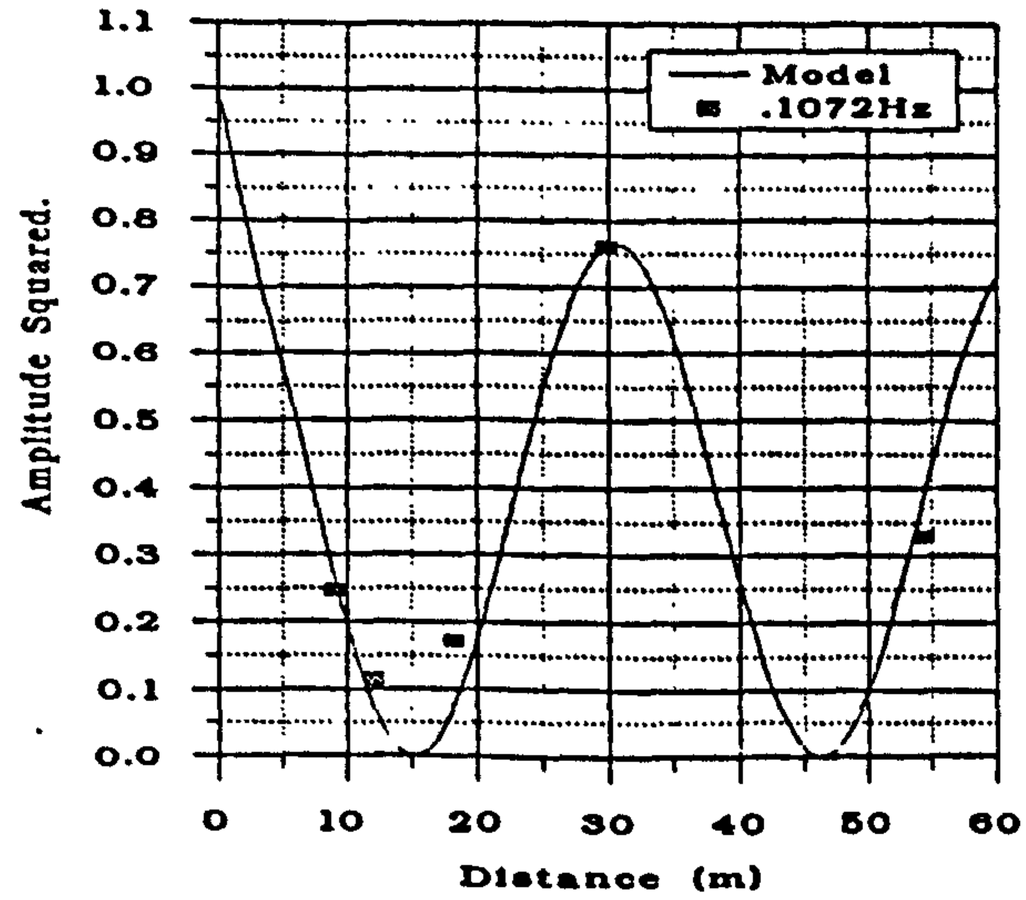

Figure 5.61 Elmer, 0233 5.7.92 - Comparison between measured data and theory for different freqency bands (from Davidson *et al* 1993)

/cont...

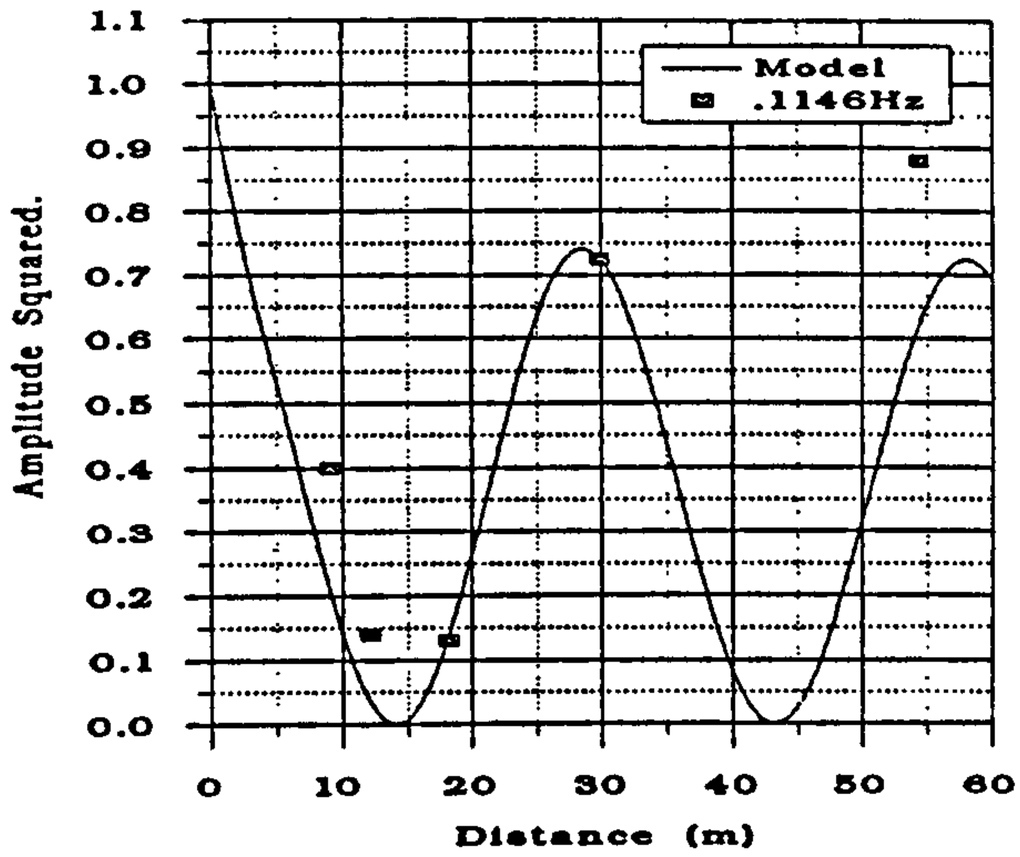

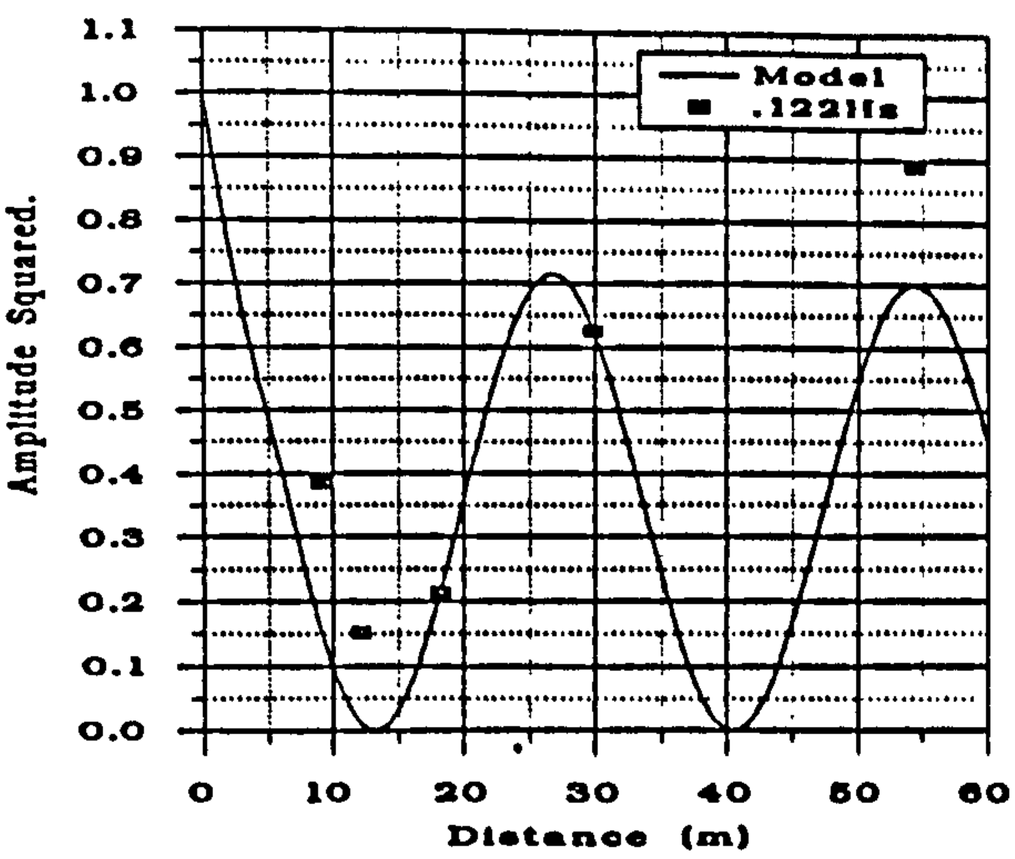

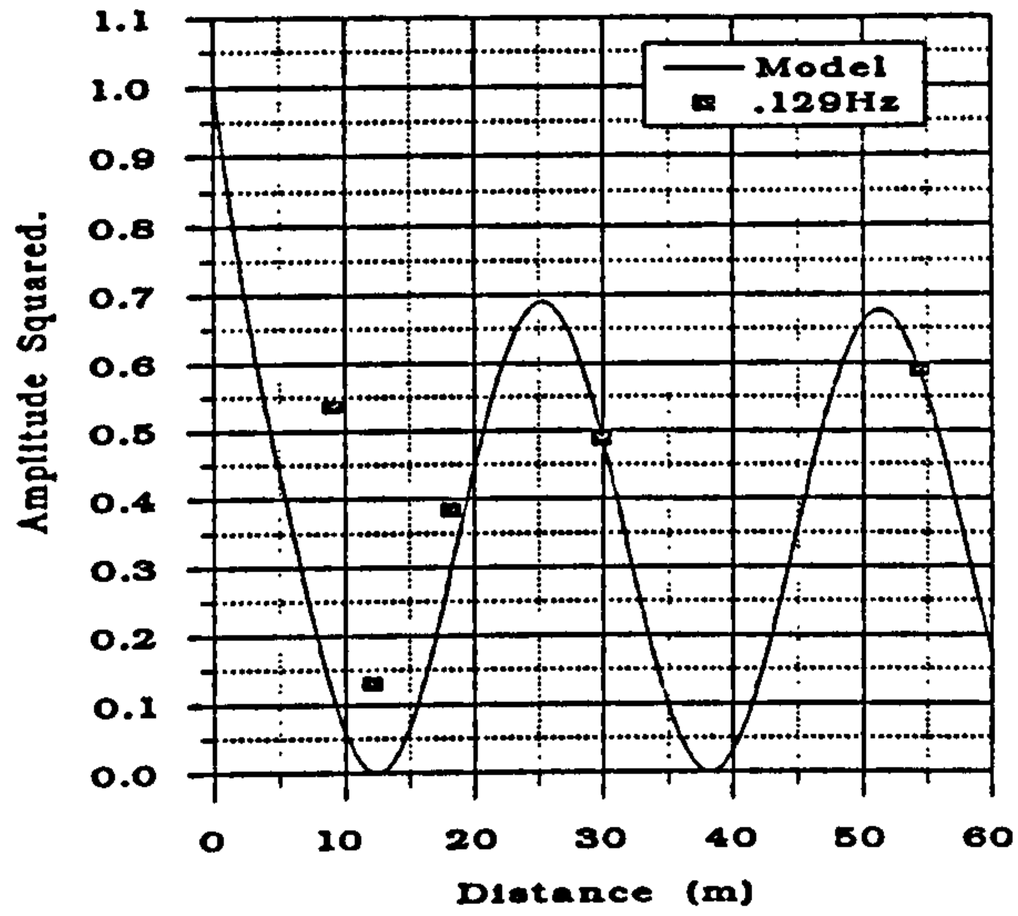

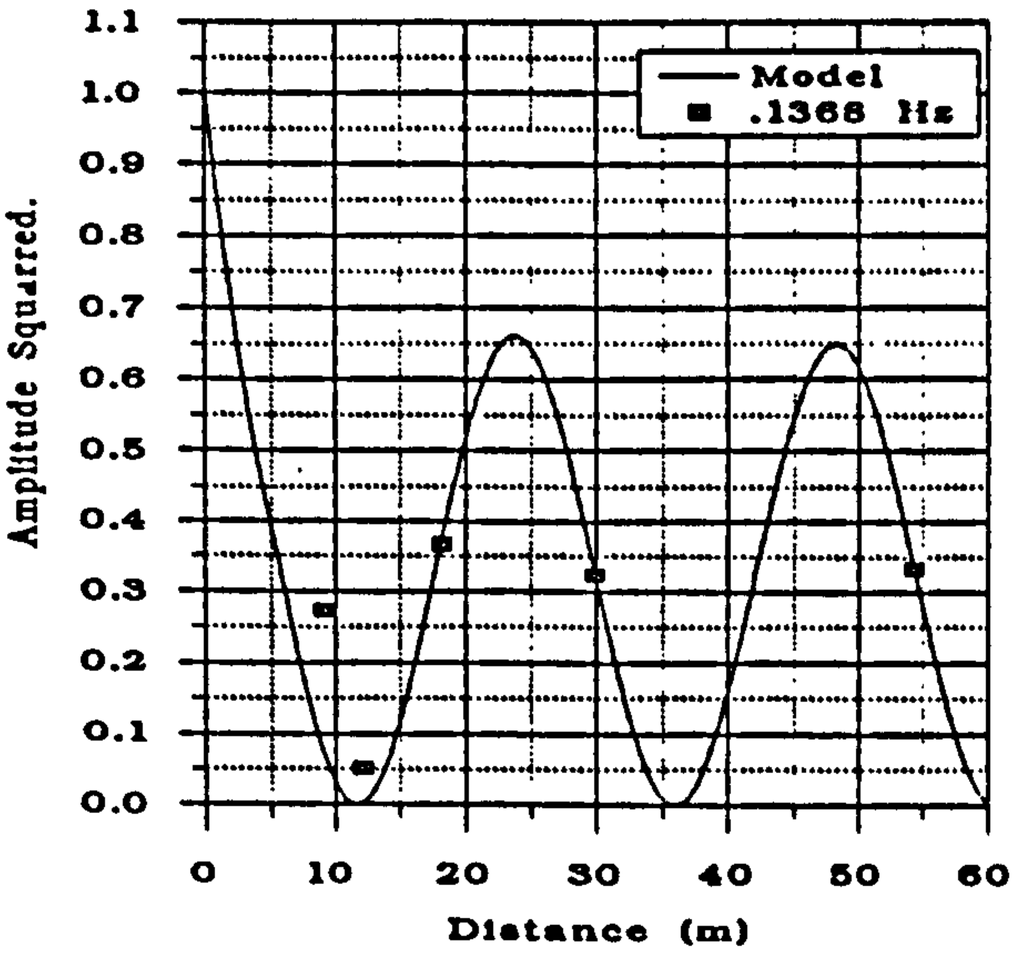

Figure 5.61 (cont)

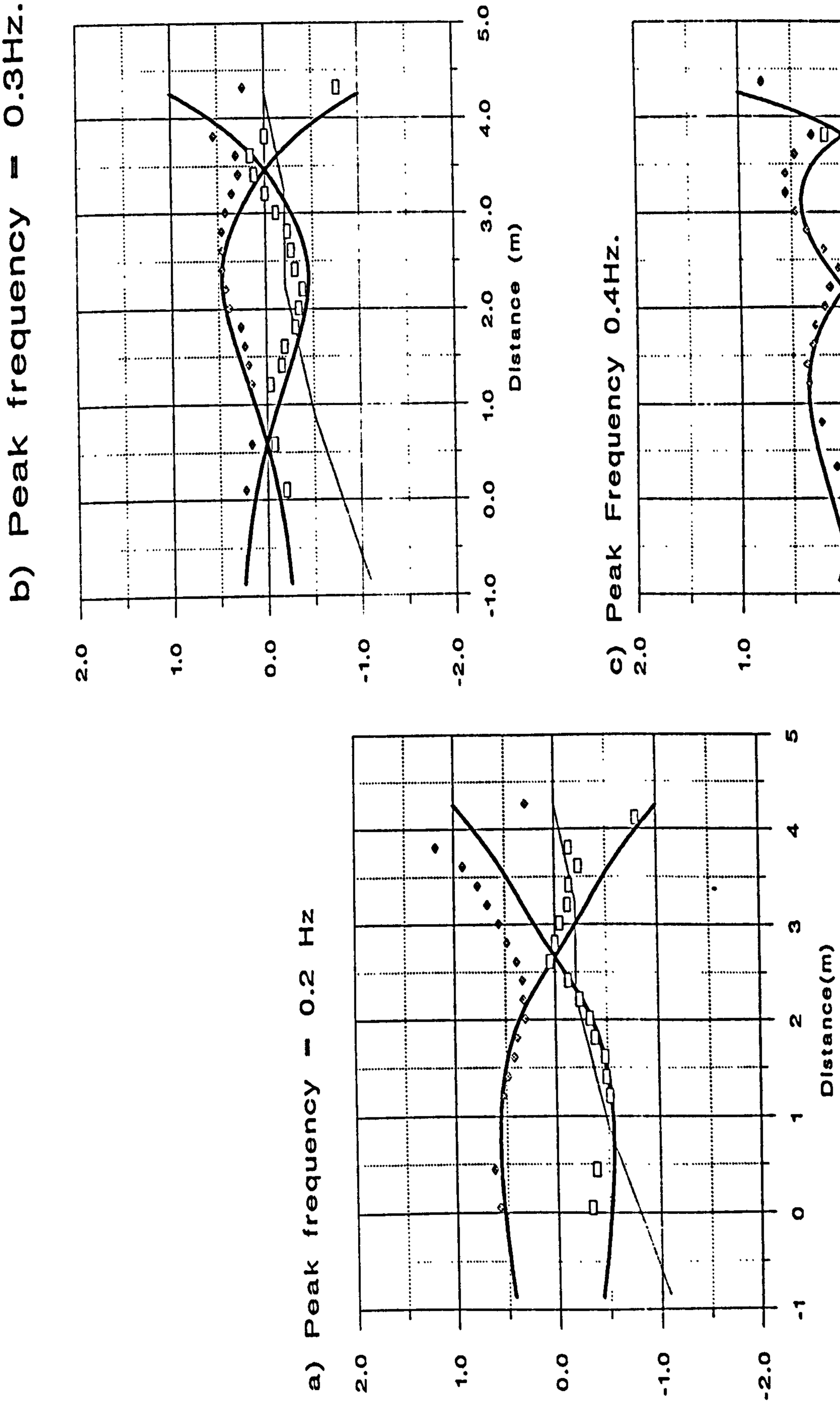

Figure 5.62 Comparisons between Plymouth Breakwater model data and theoretical curves for different frequency monochromatic waves (from Davidson *et al* 1993)

CHAPTER 6
CONCLUSIONS

CHAPTER 6
CONCLUSIONS

6.1 GENERAL

The wave recording system is a fairly complex instrument comprising about 2000 bought-in components mainly assembled at the University, and defined by approximately 100 drawings backed up by a part numbering and engineering change control system. Some of the lessons learnt during development and operation, and its performance, are discussed in this chapter.

The results and validation described in Chapter 5 indicate that the wave recorder has fulfilled the objective of measuring sea waves near a reflective structure. It has provided data from a number of sites, and is currently underpinning a number of research projects (eg SERC 1991 and 1992) and playing an important part in others (eg PCFC 1992). The first of these includes the deployment of the wave recorder at sites in addition to the original one at Plymouth Breakwater with the objective of learning more about their wave reflection characteristics, and of the reflection process in general.

That work is an extension to, but falls outside, the scope of this project. However it can be seen from the initial examination of results contained in the last chapter that for no wave breaking, reflection coefficients are slightly greater at low frequencies, and increase also with steeper gradients in accordance with expectations. For large waves, reflection coefficients are low as most of the energy is dissipated in breaking. It is for those conditions, in which theoretical models are less well developed, and laboratory models suffer more from scale effects, that the system will be of most value in investigating structural performance.

In the other two current projects the wave recorder establishes the input conditions for measurements of structural loadings and performance. These

include wave impact pressures, the effectiveness of a breakwater in preventing the transmission of waves, and the degree of scour of bed material. The essential feature is the ability to determine incident wave energy from the mixture of incident and reflected, for that is the true 'input'. A single point measurement fails to distinguish between the two, and (as Figures 5.58 and 5.59 show) produces a value anywhere from the difference to the sum of the two constituents, depending on location within the nodal structure, which is itself a function of frequency. Field measurements in the past heve relied on such measurements, or on the deduction of input conditions at the shoreline from offshore measurement, or on hindcasting from weather records. However since the purpose of field work in coastal engineering is to explore effects outside the range of current theories (or to validate or extend theoretical knowledge) then it would seem desirable to acquire input conditions directly.

A second advantage of measuring close to the shore comes from the extra detail obtainable: wave crests may be followed in across the array and related to individual impact events, whereas predictions and hindcasts yield only statistical summaries of the wave conditions.

6.2 SEA BED FIXINGS AND DEPLOYMENT PROCEDURE

The sea bed fixing arrangements have proved satisfactory at both Plymouth (13m below chart dataum) and Elmer (in the surf zone), given that extra protective steelwork was provided for the latter site.

At Plymouth the system was in place (though not, unfortunately recording) during a particularly violent storm that washed two of the 100 tonne and many smaller armouring blocks right over the breakwater, and caused millions of pounds worth of damage to the city. On recovery the system was found to be substantially intact, although one cable had been damaged.

The deployment and recovery procedures were effective but proved to be major operations that had to be spread over several days' work. It is hoped to reduce this to a one day exercise by redesigning the mounting blocks and platforms, and employing new equipment such as through-water diver communications, two-way radio for surface communications, and a Global Positioning System (GPS) receiver.

6.3 MECHANICAL DESIGN

Experience has shown that, despite good intentions, handling conditions are likely to be rough for heavy equipment deployed by boat in difficult conditions. The anodised aluminium pressure housing performed well against abrasion, but its resistance to impacts was less satisfactory due to the softness of the aluminium. Once the protective coating had been damaged corrosion rates were high. The housing for the second system was re-designed in polyacetal (eg delrin), with silicon bronze fastenings. So far that has shown excellent resistance to corrosion and fouling, while retaining dimensional stability.

Stainless steel performed badly underwater, and the transducer housings were redesigned to replace the central plate in that material (on which sealing depended) with, again, polyacetal. There have been no sealing failures in any of the units to date.

Silt can accumulate in the depression above the neoprene diaphragm. This is not thought to cause appreciable error as it remains in suspension while the unit is immersed. Also the transducer is very 'stiff', deforming little with a change in pressure. Tucker (1992) reports good performance from similarly arranged pressure transducers under tens of centimetres of sand.

6.4 ELECTRONICS DESIGN

Components and techniques in electronic engineering have advanced at a rapid pace. At the time the design was started (1987) the key devices were all either fairly new or just introduced. Inevitably, by the time of writing even better products have become available. The same performance could now be achieved at less cost and in a smaller space, although the cost of the complete system is dominated by the mechanical components, wet-mateable connectors and cable.

Performance has met expectations. Figures 5.41 and 5.61 indicated that the instrument successfully handled wave components down to 0.3×10^{-3} m^2, or approximately 17mm, in height even though within a 14mWG standing signal and having passed through all the data analysis procedures. Inspection of the 'cal voltages' columns in the Decode reports (Figure 3.8) shows that the major parts of the analog sections held their calibration well, with no adjustments, over a period of years.

It was mentioned in Chapter 2 that the anti-aliasing decimation filter had not been implemented. Protection against aliasing was therefore only provided above 20Hz, by the analog filters, leaving a gap between 1 and 20 Hz. However inspection of the records consistently showed an absence of energy anywhere near the Nyquist ferquency of 1Hz or above, and it seems unlikely (given the dependence of pressure attenuation on frequency) that any aliasing was occuring.

The data compression scheme was simple. In view of the volume of research that has taken place recently in this field it is likely that a more advanced scheme could be selected and implemented to maximise the effectiveness of the data store.

6.5 DATA ANALYSIS

Futher research will undoubtedly increase the information that can be extracted from the data. Provided the data is archived in its original state it remains possible to try out new procedures. The main areas for further work are the conversion from sub-surface pressure to surface elevation, and the directional analysis. A comparative test is at the time of writing underway to establish the corresondence between the elevation predicted by the wave recorder and that measured directly by a wave staff.

As stated in Section 4.5 the location of the effective reflection line is an input to the Modified Maximum Likelihood Method (MMLM) of directional analysis that is not yet fully resolved. This is receiving further attention.

The data set length, for the results presented here, was fixed at about 12 minutes, and that is now considered to be rather short. A useful improvement in the statistical reliability of the spectral coefficients would be given by a length of , say, 17 minutes. The trade-offs are data storage capacity, battery life and reduced stationarity of the records on rising and falling tides. As mentioned in Chapter 4 the reliability of these coefficients is critical for the good behaviour of the directional analysis. Work is also proceeding on identifying the optimum window function for sea wave data.

The wave simulation programs written so far have been relatively simple, designed for fault-finding rather than true validation, and it is proposed to extend them to gain more experience with directional analysis techniques.

6.6 FUTURE ENHANCEMENTS

Data storage technology has, as expected, advanced quickly, and a quadrupling of the capacity to 16MB would be achievable if desired. Two developments currently underway at the University of Plymouth, however,

will remove this parameter as a limitation (PCFC, 1992). These are firstly a radio buoy to allow communication with the recorder from a distance of up to 10km, and secondly a satellite link between Plymouth and the shore station at the remote site.

The limiting factor for deployment period would then be battery capacity, and this could be multiplied several times by using lithium cells with relatively minor modifications to the regulators and control circuits.

REFERENCES

SERC (1991)
'Wave reflection characteristics of coastal structures'
P.A.D. Bird, G.N. Bullock, P.J.Hewson, D.A. Huntley

SERC (1992)
'Role of offshore breakwaters in coastal defence'
G.N. Bullock, P.A.D. Bird, D.A.Huntley

PCFC (1992)
'Coastal Engineering'
G.N. Bullock, P.A.D. Bird, P.J. Hewson

Tucker M.J. (1992)
Waves in ocean engineering
Ellis Horwood, p62.

APPENDICES

APPENDIX A:

LIST OF MANUFACTURERS OF OCEANOGRAPHIC MEASURING EQUIPMENT (1987)

Anderaa Instruments (agent: WS Ocean Systems)	Bergen	Norway
Ameeco (Hydrospace)	Andover	UK
B&P Instrumentation	Hull	UK
BAJ Ltd	Weston-S-Mare	UK
Benthos Inc	North Falmouth, MA	USA
Burmarc Ltd	Liphook	UK
NBA Controls Ltd	Farnborough	UK
Niel Brown Inst. Systems Inc	Cataumet, MA	USA
Chelsea Environmental Instruments	Colchester	UK
Kahl Scentific Instr Corp	El Cajon, CA	USA
Klein Associates Inc	Salem, NH	USA
Liebnitz-Lann Ltd	Nairn	UK
Magnevox Systems	Slough	UK
Marine Electronics Ltd	Guernsey	UK
Marintech NW Ltd	Manchester	UK
Metocean Data	Nova Scotia	Canada
MIROS Ltd	Colnbrook	UK
Navitronic A.S.	Aarhus	Denmark
Nekton Systems	Swindon	UK
Nereides	Paris	France

Oceano Instruments (UK) Ltd	Edinburgh	UK
Paroscientific Inc	Redmond, WA	USA
Qubit Ltd	Aldershot	UK
Sea Data Corp (agent: Burmarc Ltd)	Newton, MA	USA
Seastar Instruments	Sidney, BC	Canada
Seatronics Ltd	Alton	UK
Sipro A.S.	Sandefjord	Norway
Slingsby Engineering Ltd	Kirkbymoorside	UK
Sonardyne Ltd	Fleet	UK
Suber	Brest	France
Tower Computer Systems	Newmarket	UK
Valeport Marine Scientific Ltd	Dartmouth	UK
WS Ocean Systems	Haslemere	UK
Waverley Electronics	Weymouth	UK

MARINE AND SITE DATA RECORDER

The Marine and Site Data Recorder is a high capacity, intelligent measuring instrument for use in remote and hostile environments. It was originally developed at University of Plymouth to measure waves near breakwaters and sea walls.

Features:

- self contained
- rugged
- high data storage capacity
- high-precision
- automatic self calibration
- flexible operation
- PC interface

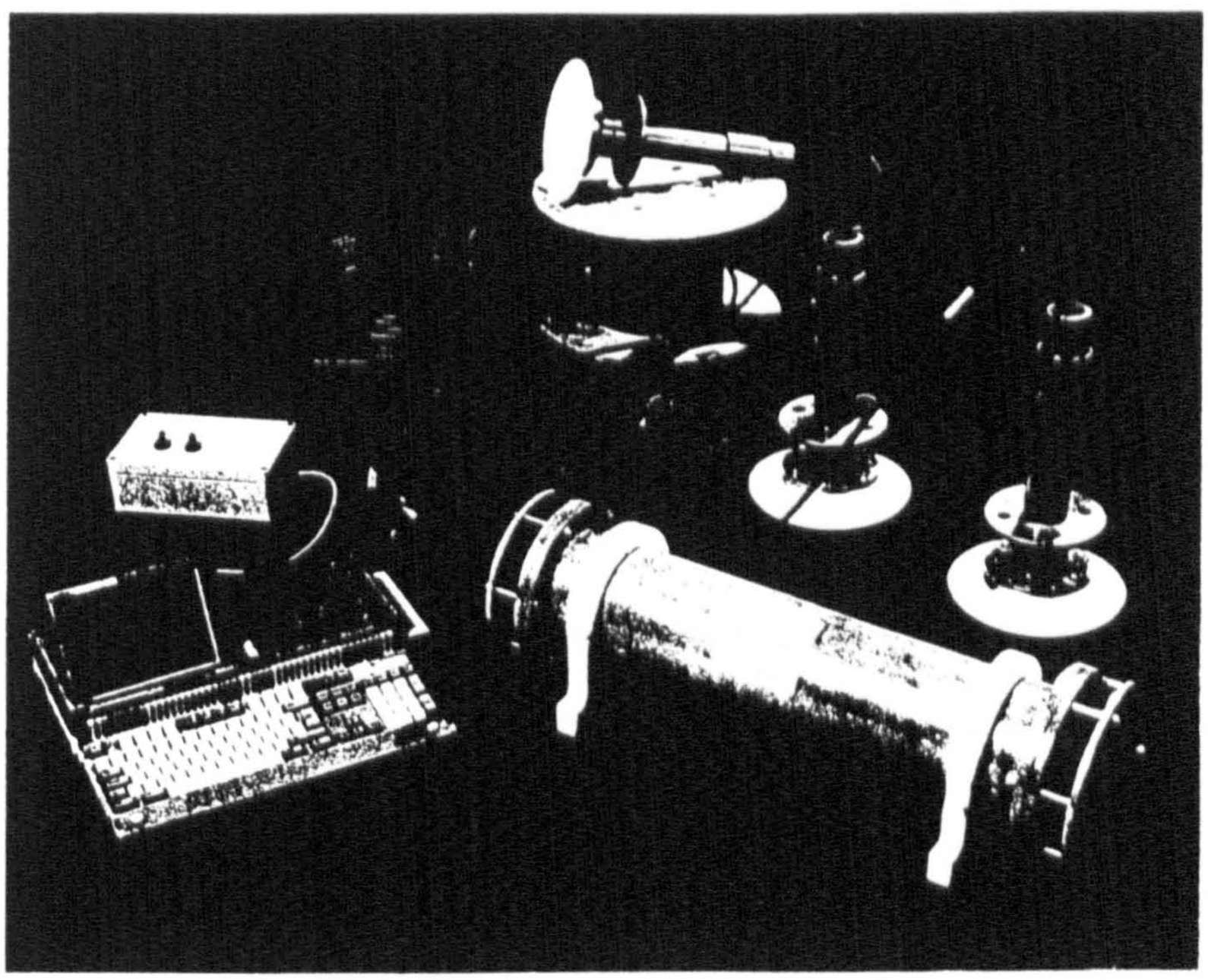

The Marine and Site Data Recorder
with three sub-sea pressure transducers

Description

The signal processing, semiconductor data storage, battery pack and microprocessor control sections are all housed in a sealed pressure casing. Sensors and transducers, and the personal computer link, are connected by wet-mateable connectors. The instrument and transducers may be deployed to measure over a long period before recovery is necessary to change the batteries. At any time a PC may be connected via the interface box and cable shown in the photograph to change measurement parameters or to download measured data.

For further details please contact:

Paul A. D. Bird School of Civil and Structural Engineering,
University of Plymouth, Palace Court, Palace Street, Plymouth PL1 2DE Tel: (0752) 233664

Specification

Some of the performance figures depend on the precise application. For example since external transducers may be powered by the internal batteries of the recorder, battery life will depend on those, as well as on measuring intervals which are under the control of the user. Generally applicable information is given below, together with, in brackets, figures for the Marine and Site Recorder as used to measure sea waves with six pressure transducers.

Input channels	(6 no., 0 - 5 volt analog) (input impedance 47 kilohm) Over voltage protection on each channel.
Signal processing	Anti-alias filter on each channel. Track-and-hold for simultaneous readings of all channels. Amplifiers have 4 gain settings and 4 offset settings, selectable automatically or manually to ensure full use of ADC resolution. On automatic - settings chosen as function of input signal excursions.
Accuracy	Dependent on gain and offset setting. Accuracy of individual circuits is better than 0.1% Automatic self-calibration using internal voltage references.
A to D Converter	12 bit resolution (1 part in 4096). 100 microsecond conversion time.
Data Storage	
Capacity	4 megabytes
Organisation	Subject to software version installed. Typically:- 1) an area for instrument parameters such as memory remaining and battery condition, and 2) measurement data records, date and time stamped. First and last readings at 2 bytes per reading, the rest compressed to 1 byte per reading, giving a capacity of about 4 million readings.
PC link	Serial 9600 baud with 30m cable, 19200 with shorter cable. RTS/CTS handshaking. All lines opto-coupled for electrical isolation.
Power Supply	Main battery pack: primary, alkaline-manganese. (Including six pressure transducers, and measuring for 17 minutes every 3 hours, battery life is 4 months). Measuring intervals may be pre-set, or automatic governed by comparison of input signal activity with a threshold.
Mechanical	Double O-ring sealed pressure housing in corrosion resistant materials.
Dimensions	875 mm long, 150 mm diameter (220 mm over flanges).
Weight	18.5 kg (in air) 3.3 kg (in water)

David Jackson

● Sea check: Bullock and Bird with seabed data recorder

Sensors shore up sea defences

METROLOGY

by JANE BIRD

DEVASTATION to coastal areas caused by breaches of sea walls, such as those which occurred in Wales recently, could be avoided with a new instrument that measures the power, direction and frequency of waves.

It uses six sensors spread across the sea-bed to detect fluctuations in water pressure – an accurate indicator of what happens at the surface.

The instrument should enable engineers to provide better defences against storm waves and the rising tide levels expected from the greenhouse effect.

Three years ago a team from the civil engineering department at Polytechnic South West in Plymouth, under Dr Geoff Bullock, searched the market for a machine to measure the strength and direction of waves close to sea walls. The behaviour of waves there is quite different from those out at sea because much of their energy is reflected back. The team was also looking for an instrument that was strong – in the recent gales, two 100-ton boulders were forced over the top of a Plymouth breakwater.

They could find nothing to meet all three criteria, but managed to get a £50,000 grant from the Science and Engineering Research Council to develop their own. The result is an instrument consisting of six pressure sensors placed just offshore in Plymouth where the water depth varies from 10 metres to 15 metres, depending on the tide. The sensors are encased in strong plastic and mounted on concrete blocks. As a wave passes over them, they measure the pressure fluctuation, from which the surface fluctuation can be accurately calculated.

The sensors are placed at distances from 60 metres to 160 metres from the breakwater and connected by cables sheathed in steel wire. They take their readings simultaneously to get a snapshot of the sea above and to work out the direction in which each wave is travelling.

Paul Bird, the instrument's designer, says: "The sensors allow us to unravel the approaching waves from the reflected ones. This means we can work out how much the sea wall reflects and learn how effectively it resists wave attack."

The pressure fluctuation readings are stored in a battery-powered data recorder on the sea-bed for six weeks at a time, and later retrieved by connecting this, through a cable, to a computer on board a boat.

Bird believes the instrument could be useful to coastal authorities and water companies for whom taking wave measurements has been very expensive.

"A follow-up we're developing will measure air in waves. Those that are highly aerated, such as the white horses seen on a windy day, are much less forceful than dark green sea which is so devoid of air as to be almost incompressible."

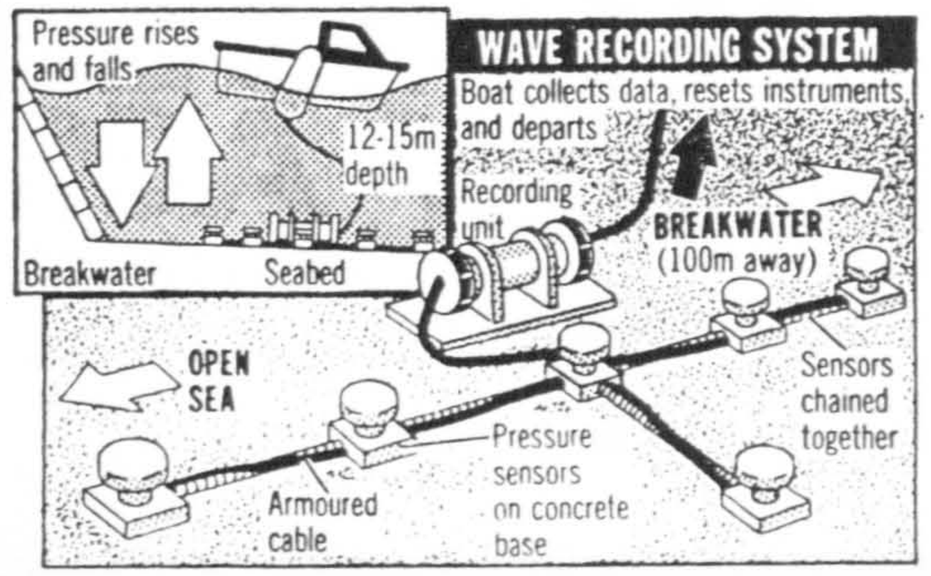

APPENDIX D

Druck

AMPLIFIED OUTPUT PRESSURE TRANSDUCERS

Types: PDCR 130/W & PDCR 135/W

Excellent linearity
±0.1% B.S.L. for all ranges

Aircraft compatible excitation:
10-32V d.c. or ± 15V d.c.

Amplified output
Up to 10V

Input/output isolation
PDCR 130/W series

Integral zero and span adjustments

Stainless steel wetted parts

Good thermal stability
± 1.5% total error band −20° to +80°C

This series of pressure transducers provide the user with a high level output signal for industrial, marine and aerospace applications, with all wetted parts manufactured from stainless steel.

Military grade electronic components are used to ensure maximum integrity, and the units are individually tested and compensated before despatch.

Zero and span potentiometers are provided in the rear of the transducer body and user access is via two sealed blanking plugs.

Linearizing and temperature compensation is provided within the instrument, and the rationalised outputs ensure interchangeability without system re-calibration.

During manufacture the transducers are set to customer requirements for any intermediate pressure range or pressure units specified.

Operating pressure range
350mbar, 700mbar, 1, 1.5, 2, 3.5, 5, 7, 10, 15, 20, 35, 60 and 70 bar gauge or absolute. 175mbar gauge only.
135, 200, 350, 500 and 700 bar sealed gauge or absolute.
Other pressure units can be specified, e.g. psi, kPa, etc.

Overpressure
The rated pressure can be exceeded by the following multiples causing negligible calibration change:-
10× for 175mbar range
6× for 350mbar range
4× for 700mbar to 15 bar ranges.
100 bar for 35 bar to 70 bar ranges
2× for 135 bar to 500 bar ranges.

Pressure media
Fluids compatible with 316 stainless steel.

Transduction principle
Integrated silicon strain gauge bridge.

Supply voltage. PDCR 135/W and PDCR 135/W/C
+15, 0, −15 Volts d.c.
+15 Volts (±0.5 Volts) 1mA nominal
−15 Volts (±0.5 Volts) 6mA nominal
These currents are quoted for zero output current.
+12, 0, −12 Volts d.c. available.

Supply sensitivity. 0.02% F.S.O./Volt

Supply voltage. PDCR 130/W and PDCR 130/W/C
10-32V d.c. @ 20mA isolated from output.

Supply sensitivity. 0.005% F.S.O./Volt
Polarity reversal protected.

Output voltage (isolated on PDCR 130/W)
±2.5V maximum for 175mbar range
±10V maximum for 350mbar range and above.

Output current
PDCR 135: 5mA maximum. PDCR 130: 2mA maximum.

Combined non-linearity and hysteresis
±0.1% B.S.L. for all ranges.
±0.05% B.S.L. available for ranges up to 20 bar on request.

Zero offset and span setting
Integral trim potentiometers giving total adjustment of nominally 10% F.S.O. available on most models.

Operating temperature range
−40° to +80°C standard
−40° to +125°C connector version
This temperature range can be extended.

Temperature effects

±0.5% total error band 0° to 50°C
±1.5% total error band −20° to +80°C
175mbar range, ±0.5% total error band 10° to 40°C.
For special applications it is possible to give improved temperature compensation over a wider range.

Natural frequency (mechanical)

10.5kHz for 350mbar range increasing to 210kHz for 35 bar range.

Amplifier band width −3dB at 2kHz nominal

Acceleration sensitivity

0.044% F.S.O./g for 350mbar range decreasing to 0.0005% F.S.O./g for 35 bar range.

Mechanical shock

1000g for 1ms in each of three mutually perpendicular axes will not affect calibration.

Weight. 250 grams nominal.

Electrical connection. PDCR 130/W and PDCR 135/W

1 metre integral vented cable supplied.
Longer lengths available on request.

Electrical connection. PDCR 130/W/C and PDCR 135/W/C

6 pin Bayonet fixed plug tested to MIL-C-26482 or DEF 5325 shell size 10. Free mating socket not supplied.
Free mating socket Amphenol type 62GB-16F10-6S available on request.

Options available

Internal "R" calibration facility.

An extra electrical connection is provided on the transducer and if the voltage applied (referenced to the signal 0 Volt) is less than 0.8V (or open-circuit) the R-cal will not operate, and if greater than 2.4V the output will change in a positive direction by a percentage specified during manufacture (up to the maximum output available).

General purpose gauge transducer PDCR 135 and PDCR 130 (separate data sheet).

Differential transducer PDCR 130/WL and PDCR 135/WL (separate data sheet).

Submersible transducer: contact manufacturer.

Flush mounting transducer: contact manufacturer.

Ordering information

Please state the following:-

(1) Type number
(2) Pressure range
(3) Gauge, sealed gauge or absolute
(4) Temperature range
(5) Pressure connection
(6) Pressure media
(7) Supply voltage
(8) Output voltage
(9) Mating electrical socket (if required)

For non-standard requirements please specify in detail.

Continuing development sometimes necessitates specification changes without notice.

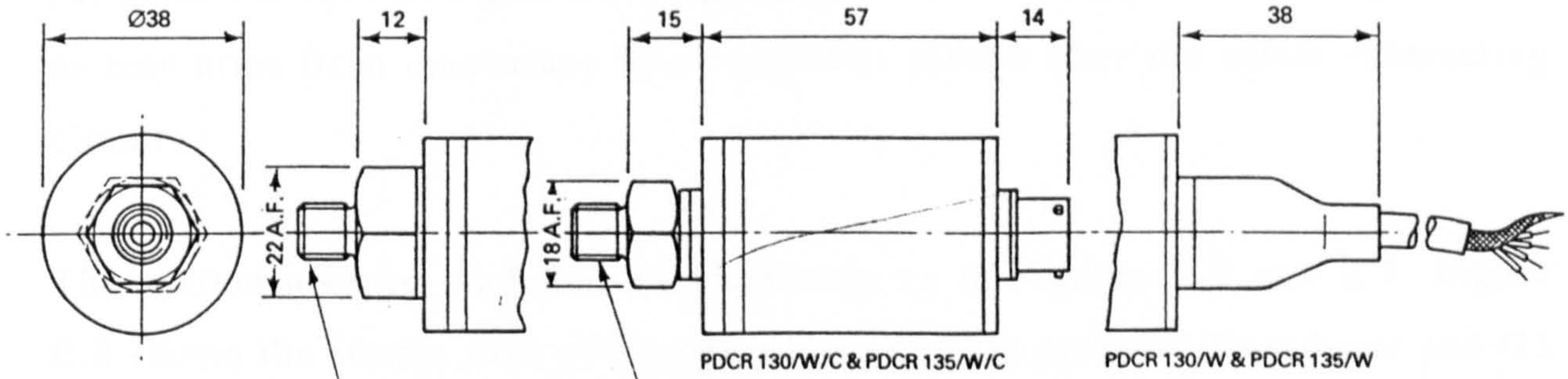

PDCR 130/W/C & PDCR 135/W/C

PDCR 130/W & PDCR 135/W

Pressure connections
G¼B
¼" N.P.T. } Flat end

Pressure connections
G¼B
¼" N.P.T. } Flat end
G¼B 60° Internal cone
7/16" U.N.F. as MS.33656-4
M12×1.5 Ermeto
M14×1.5mm 6 DIN
Others available on request.

Electrical connection

Connector version	Cable version	Function	Function
Pin	Colour	PDCR 130	PDCR 135
A	Red	Supply positive	Supply positive
D	White	Supply OV	Supply negative
B	Yellow	Output positive	Output positive
C	Blue	Output negative	OV common
F connected to C	—	R cal when spec.	R cal when spec.
E	Orange		

Installation

Dimensions: mm

Druck Limited
Fir Tree Lane, Groby,
Leicestershire LE6 0FH, England.
Telephone: Leicester (0533) 878551
Telex: 341743
Facsimile: (0533) 875022

Agent:

D2

APPENDIX E:

METHOD FOR ESTIMATING OVERALL SYSTEM ACCURACY

The effects of individual component inaccuracies on the standing part of the pressure signal (corresponding to mean depth) and on the time-varying part (wave activity) of the whole system are calculated separately. Figure E.1 shows the effect of gain and offset error on these two parts of the pressure signal.

In the figure:- (a) shows the actual signal: a 10 mb peak-to-peak variation about a 2000 mb mean, while

(b) gives the result of this measurement for the case of a 10% gain error. Both standing part (still water level) and varying part (wave) are too small.

(c) shows the effect of an offset error in the circuits: only the standing part is affected. Gain errors are expressed in relative terms (eg -10%) while offset errors may be expressed either in relative (eg -5% of full scale) or absolute (eg -100mb) terms.

(d) gives the case of a gain error applying to the varying part of the signal only, as may arise from inaccuracy in an amplifier placed after the offset-subtracting circuit.

The system may be modelled quantitatively as in Figures E.2 and E.3. Figure E.2 shows the simple case of two gain blocks, G1 a pressure transducer and G2 some sort of amplifying or attenuating function. Clearly

$$B = G_2 A = G_1 G_2 P$$

In Figure E.3 two offset voltages have been added. These may be intentional such as the output of the offset amplifiers, or undesirable such as input errors of an operational amplifier gain block. We now have

$$B = G_2 A + Z_2 = G_2(G_1 P + Z_1) + Z_2$$

$$= P G_1 G_2 + Z_1 G_2 + Z_2 \qquad \text{(E.1)}$$

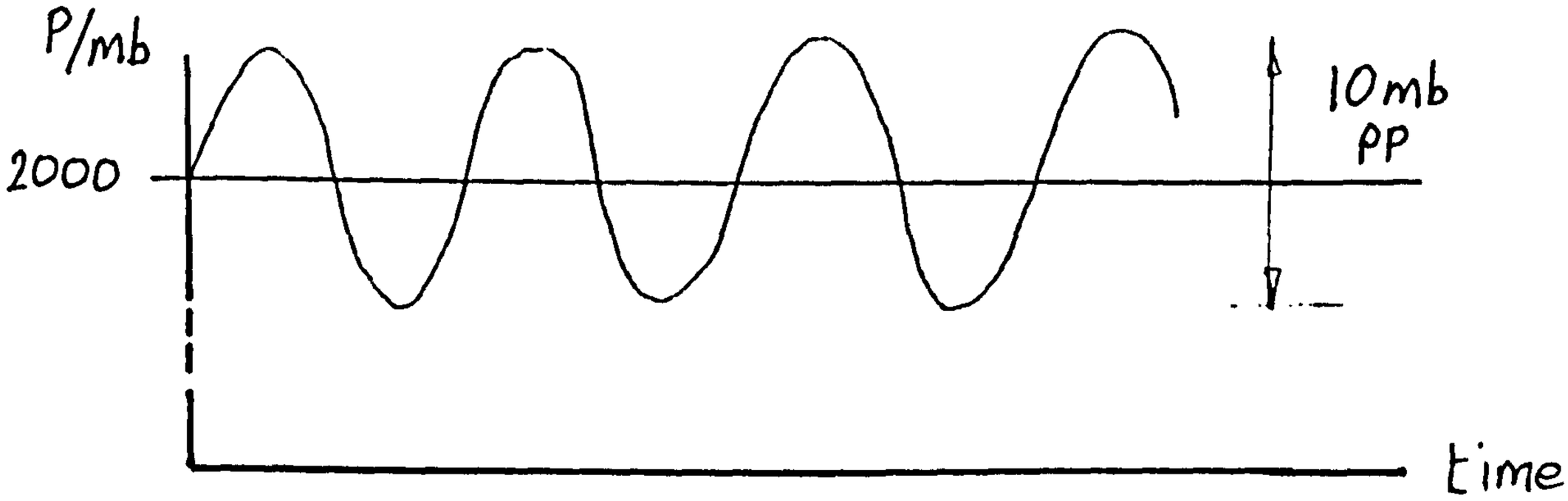

a) indicated and actual pressure : no error

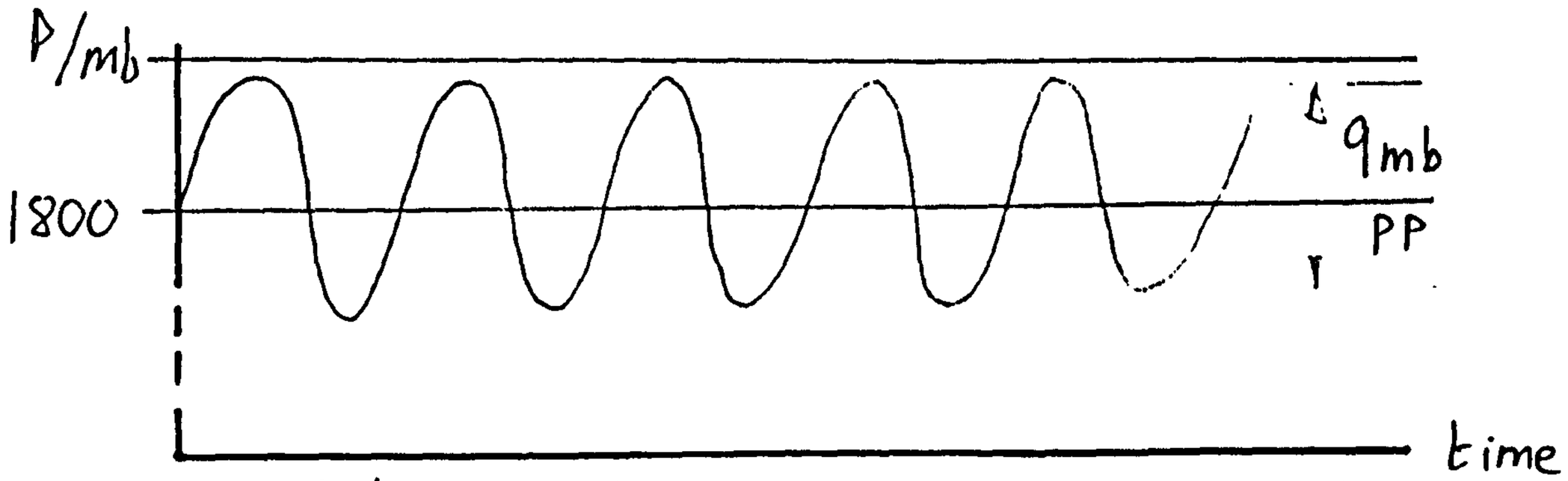

b) indicated pressure : gain error -10%

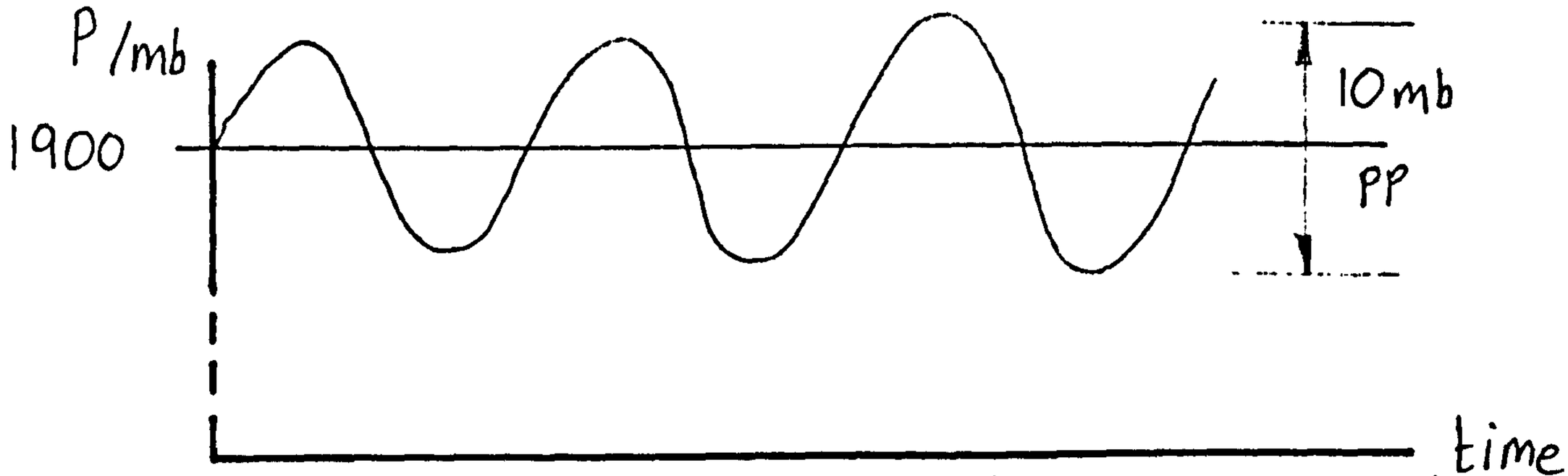

C) indicated pressure : offset error -100mb

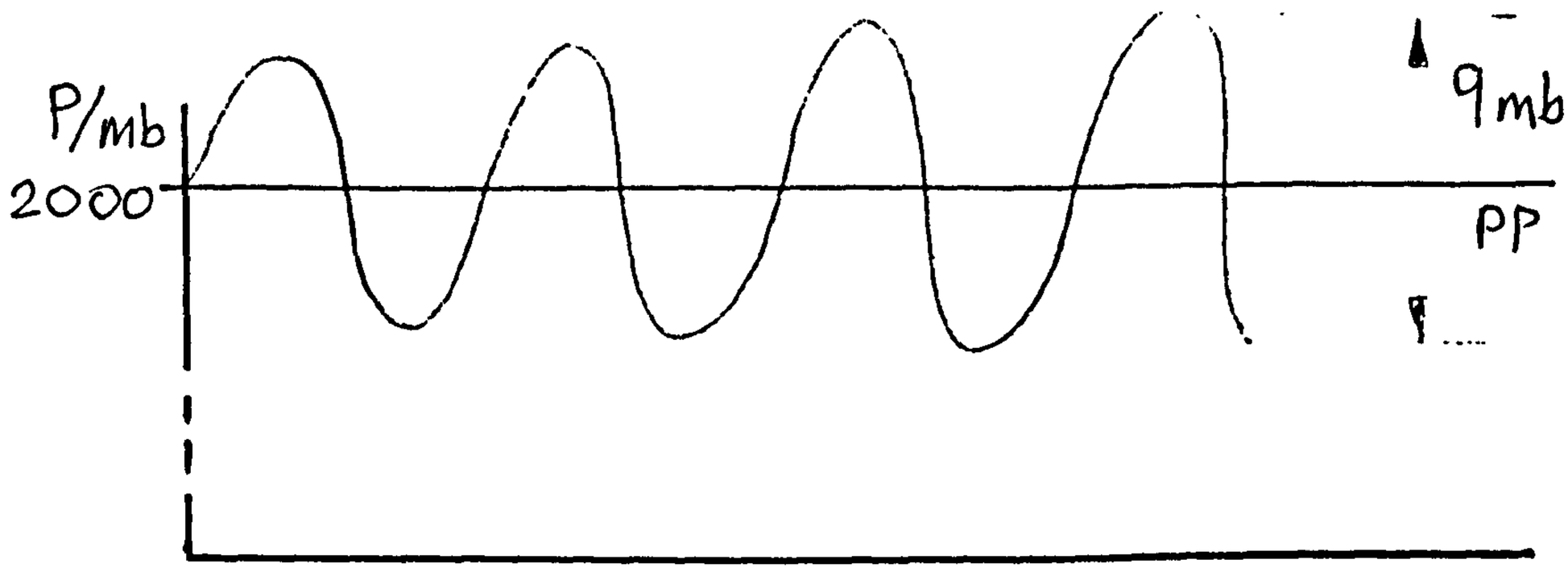

d) indicated pressure : gain error in varying part only.

Figure E.1 : Effects of gain and offset errors on measured pressure signal

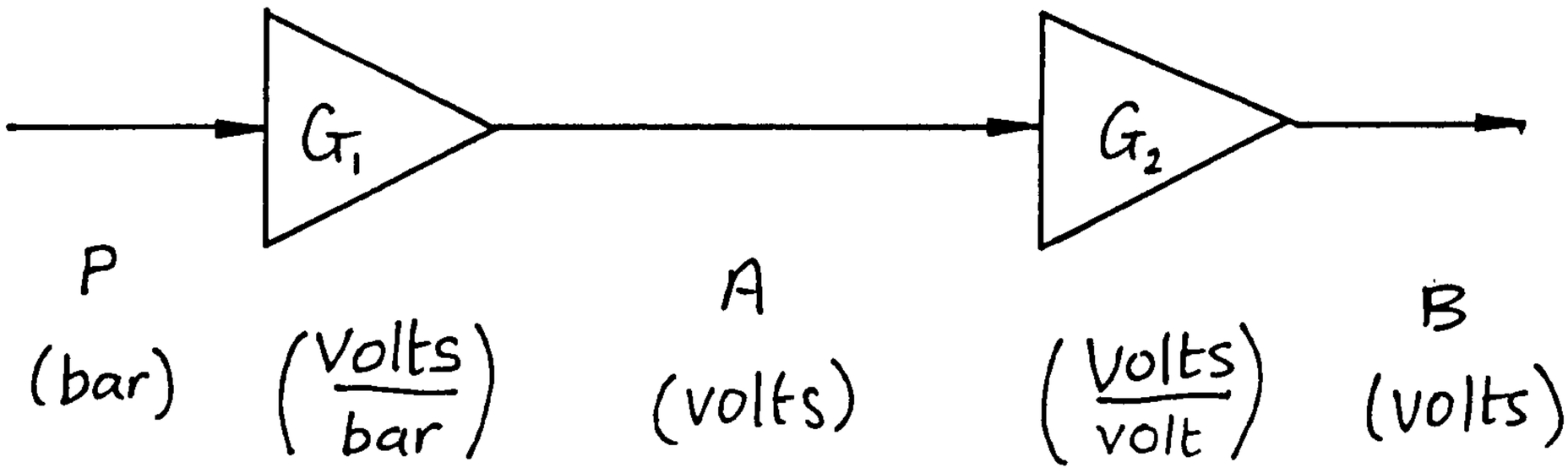

Figure E.2 : Signal flow diagram with two gain blocks

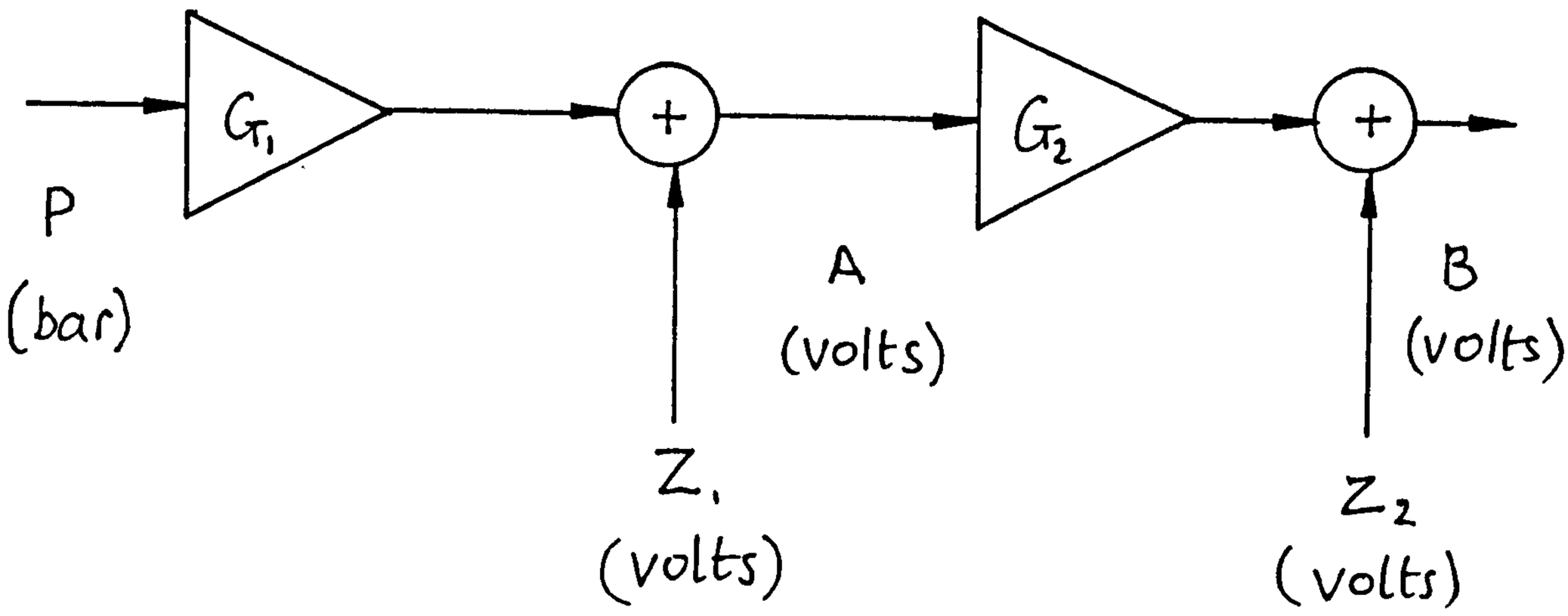

Figure E.3 : Signal flow diagram with two gains and two offsets

Thus, the output of the system B is the sum of a term proportional to the input pressure P and two offset terms. When using the system, its output is known and the measurand (pressure) is inferred assuming that the gains and offsets are as they should be, that is:

$$P_i = \frac{B - (Z_1 G_2 + Z_2)}{G_1 G_2} \qquad \text{(E.2)}$$

with the subscript denoting indicated pressure. As stated above, for comparison to the specification the standing and varying parts of the pressure signal are considered separately. If these are denoted by suffices s and v, then:

$$P = P_s + P_v$$

and $B = B_s + B_v$

The varying part of P will therefore be:

$$P_{iv} = \frac{B_v}{G_1 G_2}$$

since the other terms from Equation E.2 are constant over time and the standing part:

$$P_{is} = \frac{B_s - (Z_1 G_2 + Z_2)}{G_1 G_2} \qquad \text{(E.3)}$$

The effect of errors in gains and offsets is therefore to cause an incorrect pressure to be inferred from the known output according to Equations E2 and E3. Offsets have no effect on the varying part, but both gains and offsets affect the standing part. The terms containing the offsets Z in Equation E3 are each the respective offset referred to the input, and may be denoted by a prime:

$$\frac{Z_1 G_2}{G_1 G_2} = \frac{Z_1}{G_1} = Z_1'$$

and $\frac{Z_2}{G_1 G_2} = Z_2'$

In the system error calculations, of which an example is given in Appendix F, all offset errors are referred to the input and expressed in millibars before they are combined.

Combining errors

Overall relative (ie fractional) gain error may be considered the sum of the relative gain errors of each contributing stage, since they are small and second order effects may be ignored. Overall offset errors, referred to the input, are also the sum of those from each contributing stage.

However. in the case of random (as opposed to systematic) errors, simple addition leads to an overly pessimistic result as they are very unlikely all to be at maximum limit and of the same sign. Instead these are combined into an error for the 99% confidence interval using the statistical arguments below.

If a quantity Q is a function of some other variables, x_k

$$Q = Q(x_1, x_2, ..., x_k, ...x_n) \qquad \text{(E.5)}$$

and if these variables are random with a Gaussian distribution (means: $\bar{x}_k$ and standard deviations: σ_{xk}) then Q will also have a Gaussian distribution (mean: $\bar{Q}$, standard deviation: σ_Q).

It can be shown (Massey 1986) that the standard deviation of Q is related to those of the x's by

$$\sigma_Q^2 = \left(\frac{\partial Q}{\partial x_1}\right)^2 \sigma_{x1}^2 + \left(\frac{\partial Q}{\partial x_2}\right)^2 \sigma_{x2}^2 + ... + \left(\frac{\partial Q}{\partial x_k}\right)^2 \sigma_{xk} + ... \qquad \text{(E.5)}$$

So, for the model of Figure E.3 we have, for the offsets:

$$Z'_{total} = Z'_1 + Z'_2 + Z'_3 + ... \qquad \text{(E.6)}$$

The total offset referred to the input is the sum of the contributory offsets. For the random errors in offsets we apply Eq E5, in which the terms dQ/dx_k are all unity and so

$$\sigma_{Z'_{total}} = \sqrt{\sigma^2_{Z'_1} + \sigma^2_{Z'_2} + \sigma^2_{Z'_3} + \ldots} \qquad \text{(E.7)}$$

that is, the total standard error (ie standard deviation) in offset is the root of the sum of the squares of the contributing standard errors.

Component data sheets quote 'typical' or 'maximum' errors rather than standard errors. For a Gaussian distribution there is a 99% likelihood that the actual error will fall within 2.576 standard deviations, and so that figure is equated to the data sheet's maximum error value. (Caution is in order here, though, as common selection processes result in highly non-standard distributions.) Substituting into Equation E7, it follows that

$$Z'_{T_{e\,max}} = \sqrt{Z'^{\,2}_{1_{e\,max}} + Z'^{\,2}_{2_{e\,max}} + Z'^{\,2}_{3_{e\,max}} + \ldots} \qquad \text{(E.8)}$$

There is a 99% chance that the overall offset error (denoted by suffix e), referred to the input, is less than the root of the sum of the squares of the contributing offset errors. There is a 1% chance that the overall offset error will fall between this value and the arithmetic sum of the contributing errors.

In the case of gains, for three contributing stages:

$$G_T = G_1 G_2 G_3 \ldots \qquad \text{(E.9)}$$

$$\frac{\partial G_T}{\partial G_1} = G_2 G_3, \quad \frac{\partial G_T}{\partial G_2} = G_1 G_3 \qquad \text{etc} \qquad \text{(E.10)}$$

and for random errors in gain (from E5):

$$\sigma_{G_T} = \sqrt{G_2^2 G_3^2 \sigma^2_{G_1} + G_1^2 G_3^2 \sigma^2_{G2} + G_1^2 G_2^2 \sigma^2_{G3}} \qquad \text{(E.11)}$$

and dividing throughout by G_T:

$$\frac{\sigma_{G_T}}{G_T} = \sqrt{\left(\frac{\sigma_{G_1}}{G_1}\right)^2 + \left(\frac{\sigma_{G_2}}{G_2}\right)^2 + \left(\frac{\sigma_{G_3}}{G_3}\right)^2} \qquad \text{(E.12)}$$

the total fractional standard error in gain is the root of the sum of the squares of the contributing fractional standard errors.

Finally, to the 99% confidence limit:

$$\frac{G_{T\,e\,\max}}{G_T} = \sqrt{\left(\frac{G_{1\,e\,\max}}{G_1}\right)^2 + \left(\frac{G_{2\,e\,\max}}{G_2}\right)^2 + \left(\frac{G_{3\,e\,\max}}{G_3}\right)^2} \qquad \text{(E.13)}$$

REFERENCE

Massey B.S. (1986)
Measures in science and engineering p81ff
Ellis Horwood Ltd UK

APPENDIX F: ERROR CALCULATION

On the analog sections from pressure transducer to ADC

NOTES

1) Input is assumed to be 10mb peak-to-peak on a 2000mb standing level.

2) Maximum (not typical) data sheet values are used.

3) Systematic errors are combined by arithmetical sum.
Random errors are combined by root sum of squares.

Error Source	Effect on Varying Part			Effect on Standing Part					
	Systematic	Random		Systematic		Random			
						Non Parametric		Parametric over 15°C	
	%	Non-param ± %	Param ± % over 15°C	Actual	Referred to I/P mb	Actual ±	Ref I/P ± mb	Actual ±	Ref I/P ± mb
1 TRANSDUCER (Signal: 10mb pp on 2000mb standing) Both gain and offset errors are adjusted out. Long term drift, temperature errors, non-linearity and hysteresis are quoted in terms of total error bands: ±0.15%FR, ± 0.5% over 0-50°C.	-	0.15	0.25	-	-	0.15%FR	6.0	0.25%FR	10.0
2 CABLE: AAF AMP (Av=1) (Signal: 12.5 mV pp on 2500mV standing) Potential drop: cable & input impedance	-0.05	-	-	-0.05% RDG	-1.0	-	-	-	-
I/P bias current through unequal Rs (25 ± 10 nA from each I/P, negl. tempco	-	-	-	+4.8mV	+3.8	1.9mV	1.5	-	-
I/P offset current (±1.3 nA in 100 kΩ) ngl tempco)	-	-	-	-	-	1.3mV	1.0	-	-
I/P offset voltage (± 250 µV max, ± 2 µV/°C	-	-	-	-	-	0.25mV	0.2	-	-
(Resistor selection and tolerance errors not applicable - unity gain)									
Filter characteristics (± 0.02dB)	-	0.2	-	-	-	-	-	-	-

Error Source	Effect on Varying Part			Effect on Standing Part					
	Systematic	Random		Systematic		Random			
						Non Parametric		Parametric over 15°C	
	%	Non-param ± %	Param ± % over 15°C	Actual	Referred to I/P mb	Actual ±	Ref I/P ± mb	Actual ±	Ref I/P ± mb
3 TRACK & HOLD (Signal I/P 12.5mV on 2500mV standing)									
I/P offset voltage (± 250µV, ± 2µV/ °C)	-	-	-	-	-	0.25mV	0.2	-	-
I/P bias current through unequal Rs, I/P offset current (25 ± 10 nA into 10.00 and 10.05 kΩ – NEGL.	-	-	-	-	-	-	-	-	-
Capacitor & switch leakages - NEGL.	-	-	-	-	-	-	-	-	-
Capacitor dielectric absorption (0.1%, applied to varying part)	-	0.1	-	-	-	-	-	-	-
Settling times, aperture time & droop rate errors - NEGL.	-	-	-	-	-	-	-	-	-
4 MULTIPLEXER Leakage current from all Off channels to ON channel, (≈100nA into 400 Ω) NEGL.	-	-	-	-	-	-	-	-	-

Error Source	Effect on Varying Part			Effect on Standing Part					
	Systematic	Random		Systematic		Random			
						Non Parametric		Parametric over 15°C	
	%	Non-param ± %	Param ± % over 15°C	Actual	Referred to I/P mb	Actual ±	Ref I/P ± mb	Actual ±	Ref I/P ± mb
5 OFFSET AMPLIFIER (1.9V setting) (I/P signal 12.5 mV pp on 2500 mV standing)									
Reference voltage (± 0.2%, 0.5 ppm/°C)	-	-	-	-	-	3.8mV	3.0	-	-
Resistor selection (E96 grid)	-	-	-	+4.3mV	+3.4	-	-	-	-
Resistor tolerance (0.1%, 15 ppm/°C)	-	-	-	-	-	1.9mV	1.5	0.3mV	0.2
Capacitor dielectric abs (0.1%) (assume adjacent channels are reading crest/trough, 10mV)	-	0.1	-	-	-	-	-	-	-
6 PROGRAMMABLE GAIN AMPLIFIER (Gain x 5) (Signal now 12.5 mVpp on 0.6 V standing)									
I/P offset voltage (5μV) NEGL.	-	-	-	-	-	-	-	-	-
I/P bias currents (175pA in ΔR ≈10 K)	-	-	-	-	-	-	-	-	-
(175pA over full temp. range) NEGL.									
I/P offset currents	-	-	-	-	-	-	-	-	-
(300 pA over full temp. range) NEGL.									
Resistor selection (E96 grid)	0.2	-	-	+0.2%(of 0.6V I/P)	+1.2	-	-	-	-
Resistor tolerance (0.1%, 15 ppm/°C)	-	0.1	0.02	-	-	0.1% (of 0.6V I/P) = 0.6mV	0.5	0.02% (of I/P)	0.1

Error Source	Effect on Varying Part			Effect on Standing Part					
	Systematic	Random		Systematic		Random			
						Non Parametric		Parametric over 15°C	
	%	Non-param ± %	Param ± % over 15°C	Actual	Referred to I/P mb	Actual ±	Ref I/P ± mb	Actual ±	Ref I/P ± mb
7 ADC (Signal now 62.5 mV pp on 3V standing) Reference voltage (± 0.2%, 0.5ppm/°C)	-	0.2	-	-	-	0.2% (of 3.0V I/P) = 6mV	1.0	-	-
Non-linearity (± 1LSB)	-	0.02	-	-	-	0.02% (of 5V) = 1.2mV	1.0	-	-
Un-adjusted zero error (± 2LSB)	-	0.05	-	-	-	0.05% (of 5V) = 2.5mV	0.4	-	-
Un-adjusted span error (± 30 LSB) (CONSIDER PROVIDING ADJUSTMENT)	-	0.73	-	-	-	0.73% (of 3V) = 22mV	3.5	-	-
Quantisation error (± ½ LSB) (Defines system resolution - treated separately from error calculation)	-	-	-	-	-	-	-	-	-

F5

Error Source	Effect on Varying Part			Effect on Standing Part					
	Systematic	Random		Systematic		Random			
						Non Parametric		Parametric over 15°C	
	%	Non-param ± %	Param ± % over 15°C	Actual	Referred to I/P mb	Actual ±	Ref I/P ± mb	Actual ±	Ref I/P ± mb
TOTALS (Systematic errors combined by arithmetic sum, Random errors by root of sum of squares)	+0.15	±0.82%							
MAXIMUM ERRORS:- (99% confidence) All:	+0.15%	±0.82%	±0.25%		+7.4mb		±8.1mb		±10mb
	+0.15%	1.01% 0.71%					+20.3 mb -5.5	(+2.0 % of 10m −0.5)	
Without ADC span error:	+ 0.15%	± 0.37%	±0.25%		+7.4mb		± 7.3mb		± 10mb
		+0.60% -0.30%					+19.8 mb -5.0		

APPENDIX G

SEMICONDUCTOR MEMORIES

1. Mask ROM — Mask Programmed Read Only Memory
Program defined by a mask during assembly.

Strengths : v. cheap, high capacity.
Weaknesses: changes expensive, long lead time, difficult stock control, slow.

Applications: v. high volume.
character generators, look up tables, compilers, operating systems, games.

Example : Hitachi HN 62412P
2Mb (256*8), CMOS, 5 uW standby, 5 V, 150 ns
£5 each (100,000 up). Mask charge £4000.

2. PROM — Programmable Read Only Memory
Normally means programmable by blowing fusible links on the chip, either by user or distributor

Strengths : cheap, high capacity, changes and stock control easier than mask ROM, fast.
Weaknesses: still cannot re-program the chip.

Applications: fairly high volume.
peripheral controllers, digital equipment control.

3. EPROM — Electrically Programmable Read Only Memory

UVEPROM — Ultra-Violet erasable and Electrically Programmable ROM

Programmed on dedicated machine, with 10 to 30 V pulse.
Erased by exposure to UV light for about 30 minutes.

Strengths : fairly cheap, high capacity, re-programmable.
Weaknesses: requires special package with quartz window, and a socket for re-programming out of circuit. Erases all data together.
limited number of erase/program cycles (eg 1000)

Applications: low volume, or prototypes for high volume products.

Example: Hitachi HN27C301G-20
1 Mb (128*8), CMOS, 5 uW standby, 5 V, with 12.5 V programming pulse, 200 ns.
£20 each (100 up).

OTP EPROM One Time Programmable Electrically Programmable ROM

Chip is same as UVEPROM but in standard plastic package.

Strengths : 15% cheaper than UVEPROM.
surface mount packages possible.
Weaknesses: cannot be re-programmed

Applications: for those UVEPROM applications in which changes are not likely, but where quantites are not high enough for Mask ROM or PROM.

4. EEPROM Electrically Erasable and Programmable ROM
(floating silicon gate NMOS technology)
(& EAROM Electrically Alterable ROM
metal-nitride - MNOS - technology)

Strengths : may be programmed and erased in circuit
Weaknesses: low capacity, expensive
(1 generation behind EPROMS).
still not like RAM - limit of about 10,000 write cycles.

Applications: wherever changes required to product in normal operation -
instrument calibration constants, PABX, point of sale systems, engine management, program development

Example : Xicor X28256AP
256 Kb (32K*8), read acces 150 ns, byte write 78 us, total memory re-write 2.5 s, £150 (1 up)

Flash EEPROM As EEPROM but density nearly as good as EPROM
100 - 10000 write cycles

5. NOVRAM Non Volatile Random Access Memory
Static RAM overlaid (bit for bit) on chip by EEPROM ("shadow" EEPROM)
Access through RAM only. Store and recall signals copy RAM into EEPROM. Individual bits, bytes, or pages may be copied.

Strengths : no limit to the number of write cycles
(genuine RAM)
Weaknesses: low capacity, expensive (6 * EPROM)

Applications: as RAM where non-volatility is required
programme development

Example : Greenwich Instruments NVR8
64 Kb (8K * *), 150 ns read, several ms store,
£68 (1 up)

6. Static RAM Static Random Access Memory (or Read - Write Memory)

Strengths : medium capacity, no limits to number of write cycles, no special voltage levels, low power (if CMOS).
Weaknesses: volatile.

Applications: computer main memory

Examples : CMOS - Hitachi HM622561-LP8
256 Kb (32K * 8), 10 uW standby, 5 V, 85 ns,
£9 (100 up)
Bipolar (ECL) - Hitachi HM6785-25
64 Kb (64K * 1), approx 500 mW, 25 ns
£37 (100 up)

7. Dynamic RAM Dynamic Random Access Memory
As static RAM but data must be re-written to each bit every 2 ms (refreshing)

Strengths : as static RAM but greater capaity, and cheaper.
Weaknesses: volatile, requires refreshing circuitry.

Applications: computer main memory

Example : Hitachi HM511001
1 Mb (1M * 1), 10 mW standby, 5 V, 100 ns
£19 (100 up)

8. Ferrite Original computer memory - a matrix of ferrite beads.

Strengths : resistant to radiation, high temperature
Weaknesses: very expensive, $1 per bit, compare above!
low capacity - 512 bit max

Applications: very specialised, high rad, high temp environments

Ferroelectric technology using thin-film & photolithographic techniques are now being developed.

P. A. D. Bird
1990

APPENDIX H :

LIST OF MANUFACTURERS OF UNDERWATER CONNECTORS (1987)

Brantner & Assoc, Inc	El Cajon, CA	USA
(agent: Techmation	Edgeware	UK)
Ferranti ORE	Great Yarmouth	UK
Glenair International	Mansfield Woodhouse	UK
Groove Associates Ltd	Emsworth	UK
Hawke Cable Glands Ltd	Ulveston	UK
Hellermann Deutsch Ltd	East Grinstead	UK
Hughes Microelectronics Ltd	Glenrothes	UK
Hydro-Bond Engineering Ltd	Aberdeen	UK
PDM Unelco	Farnham	UK
Slingsby Engineering Ltd	Kirkby moorside	UK
Souriau UK Ltd	High Wycombe	UK

APPENDIX I :

LIST OF MANUFACTURERS OF UNDERWATER CABLE (1987)

BICC Electronic Cables Ltd	Warrington	UK
Boston Insulated Wire (UK) Ltd	Esher	UK
De Regt Special Cable	Rotterdam	Holland
(agent: D.C. Cables	Wilmslow	UK)
Jaques Rotork	Ely	UK
Norsk Data	Drammen	Norway
(office in London)		
PDM Unelco Ltd	Farnham	UK